AD-A181 500 SOUTH ATLANTIC OMEGA VALIDATION VOLUME 1 SUMMARY 1/3
ANALYSIS APPENDICES A-E(U) SYSTEMS CONTROL TECHNOLOGY
INC PALO ALTO CA T M WATT ET AL. JAN 83
UNCLASSIFIED DTCG23-81-C-40023 F/G 17/7.3 NL

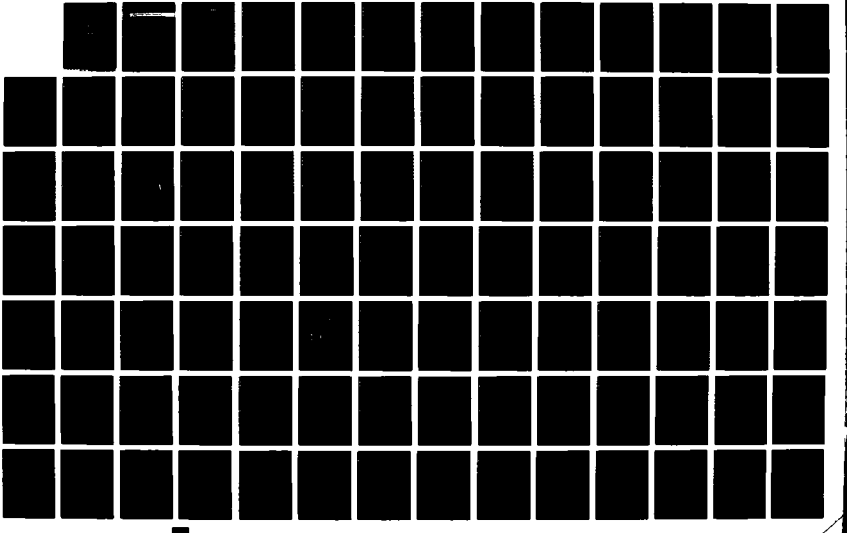

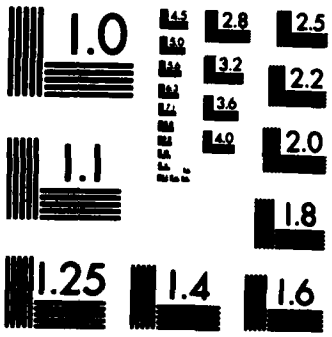

SYSTEMS CONTROL TECHNOLOGY, INC.
1801 PAGE MILL RD. □ P.O. BOX 10180 □ PALO ALTO, CALIFORNIA 94303 □ (415) 494-2233

SOUTH ATLANTIC OMEGA VALIDATION

Final Report

VOLUME I: SUMMARY, ANALYSIS, APPENDICES A-E

January 1983

Prepared by:

T. M. Watt
G. J. Bailie
M. Sutphen

Systems Control Technology, Inc.
Palo Alto, California 94304

for

OMEGA NAVIGATION SYSTEM OPERATIONS DETAIL
Washington, D.C. 20590

SECURITY CLASSIFICATION OF THIS PAGE

REPORT DOCUMENTATION PAGE

1a. REPORT SECURITY CLASSIFICATION	1b. RESTRICTIVE MARKINGS
2a. SECURITY CLASSIFICATION AUTHORITY	3. DISTRIBUTION/AVAILABILITY OF REPORT This document has been approved for public release and sale; its distribution is unlimited.
2b. DECLASSIFICATION / DOWNGRADING SCHEDULE	
4. PERFORMING ORGANIZATION REPORT NUMBER(S)	5. MONITORING ORGANIZATION REPORT NUMBER(S)
6a. NAME OF PERFORMING ORGANIZATION: Systems Control Technology, Inc 6b. OFFICE SYMBOL (If applicable)	7a. NAME OF MONITORING ORGANIZATION
6c. ADDRESS (City, State, and ZIP Code): 1801 Page Mill Rd. Palo Alto, CA 94303	7b. ADDRESS (City, State, and ZIP Code)
8a. NAME OF FUNDING / SPONSORING ORGANIZATION 8b. OFFICE SYMBOL (If applicable)	9. PROCUREMENT INSTRUMENT IDENTIFICATION NUMBER: DTCG23-81-C-40023
8c. ADDRESS (City, State, and ZIP Code)	10. SOURCE OF FUNDING NUMBERS PROGRAM ELEMENT NO. / PROJECT NO. / TASK NO. / WORK UNIT ACCESSION NO.

11. TITLE (Include Security Classification)
South Atlantic Omega Validation. Volume I: Summary, Analysis, Appendices A-E

12. PERSONAL AUTHOR(S)
T.M. Watt, G.J. Bailie, M. Sutphen

13a. TYPE OF REPORT	13b. TIME COVERED	14. DATE OF REPORT (Year, Month, Day)	15. PAGE COUNT
Final	FROM _____ TO _____	1983 January	

16. SUPPLEMENTARY NOTATION

17. COSATI CODES			18. SUBJECT TERMS (Continue on reverse if necessary and identify by block number)
FIELD	GROUP	SUB-GROUP	

19. ABSTRACT (Continue on reverse if necessary and identify by block number)

20. DISTRIBUTION / AVAILABILITY OF ABSTRACT ☐ UNCLASSIFIED/UNLIMITED ☐ SAME AS RPT. ☐ DTIC USERS	21. ABSTRACT SECURITY CLASSIFICATION
22a. NAME OF RESPONSIBLE INDIVIDUAL	22b. TELEPHONE (Include Area Code) / 22c. OFFICE SYMBOL

DD FORM 1473, 84 MAR — 83 APR edition may be used until exhausted. All other editions are obsolete.

SECURITY CLASSIFICATION OF THIS PAGE

TABLE OF CONTENTS

TABLE OF CONTENTS (Continued)

TABLE OF APPENDICES

LIST OF FIGURES

LIST OF FIGURES (Continued)

LIST OF TABLES

LIST OF TABLES (continued)

I. EXECUTIVE SUMMARY

1.1 BACKGROUND AND PROBLEM STATEMENT

A validation study has been performed of the Omega navigation system in the South Atlantic region. For purposes of the study, the validation region is bounded by 20^{0} E and 70^{0} W longitude, 20^{0} S and 60^{0} S latitude, and includes an area of about 35 million square miles.

The objectives of the study are to characterize the inherent position-fixing accuracy of the Omega system in the South Atlantic, as it will be when the eighth and final transmitting station is commissioned in Australia in 1982, and to validate Omega signal coverage and characteristics in the region.

The basic data resources available for meeting these objectives include:

- theoretical at 10.2 kHz boundaries of useful signal coverage
- a computer-based file of long-term Omega phase-difference data collected by ONSOD at eight fixed monitor sites in the region
- short-term signal amplitude and noise measurements taken with both fixed and airborne monitors for ONSOD by the Naval Ocean Systems Center (NOSC) cooperatively with the Federal Aviation Administration Technical Center (FAATC):
- shipboard phase, SNR and fix accuracy data from integrated Omega-satellite (IOS) receivers)
- operational signal quality data from the marine and aviation user communities..

1.2 METHODOLOGY OF APPROACH

The South Atlantic Omega Validation involves two main lines of inquiry. The first line of inquiry considers the availability of Omega signals, in the sense of having a sufficient SNR to be heard and to be free of modal interference. The second line of inquiry deals with the accuracies of postition fixes that can be achieved with the available signals. Fix

accuracies are fundamentally dependent on three factors; the fidelity of the phase information contained in each Omega signal, the geometrical relationships between pairs of LOPs, and the availability and accuracy of propagation prediction corrections (PPCs).

This validation effort pursues five areas of analysis; (1) signal coverage, (2) GDOP, (3) PPC error, (4) LOP error statistics and (5) fix error statistics. Except for GDOP, all analyses are performed at the two major Omega frequencies of 10.2 kHz and 13.6 kHz.

Signal coverage is analyzed in the South Atlantic from measurements of SNR from both fixed and moving platforms. Measurement results at 10.2 kHz are compared with coverage predictions at 10.2 kHz, and the coverage predictions are modified in accordance with the measurement results.

GDOP, or geometrical dilution of precision, is derived as a mathematical function of the relative locations of a hypothetical receiver and all the Omega transmitters. GDOP predicts the effect of LOP crossing angles on fix error and thus provides guidance to a user who calculates position fixes from separate LOP measurements.

PPC error can be studied by observing the diurnal behavior of LOP errors at fixed sites such as ONSOD monitors. Perfect PPCs would provide zero LOP error over all times and locations, thus a study of observed LOP errors can lead to improved PPCs.

In contrast to diurnal mean LOP errors which, in principle, are correctable by improved PPCs, random errors in LOPs observed at similar times and locations leads to an understanding of inherent limits in Omega accuracy, which errors must be described statistically. In addition, a comparison of random errors between different LOPs provides some guidance to a potential user as to the best choice of LOPs as a function of time and position.

Fix errors represent an accumulation of PPC errors, phase measurement errors, and GDOP. Fix errors define navigational accuracy and along with signal coverage, represent the most important criteria of the efficacy of Omega.

The present validation makes extensive use of measurement data from maritime vessels equipped with integrated Omega-satellite (IOS) receivers. The IOS data provide greatly-needed spatial diversity to the data base, but

because IOS fix measurements are not uniformly distributed across the South Atlantic region, it has been found useful to establish a method for quantizing the spatial dimensions of the South Atlantic region.

The spatial correlation to be expected between Omega measurements in the South Atlantic is likely to be fairly high over distances of several hundreds of miles, especially in oceanic areas. Accordingly, it seems quite reasonable to limit the spatial detail of the SNR and phase data analysis. The approach followed here has been to divide the South Atlantic region onto a grid of rectangular spaces defined by latitude boundaries at 10^{o} intervals and longitude boundaries at 10^{o} intervals. The South Atlantic region of 20^{o} N to 60^{o} S and 70^{o} W to 20^{o} E is then divided into 72 rectangular areas. Within each given area, all available fixed-monitor data for a given circumstance (transmitter, month, GMT) can be combined to yield a single set of statistics. Within each area, all available IOS data for a given circumstance (transmitter, month, GMT) can be combined to yield a single set of statistics. Figure 1-1 illustrates the grid used for quantizing results.

IOS data are available from eight ship voyages in the South Atlantic during the period November 18, 1979 through April 16, 1981. IOS measurements from maritime vessels provide a very important adjunct to the Omega data base. IOS measurements are based on simultaneous Omega fixes and satellite fixes using the Transit satellite system.

Transit signals are not available continuously, since the satellites are in near-polar orbits. In fact, Transit signals are available only at irregular intervals ranging from one-half hour to three hours.

Since the IOS data base contains entries only at times corresponding to satellite fixes, IOS data are not generally available at 0600 and 1800 GMT. Since the validation applies, strictly speaking, only to these two times and to the months of February, May, August and November, then it becomes necessary to interpret the actual IOS data in terms of imputed values that would have been observed had measurements been made at 0600 and 1800 GMT during February, May, August and November.

This requirement to infer measurements that were not actually made from measurements that were made suggests the use of some interpolation or extrapolation on the available data. Moreover, because of the rapid variation

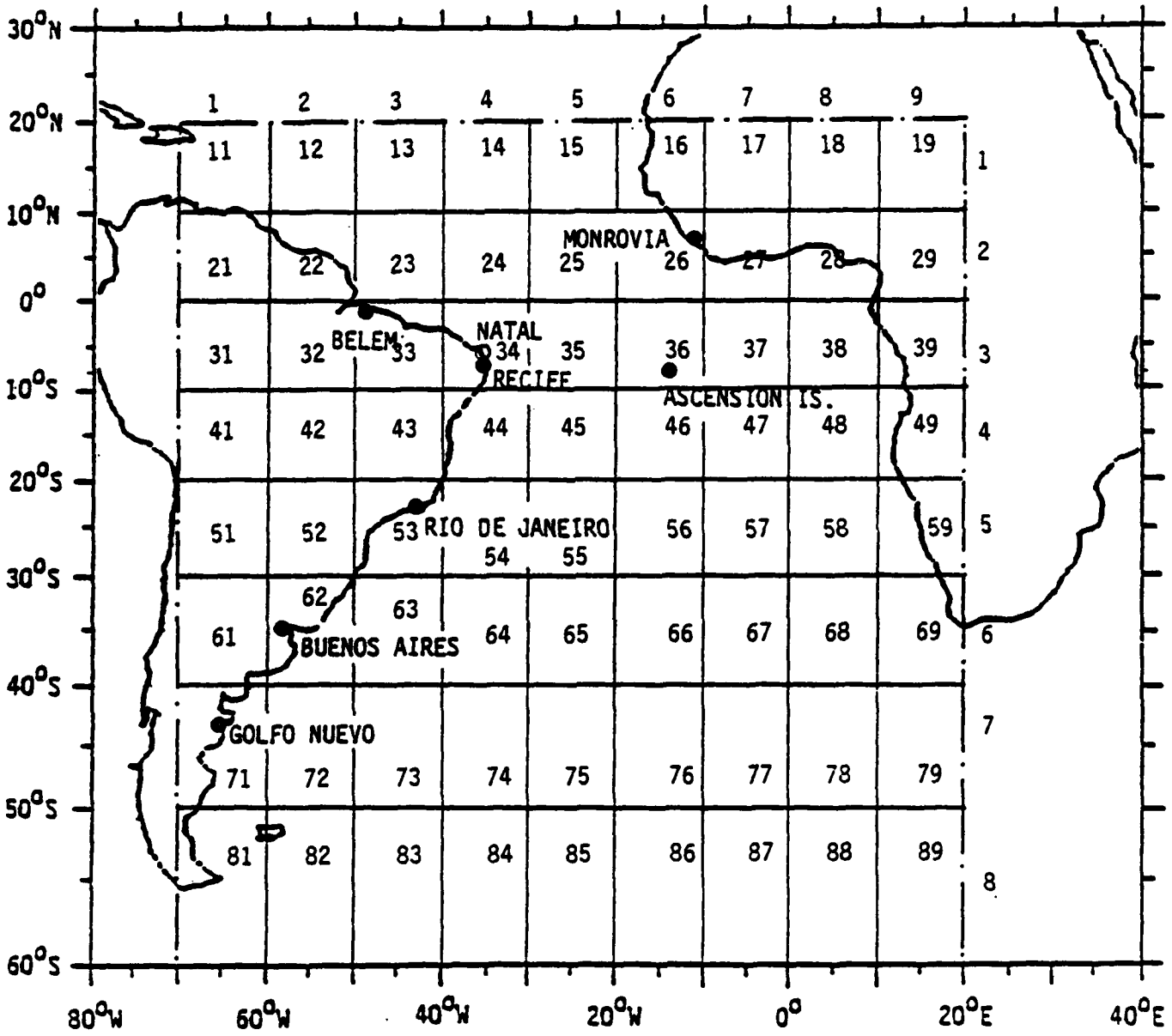

Figure 1-1. Grid used for Grouping Measurement Data in South Atlantic Region.

of radiowave propagation conditions with GMT, it is immediately obvious that the value of IOS data is related to the proximity of measurement times to 0600 and 1800 GMT. In order to delete non-utile data, time windows of 0400-0800 GMT and 1600-2000 GMT have been arbitrarily established. Data falling outside these windows are not considered in the analysis.

In order to utilize as much of the limited IOS data base as possible, "date windows" have been used, as follows. All IOS data acquired during the months of January, February, and March have been consolidated and are assumed to be representative of February. Similarly, April, May, and June data are grouped as representative of May, and so on for the 3-month periods centered on August and November. In the case of the IOS data, then, a label of any particular month means that a validation is being performed for that month based on data available in a 3-month window centered on the month being labelled in the validation.

The use of 4-hour time windows and 3-month date windows must be performed with care. In particular, it is important that daytime data and night-time data not be combined.

It is known that propagation of Omega signals from a transmitter changes rapidly as a terminator passes over the transmitter. The effects of propagation changes can be readily ovserved as a rapid variation in SNR at a receiver. In order to avoid the possibility of interpolating or extrapolating measurement data across a terminator, it is necessary to define, for each Omega transmitter, the propagation condition (night or day) at the two times 0600 GMT and 1800 GMT, and for the date of the measurement, and to forshorten the time window as appropriate to provide a single illumination condition for all data in any time block.

1.3 ANALYSIS CATEGORIES

The following aspects of Omega performance in the South Atlantic are addressed in this validation study:

(1) Signal Coverage at 10.2 kHz at 0600 and 1800 GMT for February, May, August and November.

(2) Signal Coverage at 13.6 kHz at 0600 and 1800 GMT for February, May, August and November.

(3) Geometric Dilution of Precision (GDOP).

(4) Diurnal Error in LOPs at 10.2 kHz for February, May, August and November.

(5) Diurnal Error in LOPs at 13.6 kHz for February, May, August and November.

(6) LOP Error Statistics at 10.2 kHz at 0600 and 1800 GMT for February, May, August and November.

(7) LOP Error Statistics at 13.6 kHz at 0600 and 1800 GMT for February, May, August and November.

(8) Fix Error Statistics at 10.2 kHz at 0600 and 1800 GMT for February, May, August and November.

(9) Fix Error Statistics at 13.6 kHz at 0600 and 1800 GMT for February, May, August and November.

Each analysis is independent of the others, and requires its own data base. The GDOP analysis requires no data other than Omega transmitter locations. All other analyses are based on actual measurements of Omega signals.

Except for the GDOP case, all these analyses are statistical in nature, and the validity of the results for each analysis is strongly dependent on the size and breadth of the data base used for the analysis, as well as the quality of any measurements that contribute to the data base.

1.4 ANALYSIS AND INTERPRETATION OF DATA

1.4.1 Omega Signal Coverage at 10.2 kHz

Global coverage of Omega signals 10.2 kHz has been determined theoretically by The Analytical Sciences Corporation (TASC) [18].

The threshold for usable Omega signals is either -20 dB or -30 dB SNR depending on which of two criteria is used. Contours for each Omega station corresponding to these two thresholds have been published by TASC in the form of regional and global maps with the contours overlaid. Published contours are available only for two times (0600 and 1800 GMT) and four months (February, May August and November). No allowance is made in the published

contours for long-term variations such as might be associated with the solar cycle. The contours are secondary results of the TASC analysis in that the fundamental variation of SNR is calculated along a series of radials projecting outward from each Omega station.

The contour plots available from TASC are large scale and global in their presentation. In order to focus attention on the South Atlantic, it has been necessary to redraw the contours to a much smaller scale. Appendix F presents redrawn versions of the original 64 contour plots available from TASC.

The approach followed here has been to divide the South Atlantic region onto a grid of rectangular spaces defined by latitude boundaries at 10^{o} intervals and longitude boundaries at 10^{o} intervals. The South Atlantic region of 20^{o} N to 60^{o} S and 70^{o} W to 20^{o} E is then divided into 72 rectangular areas. Within each given area, all available fixed-monitor SNR data for a given circumstance (transmitter, month, GMT) can be statistically combined to yield a single mean and a single standard deviation. Within each area, all available IOS SNR data for a given circumstance (transmitter, month, GMT) can be statistically combined to yield a single mean and a single standard deviation.

The results of all SNR data were plotted on maps that conformed to the maps presented in Appendix F, except that theoretical contours of SNR were replaced with a matrix grid defining the spatial detail of the results.

Appendix G presents the data in the form of means and standard deviations. Appendix G contains 64 maps on which are presented all the analyzed measurement data that are to be compared with theoretical predictions. Each map in Appendix G corresponds to a map of theoretical contours in Appendix F, to the same scale. A comparison of any corresponding maps enables one to make a judgment about the extent, if any, to which a theoretical contour should be modified.

The theoretical contours of SNR presented in Appendix F and based on the predictions of Reference 18 were modified in accordance with the measurement results obtained in this study and presented in Appendix G. The following rules were followed in modifying the contours:

(1) Smooth curves were employed where ever possible.

(2) Modified contours were defined only in regions where modal interference was predicted to be less than 20 cec.

(3) Modified contours were required to be consistent with measurement data.

(4) Contours were modified only to the extent necessary to accommodate measurement data. Original conours, or segments of original contours were retained wherever possible.

(5) The measurement data in Appendix G demonstrates the well-known tendency of radio noise in the Omega band to be higher over land masses than over oceanic areas. This tendency has been assumed to hold even where no supporting data exist, thus modified SNR contours were drawn to be approximately parallel to coastal outlines in the South Atlantic region.

Appendix H presents modified signal coverage predictions for the South Atlantic region. The predictions are in the same form as the theoretical predictions presented in Appendix F; that is, 64 maps depicting cases for 8 transmitters, 4 months and two GMTs. The maps in Appendix H thus provide a simple and straightforward prediction of Omega availability in the South Atlantic region.

An example of this analysis is illustrated in Figures 1-2, 1-3, and 1-4. Figure 1-2 presents predicted contours of signal coverage for Norway (A) at 0600 GMT in February, as taken from Appendix F. Figure 1-3 presents an example from Appendix G of the results of the analysis of all available data, labeled according to source [Fixed site = F, IOS = S], the number of measurements following the source designator, and the mean value of SNR for the grid block in SNR. Where multiple measurements exist, standard deviation is also indicated. Figure 1-4 presents modified contours resulting from a comparison of theoretical contours and measurement results.

1.4.2 Omega Signal Coverage at 13.6 kHz

Measurement data on SNR have been obtained at 13.6 kHz as well as at 10.2 kHz. Although signal coverage predictions are not available at 13.6 kHz, nevertheless, it is instructive to examine SNR data at 13.6 kHz and to compare results at 13.6 with results at 10.2 kHz.

Appendix M presents plots of 13.6 kHz SNR statistics obtained from measurement at fixed monitor sites and aboard IOS vessels. Appendix M applies to the same circumstances and is in the same format as Appendix G except that Appendix M contains no prediction contours for modal interference.

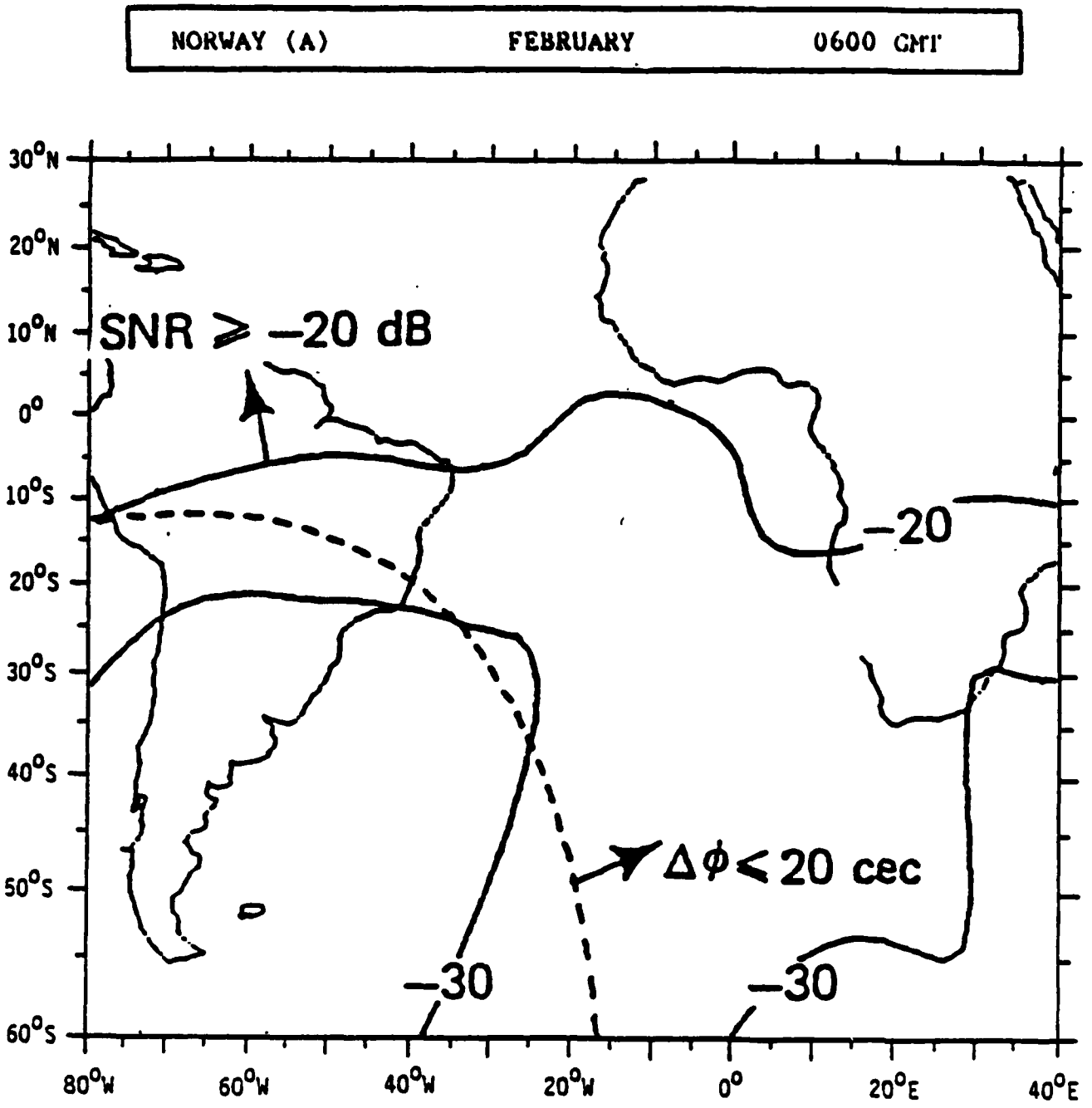

Figure 1-2. Example of Predicted Omega Signal Coverage Contours at 10.2 kHz.

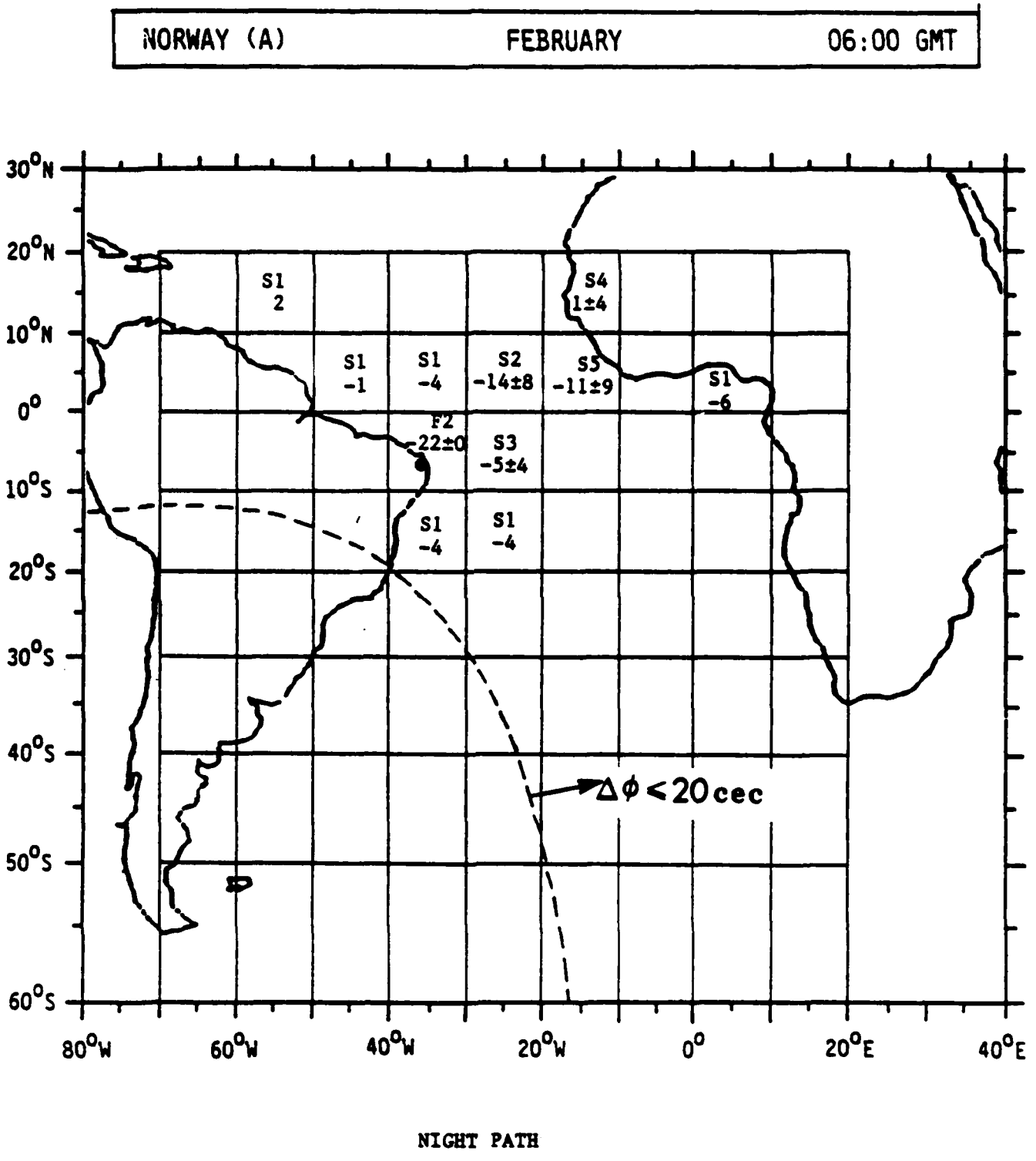

Figure 1-3. Example of Omega SNR Measurement Results.

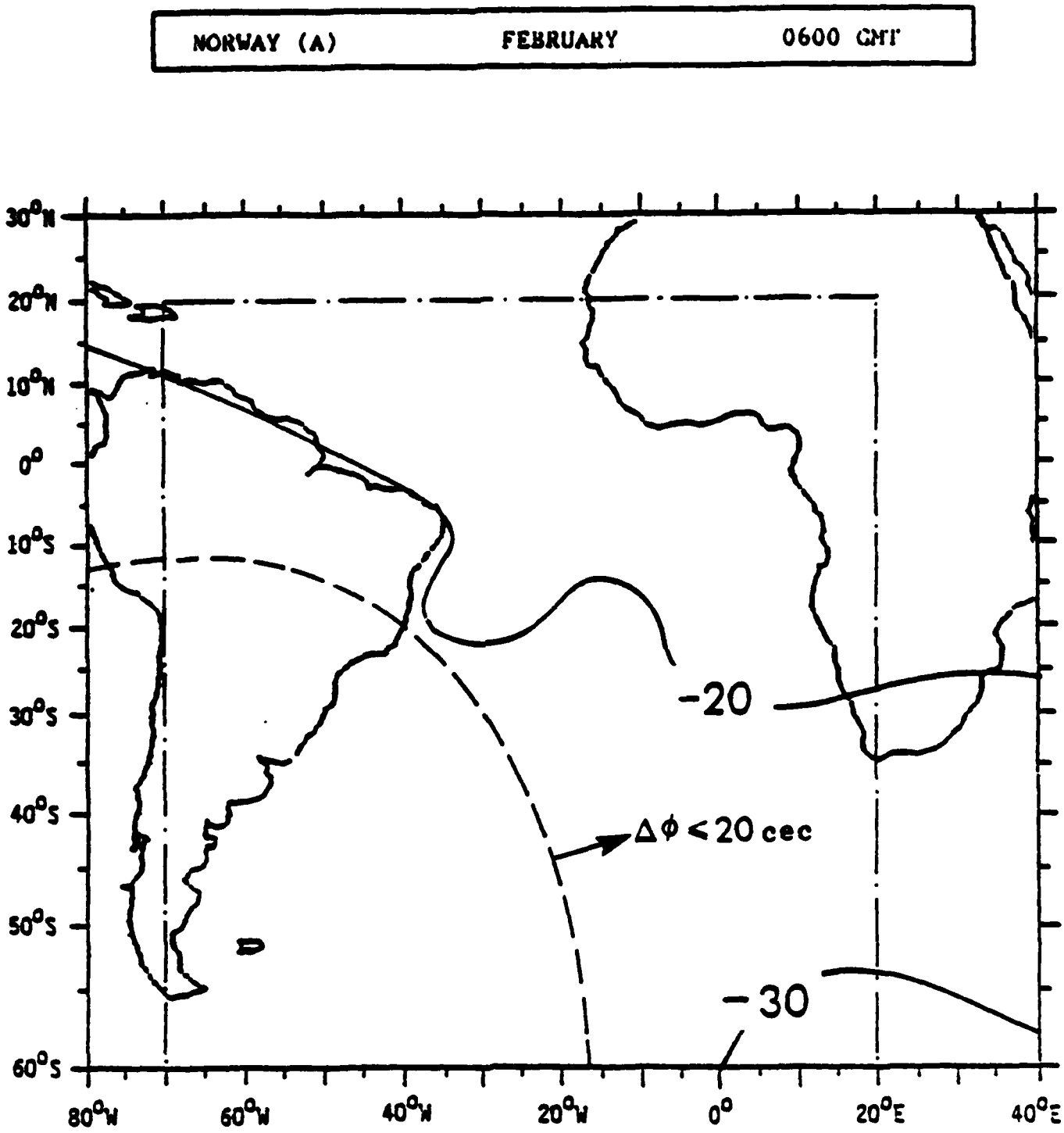

Figure 1-4. Example of Modified Omega Signal Coverage Contours at 10.2 kHz.

A comparison of the 10.2 kHz results shown in Appendix G and the 13.6 kHz results shown in Appendix M indicates a fairly good agreement in both the availability of signals and the SNR of signals at 10.2 kHz and 13.6 kHz. Although signal coverage predictions at 13.6 kHz have not been performed to date, when such predictions become available, the statistical results presented in Appendix M can be used to validate such predictions and to lead to modified coverage diagrams, just as in the case of 10.2 kHz.

1.4.3 Calculation Of GDOP

Geometrical Dilution of Precision (GDOP) is a useful predictor of fix accuracy. GDOP relates achievable fix accuracy for a particular circumstance to the accuracy that would be achievable for an ideal geometry. GDOP is based entirely on relative locations of Omega transmitters and a hypothetical receiver and is independent of phase measurement data.

A knowledge of predicted GDOP, as a function of receiver position, can be very useful to a navigator who is capable of measuring only LOPs, as it provides some guidance as to the best choice of LOPs to use to obtain a position fix.

GDOP is calculated according to a standard algorithm given in Appendix E. GDOP can be calculated for any receiver location and for any pair of LOPs, thus the possible number of GDOP calculations for the South Atlantic region could become prohibitively large unless some effort is made to limit the number of cases.

GDOP calculations are performed in the South Atlantic region according to the following criteria:

(1) GDOP clculations are performed at the center of each 10°x10° grid block defined in Section 3.3, thus 72 hypothetical receive locations are considered.

(2) GDOP calculations are performed for all possible pairs of LOPs, representing all transmitters. No effort is made to limit calculations based on SNR predictions or measurement data.

(3) For any three transmitters, three pairs of LOPs are possible, leading to three GDOP values. For this situation, all three GDOP values are calculated, but only the best, (smallest) GDOP is retained for presentation.

(4) Using four transmitters, three pairs of LOPs are possible, leading to three GDOP values. For this situation, all three GDOP values are calculated, but only the best, (smallest) GDOP is retained for presentation.

(5) GDOP values greater than 2 are rejected.

Appendix E presents the results of this GDOP analysis. Each grid block is associated with one set of calculations and the GDOP values are considered to be representative of the region represented by the grid block. Appendix E thus presents to a navigator anywhere in the South Atlantic region, achievable GDOP for any possible set of three or more transmitters, unless GDOP >2.

1.4.4 Diurnal Variations In LOP Error at 10.2 kHz and 13.6 kHz

Appendix I and Appendix N present diurnal plots of phase-difference errors at 10.2kHz and 13.6 kHz, respectively, measured at ONSOD fixed sites and recorded in Masterfile.

Phase-difference errors or LOP errors as they are also called, may be equated directly to errors in LOP-PPCs where a LOP-PPC is defined as composite propagation corrections applied to a phase difference measurement to yield a corrected LOP. Observed errors in LOP-PPCs provide valuable information regarding the accuracy of propagation corrections that are applied to Omega signals.

The plots in Appendix I and Appendix N provide information from fixed sites at Belem, Buenos Aires, Golfo Nuevo, Monrovia, Natal and Recife, and propagation paths from transmitters at Norway (A) Liberia (B), Hawaii (C), North Dakota (D), La Reunion (E), Argentina (F) and Japan (H), although not every possible combination of transmitters and receivers is represented. In the cases of the monitor at Monrovia receiving signals from Transmitter B, and the monitor at Golfo Nuevo receiving signals from Transmitter F, the proximity of transmitter and receiver means that propagation errors are negligible, hence LOP errors may be interpreted entirely in terms of propagation errors on the other path of the LOP. In these special cases, LOP-PPC errors may be interpreted directly as single-path propagation-correction errors.

In a number of cases, LOP error data are available for the same month during different years. No attempt has been made to combine data from more than one year into a single diurnal plot. Comparing diurnal behavior of LOP errors that represent different years can provide valuable insight into the relationship between propagation errors and solar cycle. At present, this relationship is poorly known, as it is virtually impossible to predict theoretically, and empirical relationships can only be deduced from comparisons of observations made during different parts of the solar cycle.

LOP Errors at 10.2 kHz and 13.6 kHz

Appendix J and Appendix O present maps of LOP error statistics for 10.2 kHz and 13.6 kHz, respectively, arranged by LOP, month and GMT. The statistics are based on measurements from ONSOD fixed monitor sites and from IOS-equipped vessels.

Results are quantized in 10^{o} latitude x 10^{o} longitude grid blocks. Within each grid block, LOP errors obtained from fixed monitors are described by a mean value and a standard deviation, and LOP errors obtained from IOS measurements are described by a mean value and a standard deviation.

Each map describes one LOP for one month (February, May, August or November) and one GMT (0600 or 1800). No attempt is made to distinguish between calendar years. Fixed monitor data correspond to specific months and specific times. However, it was pointed out in Section 4.5 that, in order to retain a reasonable sample size in the IOS data base, it has been necessary to establish finite time windows of 4 hours centered on the labeled times of 0600 GMT and 1800 GMT, and date windows of 3 months centered on the labeled months of February, May, August and November. The data windows thus include all 12 months and 8 hours of each day. This scheme accepts some smearing of results over times and over seasons in return for obtaining a meaningful sample size for each case. Table 1-1 presents an example of these results.

Table 1-1

EXAMPLE OF LOP ERRORS IN CENTI-CYCLES AT 10.2 KHz

FEBRUARY

LOP: AB

MAP GRID	0600 GMT			1800 GMT		
	NUMBER OF POINTS	MEAN ERROR	STANDARD DEVIATION	NUMBER OF POINTS	MEAN ERROR	STANDARD DEVIATION
16	4	8	12	5	9	3
26	4	18	23			
35	1	8	0	8	18	4
25	2	26	9	1	27	0
44				4	1	3
45				3	8	0
53	11	-8	42	8	4	7
54	1	-5	0			

1.4.5 Fix Errors at 10.2 kHz and 13.6 kHz

Fix errors are calculated by comparing an Omega fix with a reference position. In the case of IOS fixes, the reference position of the platform is usually the position determined from a transit fix.

The data base for analysis of fix errors is taken entirely from IOS measurements. Each IOS measurement in the data base represents a transit fix along with phase measurements, at both 10.2 kHz and 13.6 kHz, from several stations. Since any combination of 3 stations yields a potential fix, it follows that several Omega fixes can be associated with a single IOS measurement. In a situation where more than one Omega fix, at either 10.2 KHz or 13.6 kHz, is available for a particular IOS measurement, the procedure followed in this study is to discard all fixes but the "best" fix, where the best fix is defined as that fix having the smallest error magnitude. Omega fixes are calculated separately at 10.2 kHz and 13.6 kHz, thus for any IOS measurement, a best fix at 10.2 kHz and a best fix at 13.6 kHz are obtained. At each of the frequencies 10.2 kHz and 13.6 kHz, a best fix yields a fix error; this fix error is considered to be the smallest fix error achievable under the circumstances, and is entered into the fix error data base.

Fix errors are calculated, for 10.2 kHz and for 13.6 kHz, at 0600 GMT and at 1800 GMT, and for the months of February, May, August and November. As in the LOP error analysis, IOS data are used that fall within time windows of 4 hours centered on the times 0600 GMT, and that fall within 3 month windows centered on the validation months of February, May, August and November. These rather wide windows of data accessability cause some diurnal and seasonal smearing of results, but result in much larger statistical samples than would otherwise be possible. Appendix K presents fix error results obtained at 10.2 kHz and Appendix P presents fix error results obtained at 13.6 kHz. Table 1-2 presents an example of these results.

1.4.6 Modal Interference at 10.2 kHz and 13.6 kHz

One of the experiments performed by NOSC was a series of aircraft flights along approximate radials for several transmitters. During each flight, signal amplitudes were monitored from several transmitters.

Table 1-2

EXAMPLE OF FIX ERRORS IN NAUTICAL MILES

FEBRUARY, 0600 GMT

MAP GRID	NORTH ERROR			EAST ERROR		
	NUMBER OF POINTS	MEAN ERROR	STANDARD DEVIATION	NUMBER OF POINTS	MEAN ERROR	STANDARD DEVIATION
11	4	0.5	2.4	4	1.0	2.9
12	3	-7	1	3	1.4	0.2
16	21	-2.0	0.6	21	-0.1	1.1
23	5	1.6	7	5	3.3	3.6
24	4	-2.8	1.2	4	-0.9	1.7
25	8	-1.7	1.8	8	-1.2	1.9
26	10	0	1.6	10	0.0	1.4
34	2	-2.5	2.4	2	-1.2	1.7
35	12	0.0	3.5	12	-1.2	2.9
44	4	-3.7	1.7	4	-6.2	2.3
45	1	-0.9	0	1	-2.4	0.0
53	22	-0.8	1.1	22	-1.9	2.7
54	1	-0.3	0.0	1	-3.5	0.0

The presence of higher-order propagation modes gives rise to both amplitude and phase fluctuation of the Omega signal with distance along a radial. Phase fluctuations resulting in modal interference are a direct cause of navigational errors for Omega. Amplitude fluctuations, while not affecting accuracy directly, indicate the presence of higher-order modes and modal interference.

Analysis of NOSC airborne amplitude measurements is based on results presented in References 21 and 22. Since the conclusions being sought are transmitter specific, it is convenient to arrange the measurements according to Omega transmitters rather than by flight.

Figure 1-5 illustrates radials for Omega Norway in the South Atlantic, along with flight tracks for the various NOSC flights receiving Norway signals during the Omega experiments. It can be seen that each flight can be associated with one or more specific radials from Norway.

Figure 1-6 presents an overlay of theoretical 10.2 kHz signal amplitude profiles for Norway along selected radials, and measured 10.2 kHz signal strength profiles for Norway obtained during Flights 1B, 2, and 3.

Figures 1-5 and 1-6 are duplications of Figures L-1 and L-2 (Appendix L) and are presented here to provide an example of the approach that is used to analyze the NOSC airborne test data. Appendix L presents the available results for all Omega transmitters at 10.2 kHz, and Appendix Q presents analogous results at 13.6 kHz.

1.5 CONCLUSIONS AND RECOMMENDATIONS

The conclusions to be drawn from any study should include the following elements:

(1) answers to questions explicitly or implicitly posed at the beginning of the study;

(2) a description of significant results that were not expected and were not the basis of inquiry at the beginning of the study

(3) comments on the parameters of the study itself, as opposed to the results obtained; typical parameters might include methodology of the study, data breadth and quality, etc.

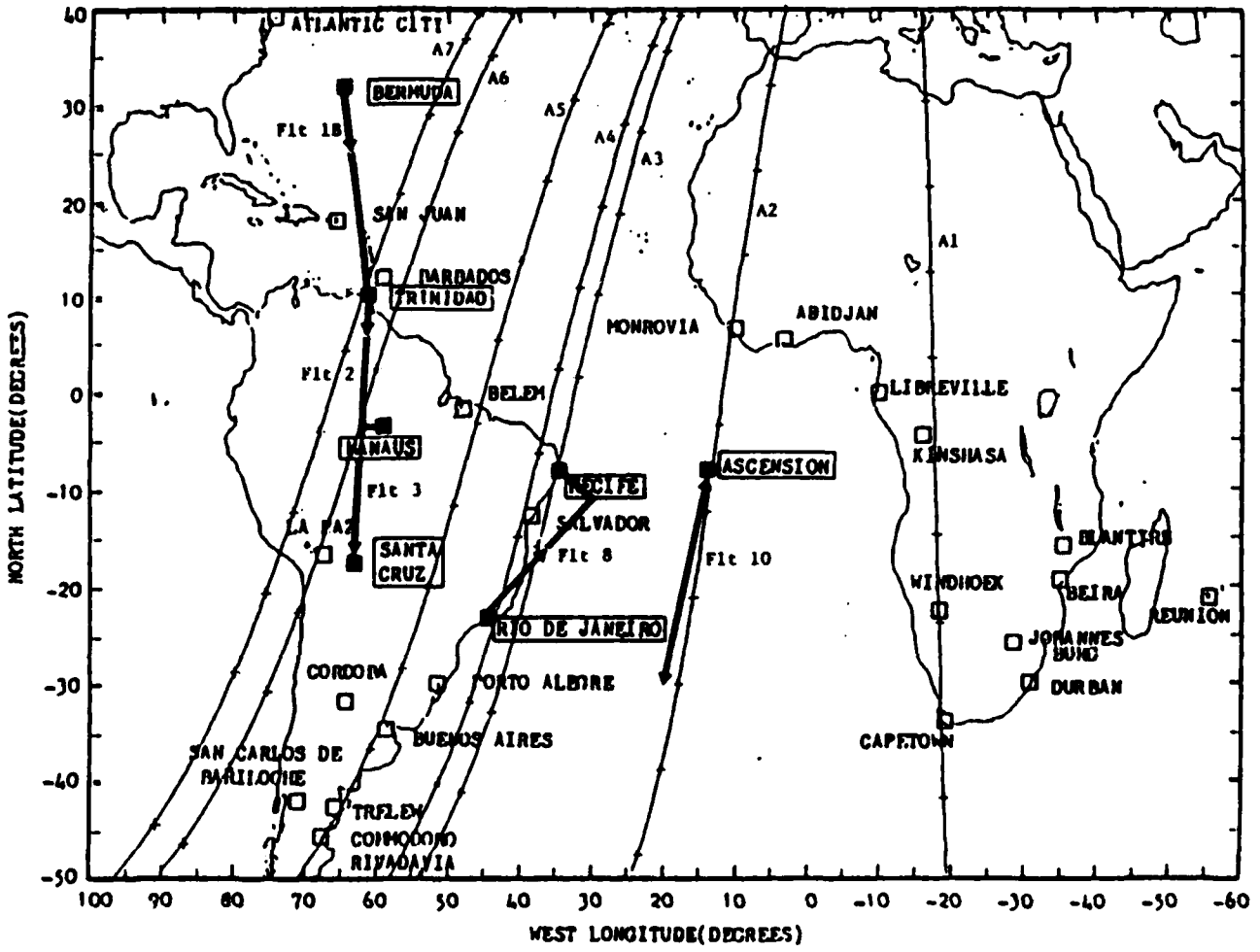

Figure 1-5. Azimuths for predicted radials from Omega Norway and ground tracks for NOSC test flights.

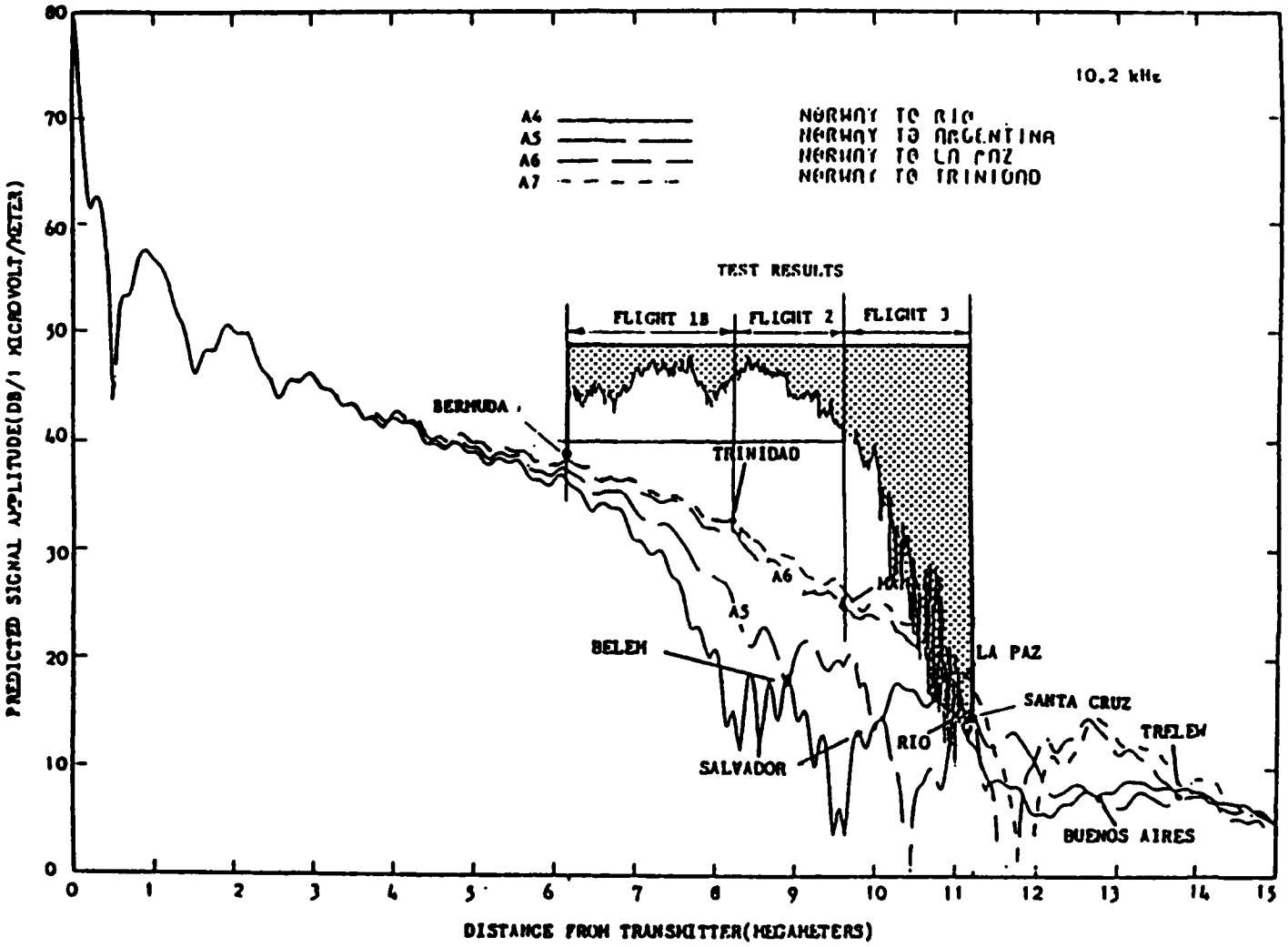

Figure 1-6. Predicted nighttime signal amplitudes at 10.2 kHz as functions of distance from an assumed 1-KW transmitter at Norway along selected radials, and observed signal amplitudes as functions of distance from Norway during Flights 1B, 2 and 3 (References 21 and 22).

In drawing conclusions from this study, not only should one address the above elements, but one must also make a decision, or series of decisions about tradeoffs between generality and specificity of the conclusions. These tradeoffs are properly determined according to the audience one is attempting to reach.

In this study, it is assumed that the two most important criteria determining this efficacy are signal coverage and available accuracy. Other possible criteria, such as reliability, power consumption, and user cost, have not been addressed in this study.

Available accuracy is, of course, strongly dependent on the sophistication of a user's receiver. In this study, available accuracy has been characterized according to two levels of receiver sophistication. Specifically, accuracy assessments have been performed for (a) a hypothetical receiver providing single-frequency LOP's and (b) a hypothetical automatic receiver that makes optimal use, in a least squares sense, of all available Omega signals. It is doubtful that even a sophisticated Omega receiver can interpret, in real time, the effects of transient propagation phenomena such as SIDs and PCAs. These phenomena are not predictable, are unavoidable, and cause significant degradation in navigation performance of a users receiver. In this study, attainable accuracy assumes that SIDs and PCAs are absent; that is, accuracy estimates are based on data from which all known SIDs and PCAs have been removed.

Omega Signal Coverage

Omega signal coverage at 10.2 kHz in the South Atlantic is presented in Appendix H. The results of this study indicate that Omega signal coverage in the South Atlantic is somewhat better than had been predicted by the TASC study. The results are conservative in the sense that the eventual presence of a transmitter in Australia can only improve coverage, although the TASC predictions indicate that expected coverage from Station G should be quite poor in the South Atlantic.

There is no comprehensive prediction of Omega signal coverage at 13.6 kHz in the South Atlantic. A comparison of measured results at 13.6 kHz (Appendix M) with measured results at 10.2 kHz (Appendix G) suggests that, broadly

speaking, signal coverage at 13.6 kHz is comparable to signal coverage at 10.2 kHz, although large variations exist in particular cases.

Measurement results are quite sparse in the southern part of the South Atlantic, except near the coasts of Africa and South America, and the quality of predictions is lower in those areas without confirming measurements.

The modified predictions resulting from this study suggest that Omega signal coverage, in terms of adequate SNR and freedom from excessive modal interference, should be reasonably good during most times and seasons in the entire South Atlantic from at least three of the Omega stations B, C, D and E.

LOP Errors

LOP errors have been considered in two way in this study. First, LOP mean errors obtained at ONSOD monitor sites have been determined on a diurnal basis for specific years and for the possible months of February, May, August and November. The results have been presented in Appendix I for 10.2 kHz and in Appendix N for 13.6 kHz. No further analysis of the results in Appendixes I and N have been performed, as any further analysis would be beyond the scope of this study. However, the results as presented provide potentially valuable input to any study designed to improve the PPC model presently used by ONSOD.

The second consideration of LOP errors has been a statistical analysis of LOP errors at 0600 GMT and 1800 GMT for the months of February, May, August* and November. This analysis has used data from IOS vessels, and has averaged measurements over more than one year. Appendix J presents LOP error statistics at 10.2 kHz, and Appendix O presents LOP error statistics at 13.6 kHz.

Apparent accuracies of LOP measurements in the South Atlantic are moderately good. Within the circumstances actually measured, median LOP errors are typically about 15 cecs, and 90% of the observed mean errors are less than 25 cecs.

The results shown in Appendixes J and O suggest that fix accuracies better than ± 2 NM are regularly achievable in the South Atlantic. A caveat to this conclusion is that little or no data are available for the southern part

*No August data were available.

of the region where theoretical predictions of SNR indicate poorer signal quality than in the northern part of the region where most of the data were taken.

Fix Errors

Fix errors have been estimated entirely from the IOS data. The IOS data file supplied by ONSOD provides, at each location and at each of the frequencies 10.2 kHz and 13.6 kHz, fix errors for a number of Omega fixes, where the various fixes are obtained using various combinations of available LOPs. Out of each set of fixes obtained at one location using one frequency, one "best" fix is obtained, in the sense of having the smallest total error. Fix errors associated with the best fix characterize the Omega fix accuracy that is attainable under the circumstances for the IOS operation.

Attainable fix accuracies, described in terms of northern and eastern components, are estimated by averaging individual results. Appendix K presents attainable fix accuracies for 10.2 kHz and Appendix P presents attainable fix accuracies for 13.6 kHz.

As in all other data analyses, conclusions for situations where no data exist must be drawn cautiously. Nevertheless, the results presented in Appendix K and Appendix O indicate that attainable Omega accuracy in the South Atlantic is characterized by a median error of about $\pm$ 1 NM and that 90 of all fixes should have errors less than $\pm$ 2 NM. Accuracies in the southern part of the South Atlantic may be somewhat worse than these estimates because of the predicted diminishment of signal quality in the southern part of the region.

Modal Interference

Modal interference, caused by the presence of higher-order propagation modes, gives rise both to amplitude fluctuations and to phase fluctuations as functions of range along a propagation path. Amplitude fluctuations thus indicate the presence of modal interference.

The results obtained from Norway show substantial, although not complete, agreement between observed and predicted signal amplitude effects due to modal

interference. If anything, the observed effects indicate slightly more severe modal interference at 10.2 kHz than has been predicted in the South Atlantic, and also indicate comparable modal interference at 10.2 kHz and 13.6 kHz.

The results obtained from Liberia confirm the predictions of strong modal interference effects, at least along radials to the southwest of Liberia. Observed and predicted effects were consistent in all cases, at both 10.2 kHz and 13.6 kHz.

The results obtained from La Reunion confirm the predictions of moderate to weak modal interference effects in the South Atlantic. Observed and predicted effects were consistent in all cases, at both 10.2 kHz and 13.6 kHz.

The results obtained from Argentina suggest that, while modal interference is present out to ranges of 5 to 7 megameters, the severity of the modal interference may be less than predicted at 10.2 kHz. At 13.6 kHz, on the other hand, modal interference may be somewhat more severe than predicted out to ranges exceeding 8 megameters.

Recommendations

The most serious limitation on the results of this study has been the lack of measurement data over large sections of the South Atlantic Region. This limitation was recognized early in the study. In order to provide for an augmentation of the results should additional data become available at a later time, the analysis results have been quantized into small geographical areas, and presented in this form in the various appendixes. The results have thus been preserved at a fairly detailed level for ease of augmentaiton.

It is recommended that some effort be made to collect more IOS data in geographical areas of the South Atlantic that are presently under-represented. Additional data should include measurements of Station G, in Australia, so that benefits of the Australia signal can be evaluated, especially in the southern part of the South Atlantic Region.

II. BACKGROUND AND PROBLEM STATEMENT

2.1 INTRODUCTION AND OBJECTIVES

This is the fourth in a series of regional validations of the Omega navigation system conducted for the U.S. Coast Guard's Omega Navigation System Operations Detail (ONSOD), previous studies having addressed the Western Pacific [1-4], the North Atlantic [5], and the North Pacific [6]. Subsequent efforts will address the Indian Ocean and the South Pacific [7, 8].

A regional validation of Omega is a procedure for determining the efficacy of Omega as a navigational aid in a specific region of the earth. This proposition is simply stated, but its logical extension into a concrete program of measurement, analysis and conclusion is complicated by several factors. First of all, one must decide what one means by "efficacy as a navigation aid." Efficacy--the power to produce a desired effect--can be taken to mean the power to produce good navigation. In its most general sense, navigation can involve the determination of any or all dimensions of a seven-dimensional state vector that includes position, velocity and time. "Good" can mean a large number of state vector dimensions, or great precision associated with one or two dimensions, or promptness of information, or ready availability of new information, or many other indications of quality. The mission of Omega, for our purposes, is limited to providing two-dimensional (horizontal) position information, worldwide, to appropriately-equipped users. Although Omega has an intrinsic capability to provide time transfer and user horizontal velocity (through differentiation of user position), and may also have some utility as a tool for studying radiowave propagation, the validation described herein is limited to consideration of the Omega mission just described.

A second factor to be considered is the Omega user. The Omega user may be anyone from a commercial aircraft or oil tanker with sophisticated equipment and redundant navigation systems all the way to a small sailboat. The commercial user is likely to be interested in following a route that maximizes fuel savings, while the sailboat user is likely to emphasize low

equipment cost and low power drain. Intuitively, it seems that a user with sophisticated equipment can derive more benefit, in a navigational sense, than can a user with a low-cost, simple receiver. There is an obvious difference between these two classes of users in the efficacy of Omega as a navigation aid. A validation program must be cognizant of the class, or classes, of users to which the validation is addressed.

A third factor to be considered in an Omega validation is the type of data base to be used. It is well known that a comprehensive description of any system depending on ionospheric propagation of radio waves must be based fundamentally on measurements and measurement data, and Omega is no exception to this rule. The choice of parameters to be measured and analyzed is obviated to a large extent by the simple expedient of using navigational receivers to obtain test data. The quantities that are available from a navigational receiver being used for acquisition of validation data are the same quantities that are intrinsic to the navigation function. The fundamental quantities associated with any Omega navigation problem involving a transmitter, a receiver and an operating frequency are signal strength (or signal-to-noise ratio, SNR) and signal phase (or phase difference between two signals at a common frequency). The data base used for Omega validations consists of SNR and phase difference measurements obtained over a range of locations, diurnal conditions and seasons.

A fourth factor, and an extremely important one, is the limited quantity of available measurement data and the limited spectrum of measurement conditions, in comparison with the range of spatial, temporal and geophysical circumstances contemplated by a single regional validation of Omega. One discrepancy between available data and validation requirements that is especially acute for the present validation lies in the fact that, with the single exception of Ascension Island, no fixed-site measurements are available for the interior of the validation region; that is, except for Ascension Island, the fixed-site measurements to be used for a validation of Omega navigation <u>within</u> the South Atlantic region are available only around the <u>boundaries</u> of the South Atlantic region. In general for all regional validations, and in particular for the South Atlantic validation, a useful

product from the validation effort requires a good deal of thoughtfulness in extrapolating data obtained under certain conditions to other conditions for which little or no data are available.

This observation in no way implies a criticism either of the goals of the Omega validation program or of the measurement program. Navigators will journey through the South Atlantic with good navigation or poor navigation; it is a worthwhile endeavor to provide navigators with a realistic assessment of the value that should be placed on Omega as a navigational aid. On the other hand, the resources that would be required to provide a data base that is "adequate" in some rigid sense, would be prohibitive. The challenge, then, is to perform a validation that will be utile to users and planners, based on a limited quantity and distribution of data and sound engineering judgment.

One of the more important criteria of Omega performance is known as available accuracy. The meaning of this term is not immediately apparent, nor is its applicability, inasmuch as the accuracy of Omega navigation depends not only on geophysical variables but on the sophistication of both the users' receiver and the propagation-prediction corrections (PPCs) that are available to the user. A user can provide its own PPCs if it has the motivation and resources to do so, or it can use PPCs that are provided by ONSOD [9-11]. In this report, the available accuracy of Omega navigation will assume the use of existing ONSOD - supplied PPCs. These PPCs, which will also be evaluated during this study, are subject to continuing improvement as the propagation of Omega signals becomes better understood. Improved PPCs will lead to improvements in available accuracy. Although we cannot speculate today on the future effectiveness of PPCs, we can evaluate, according to some simple criteria, the effectiveness of PPCs that are presently supplied by ONSOD.

Available accuracy is, of course, strongly dependent on the sophistication of a user's receiver. In this study, available accuracy will be characterized according to two levels of receiver sophistication. Specifically, accuracy assessments will be performed for (a) a hypothetical receiver providing single-frequency LOP's, and (b) a hypothetical automatic receiver that makes optimal use, in a least squares sense, of all available Omega signals. It is doubtful that even a sophisticated Omega receiver can interpret, in real time, the effects of transient propagation phenomena such

as SIDs and PCAs. These phenomena are not predictable, are unavoidable, and cause significant degradation in navigation performance of a users receiver. In this study, attainable accuracy assumes that SIDs and PCAs are absent; that is, accuracy estimates are based on data from which all known SIDs and PCAs have been removed.

In addition to its primary objective of determining available accuracy, this study will address a comparison of the attainable fix accuracies with user navigation requirements and system design objectives, and an evaluation of the effectiveness of the ONSOD propagation phase corrections (PPC's) in the South Atlantic.

The South Atlantic region of interest, for purposes of Omega validation, is bounded by 20^{o}E and 70^{o}W longitude, 20^{o}N and 60^{o}S latitude, and includes an area of about 35 million square miles. Available Omega measurement data are not uniformly distributed over the region of interest as noted earlier. In the southern (30^{o} - 60^{o}S latitude) oceanic areas especially, Omega phase data are quite sparse. Accordingly, Omega validation of the entire South Atlantic region will require considerable extrapolation of measurement data, and the application of sound engineering judgement.

2.2 DESCRIPTION AND STATUS OF THE OMEGA SYSTEM

The Omega navigation system was initially conceived by the U.S. Navy to meet general navigation needs on a worldwide basis. In the early stages (pre-1966), the program was handled largely under the auspices of the research and development elements of the Navy, notably the Naval Electronics Laboratory in San Diego, California, which designed, developed and tested the prototype transmitting equipment. Successful testing of a four-station experimental 1-KW chain in the mid-1960's validated the feasibility of a full-power, world-wide network. In 1966, a special office, the Omega Project Office, now known as PME-119, was established within the Navy as the DOD Executive Agent for implementing the full system. Form the outset, however, the permanent Omega system was to be built and operated under very different ground rules from similar hyperbolic systems such as Loran [12]. Today, seven permanent stations are on the air at full power and construction of an eighth station in Australia is under way with an estimated operational date of mid 1982.

Recognizing the international nature and long-term benefits to the non-military community, the DOD authorized the permanent system on the basis that the nations hosting the transmitting facilities would share in the management responsibilities and, where possible, assist financially. To this end, the Navy and State Department successfully negotiated agreements with Japan, Norway, Liberia, France, Argentina, and most recently, with Australia, wherein the host nations provide land and varying levels of resources to build, operate, and maintain the transmitting stations [12, 13].

Within the U.S. government, responsibility for the operation and maintenance of the international Omega Navigation System transferred, in June 1978, from the U.S. Navy to the U.S. Coast Guard. ONSOD will continue to manage the technical efforts of system engineering, daily operations, and navigational matters. However, the overall direction of ONSOD within the U.S. government will be the responsibility of the Commandant, U.S. Coast Guard, rather than the U.S. Navy Omega Project Office (PME-119).

The U.S. Navy will retain the U.S. responsibilities for the completion of the last transmitting station in Australia. The U.S. Coast Guard will assume the U.S. support commitments towards this station upon operational status [14].

The Omega system has been in a state of continuous evolution since 1966, when four developmental cesium-controlled transmitting stations first began operations on a 24-hour schedule. Over the subsequent years, stations have been added and deleted, new frequencies have been implemented in the signal format, propagation phase corrections (PPC's) have been improved, techniques of station synchronization have matured, and receiver technology has progressed from the early manual single-frequency units to the microprocessor-controlled automatic multifrequency receivers of today. It is therefore very important to define clearly the various elements of the Omega "system" whose performance is to be assessed. As a general guideline, the goal is to characterize conservatively the performance of the Omega system as it will be in 1985 when it is declared fully operational at the completion of the regional validation program.

2.2.1 Transmitter Network

The operational Omega system will contain the transmitter network listed in Table 2-1. The Australia Station "G" was not completed in time for this study, and is not expected to become operational before mid-1982. A temporary Omega station at Trinidad transmitted in the "G" time slot until December 1980 when it was decommissioned. In all Omega measurements to date, G-data refer, by definition, to Trinidad. Prospective users of operational Omega will, of course, be interested in the Omega system that includes Australia but not Trinidad. This study will ignore the Trinidad G measurements in the data base and will estimate the prospective performance of the operational system that includes Australia but not Trinidad. The methodology of this approach is discussed in Section III.

2.2.2 Signal Frequencies and Receiver Timing

Each of the four frequencies (10.2, 11.05, 11 1/3 and 13.6 kHz) shared among all stations are given equal weight in the Omega signal format shown in Figure 2-1. Although traditionally the 10.2 kHz signal has been viewed as the "primary" Omega frequency, the trend in design of modern sophisticated receivers has been to utilize all of the shared frequencies for navigation, thereby exploiting the gains in position fixing accuracy which accrue from such redundancy.

2.3 OMEGA MONITOR NETWORK

A world-wide network of land-based fixed Omega monitors is maintained by ONSOD. The primary function of the network is to acquire Omega phase data over a sufficiently broad range of diurnal and seasonal conditions to support efforts to confirm and, if necessary, upgrade propagation phase corrections (PPC's) and the underlying models from which they are derived. Analysis of such phase data also provides assessments of signal coverage, modal interference, phase stability and other signal characteristics required for system calibration and validation in the geographical area served by the monitor.

TABLE 2-1

OMEGA TRANSMITTING STATIONS

STATION LETTER DESIG.	SITE[4]	LATITUDE/LONGITUDE[1]	OPERATING AGENCY
A	Aldra, Norway	66.4202°N/13.1368°E	Norwegian Telecommunications Administration
B	Monrovia, Liberia	6.3053°N/10.6646°W	Liberian Ministry of Commerce, Industry and Transportation[2]
C	Haiku, Oahu I, Hawaii	21.4047°N/157.8310°W	U.S. Coast Guard
D	La Moure, North Dakota	46.3659°N/98.3358°W	U.S. Coast Guard
E	La Reunion I, Indian Ocean	20.9742°S/55.2897°E	French Navy
F	Golfo Nuevo, Argentina	43.0536°S/65.1909°W	Argentine Navy
G	Woodside, Australia[3]	38.4813°S/146.9351°E	Australian Dept. of Transportation
H	Tsushima, Japan	34.6147°N/129.4535°E	Japanese Maritime Safety Agency

Notes:

1. Transmitter Position Datum: World Geodetic System 1972 (WGS-72)

2. Station B, Liberia, is jointly operated by Liberian personnel and a U.S. contractor.

3. A temporary station at Trinidad (10.6995°N/61.6383°W) transmitted in the G station segment until December 1980 when it was decommissioned. The Australia station is expected to be operational in 1982.

4. Stations A and D have been on-the-air since 1972-3, stations B,C,E,F and H since 1975-6.

Since the inception of the monitoring program in 1966, the network has been systematically expanded to keep pace with the addition of new transmitters and the progress of Omega towards full implementation. The majority of sites are instrumented with a Magnavox MX-1104 receiver which outputs one-way phase (relative to an internal quartz oscillator) and a measure of SNR for three of the four common Omega frequencies (10.2, 11 1/3, 13.6 kHz) on a once-per-hour basis to a digital data logging device. Data are logged for a full month on a digital cassette which is then sent to ONSOD for processing. Since the receivers are generally not equipped with precision time standards, one-way phase measurements are not directly useful and must be combined into station- pair phase differences to remove effects of timing errors.

In the South Atlantic validation effort, the eight monitor sites listed in Table 2-2 and shown in Figure 2-2 were chosen for use.

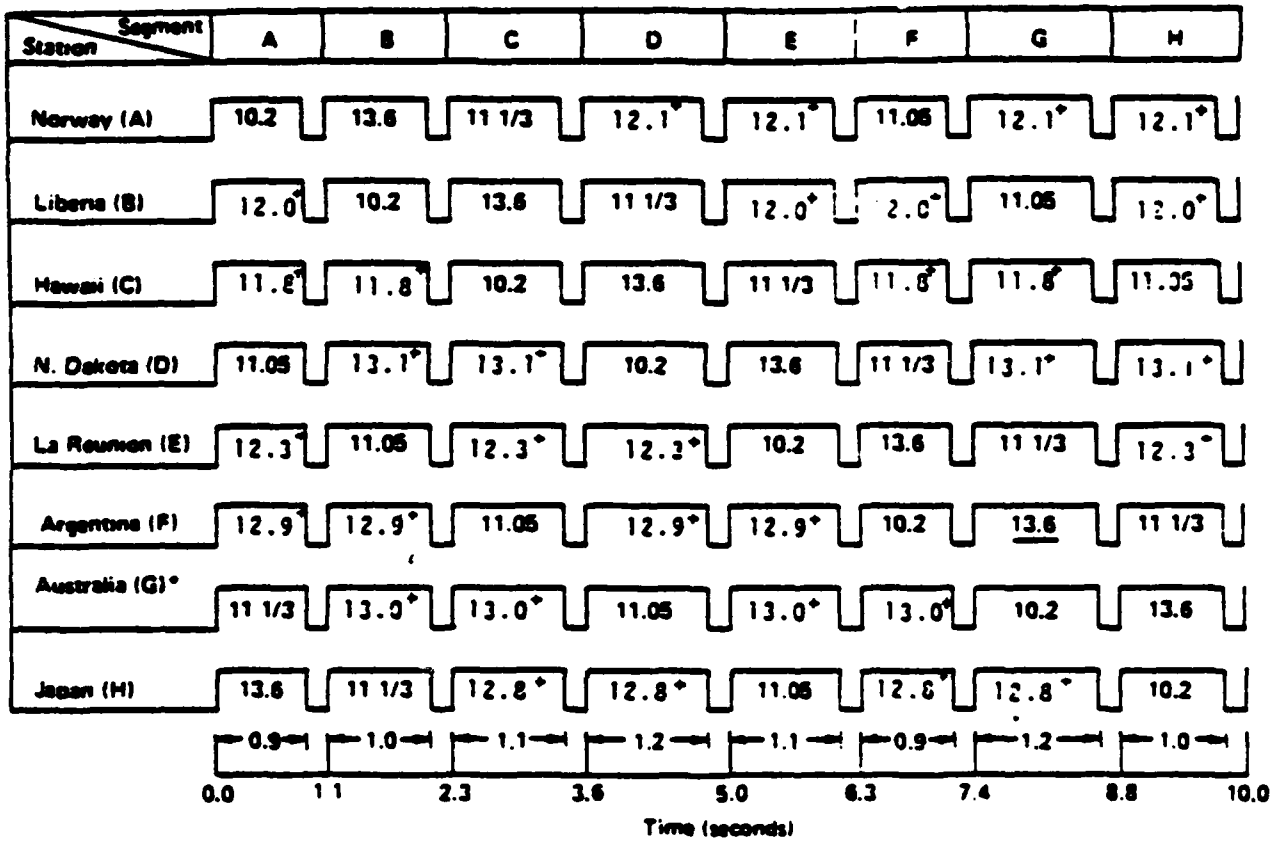

* Signal "G" was transmitted from Trinidad until December 1980. Australia "G" is expected to begin operation in mid-1982.

Figure 2-1
Omega Signal Transmission Format

Table 2-2

SOUTH ATLANTIC ONSOD SITES

SITE	LATITUDE	LONGITUDE
1. Belem, Brazil	1.39159 S	48.44497 W
2. Monrovia, Liberia	6.42627 N	10.81398 W
3. Recife, Brazil	8.07971 S	34.89603 W
4. Rio de Janeiro, Brazil	22.87175 S	43.13303 W
5. Natal, Brazil	5.92785 S	35.16464 W
6. Buenos Aires, Argentina	34.62199 S	58.35512 W
7. Golfo Nuevo, Argentina	43.22392 S	65.27159 W
8. Ascension Island, U.K.	7.95492 S	14.32682 W

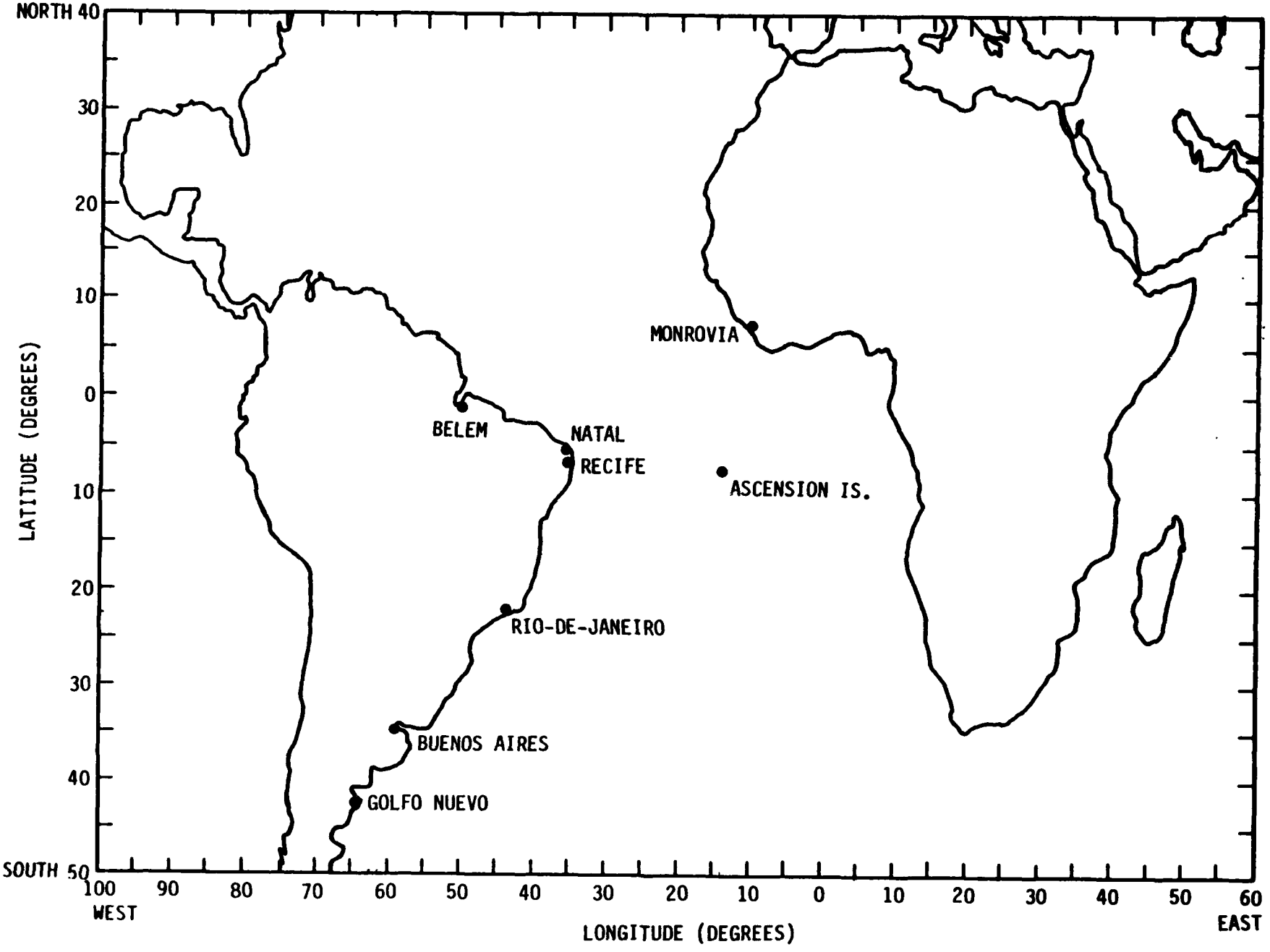

Figure 2-2 South Atlantic GNSOD Sites

III. METHODOLOGY OF APPROACH

3.1 OVERVIEW

The South Atlantic Omega Validation involves two main lines of inquiry. The first line of inquiry considers the availability of Omega signals, in the sense of having a sufficient SNR to be heard and to be free of modal interference. The second line of inquiry deals with the accuracies of position fixes that can be achieved with the available signals. Fix accuracies are fundamentally dependent on three factors; the fidelity of the phase information contained in each Omega signal, the geometrical relationships between pairs of LOPs, and the availability and accuracy of propagation prediction corrections (PPCs).

Omega signals are transmitted in the VLF band, where propagation can be modeled as being in a waveguide formed by the earth's surface and the lower boundary of the ionosphere. Spatial variation in the earth's-surface electrical characteristics, primarily surface conductivity, affect the waveguide propagation. In addition, the morphology of the ionosphere is subject to changes due to variations in solar illumination caused both by the earth's rotation and by solar disturbances. These ionospheric changes cause time variations in the phase and amplitude of Omega signals at various locations in the coverage regions [9-11].

Another characteristic of Omega signal propagation is signal attenuation due to geometric spreading. As the distance between receiver and transmitter increases, the received signal becomes weaker. This lowering in signal strength makes phase measurements of the Omega signal progressively less accurate and more difficult, until ultimately, the Omega signals are not measurable.

A third characteristic of Omega signals is modal interference. In the waveguide of the earth's surface and the ionosphere, various propogation modes are excited by the transmitter. These modes travel at different speeds. Additionally, higher order modes can be converted to lower order modes at day/night transitions. At the receiver, the various modes are not separable, and can cause unacceptable distortion in phase and amplitude of the received

signal. Modal interference is particularly noticeable on westerly propagation paths, as the interaction of the earth's magnetic field and free-charged particles in the ionosphere favors high-order mode propagation (15, 16].

Analytical models can be and have been developed that simulate the behavior and noise phenomena of VLF signals as they propagate though their unique waveguide. With these models, it is possible to generate predictions of likely Omega signal coverage. Not all of the phenomena discussed above are predictable. For example, the diurnal effects are predictable, but the solar disturbance effects, such as sudden phase anomaly and polar cap disturbances are not predictable. Smaller regular changes resulting from solar zenith angle variations, which vary with the season of the year and the latitude of the receiver position, are also predictable to a reasonable degree of accuracy. Although precise parameters for all individual propagation modes have not been quantified, it is possible to predict those regions where acceptable phase and amplitude are likely to be observed with parameters that are available [9, 17, 18].

Knowledge of the time history of recorded monitor data (obtained from the measurements data base) and the availability of prediction data provides the necessary information to evaluate the effects of any anomalous ionospheric events. Any gross discrepancies between the two data sets can be identified and the corresponding date and time of day noted. By means of the National Geographic and Solar-Terrestrial Data Center reports, it is possible to verify these ionospheric occurrences [19, 20].

3.2 AREAS OF STUDY

This validation effort pursues five areas of analysis; (1) signal coverage, (2) GDOP, (3) PPC error, (4) LOP error statistics and (5) Fix error statistics. Except for GDOP, all analyses are performed at the two major Omega frequencies of 10.2 kHz and 13.6 kHz.

Signal coverage is analyzed in the South Atlantic from measurement data of SNR from both fixed and moving platforms. Measurement results at 10.2 kHz are compared with coverage predictions at 10.2 kHz, and the coverage predictions are modified in accordance with the measurement results.

GDOP, or geometrical dilution of precision, is derived as a mathematical function of the relative locations of a hypothetical receiver and all the Omega transmitters. GDOP predicts the effect of LOP crossing angles on fix error and thus provides guidance to a user who calculates position fixes from separate LOP measurements.

PPC error can be studied by observing the diurnal behavior of LOP errors at fixed sites such as ONSOD monitors. Perfect PPCs would provide zero LOP error over all times and locations, thus a study of observed LOP errors can lead to improved PPCs.

In contrast to diurnal mean LOP errors which, in principle, are correctable by improved PPCs, random errors in LOPs observed at similar times and locations leads to an understanding of inherent limits in Omega accuracy, which errors must be described statistically. In addition, a comparison of random errors between different LOPs provides some guidance to a potential user as to the best choice of LOPs as a function of time and position.

Fix errors represent an accumulation of PPC errors, phase measurement errors, and GDOP. Fix errors define navigational accuracy and, along with signal coverage, represent the most important criteria of the efficacy of Omega.

3.3 DATA QUANTIZATION

The present validation makes extensive use of measurement data from maritime vessels equipped with integrated Omega-satellite (IOS) receivers. The IOS data provide greatly-needed spatial diversity to the data base, but because IOS fix measurements are not uniformly distributed across the South Atlantic region, it has been found useful to establish a method for quantizing the spatial dimensions of the South Atlantic region.

The spatial correlation to be expected between Omega measurements in the South Atlantic is likely to be fairly high over distances of several hundreds of miles, especially in oceanic areas. Furthermore, the spatial resolution intrinsic to the theoretical signal-coverage predictions is not great since the theoretical calculations were performed along radials from each transmitter that are displaced 15 degrees azimuth intervals.

Accordingly, it seems quite reasonable to limit the spatial detail of the SNR and phase data analysis. The approach followed here has been to divide the South Atlantic region onto a grid of rectangular spaces defined by latitude boundaries at 10^{o} intervals and longitude boundaries at 10^{o} intervals. The South Atlantic region of 20^{o} N to 60^{o} S and 70^{o} W to 20^{o} E is then divided into 72 rectangular areas. Within each given area, all available fixed-monitor data for a given circumstance (transmitter, month, GMT) can be combined to yield a single set of statistics. Within each area, all available IOS data for a given circumstance (transmitter, month, GMT) can be combined to yield a single set of statistics.

Geometrical relationships between LOPs, which influence fix accuracies independently of phase accuracies, are also closely correlated over distances of hundreds of miles except when the receiver is close to one of the transmitters being received, in which case, LOP crossing angles can very rapidly.

The effect on fix accuracy of geometrical relationships between LOPs is expressed by a factor known as geometrical dilution of precision (GDOP). GDOP relates achievable fix accuracy to the accuracy that would be achievable for an ideal geometry between LOPs. GDOP is based entirely on relative locations of Omega transmitters and a hypothetical receiver, and is independent of actual measurement data. In this study, GDOP is calculated at the center of each 10^{o} x 10^{o} grid block and may be used to estimate the potential accuracy of fixes that can be obtained for any hypothetical LOPs actually measured.

Figure 3-1 illustrates the basic grid approach that is used in this study.

3.4 GEOMETRIC DILUTION OF PRECISION

A factor that is extremely useful in interpreting LOP data is GDOP. This is an overall factor which indicates how phase difference errors are reflected into position errors. Hyperbolic GDOP is defined as the ratio of RMS position error to the RMS position error of "ideal" geometry assuming

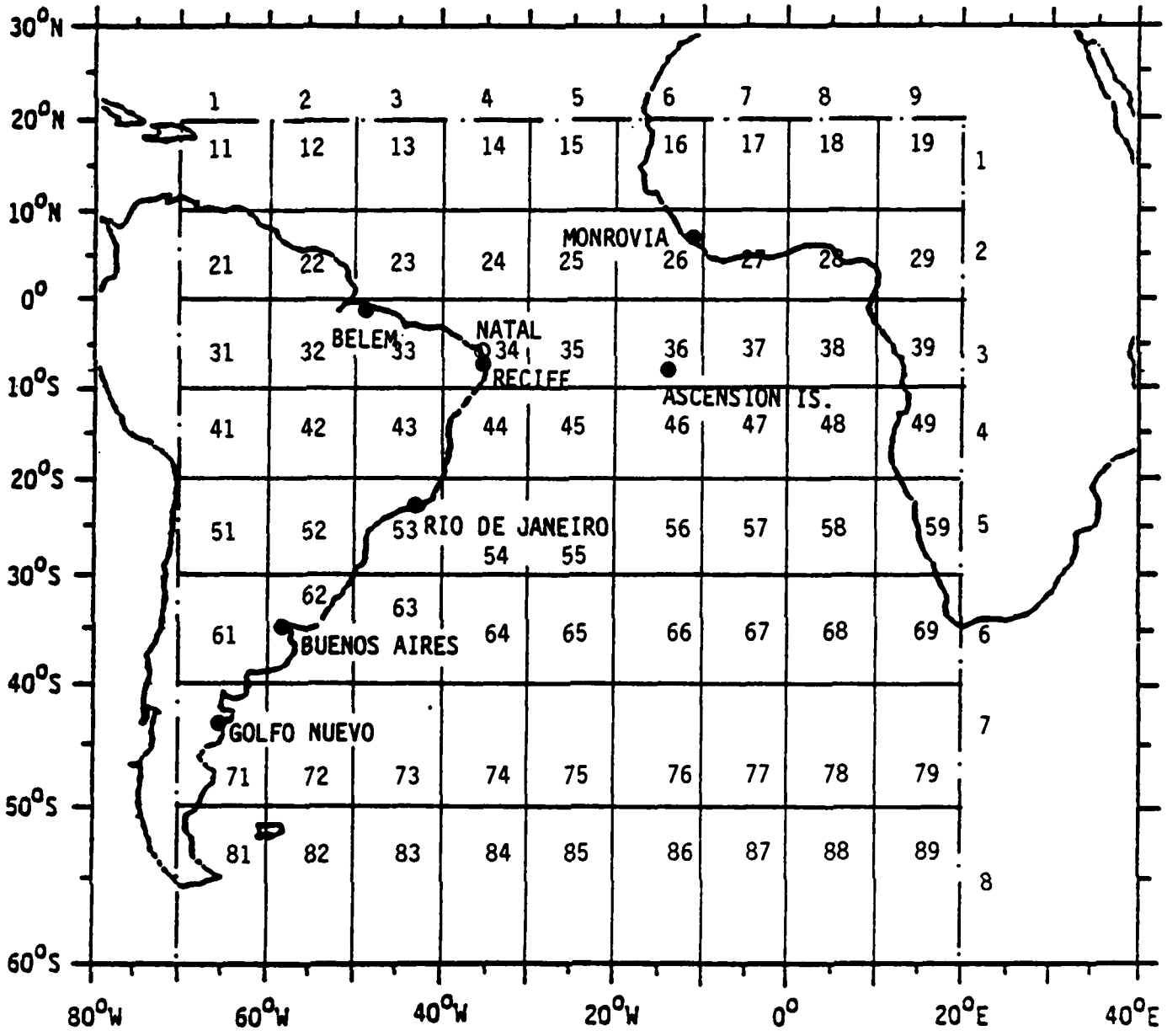

Figure 3-1. Grid used for Grouping Measurement Data in South Atlantic Region.

equal RMS errors on all received phases. For Omega hyperbolic geometry, the "ideal" configuration is represented by four stations at multiples of 90^{o} in bearing from the receiver.

for four stations forming LOPs A and B, GDOP is

$$GDOP_4 = \frac{2}{\sqrt{2}} \frac{1}{\sin \theta_4} \sqrt{\frac{1}{LOPA^2} + \frac{1}{LOPA^2}}$$

where θ_4 is the crossing angle of the two LOPs and $\nabla LOPA$ is the magnitude of the gradient of the LOP. θ_4 can be found from

$$\theta_r = \frac{BR1 - BR2}{2} + \frac{BR3 - BR4}{2}$$

where BR1 through BR4 are the bearing angles to the four stations used in the position fix. The magnitude of the gradient is found from

$$\nabla LOPA = 2 \sin \left(\frac{BR1 - BR2}{2}\right), \quad \nabla LOPB = 2 \sin\left(\frac{BR3 - BR4}{2}\right)$$

For three stations GDOP becomes

$$GDOP_3 = \frac{2}{\sqrt{2}} \frac{1}{\sin \theta_3} \sqrt{\frac{1}{|\nabla LOPA|^2} \frac{1}{|\nabla LOPB|^2} \frac{\cos \theta_3}{|\nabla LOPA||\nabla LOPB|}}$$

where θ_3 is the crossing angle of the LOPs given by

$$\theta_3 = \frac{BR1 - BR2}{2} + \frac{BR2 - BR3}{2}$$

where BR1 through BR3 are the bearing angles to the three stations in the triad, the magnitude of the gradients is

$$\nabla LOPA = 2 \sin \left(\frac{BR1 - BR2}{2}\right), \quad \nabla LOPA = 2 \sin \left(\frac{BR2 - BR3}{2}\right)$$

3.5 MASTERFILE DATA PROCESSING

Masterfile data from the monitor sites are processed in this study using a modified version of the program developed by SCT for processing the data from the Western Pacific region. A flow diagram of the modified program is shown in Figure 3-2.

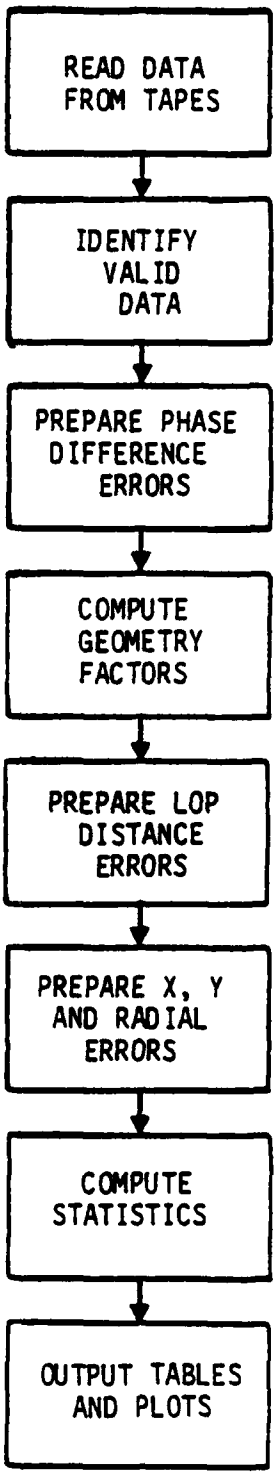

Figure 3-2. Masterfile Data Processing Flow Diagram

Significant blocks of data in Masterfile are flagged with warning indicators. These indicators are as follows:

Indicator	Definition
S	Sudden ionospheric disturbance
P	Polar cap absorption
U	Unknown anomaly
T	Transmitter out
M	Monitor out
L	Insufficient data for statistical analysis
Q	Data is beyond acceptable value

L and Q flags require careful definition. The average and standard deviation for phase readings taken at a given hour for the month are computed. Any data beyond the larger of two standard deviations, or 8 centicycles from the average, are flagged Q and called outliers. The statistics are recomputed and another search for outliers is made. The process is completed when no additional outliers are found or if less than 10 unflagged data points remain. If less than 10 unflagged data points remain or the phase error standard deviation is greater than 15.0, all data points not yet flagged are flagged L.

To identify valid data, the first step is to remove data flagged T or M. These data are flagged when either the transmitter or the monitor receiver is not functioning. The second step is to restore the whole part of the lane count. This is required because in some cases the LOP error may exhibit more than $\pm$0.5 cycle variation. The whole part of the lane count is restored by working sequentially through the hourly data and adjusting the whole lane count so that the change in the LOP error (with PPCs applied) is within the range of $\pm$0.5 cycle. If this cannot be done, the data cannot be interpreted, and are flagged as unusable. Data containing other flags are retained.

Tables of phase difference errors are now prepared. For a single frequency (10.2, 13.6, 11-1/3 kHz), the phase difference is described as:

Phase Difference Error. Ephd (h,d). Difference between the observed phase difference and the predicted phase difference.

$$Ephd\ (h,d) = PHDo\ (h,d) - PHDp\ (h,d)$$

$$Ephd\ (h,d) = PHDo\ (h,d) + PPC\ (H,d) - LOP$$

$$Ephd\ (h,d) = PHDc\ (h,d) - LOP$$

where we define:

Predicted Phase Difference, PHDp (h,d). Phase difference at a position, predicted from models or measurements.

Propagation Correction, PPC (h,d). Difference between the predicted phase difference at a position and the nominal phase difference, i.e.,

$$PPC\ (h,d) = LOP - PHDp\ (h,d)$$

Observed Phase Difference, PHDo (h,d). Measurement of a phase difference from a receiver.

Corrected Phase Difference, PHDc (h,d). Sum of the observed phase difference and the propagation correction, i.e.,

$$PHDc\ (h,d) = PHDo\ (h,d + PPC\ (h,d).$$

Where a difference frequency i.e., 3.4 kHz, is being analyzed, the individual frequencies are first processed and then differenced to produce the difference frequency errors. An additional critical error is then computed. This is the laning error. The laning error is the difference between the difference frequency error and the next laning frequency error. The laning error will provide the information required to determine the probability of a mislane.

For conversion of the LOP errors into distance errors, the geometry of the stations as observed from the monitor site must be considered. Three or four station are selected for a position fix. At each location several

combinations representing preferred and alternate combinations are selected. For the selected stations several factors are computed for processing and for aiding the interpolation of data. The LOP spacing (or gradient) is computed to convert LOP Phase difference errors into LOP distance errors. The bearing angle to each station is computed.

For small errors about the monitor site, the errors in a North and East coordinate system (E_N, E_E) can be expressed as

$$\begin{bmatrix} E_N \\ E_E \end{bmatrix} = \begin{bmatrix} A & B \\ C & D \end{bmatrix} \begin{bmatrix} E_{phda} \\ E_{phdb} \end{bmatrix}$$

where

$$A = \frac{\text{COS [Bearing (LOP B)]}}{\text{Grad A} \bullet \sin(\text{crossing angle})}$$

$$B = \frac{-\text{COS [Bearing (LOP A)]}}{\text{Grad B} \bullet \sin(\text{crossing angle})}$$

$$C = \frac{-\sin \text{ (Bearing LOP B)}}{\text{Grad A} \bullet \sin(\text{crossing angle})}$$

$$D = \frac{\sin \text{ (Bearing LOP A)}}{\text{Grad B} \bullet \sin(\text{crossing angle})}$$

Positional errors, North and East, are computed using the procedure defined above. Radial error is computed as

Radial Error, $E_r(h,d)$. Magnitude of the error vector.

$E_r(h,d)$ and $E_e(h,d)$

refer to the North and East components of position errors.

Statistics of the data are computed. The most meaningful are:

Hourly Mean Phase Difference Error, Ephd(h). Average value, over the month of the phase difference error. D is the number of days for which there is data.

$$Ephd(h) = \frac{1}{D}\sum_{d=1}^{D} Ephd(h,d)$$

Hourly Standard Deviation of the Phase Difference Error. $SD_{ephd}(h)$. Standard deviation of the phase difference errors about the hourly mean phase difference error.

$$SD_{ephd}(h) = \frac{1}{D}\sqrt{\sum_{d=1}^{D}\left(E_{phd}(h,d) - E_{phd}(h)\right)^2}$$

Hourly Mean Position Component Errors, $E_n(h)$ and $E_e(h)$.

Average value, over the month, of the position component errors.

$$E_n(h) = \frac{1}{D}\sum_{d=1}^{D} E_n(h,d)$$

$$E_e(h) = \frac{1}{D}\sum_{d=1}^{D} E_e(h,d)$$

Hourly Mean Radial Error, $E_r(h)$. Average value, over the month, of the radial error.

$$E_r(h) = \frac{1}{D}\sum_{d=1}^{D} E_r(h,d)$$

Hourly Standard Deviation of the Radial Error, SD(h). Standard deviation of the radial errors about the hourly mean radial errors.

$$SD(h) = \frac{1}{D}\sum_{d=1}^{D} (E_n(h,d) - E_n(h))^2 + (E_e(h,d) - E_e(h))^2$$

Maximum Radial Error, $E_r(M)$. Maximum value of the hourly mean radial errors. M is the hour the maximum value occurs.

Maximum Standard Deviation, SD(M). Maximum value, over the hours, of the hourly standard deviations.

Mean Radial Error, ME_r. Average value, over the hours, of the hourly mean radial errors. H is the number of hours for which there are data.

$$ME_r = \frac{1}{H} \sum_{h=1}^{H} E_r(h)$$

Mean Standard Deviation of the Radial Error. MSD. Average value, over the hours, of the hourly standard deviation.

$$MSD = \frac{1}{H} \sum_{h=1}^{H} SD(h)$$

Finally, the data are outputted. Tables are printed of the phase difference errors, LOP distance errors, x errors, y errors, radial errors, and laning errors. Geometric factors for the site are printed including; distance to stations, bearing to stations, LOP gradients, LOP crossing angles, conversion constants , and GDOP. Statistics of the data are printed including; hourly mean phase difference errors, hourly standard deviation of phase radial errors, hourly standard deviation of the radial error, maximum radial error, maximum standard deviation mean radial error, mean standard deviation of the radial error and the number of data points included for each statistic.

3.6 DIURNAL VARIATIONS IN LOP ERRORS

Measured phase differences are used by the Omega navigator to estimate his line of position, or LOP, with respect to a pair of Omega transmitters. This estimated LOP contains some error because of the impossibility of accounting fully for propagation anomalies of Omega signals. Propagation prediction corrections (PPCs) have been developed to provide first-order corrections to measured LOPs. PPCs generally offset 50% to 80% of the initial error in measured LOPs, leaving residual errors that are much smaller than the uncorrected errors.

The physical processes involved in Omega signal propagation are far too

numerous, complex and poorly understood to support the generation of complete corrections to measured LOPs. Nevertheless, it is useful to examine the residual errors associated with corrections of measured LOPs.

Residual error may be defined by the following relationships. First, a perfect correction can be expressed as

$$LOP_A = LOP_M + LOP\text{-}PPC_0$$

where LOP_A is the actual LOP that would be determined from surveys, LOP_M is the measured LOP, or phase difference and $LOP\text{-}PPC_0$ is an imaginary, "perfect" correction applied to the LOP, where we are using the term LOP-PPC to describe a single correction that is applied to a measured LOP and thus may be thought of as a composite of two PPCs. A LOP-PPC is actually a result of propagation-prediction corrections that have been applied separately to each of the two propagation paths involved in the LOP.

A real, imperfect LOP-PPC can be expressed as $LOP\text{-}PPC_R$, where

$$LOP\text{-}PPC_R = LOP\text{-}PPC_0 + \Delta(LOP\text{-}PPC)$$

and $\Delta(LOP\text{-}PPC)$ is a residual error in the calculated LOP-PPC due to our imperfect understanding of Omega signal propagation.

If we now recognize that it is $LOP\text{-}PPC_R$, not $LOP\text{-}PPC_0$, that is actually applied to the measured LOP, then we have

$$LOP_A + \Delta(LOP) = LOP_M + LOP\text{-}PPC_0 + \Delta(LOP\text{-}PPC)$$

where $\Delta(LOP)$ is just the residual error in estimated LOP resulting from the application of an imperfect LOP-PPC to the measurement. Specifically,

$$\Delta(LOP) = \Delta(LOP\text{-}PPC)$$

If we neglect errors in signal processing within Omega receiving equipment, then the <u>observed</u> phase difference error (LOP error) may be equated to errors in LOP-PPCs that have been applied to the measured values.

Phase difference errors are routinely calculated and are available from Masterfile for each month, GMT, monitor site and LOP in the data base. In this study, phase difference errors are averaged over a full month at each hour, and these hourly averaged values are plotted over a 24-hour period to describe graphically the diurnal variations in the monthly-averaged phase difference errors. By the argument just given above, such plots are also plots of the diurnal variation in monthly-averaged LOP-PPC errors. The magnitudes and variability of LOP-PPC errors provide information that can be useful in improving algorithms that are used to compute propagation corrections in navigation receivers.

The interpretation of errors in LOP-PPCs in terms of errors in those propagation corrections that are applied to individual propagation paths is a complex process that is beyond the scope of this study. Nevertheless, the results obtained here provide essential inputs to any effort to improve the quality of propagation corrections for Omega.

IV. DESCRIPTION OF NON-TEST DATA

4.1 OVERVIEW

Non-test data are those data obtained by means of measurements that took place independently of the NOSC South Atlantic Omega Validation Tests. Non-test data are of three general types; (a) phase or phase-difference data, (b) signal amplitude or signal-to-noise data, and (c) operational data.

Phase-difference data are available from the ONSOD monitor sites. Phase-difference data are also available from Integrated Omega-Satellite (IOS) measurements performed aboard certain ships in the South Atlantic.

Signal-to-noise data are available both from measurements at ONSOD sites and from IOS measurements. Signal-to-noise data from ONSOD sites are obtained from a different file than phase-difference data, and, indeed, the ONSOD signal-to-noise data base is much smaller than the ONSOD phase-difference data base. On the other hand, IOS signal-to-noise data and IOS phase-difference data are obtained from the same files and from the same sets of measurements.

Operational data are obtained from a limited number of ship voyages and aircraft flights, and are in the form of operational logs and reports. These data do not benefit from precise reference information and are therefore less important than the other data sets. A detailed description of each non-test data set follows.

4.2 FIXED OMEGA MONITOR DATA

4.2.1 Phase Difference Data

Raw phase data from the ONSOD monitor sites are processed at ONSOD to obtain the structured data base of phase-difference data called Masterfile. Primary emphasis is given to the 10.2 and 13.6 kHz data in constructing the Masterfile, as the 11 1/3 kHz data is of secondary importance in the validation program. The breadth of the Masterfile is illustrated by Tables 4-1 and 4-2 and by reference to Figure 2-2. Table 4-1 lists the monthly

TABLE 4.1
MASTERFILE PHASE DATA BY SITE,
FREQUENCY, MONTH, AND YEAR

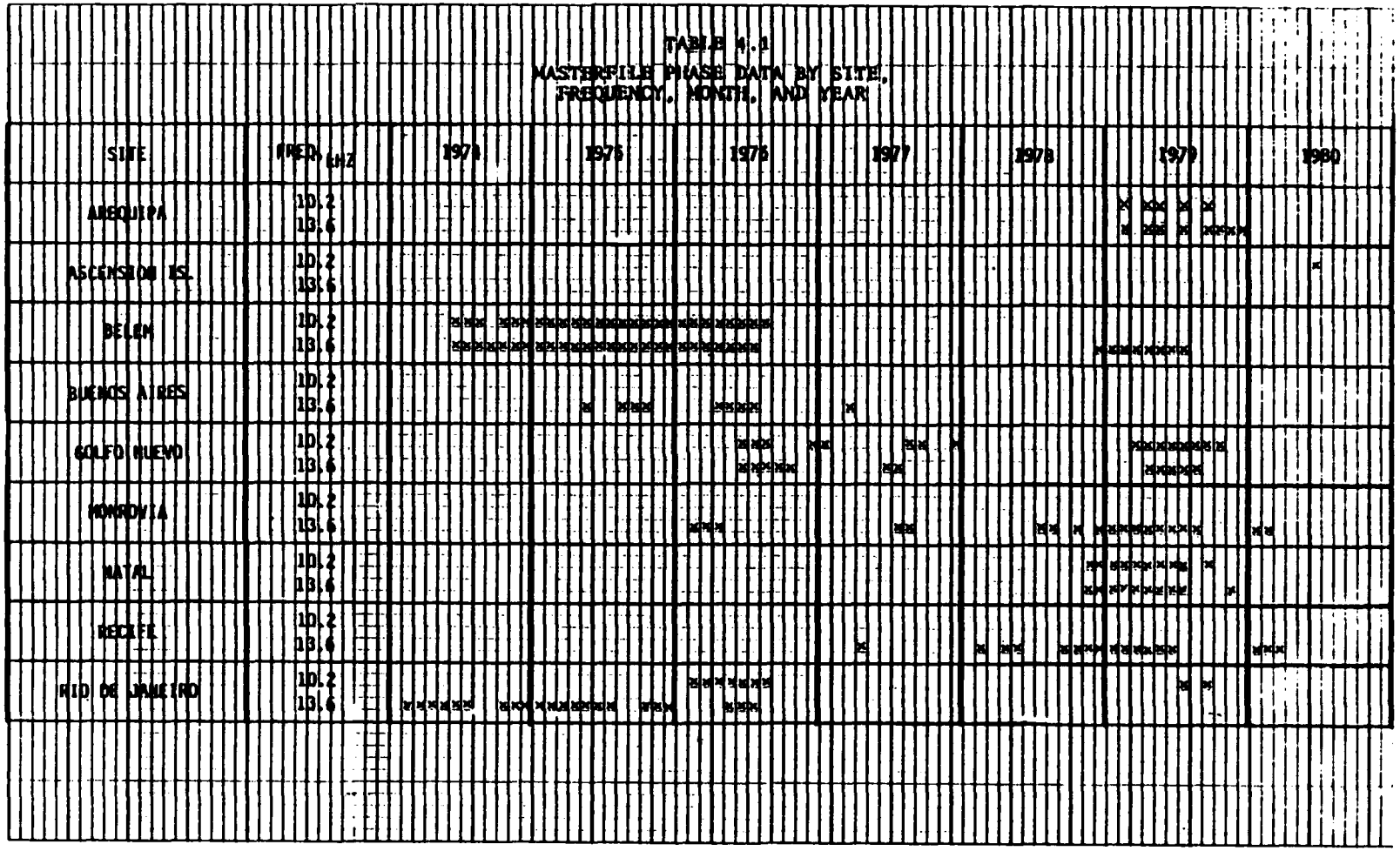

representation of each of the monitor sites in the 10.2 and 13.6 kHz Masterfile. An entry in Table 4-1 simply indicates that some data are available during the month from the monitor site. Table 4-2 extends Table 4-1 to include the monthly representation of LOP, or station-pairs, in the data base. An entry in Table 4-2 simply indicates that some data are available during the month for the particular LOP from the monitor site.

We may define a "reduced" set of phase-difference data, which will be used for the various statistical analyses required by the validation efort. A reduced data set consists of the set of useful data corresponding to 0600 and 1800 GMT during the months of February, May, August and November. In this case, where all data are obtained from Masterfile, there is no need to create an additional data file, since the reduced data set is easily accessed directly from Masterfile. However, it is instructive to consider the size of the reduced data base, i.e., the numbers of data points that are actually available from the Masterfile for analysis. Table 4-3 lists the numbers of unflagged data points that are available from Masterfile by site, frequency, LOP (station pair), month and GMT.

4.2.2 Signal-to-Noise Data

Signal-to-noise data are available from ONSOD monitor sites for the year 1980. The quantity that is recorded and that corresponds to a given measurement, contains information on the signal-to-noise ratio (SNR) appropriate to a signal from a particular station at a particular frequency. In order to obtain SNR expressed in dB, it is necessary to apply a calibration factor to each recorded quantity. The calibration that has been used is described in Appendix A. Table 4-4 describes the availability of signal-to-noise measurement data from ONSOD sites.

We may define a reduced data set of signal-to-noise data from ONSOD sites corresponding to 0600 and 1800 UT during the months of February, May, August and November. Tables 4-5 and 4-6 describe the availability of data in the reduced set. A separate file has been created at SCT to contain the reduced set of SNR data from ONSOD sites. The calibration described in Appendix A has been applied to all reduced data contained in the file.

TABLE 4-2

SOUTH ATLANTIC OMEGA VALIDATION

MASTERFILE DATA AVAILABLE BY SITE, FREQUENCY, LOP AND MONTH

ASCENSION ISLAND

DATE	10.2 KHz					
	LOP					
	AD	AE	BF	CD	CF	DE
6/80	✓	✓	✓	✓	✓	✓

BELEM

DATE	10.2 KHz LOP			13.6 KHz LOP						
	AC	AD	CD	AC	AD	CD	AF	DF	BF	BD
6/74		✓			✓					
7/74		✓								
8/74		✓			✓					
9/74					✓					
10/74		✓			✓					
11/74		✓								
12/74	✓	✓	✓	✓	✓	✓				
1/75	✓	✓	✓	✓	✓	✓				
2/75	✓	✓	✓	✓	✓	✓				
3/75	✓	✓	✓	✓	✓	✓				
4/75	✓	✓	✓	✓	✓	✓				
5/75	✓	✓	✓	✓	✓	✓				
6/75	✓	✓	✓	✓	✓	✓				
7/75	✓	✓	✓	✓	✓	✓				
8/75	✓	✓	✓	✓	✓	✓				
9/75	✓			✓						
10/75	✓	✓	✓	✓	✓	✓				
11/75	✓	✓	✓	✓	✓	✓				
12/75	✓	✓	✓	✓	✓	✓				
1/76	✓	✓	✓	✓	✓	✓				
2/76	✓	✓	✓	✓	✓	✓				
3/76	✓	✓	✓	✓	✓	✓				
4/76	✓	✓	✓	✓	✓	✓				
5/76	✓	✓	✓	✓	✓	✓				
6/76	✓	✓	✓	✓	✓	✓				
7/76	✓	✓	✓	✓	✓	✓				
8/76	✓	✓	✓							
12/78							✓	✓		
1/79							✓	✓		
2/79							✓	✓		
3/79							✓	✓		
4/79							✓	✓	✓	
5/79							✓			✓
6/79							✓	✓	✓	✓
7/79							✓	✓	✓	✓

BUENOS AIRES

DATE	13.6 KHz LOP		
	BC	CD	DH
5/75			
8/75		✓	✓
9/75		✓	
10/75		✓	
1/76			
4/76	✓	✓	✓
5/76	✓	✓	✓
6/76		✓	✓
7/76	✓	✓	✓
3/77	✓	✓	✓

GOLFO NUEVO

DATE	10.2 KHz LOP			13.6 KHz LOP		
	BF	DF		BF	DF	FB
6/76				✓	✓	✓
7/76				✓	✓	✓
8/76				✓	✓	✓
9/76				✓	✓	✓
]0/76				✓	✓	✓
12/76	✓	✓				
1/77						
6/77				✓	✓	✓
7/77				✓	✓	✓
8/77	✓	✓				
9/77	✓	✓				
12/77	✓	✓				
3/79	✓	✓				
4/79	✓	✓				
5/79	✓	✓				
6/79	✓	✓				
7/79	✓	✓				
8/79	✓	✓				
9/79	✓	✓				
10/79	✓					

MONROVIA

DATE	13.6 KHz LOP AB	BE	BF
2/76	✓		
3/76	✓		
4/76	✓		
6/76			
7/76			
8/76			
7/77	✓	✓	✓
8/77	✓	✓	✓
7/78	✓	✓	✓
8/78		✓	✓
10/78			✓
12/78			✓
1/79	✓	✓	✓
2/79	✓		✓
3/79	✓	✓	
4/79	✓	✓	✓
5/79	✓	✓	✓
6/79	✓	✓	✓
7/79	✓	✓	✓
8/79	✓		✓
1/80	✓	✓	✓
2/80	✓	✓	✓

NATAL

DATE	10.2 KHz LOP							13.6 KHz LOP					
	AD	AE	BF	CD	DF	EF		AD	AE	BF	CD	DF	EF
11/78	✓	✓	✓	✓	✓	✓		✓	✓	✓	✓	✓	✓
12/78	✓	✓	✓	✓	✓	✓		✓	✓	✓	✓	✓	✓
1/79	✓	✓	✓	✓	✓	✓		✓	✓	✓	✓	✓	✓
2/79	✓	✓	✓	✓	✓	✓		✓	✓	✓	✓	✓	✓
3/79	✓	✓	✓	✓	✓	✓		✓	✓	✓	✓	✓	✓
4/79	✓	✓	✓	✓	✓	✓		✓	✓	✓	✓	✓	✓
5/79	✓	✓	✓	✓	✓	✓		✓	✓	✓	✓	✓	✓
6/79	✓	✓	✓	✓	✓	✓		✓	✓	✓	✓	✓	✓
7/79	✓	✓	✓	✓	✓	✓		✓	✓	✓	✓	✓	✓
9/79	✓	✓	✓	✓	✓	✓							
11/79								✓	✓	✓	✓	✓	✓

RECIFE

DATE	13.6 KHz			
	LOP			
	CF	DE	DF	EF
4/77	✓	✓	✓	✓
2/78	✓	✓	✓	✓
4/78	✓	✓		✓
5/78	✓	✓		✓
9/78	✓	✓	✓	✓
10/78	✓	✓	✓	✓
11/78	✓	✓	✓	✓
12/78	✓	✓	✓	✓
1/79		✓	✓	✓
2/79	✓		✓	✓
3/79	✓	✓	✓	✓
4/79	✓	✓	✓	✓
5/79	✓	✓	✓	
6/79	✓	✓		✓
1/80	✓	✓	✓	✓
2/80	✓	✓	✓	✓
3/80	✓	✓	✓	✓

TABLE 4-3

REDUCED MASTERFILE DATA AVAILABLE BY SITE, FREQUENCY, LOP, MONTH AND GMT

BELEM

DATE	FREQ. KHz	LOP					
		AC		AD		CD	
		06	18	06	18	06	18
8/74	10.2			21	26		
11/74				23	25		
2/75		25	24	23	22	23	22
5/75		22	24	23	23	25	23
8/75		11	10	0	11	24	20
11/75		14	14	13	15	27	15
2/76		26	26	25	27	24	25
5/76		21	23	17	21	19	23
8/76		30	28	29	29	24	29

DATE	FREQ. KHz	LOP											
		AC		AD		CD		AF		DF		BD	
		06	18	06	18	06	18	06	18	06	18	06	18
8/74	13.6	0	0	26	25								
11/74													
2/75		25	23	23	21	25	22						
5/75		23	24	18	24	22	24						
8/75		0	11	0	11	25	19						
11/75		15	13	13	12	24	13						
2/76		25	26	21	26	22	26						
5/76		21	23	20	23	19	22						
2/79								15	17	21	19		
5/79								0	24			27	24

BUENOS AIRES

DATE	FREQ. KHz	LOP					
		BC		CD		DH	
		06	18	06	18	06	18
5/75	13.6	0	0				
8/75				0	0	0	0
5/76		19	23	21	23	19	23

GOLFO NUEVO

DATE	FREQ. KHz	LOP			
		BF		DF	
		06	18	06	18
8/76	10.2				
8/77		23	22	27	21
5/79		29	26	28	26
8/79		26	22	21	14
8/76	13.6	23	28	28	27
5/79		27	26	29	26
8/79		27	23	21	13

MONROVIA

DATE	FREQ. KHz	LOP					
		AB		BE		BF	
		06	18	06	18	06	18
2/76	13.6	23	22				
8/77		27	22	24	19	28	22
8/78				22	21	24	21
2/79		15	15			24	15
5/79		29	26	0	0	28	26
8/79		25	21			21	22
2/80		0	0	0	0	14	0

NATAL

DATE	FREQ. KHz	LOP											
		AD		AE		BF		CD		DF		EF	
		06	18	06	18	06	18	06	18	06	18	06	18
11/78	10.2	0	23	0	0	23	23	28	21	26	19	0	19
2/79		0	0	0	0	0	10	0	0	14	0	0	0
5/79		0	14	17	19	22	19	23	0	26	18	0	18
11/78	13.6	20	21	0	18	18	22	28	19	28	21	17	19
2/79		0	0	0	0	0	0	0	10	14	0	0	0
5/79		23	19	0	18	17	19	22	18	24	19	18	18
11/79		0	0	0	0	0	0	11	0	12	0	0	0

RECIFE

DATE	FREQ. KHz	LOP							
		CF		DE		DF		EF	
		06	18	06	18	06	18	06	18
2/78	13.6	21	21	14	21	24	21	18	22
5/78		14	0	11	0			0	0
11/78		27	25	26	25	29	25	23	24
2/79		17	15			24	19	18	19
5/79		26	25	22	25	30	25		
2/80		10	10	0	0	25	10	11	0

TABLE 4-4

SNR DATA AT 10.2 and 13.6 KHz FROM ONSOD SITES IN 1980
MONTHS REPRESENTED IN TOTAL DATA BASE

SITE	JAN	FEB	MAR	APR	MAY	JUN	JUL	AUG	SEP	OCT	NOV	DEC
AREQUIPA		*	*	*	*	*	*	*			*	*
ASCENSION						*	*	*		*		
BUENOS AIRES	*	*	*		*	*		*				
NATAL	*		*		*		*				*	

TABLE 4-5

REDUCED SNR DATA AT 10.2 kHz AND 13.6 kHz FROM ONSODE SITES IN 1980. NUMBER OF DAYS OF DATA BY MONTH AND TIME.

SITE	FEBRUARY		MAY		AUGUST		NOVEMBER	
	0600	1800	0600	1800	0600	1800	0600	1800
AREQUIPA	2	1	26	27	5	4	23	19
ASCENSION					14	14		
BUENOS AIRES	21	24	16	16	25	26		
NATAL	2	2	10	12	15	13		

TABLE 4-6

REDUCED SNR DATA AT 10.2 kHz AND 13.6 kHz FROM ONSOD SITES IN 1980. NUMBER OF DATA POINTS BY MONTH AND GMT.

MONTH	GMT	OMEGA TRANSMITTERS						
		A	B	C	D	E	F	H
		ASCENSION ISLAND						
8	06	14	14	14	14	14	14	14
	18	14	14	14	14	14	14	14
		AREQUIPA						
2	06	2	2	2	2	2	2	-
	18	1	1	1	1	1	1	-
5	06	26	26	26	26	26	26	-
	18	27	27	27	27	27	27	-
8	06	5	5	5	5	5	5	-
	18	4	4	4	4	4	4	-
11	06	23	23	23	23	23	23	1
	18	19	19	19	19	19	19	-
		BUENOS AIRES						
2	06	-	21	21	21	21	21	21
	18	-	24	24	24	24	24	24
5	06	-	16	16	16	16	16	16
	18	-	16	16	16	16	16	16
8	06	-	25	25	25	25	25	25
	18	-	26	26	26	26	26	26

TABLE 4-6

(CONTINUED)

REDUCED SNR DATA AT 10.2 kHz AND 13.6 kHz FROM ONSOD SITES IN 1980. NUMBER OF DATA POINTS BY MONTH AND GMT.

MONTH	GMT	OMEGA TRANSMITTERS						
		A	B	C	D	E	F	H
		NATAL						
2	06	2	2	2	2	2	2	-
	18	2	2	2	2	2	2	-
5	06	10	10	10	10	10	10	-
	18	12	12	12	12	12	12	-
11	06	15	15	15	15	15	15	-
	18	13	13	13	13	13	13	-

4.3 SHIPBORNE OMEGA DATA

Omega data are available from four cruises of commercial vessels. All four cruises involved passages around the Cape of Good Hope and through the eastern part of the South Atlantic. Table 4-7 lists the essential circumstances of these measurements and Figures 4-1 and 4-2 illustrate the approximate routes involved.

The value of these data is somewhat limited. The presentation of LOPs provides a positive indication of Omega coverage from the transmitters involved, but no information is available on what Omega frequencies were received at any time or even what frequencies were within the tuning range of the navigation receivers aboard the ships. Obviously, one cannot conclude anything about coverage from the absence of any station in the data.

In the same vein, no quantitative conclusions regarding available accuracy of Omega can be derived from these data since the quality of the reference position data cannot be assessed from the measurement records.

At most, these data provide positive confirmation of Omega coverage and a tentative confirmation of reasonable fix accuracy in the cases measured.

4.4 AIRBORNE OMEGA DATA

Non-test Omega data are available from two commercial aircraft flights for this study. In addition, Omega performance summaries are available that list certain performance criteria for commercial flights between December 1977 and July 1978. Appendix B summarizes Omega performance results in terms of operational/non-operational status and reported lane slips during 1227 flights without attempting to relate performance to season, flight location, solar illumination, or transmitter. Appendix B also provides a breakdown of the geographical distribution of reported lane slips for 168 flights between 12 June 1978 and 27 June 1978. It can be seen that airborne Omega data available for this study are of little quantitative value, and can be useful only to verify results obtained from other data.

Appendix C describes observations of Omega signals during a round-trip flight from New York to San Jose, Guatamala, on 5 April and 6 April 1978.

TABLE 4-7. Shipborne OMEGA Data

VESSEL	DATES	DAILY READINGS	OMEGA LOPs	REFERENCE POSITION (LAT/LON) SOURCES
United Overseas I	Jan 11/21 1978	every hour	BE,BF,EF, AE & AD	None given
Alabama Getty	Nov 12-23 1976	4-12	BE,BF,EF	Satellite/ radar, sight
British Respect	Oct 21-30 1977	every 2 hours	AD,DF,AF	Satellite/ radar, sight dead reckoning
British Respect	July 13-23 1977	every 2 hours	BE,BF,EF	Radar, visual dead reckoning

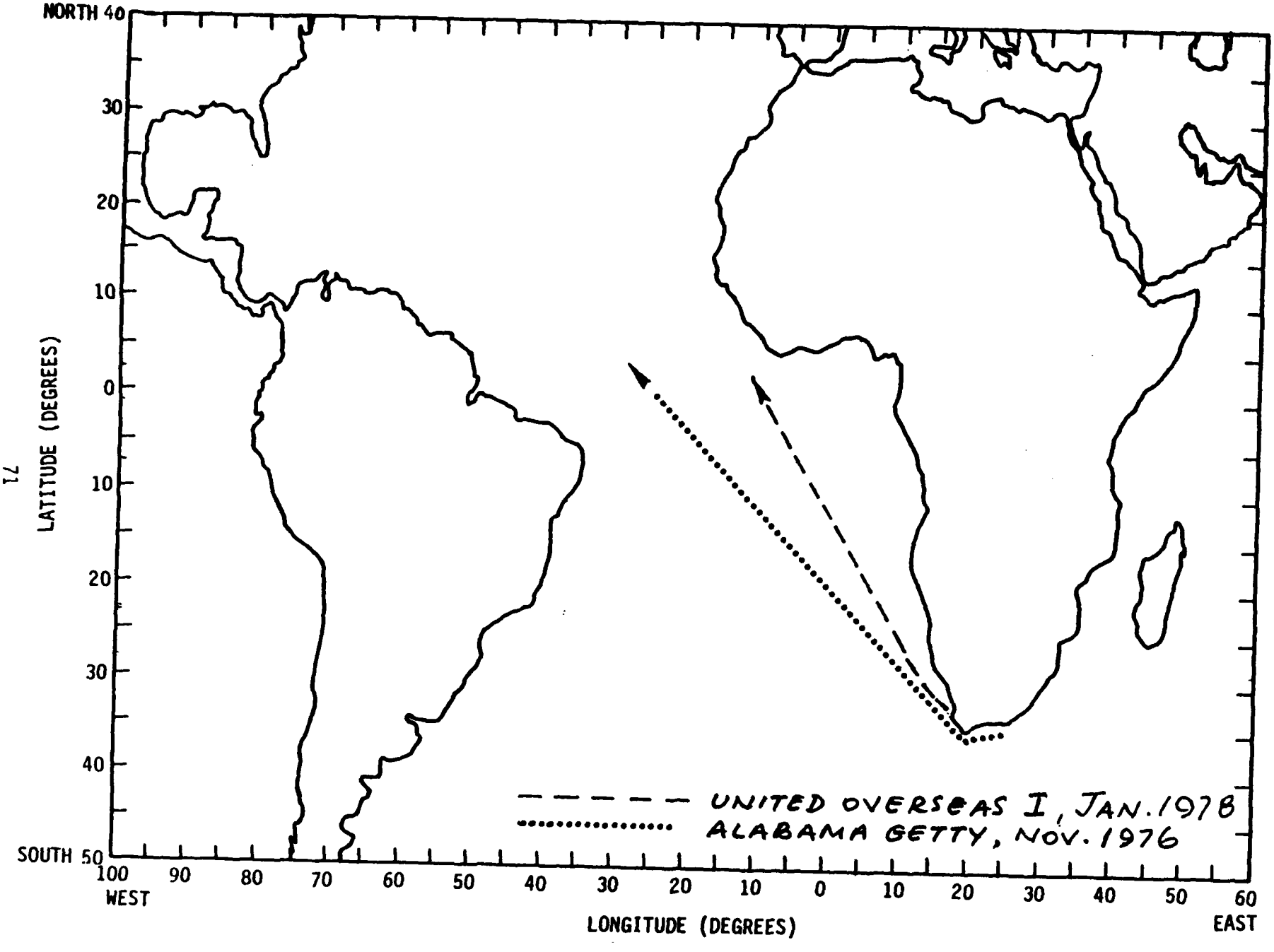

FIGURE 4-1. Routes of United Overseas and Alabama Getty.

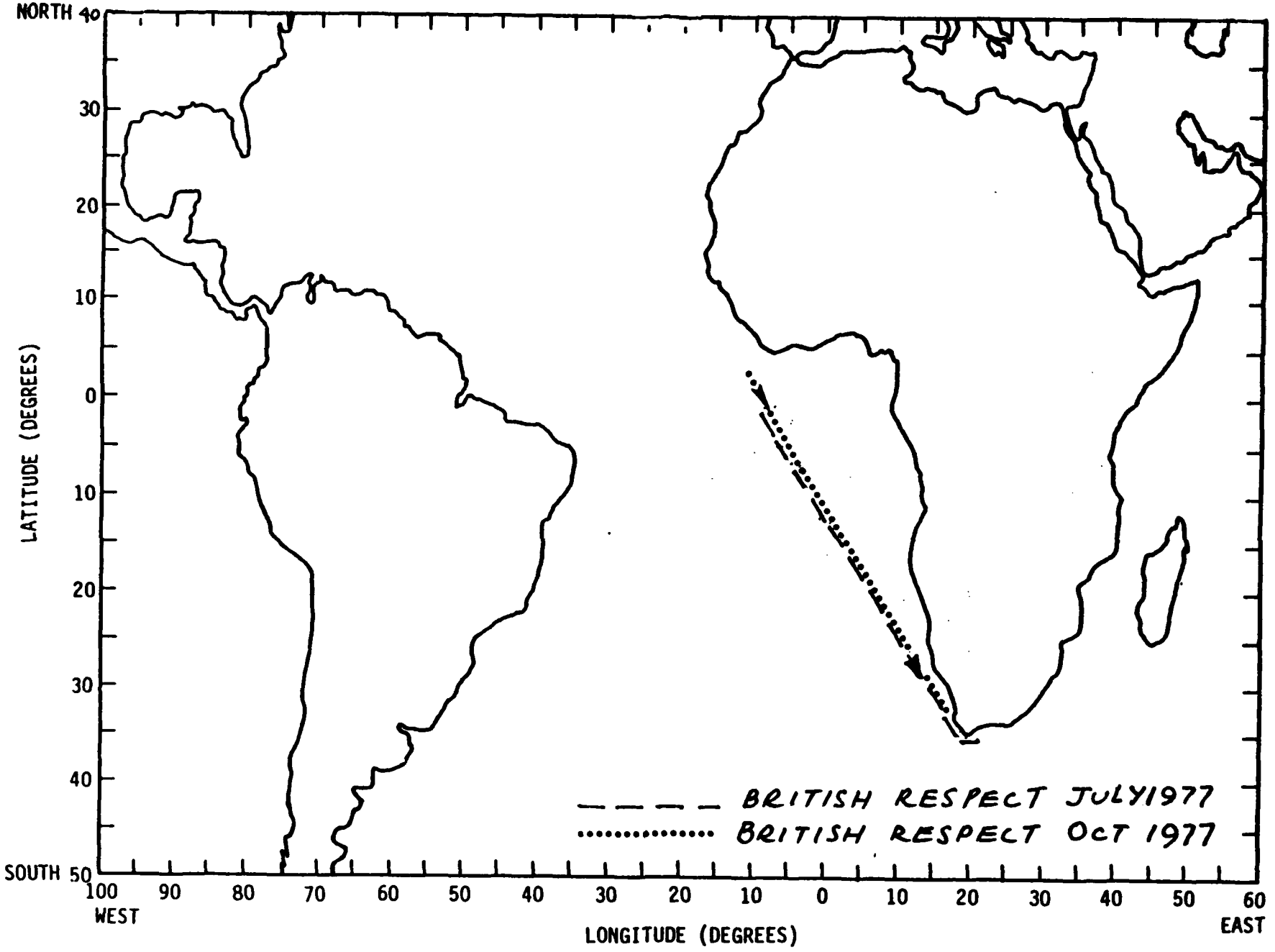

FIGURE 4-2. Routes of British Respect.

Table 4-8 lists these observations by frequency and transmitter. We assume, from the appearance of the data in Table 4-8, that the airborne observer attempted routinely to receive all available signals, thus the absence of any observation provides a positive indication that the signal being sought was not available during the observation period.

4.5 INTEGRATED OMEGA-SATELLITE RECEIVER DATA

Integrated Omega/Satellite (IOS) data are available from eight ship voyages in the South Atlantic during the period November 18, 1979 through April 16, 1981. IOS receivers built by Magnavox provide Omega measurement data similar to the data provided at the ONSOD sites. In addition, these receivers compute highly accurate position fixes based on signals received from the Transit (NAVSAT) satellites. The satellite-derived position fixes provide the necessary reference used for evaluating the navigation accuracy of Omega measurements.

Transit signals are not available continuously, since the satellites are in near-polar orbits. In fact, Transit signals are available only at irregular intervals ranging from one-half hour to three hours.

Figures 4-3 through 4-10 illustrate the routes followed by the ships during the various cruises and illustrate the approximate geographical distribution of IOS measurements, without regard to the GMT distribution of measurements.

The IOS data base contains entries only at times corresponding to satellite fixes. As a result, IOS data are not generally available at 0600 and 1800 GMT. Since the validation applies, strictly speaking, only to these two times and to the months of February, May, August and November, then it becomes necessary to interpret the actual IOS data in terms of imputed values that would have been observed had measurements been made at 0600 and 1800 GMT during February, May, August and November.

This requirement to infer measurements that were not actually made from measurements that were made suggests the use of some interpolation or extrapolation on the available data. Moreover, because of the rapid variation of radiowave propagation conditions with GMT, it is immediately obvious that

TABLE 4-8

Observations of OMEGA Signals

		OMEGA TRANSMITTERS																	
		A			B			C			D			E			F			H		
FLIGHT	G.M.T.	10.2	13.6	11.3	10.2	13.6	11.3	10.2	13.6	11.3	10.2	13.6	11.3	10.2	13.6	11.3	10.2	13.6	11.3	10.2	13.6	11.3
NEW YORK TO SAN JOSE 5 APRIL 1978	15:45	✓	✓	✓	✓	✓	✓	✓	✓	✓	✓	✓	✓	✓	✓	✓	✓	✓	✓	✓	✓	✓
	16:28	✓	✓	✓	✓	✓	✓	✓	✓	✓	✓	✓	✓	✓	✓	✓	✓	✓	✓	✓	✓	✓
	18:23	✓	✓	✓	✓	✓	✓	✓	✓	✓	✓	✓	✓	✓	✓	✓	✓	✓	✓	✓	✓	✓
	19:15	✓	✓	✓	✓	✓	✓	✓	✓	✓	✓	✓	✓	✓	✓	✓	✓	✓	✓	✓	✓	✓
	19:50	✓	✓		✓	✓		✓	✓		✓	✓		✓	✓		✓	✓		✓	✓	
	20:30	✓	✓		✓	✓		✓	✓		✓	✓		✓	✓		✓	✓		✓	✓	
	21:18	✓	✓		✓	✓		✓	✓		✓	✓		✓	✓		✓	✓		✓	✓	
SAN JOSE TO NEW YORK 6 APRIL 1978	00:33	✓	✓	✓	✓	✓	✓	✓	✓	✓	✓	✓	✓	✓	✓	✓	✓	✓	✓	✓	✓	✓
	14:15	✓	✓	✓	✓	✓	✓	✓	✓	✓	✓	✓	✓	✓	✓	✓	✓	✓	✓	✓	✓	✓
	15:03	✓	✓		✓	✓		✓	✓		✓	✓		✓	✓		✓	✓		✓	✓	
	15:40	✓	✓		✓	✓		✓	✓		✓	✓		✓	✓		✓	✓		✓	✓	
	18:00	✓	✓	✓	✓	✓	✓	✓	✓	✓	✓	✓	✓	✓	✓	✓	✓	✓	✓	✓	✓	✓
	19:12	✓	✓	✓	✓	✓	✓	✓	✓	✓	✓	✓	✓	✓	✓	✓	✓	✓	✓	✓	✓	✓
	20:10	✓	✓	✓	✓	✓	✓	✓	✓	✓	✓	✓	✓	✓	✓	✓	✓	✓	✓	✓	✓	✓
	20:45	✓	✓		✓	✓		✓	✓		✓	✓		✓	✓		✓	✓		✓	✓	
	21:19	✓	✓	✓	✓	✓	✓	✓	✓	✓	✓	✓	✓	✓	✓	✓	✓	✓	✓	✓	✓	✓

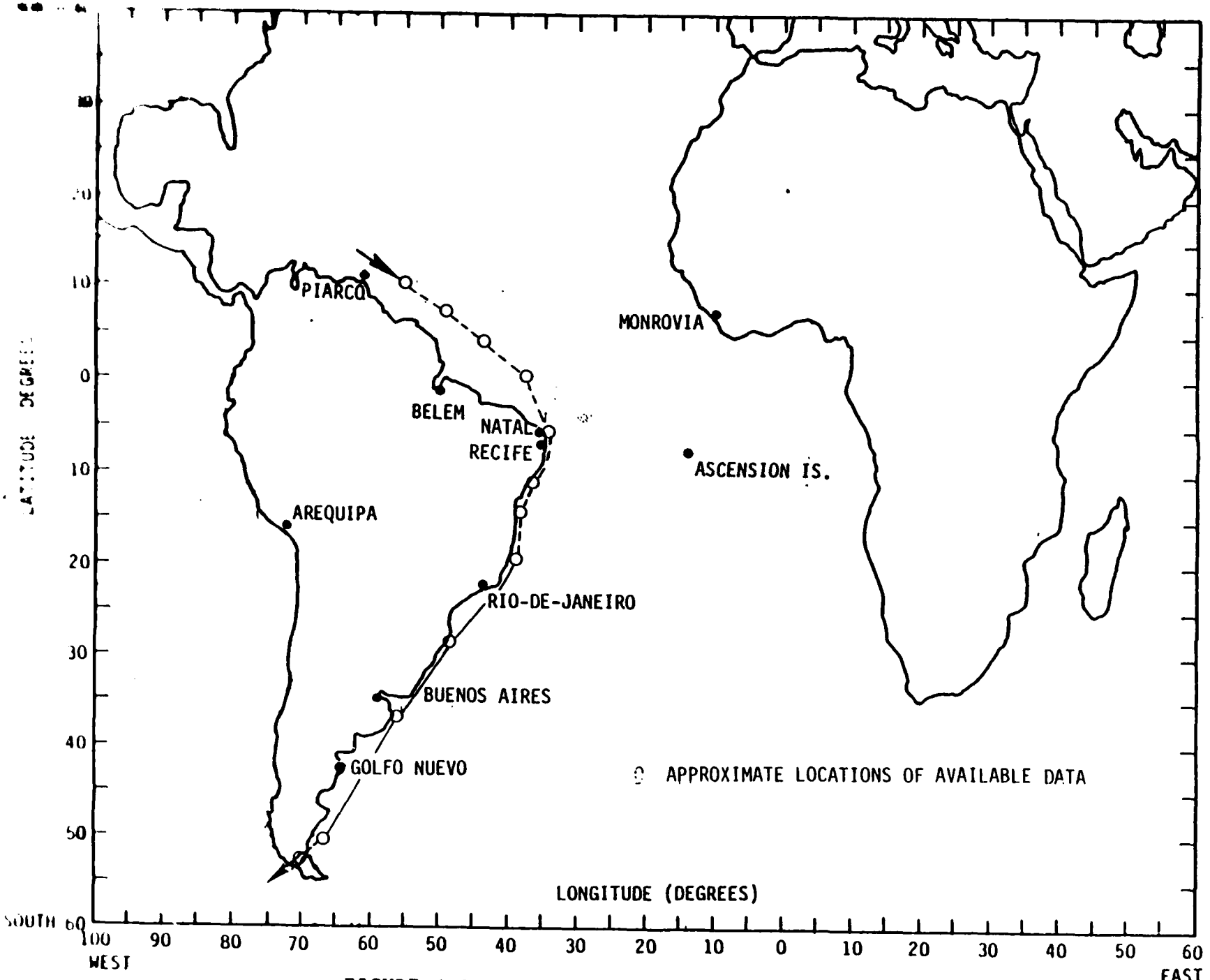

FIGURE 4-3 MAGDALENA CRUISE 11/18/79 - 12/7/79

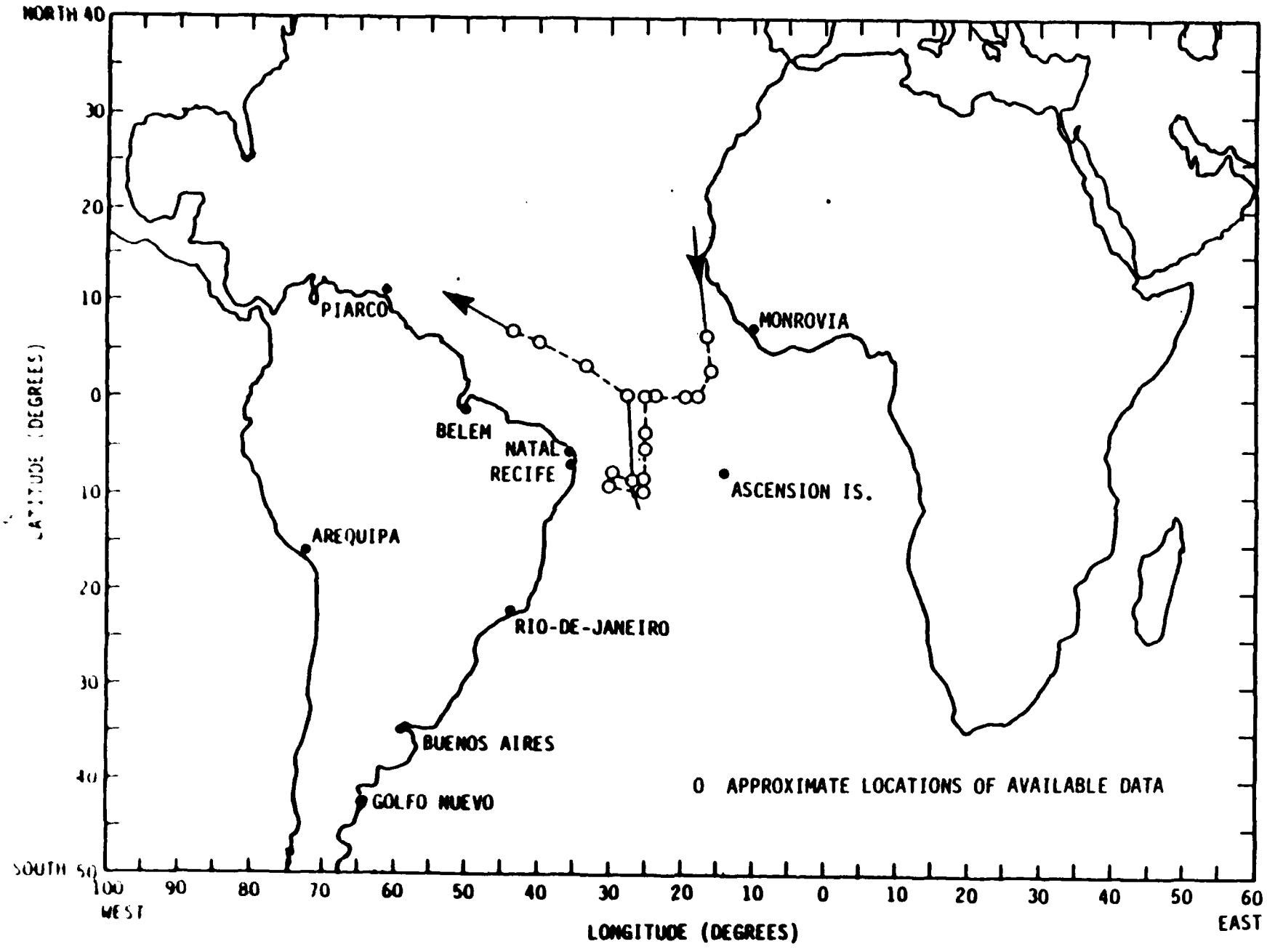

FIGURE 4-4 RESEARCHER CRUISE 2/19/80 - 3/12/80

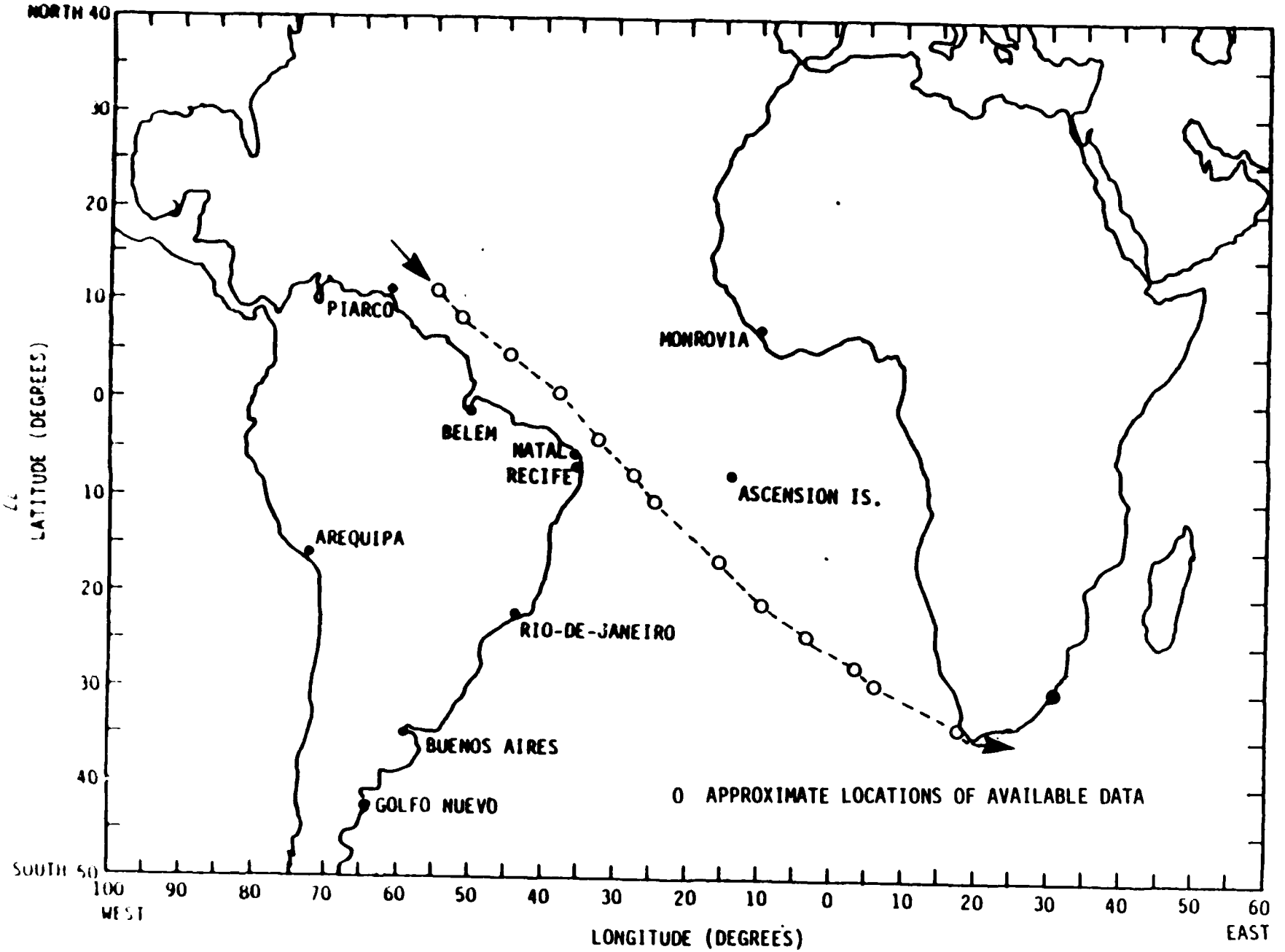

FIGURE 4-5 SHELDON CRUISE 4/22/80 - 5/4/80

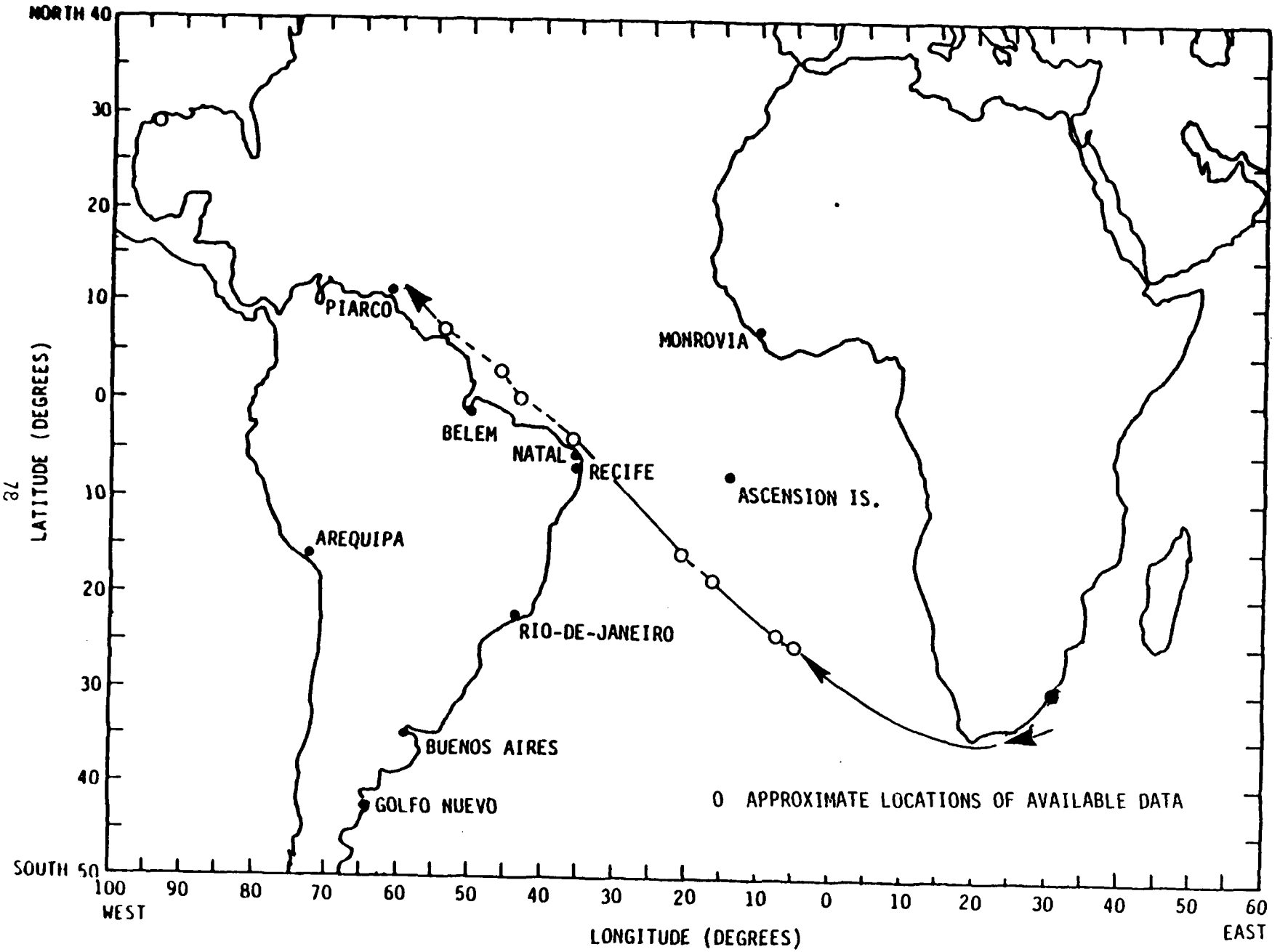

FIGURE 4-6 SHELDON CRUISE 6/10/80 - 6/18/80

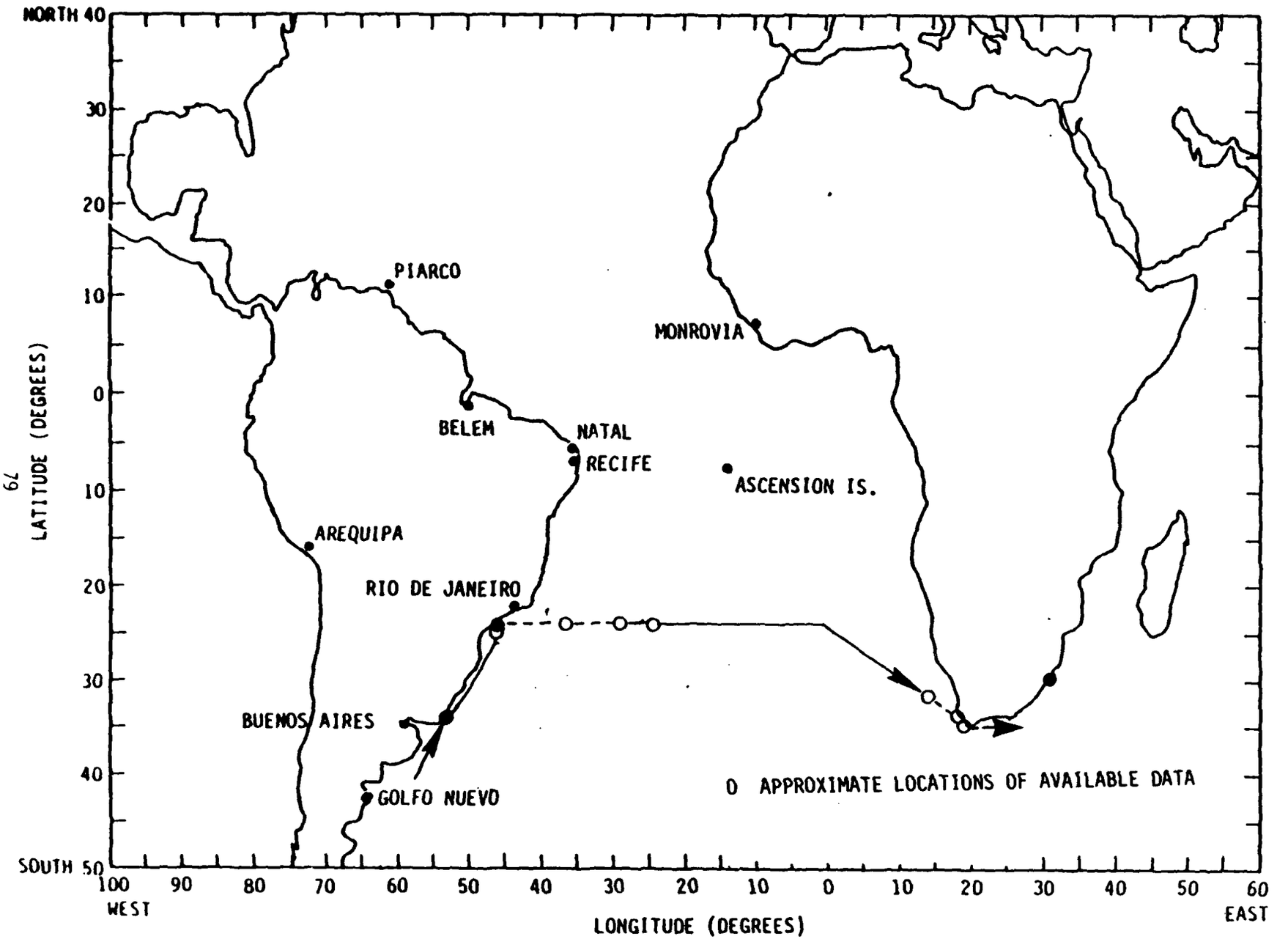

FIGURE 4-7 CATAMARCA II CRUISE 6/22/80 - 7/12/80

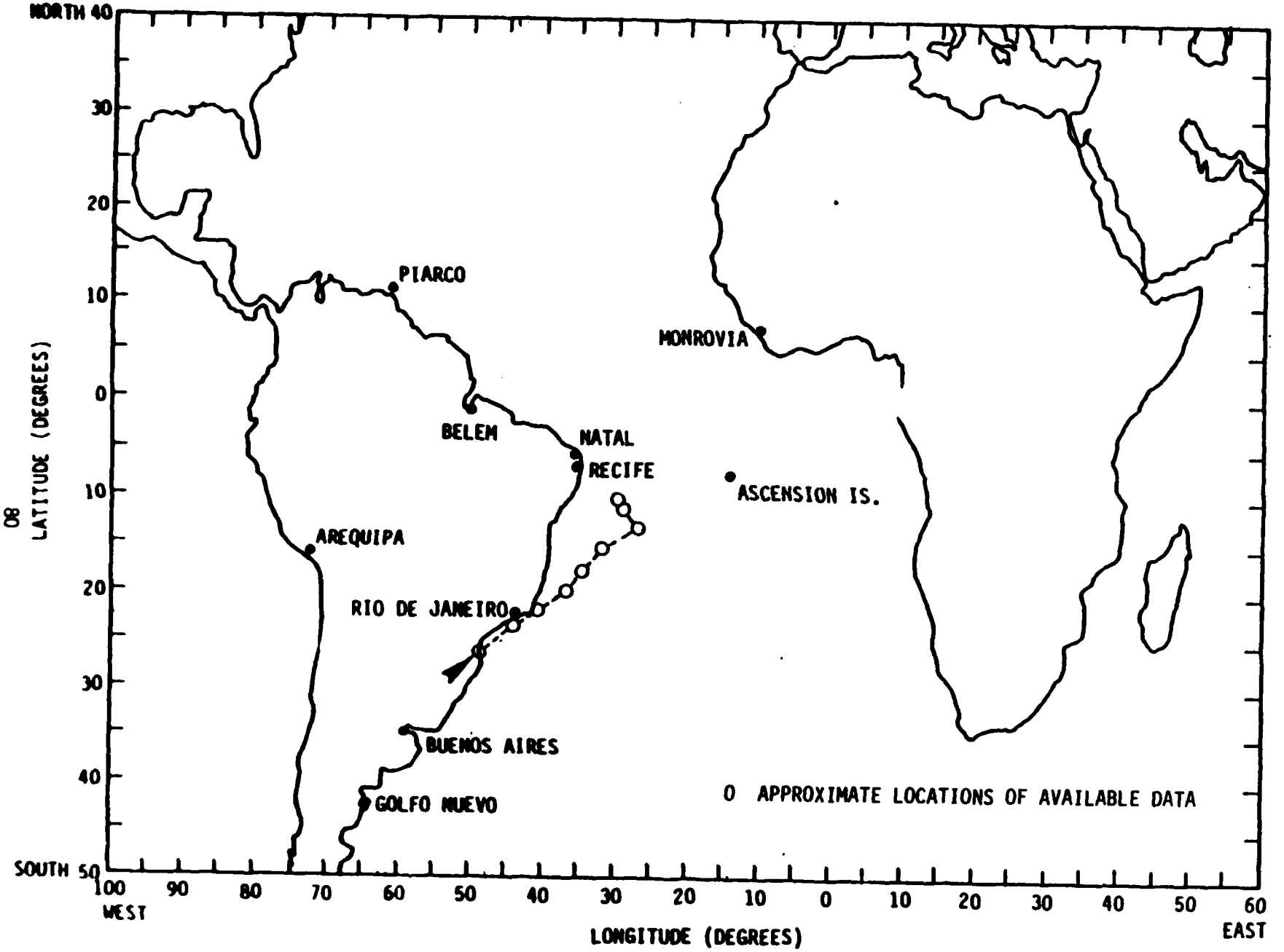

FIGURE 4-8 JULIO REGIS CRUISE 11/19/80 - 11/29/80

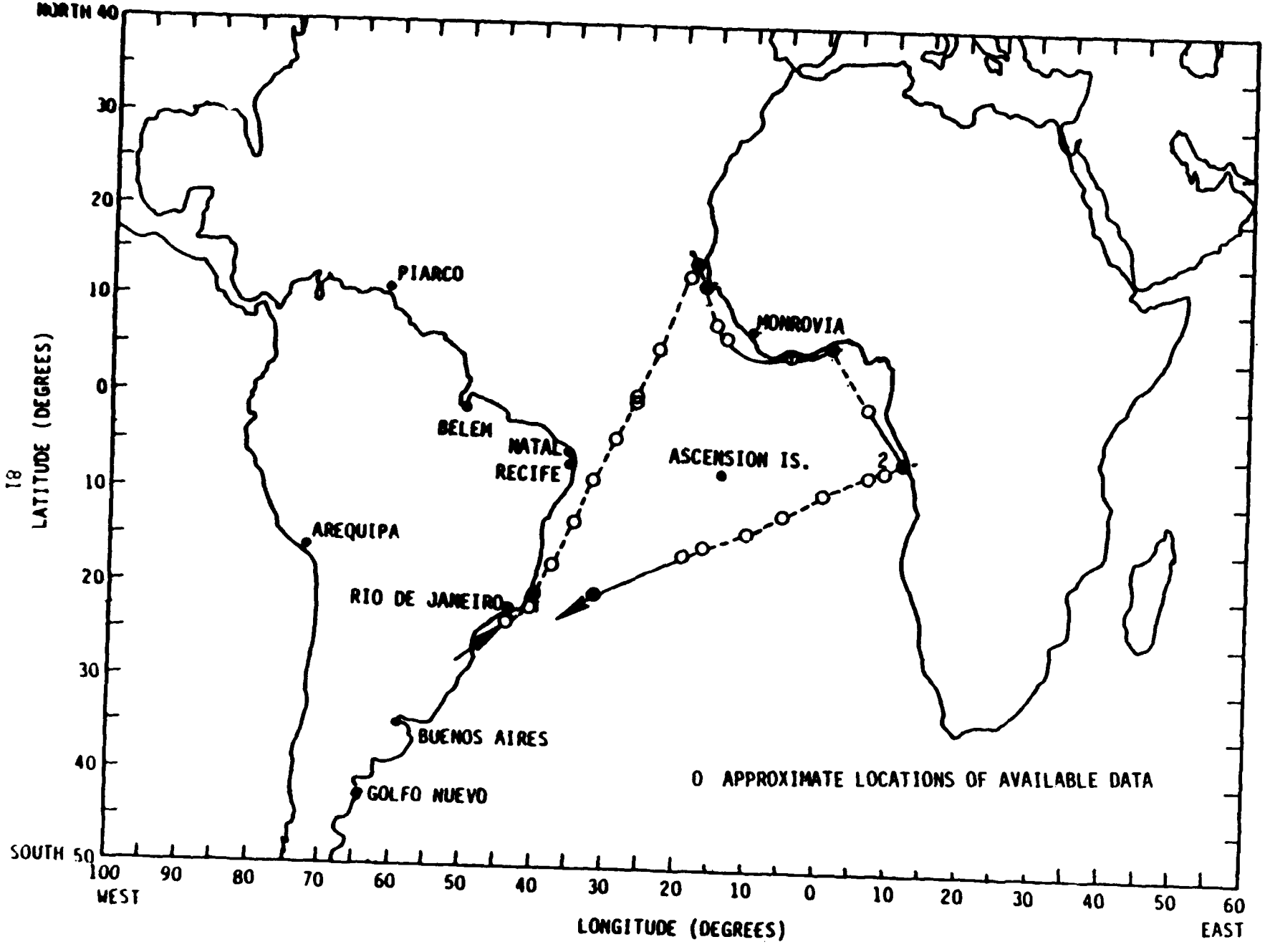

FIGURE 4-9 JULIO REGIS CRUISE 2/23/81 - 4/16/81

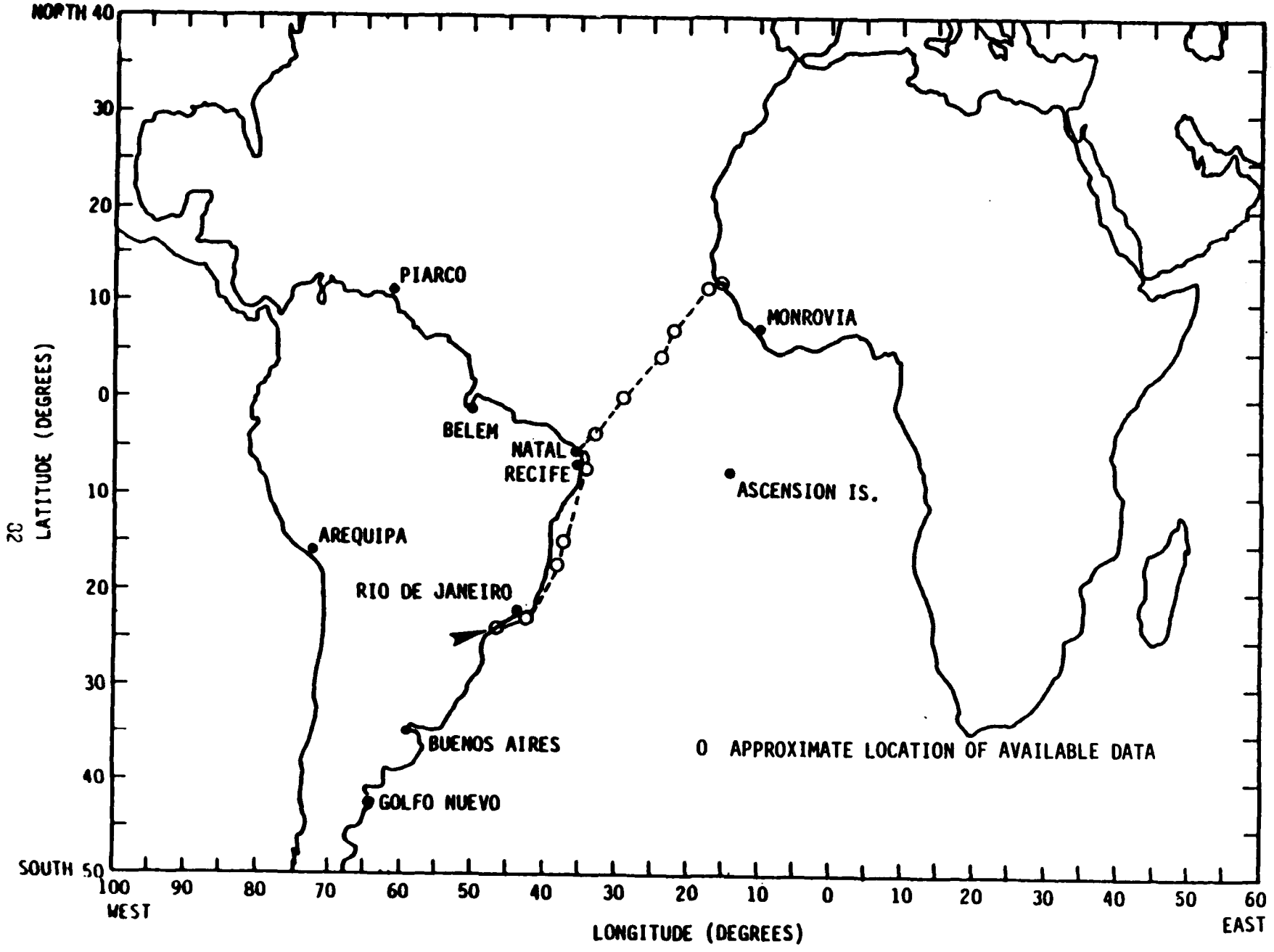

FIGURE 4-10 JULIO REGIS CRUISE 4/28/81 - 5/19/81

the value of IOS data is related to the proximity of measurement times to 0600 and 1800 GMT. In order to delete non-utile data, time windows of 0400-0800 GMT and 1600-2000 GMT have been arbitrarily established. Data falling outside these windows will not be considered in the analysis.

In order to utilize as much of the limited IOS data base as possible, "date windows" have also been used, as follows. All IOS data acquired during the months of January, February, and March have been consolidated and are assumed to be representative of February. Similarly, April, May, and June data are grouped as representative of May, and so on for the 3-month periods centered on August and November. In the case of the IOS data, then, a label of any particular month means that a validation is being performed for that month based on data available in a 3-month window centered on the month being labelled in the validation.

The use of 4-hour time windows and 3-month date windows must be perfomed with care. In particular, it is important that daytime data and night-time data not be combined.

It is known that propagation of Omega signals from a transmitter changes rapidly as a terminator passes over the transmitter. The effects of propagation changes can be readily observed as a rapid variation in SNR at a receiver. In order to avoid the possibility of interpolating or extrapolating measurement data across a terminator, it is necessary to define, for each Omega transmitter, the propagation condition (night or day) at the two times 0600 GMT and 1800 GMT, and for the date of the measurement.

The GMT of terminator crossing has been calculated for each transmitter site in the Omega network, for each day of the year. These times have been used to define acceptable windows, by GMT and month, to insure that all IOS data in any window represents either night propagation exclusively, or day propagation exclusively. Appendix D presents the results of this analysis, and defines the windows that have been used for final selection of IOS measurement data for statistical analysis.

Table 4-9 summarizes the availability of SNR measurements by transmitter, month, and GMT, where month and GMT are understood to refer to the windows just described.

TABLE 4-9

INTEGRATED OMEGA-SATELLITE DATA

OMEGA TRANSMITTER SNR MEASUREMENTS AT 10.2 kHz AND 13.6 kHz
FOR SOUTH ATLANTIC
(1979-1981)

Transmitter	Reference[1] Month	Time[2] (GMT)	Number of Readings
Norway (A)	February	6:00	29
	February	18:00	48
	May	6:00	41
	May	18:00	33
	November	6:00	12
	November	18:00	14
Liberia (B)	February	6:00	50
	February	18:00	43
	May	6:00	37
	May	18:00	34
	November	6:00	17
	November	18:00	21
Hawaii (C)	February	6:00	52
	February	18:00	47
	May	6:00	38
	May	18:00	37
	November	6:00	21
	November	18:00	21
North Dakota (D)	February	6:00	53
	February	18:00	54
	May	6:00	38
	May	18:00	39
	November	6:00	20
	November	18:00	23
La Reunion (E)	February	6:00	50
	February	18:00	49
	May	6:00	34
	May	18:00	37
	November	6:00	14
	November	18:00	11
Golfo Nuevo (F)	February	6:00	50
	February	18:00	47
	May	6:00	38
	May	18:00	40
	November	6:00	21
	November	18:00	24
Aust-alia (G)	No Data		
Japan (H)	No Data		

(1) Reference Month refers to 3-month period centered on indicated month.

(2) GMT refers to 4-hour time block centered on indicated GMT.

V. DESCRIPTION OF TEST AND TEST DATA

5.1 AIRBORNE MONITOR DATA

The Naval Ocean Systems Center (NOSC) of San Diego, California, was tasked with a significant field measurement and data analysis effort for the validation of Omega performance in the South Atlantic area. This effort included aircraft and temporary fixed-site measurements of Omega signals and the analysis of results [21, 22].

NOSC, in cooperation with the FAA, instrumented a Convair 880 aircraft with Omega receiving equipment. The aircraft was flown along the routes shown in Figure 5-1 in a sequence of fifteen flights from 19 April 1980 to 5 May 1980. Omega signal amplitude data were collected on all flights from Omega stations providing coverage for each route. The NOSC aircraft flights are summarized in Table 5-1. The flight numbers in Table 5-1 correspond to those shown in Figure 5-1. Table 5-2 lists flight terminal locations for the NOSC flights, and Table 5-3 lists the inventory of data available from the NOSC flights.

The aircraft flight routes were chosen to correspond to radials from selected transmitters, and the flights were timed to provide all-night or all-day illumination conditions along the flights. Table 5-4 summarizes the transmitters, radial bearings and illumination conditions for each of the NOSC flights.

5.2 TEMPORARY MONITORS

In addition to aircraft measurements, NOSC personnel established temporary fixed Omega monitor stations at Ascension Island, Blumenau, Brazil, and Trelew, Argentina. The temporary monitor stations provided measurement data during the same time period (March - June, 1980) as the aircraft measurements. Table 5-5 lists the locations of the NOSC temporary monitors and Table 5-6 lists the data inventory available.

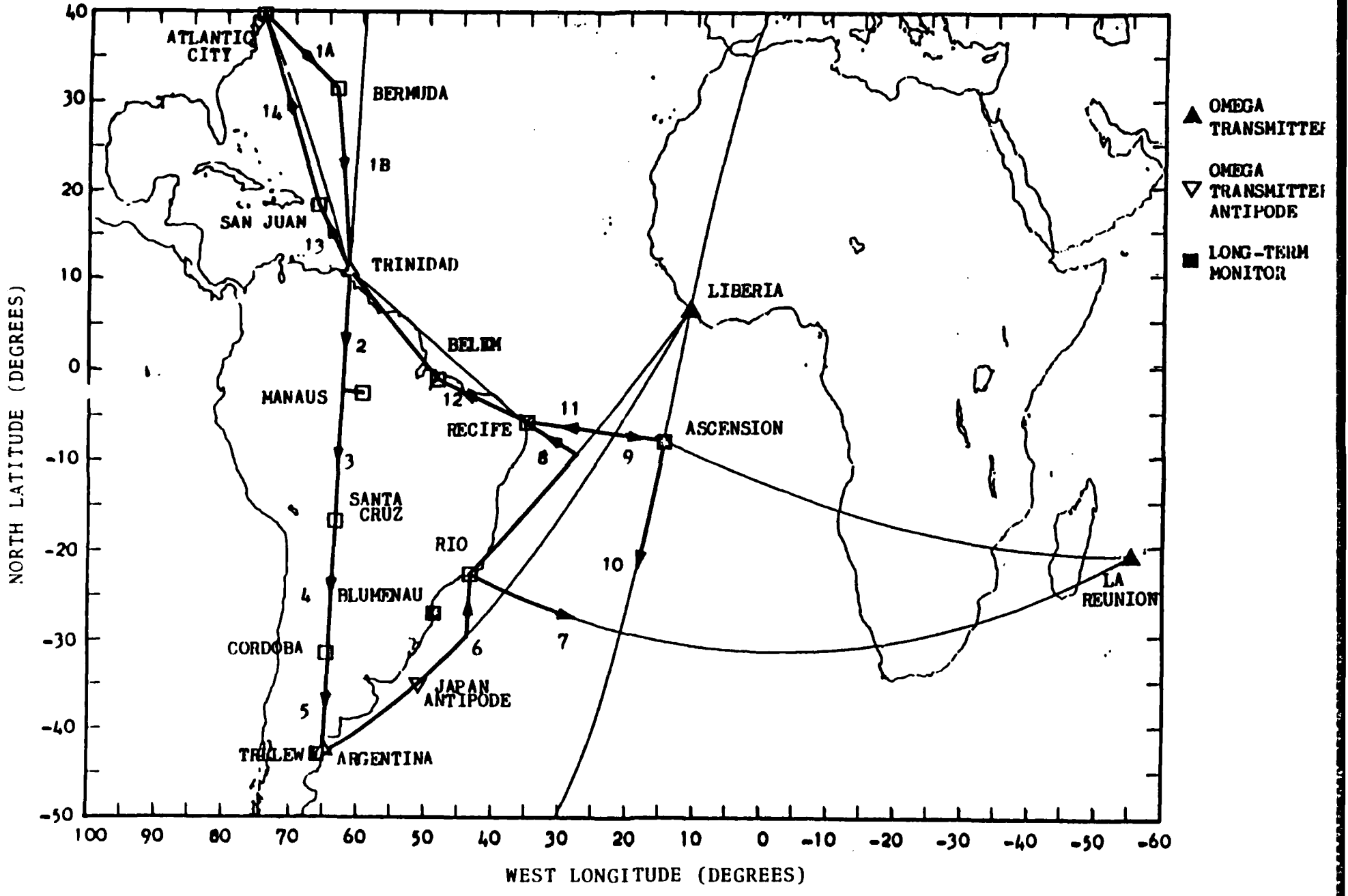

Figure 5-1 NOSC Aircraft Flight Paths and Fixed Receiver Sites

Table 5-1 1980 NOSC Aircraft Flight Itinerary
(Reference 22)

FLT. NO.	ORIGIN			DESTINATION			DURATION (HR)	OVERFLIGHT LOCATIONS
	LOCATION	DATE	GMT	LOCATION	DATE	GMT		
1A	Atlantic City	4/19	2002	Bermuda	4/19	2137	1.6	
1B	Bermuda	4/20	0022	Trinidad	4/20	0327	3.1	
2	Trinidad	4/21	0044	Manaus	4/21	0334	2.8	
3	Manaus	4/21	2314	Santa Cruz	4/22	0145	2.5	
4	Santa Cruz	4/22	2340	Cordoba	4/23	0138	2.0	
5	Cordoba	4/23	2240	Trelew	4/24	0019	1.6	Omega "F"
6	Trelew	4/25	2245	Rio de Janeiro	4/26	0233	3.8	Omega "F"
7	Rio de Janeiro	4/27	2222	Rio de Janeiro	4/28	0201	3.6	
8	Rio de Janeiro	4/28	2224	Recife	4/29	0216	3.9	
9	Recife	4/29	2304	Ascension	4/30	0145	2.7	Ascension
10	Ascension	4/30	2132	Ascension	5/1	0051	3.3	Ascension
11	Ascension	5/1	2137	Recife	5/2	0032	2.9	Ascension
12	Recife	5/2	2305	Belem	5/3	0111	2.1	
13	Belem	5/3	2310	San Juan	5/4	0242	3.5	
14	San Juan	5/5	0005	Atlantic City	5/5	0327	3.4	

Table 5-2 Location of Flight Terminals and Receiver Sites for NOSC Measurements
(References 21,22)

A. Flight Terminals

SITE NAME	COUNTRY	AIRFIELD	LATITUDE		LONGITUDE	
			DEG	MIN	DEG	MIN
Atlantic City	New Jersey	NAFEC	39	27N	74	35W
Bermuda	Bermuda	Bermuda NAS	32	22N	64	41W
Trinidad	Trinidad & Tobago	Piarco	10	36N	61	21W
Manaus	Brazil	Eduardo Gomez	3	22S	60	03W
Santa Cruz	Bolivia	El Trompillo	17	48S	63	11W
Cordoba	Argentina	Cordoba	31	19S	64	13W
Trelew	Argentina	Trelew	43	14S	65	19W
Galeao	Brazil	Galeao	22	49S	43	15W
Guararapes	Brazil	Guararapes	8	08S	34	55W
Wideawake	UK Territory	Wideawake Aux. AB	7	58S	14	24W
Val de Caes	Brazil	Val de Caes	1	23S	48	29W
Puerto Rico	Puerto Rico	Puerto Rico Int'l.	18	26N	66	00W

AD-A181 508 SOUTH ATLANTIC OMEGA VALIDATION VOLUME 1 SUMMARY ANALYSIS APPENDICES A-E(U) SYSTEMS CONTROL TECHNOLOGY INC PALO ALTO CA T M WATT ET AL. JAN 83 2/3

UNCLASSIFIED DTCG23-81-C-40023 F/G 17/7.3 NL

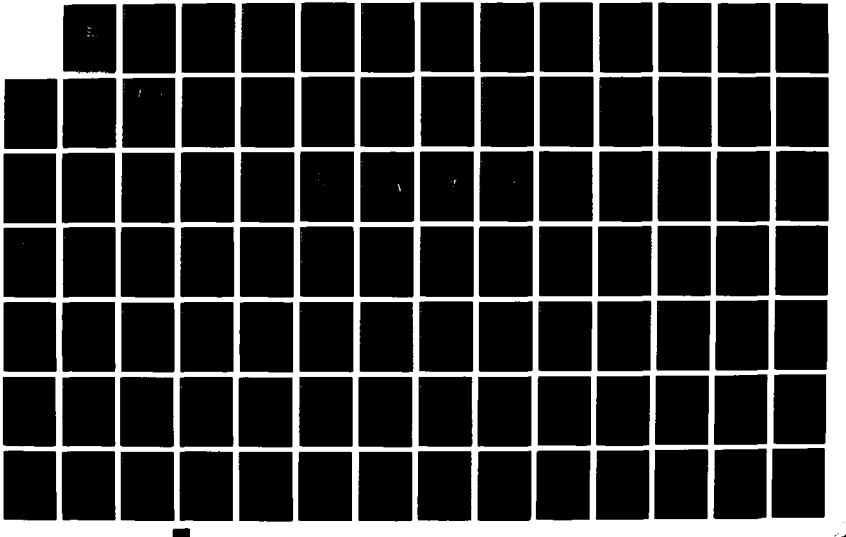

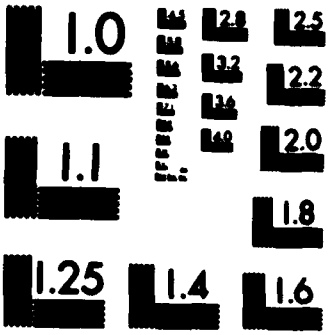

MICROCOPY RESOLUTION TEST CHART
NATIONAL BUREAU OF STANDARDS-1963-A

Table 5-3 1980 NOSC Flight Data Inventory
(References 21,22)

Flight			OMEGA TRANSMITTER									
			A		B		D		E		F	
No.	Origin	Day (D) Night (N)	10.2	13.6	10.2	13.6	10.2	13.6	10.2	13.6	10.2	13.6
1A	Atlantic City	D	X	X			X	X				
1B	Bermuda	N	X	X							X	X
2	Trinidad	N	X	X							X	X
3	Manaus	N	X	X							X	X
4	Santa Cruz						X	X			X	X
5	Cordoba	N					X	X			X	X
6	Trelew	N				X			X	X	X	X
7	Rio	N	X	X	X	X			X	X	X	
8	Rio	N	X	X	X	X			X	X	X	
9	Recife	N	X	X	X	X			X	X	X	
10	Ascension	N	X	X	X	X			X	X	X	
11	Ascension	N	X	X	X	X			X	X		X
12	Recife	N	X	X	X	X					X	
13	Belem	N	X	X	X	X					X	X
14	San Juan	N	X	X			X					X

FLT NO.	PRIMARY SIGNAL.				SECONDARY SIGNAL.				TERTIARY SIGNAL			
	XMTR	BEAR.	ILLUM.	FIG.	XMTR	BEAR.	ILLUM.	FIG.	XMTR	BEAR.	ILLUM.	FIG.
1A	NORTH DAKOTA	104-107	D	34								
1B	ARGENTINA	0-5	N	40	TRINIDAD	353	N	43	NORWAY	260-273	N	28
2	ARGENTINA	4-5	N	40	TRINIDAD	180-183	N	45	NORWAY	253-260	N	28
3	ARGENTINA	4-5	N	40	TRINIDAD	183	N	45	NORWAY	250-253	N	28
4	ARGENTINA	4-5	N	40	TRINIDAD	183	N	45	NORTH DAKOTA	145-151	SS	36
5	ARGENTINA	0-4	N	40	TRINIDAD	183	N	45	NORTH DAKOTA	151-156	SS	36
6	LIBERIA	220	N	32	ARGENTINA	49-59	N	42				
7	LA REUNION	246	N	37								
8	LIBERIA	227	N	31	ARGENTINA	49-56	N	42	NORWAY	221-231	N	20
9	LA REUNION	262-270	N	38								
10	LIBERIA	195	N	33	NORWAY	208	N	30				
11	LA REUNION	262-270	N	39								
12	TRINIDAD	124-132	N	46								
13	ARGENTINA	359-4	N	41	TRINIDAD	130/332	N	46/44				
14	ARGENTINA	353-359	N	41	TRINIDAD	332-343	N	44	NORTH DAKOTA	103-126	SS	35

N = night, D = day, SS = sunset transition

Table 5-4 Summary of Aircraft Radial Data Plots
(Reference 22)

Table 5-5 NOSC Temporary Monitor Stations
(References 21,22)

SITE NAME	OPERATING AGENCY/ACTIVITY/LOCATION	LATITUDE			LONGITUDE		
		DEG	MIN	SEC	DEG	MIN	SEC
Ascension	NASA STDN Station, Devils Ashpit, Ascension Island	7	59	19S	14	19	41W
Brazil	Institute for Space Activities, Bluemenau, Brazil	27	0	0S	48	0	0W
Argentina	Argentine Navy, Omega Station, Trelew, Argentina	43	3	13S	65	11	28W

Table 5-6 Data Available from NOSC Monitor Sites
(Reference 22)

RECEIVING SITE	MONITORING PERIOD			OMEGA TRANSMITTERS OBSERVED						
	START	END	DAYS	A	B	C	D	E	F	H
Ascension	21 Mar	30 Jun		61	41	61	41	61	41	61
Brazil	21 Mar	30 Jun		2	100	1	100	2	102	-
Argentina	25 Apr									

5.3 AMPLITUDE AND NOISE MEASUREMENTS

5.3.1 Airborne Monitor Measurements

The NOSC Report [22] presents measurement data of both signal amplitude and radio noise from the aircraft flights. Because of the limited durations of the flights and the times chosen for the flights, one can, to a first approximation, ignore the passage of time during a flight and consider the observed variations to be due to spatial movement of the observing platform.

The NOSC Report presents plots of observed signal amplitude in dB relative to 1 microvolt/meter vs time for all flights [1-14].

Continuous data from the Tracor 599H receivers generally were calibrated by fitting to the highly stable discrete measurements from a wave analyzer. Table 5-7 summarizes the signal-amplitude data available from the NOSC flights by date, frequency, flight number and transmitter.

Noise measurements were also made during the aircraft flights. Noise data were obtained at 10.2 kHz and 13.6 kHz. Table 5-8 lists all the noise measurements and the observed noise levels during the flights.

Tabulated values were derived from the HP Wave Analyzer stripchart recordings made at periodic intervals throughout most flights. Readings were calibrated to absolute levels and adjusted to an equivalent observation bandwidth of 100 Hz. However, no adjustments to convert values to equivalent RMS levels for impulsive noise have been included in the listings. Because of possible contamination by aircraft power system harmonics, the data are presented more as indications of actual noise levels encountered by the receiving systems rather than measures of true atmospheric noise. The typical values shown are consistent with those expected from the tracking response of the receivers; i.e., response deteriorates when signal levels decrease such that SNRs are in the -20 to -30 dB range, the nominal limit for the equipment.

Table 5-7 Summary of NOSC Signal-Amplitude Time Plots For Aircraft Flights 1-14

DATE	FREQUENCY KHz	FLIGHT NO.	OMEGA TRANSMITTI						
			A	B	C	D	E	F	H
4/19/80	10.2	1A	✓		✓	✓			
	13.6		✓		✓	✓			
4/20/80	10.2	1B	✓		✓	✓		✓	
	13.6		✓		✓	✓		✓	
4/21/80	10.2	2	✓		✓	✓		✓	
	13.6		✓		✓	✓		✓	
4/21-4/22/80	10.2	3	✓		✓	✓		✓	
	13.6		✓			✓		✓	
4/22-4/23/80	10.2	4		✓	✓	✓		✓	
	13.6				✓	✓		✓	✓
4/23-4/24/80	10.2	5			✓	✓		✓	✓
	13.6			✓	✓	✓		✓	✓
4/25-4/26/80	10.2	6		✓	✓	✓	✓	✓	✓
	13.6			✓	✓	✓	✓	✓	✓
4/27-4/28/80	10.2	7	✓	✓	✓	✓	✓	✓	✓
	13.6		✓	✓	✓	✓	✓	✓	✓
4/28-4/29/80	10.2	8	✓	✓	✓	✓	✓	✓	
	13.6		✓	✓	✓	✓	✓	✓	
4/29-4/30/80	10.2	9	✓	✓	✓	✓	✓	✓	
	13.6		✓	✓	✓	✓	✓	✓	
4/30-5/1/80	10.2	10	✓	✓		✓	✓	✓	
	13.6		✓	✓	✓	✓	✓	✓	
5/1-5/2/80	10.2	11	✓	✓		✓	✓	✓	
	13.6		✓	✓		✓	✓	✓	
5/2-5/3/80	10.2	12	✓	✓		✓	✓	✓	
	13.6		✓	✓		✓	✓	✓	
5/3-5/4/80	10.2	13	✓	✓	✓	✓		✓	
	13.6		✓	✓	✓	✓		✓	
5/5/80	10.2	14	✓		✓	✓			
	13.6		✓		✓	✓		✓	

FLT.	JULIAN DAY, YEAR	GMT	LAT	LONG	10.2 KHZ NOISE						13.6 KHZ NOISE					
					3 HZ BW		10 HZ BW		100 HZ BW		3 HZ BW		10 HZ BW		100 HZ BW	
					S	T	S	T	S	T	S	T	S	T	S	T
01A	11080	2023	38.0	72.8			44.0	41.5	41.0	41.5			42.0	39.0	38.0	36.0
		2102	34.2	67.9			44.0	43.5	40.0	41.5			43.0	41.0	37.0	35.0
		2140	32.4	64.7				42.5		41.5				39.0		37.0
01B	111	0009	32.4	64.7				44.5		43.5						
		0043	30.3	64.4			47.0	47.5	43.0	44.5			47.0	47.0	41.0	40.0
		0119	25.8	63.6		50.5	50.0	47.5	45.0	44.5			49.0	47.0		42.0
		0152	21.7	63.0			51.0	50.5	46.0	46.5			50.0	49.0	44.0	42.0
		0220	18.1	62.5			53.0	50.5	48.0	46.5			51.0	49.0	46.0	43.0
		0250	14.4	62.1			52.0	49.5	45.0	45.5			51.0	50.0	45.0	44.0
02		2343	10.5	61.4				48.5						41.0		
	112	0138	05.5	61.7			47.0	47.5	43.0	47.5			45.0	41.0	41.0	38.0
03		2328	-02.8	61.3		50.5	45.0	48.5	47.0	48.5			43.0	44.0		41.0
	113	0010	-07.1	62.6		53.5				50.5		50.0				45.0
		0106	-14.1	63.0			45.0	50.5	46.0	50.5		45.0		44.0		44.0
04		2332	-17.8	63.2			45.0		44.0							
		2355	-19.3	63.2			47.0	48.5								
	114	0007	-20.9	63.3	49.0	47.5		49.5	45.0	48.5	46.0				41.0	43.0
		0038	-25.1	63.7			44.0	46.5	43.0	51.5	46.0	45.0			41.0	43.0
05		2151	-31.3	64.2	45.0	43.5					43.0	41.0				
		2229	-31.3	64.2								45.0				
		2304	-34.2	64.5	49.0	46.5			43.0	46.5	48.0	43.0				
		2335	-38.7	64.8	49.0	46.5			44.0	50.5	48.0	44.0	47.0	43.0	42.0	42.0
06*	116	2315	-41.3	61.4	43.0	47.5			42.0	47.5	44.0	41.0		42.0	39.0	40.0
		2352	-38.3	56.0		44.5	42.0	47.5	41.0	48.5	47.0	45.0	41.0	44.0	39.0	41.0
	117	0038	-34.2	50.1	45.0	48.5	45.0		41.0	48.5		43.0	44.0	45.0	39.0	42.0
		0114	-31.3	45.6	42.0	45.5	41.0	46.5	40.0	47.5		44.0	40.0	43.0	38.0	42.0
		0209	-24.9	43.7		48.5	41.0	49.5	41.0	49.5			38.0	41.0	36.0	39.0
07	118	2150	-22.8	43.3							38.0				35.0	
		2245	-23.6	40.8	43.0		41.0		42.0		41.0		40.0		38.0	
		2314	-24.8	37.0	41.0											
		2323	-25.1	35.8	41.0				40.0		39.0		39.0		36.0	
	119	0003	-26.4	30.2	42.0		40.0		40.0		40.0		38.0		36.0	
		0033	-25.9	32.6	41.0		41.0		40.0		42.0		39.0		36.0	
		0103	-24.8	36.7	40.0		40.0		40.0				36.0		36.0	
		0133	-23.6	40.8	43.0		42.0		41.0				39.0		35.0	

T = TRACOR LOOP

S = SPEARS LOOP

* Tracor loop breaking loose from fuselage-noise probably too high

Table 5-8 Observed Aircraft Noise (dB/1μV/meter) for Equivalent 100 HZ Bandwidth

(Reference 22)

FLT.	DAY YEAR	GMT	LAT	LONG	10.2 KHZ NOISE						13.6 KHZ NOISE					
					3 HZ BW		10 HZ BW		100 HZ BW		3 HZ BW		10 HZ BW		100 HZ BW	
					S	T *	S	T	S	T	S	T	S	T	S	T
08		2302	-20.3	40.3	44.0		44.0		43.0		44.0		43.0		39.0	
		2332	-17.7	37.1	44.0				41.0		41.0		40.0		38.0	
	120	0003	-14.6	33.8			43.0		42.0		42.0		41.0		38.0	
		0032	-12.1	30.9			43.0		42.0				43.0		39.0	
		0132	-09.1	30.9			42.0		42.0				41.0		38.0	
		0152	-08.5	33.4			43.0		42.0				40.0		38.0	
09		2339	-08.4	30.8	45.0		44.0		42.0		43.0		44.0		40.0	
	121	0012	-08.5	26.3			45.0		42.0				44.0		41.0	
		0047	-08.4	21.5			44.0		42.0				44.0		40.0	
		0117	-08.2	17.3	47.0		45.0		42.0		44.0		40.0		40.0	
10		2109	-08.0	14.4	47.0		48.0				45.0		44.0			
		2200	-10.9	15.2			46.0		44.0		47.0		44.0		40.0	
		2234	-15.2	16.4	46.0				42.0		43.0				39.0	
		2302	-18.6	17.3	46.0		44.0		42.0		45.0		44.0		40.0	
		2338	-15.9	16.6	45.0		44.0		42.0		42.0		42.0		38.0	
	122	0008	-12.1	15.5	45.0		43.0		42.0		43.0		41.0		38.0	
11		2203	-08.2	17.2			45.0		46.0				43.0		41.0	
		2233	-08.4	21.0			45.0		42.0				43.0		40.0	
		2302	-08.5	24.6	49.0		46.0		43.0				43.0		39.0	
		2333	-08.5	28.4			43.0		42.0				43.0		39.0	
	123	0002	-08.4	31.9			45.0		42.0				44.0		40.0	
12		2326	-07.3	36.8	46.0		45.0		44.0		45.0		42.0		39.0	
	124	0009	-04.7	42.1			44.0		41.0				43.0		39.0	
		0046	-02.4	46.6			44.0		42.0				45.0		40.0	
13		2332	0.3	50.1	46.0		46.0		45.0				46.0		41.0	
	125	0002	3.2	53.0			43.0		42.0				39.0		38.0	
		0032	6.1	55.9			42.0		42.0				42.0		40.0	
		0102	8.6	59.0			42.0		42.0				41.0		39.0	
		0146	13.0	62.9			42.0		42.0				40.0		39.0	
14	126	0036	21.5	67.2	52.0		52.0		49.0		50.0		49.0		45.0	
		0105	24.9	68.1			50.0		46.0				50.0		44.0	
		0145	29.6	69.4			50.0		45.0				49.0		44.0	
		0218	33.5	70.5			53.0		48.0				47.0		44.0	
		0246	36.9	71.5			52.0		47.0				50.0		44.0	
		0320	39.4	74.4			50.0		46.0				50.0		44.0	

* Tracor loop inoperative beginning FLT 7

Table 5-8 (Continued)

5.3.2 Temporary Monitor Measurements

Temporary monitors set up at selected ground sites obtained four types of data during the NOSC tests; (a) absolute field intensities, (b) radio noise, (c) solar events, and (d) diurnal behavior of Omega signal amplitudes.

Absolute field intensity measurements were performed with a wave analyzer and represent a means of calibrating signal amplitude measurements obtained by the Omega receivers. Field intensity data were presented in Reference 22 only from Ascension Island, and these data are listed in Table 5-9. Nearly all field intensity measurements were made during local daytime hours.

A limited amount of radio noise data were also obtained at Ascension Island. Table 5-10 presents these results. Measurements were made with the same instrumentation used in the absolute field intensity observations, except that the wider bandwidths on the wave analyzer were employed.

The general procedure followed was to check any directionality of the noise and to make measurements in the maximum and minimum directions. If no preference was noted, measurements in north-south and east-west directions were made.

Although no evidence of other than wide-band noise was noted at the time of these measurements, subsequent long-term monitoring indicated significant local interference on 13.6 kHz at Ascension Island.

Table 5-11 lists the major solar flares observed during the period of the NOSC tests. The events expected to have the largest effect on Omega signals are those indicated as "X events" because of the large amount of x-rays emitted by those flares. Ionospheric disturbances produced by these flares were seen in the amplitude data. Effects were varied with some signals being affected on one frequency but not the other, or with one frequency increasing in amplitude while the other was decreasing. These phenomena could be expected to occur on those signals exhibiting modal interference, and there may be some effects associated with equatorial propagation which have been observed but not analyzed in this report. The weekly statistics presented as plotted diurnal behavior do show the effects of the larger flares, but none of the effects appear as drastic as that which typically occurs with phase data.

Table 5-9 Summary of Absolute Field Intensity Measurements
(Reference 22)

RECEIVING SITE		DATE/TIME			TRANSMITTER	FREQ (kHz)	F.I. dB/1μV/m)
NAME	NO.	MON	DAY	GMT			
Ascension	1	4	30	1548	Liberia	10.2	65.1
				1555			>63.0
	2	5	1	0939			57.7
	2	5	1	0941		11.05	57.0
				1018			>54.5
	2	5	1	0943		11.33	57.6
				1018			>56.4
	1	4	30	1545		12.0	64.9
				1608			>63.0
	2	5	1	0937			57.5
				1019			>57.9
	1	4	30	1549		13.6	65.6
				1609			>63.0
	2	5	1	0945			58.3
	1	4	30	1555	Argentina	10.2	48.2
	2	5	1	0953			45.8
	2	5	1	0955		11.05	46.7
	2	5	1	0957		11.33	46.4
	1	4	30	1554		12.9	52.3
	2	5	1	0950			45.6
				1019			>42.2
	1	4	30	1557		13.6	49.6
	2	5	1	0958			46.0

RECEIVING SITE		DATE/TIME			LOOP ANTENNA BEARING	FREQ. (KHZ)	NOISE(dB/1μV/m in B.W. below)					100 HZ RMS	CCIR PRED.
NAME	NO.	MON-DAY-GMT					3	10	30	100	300		
Ascension	1	4	30	1607	N-S	10.0				49			
				1615	E-W					52			
				1608	N-S	12.0				48			
				1616	E-W					50			
				1609	N-S	14.0				47			
				1617	E-W					47			
				0949		10.2				36			
				0953		11.05				36			
				0956	ARG	11.33				36			
				0959		13.6				35			
	2	5	1	1017	N-S	10.0				42			
				1024	E-W					42			
				1034	OMNI					42			
				1018	N-S	12.0				41			
				1025	E-W					41			
				1019	N-S	14.0				39			
				1026	E-W					39			
				1031	OMNI					40			

Table 5-10 Summary of Observed Noise Measurements
(Reference 22)

MONTH	DAY	GMT			X-RAY CLASS	PCA?
		START	MAX.	END		
MAR	27	1242	1312	1344	M2	
	27	1835	1842	1912	M5	
	28	0953	0957	1001	M1	
	28	1958	2004	2016	M2	
	28	2156	2201	2209	M4	
	29	0953	0956	1002	M1	
APR	2	1944	1956	2012	M2	
	3	0114	0124	0142	M1	
	3	0633	0725	0757	M2	
	4	1455	1523	1612	M5	✓
	5	0343	0356	0419	M2	
	5	0553	0605	0619	M1	
	5	1545	1556	1609	M5	
	6	0402	0413	0457	M5	
	6	1413	1427	1624	X2	
	7	0048	0110	0150	M4	
	7	0527	0541	0625	M8	
	7	1839	1845	1900	M1	
	8	0113	0124	0138	M1	
	8	0149	0157	0205	M1	
	8	0257	0307	0346	M4	
	9	0514	0518	0522	M1	
	10	0914	0922	0945	M4	
	10	1732	1734	1750	M3	
	11	2256	2312	2335	M2	
	12	0901	0925	0949	M1	
	12	2037	2051	2122	M2	
	12	2223	2228	2230	M2	
	12	2245	2254	2305	M1	
	13	0402	0409	0431	M1	
	14	2135	2139	2145	M1	
	15	0202	0208	0212	M1	
	15	0545	0551	0555	M1	
	15	1506	1512	1527	M8	

MONTH	DAY	GMT			X-RAY CLASS	PCA?
		START	MAX.	END		
APR	16	0056	0104	0115	M1	
	20	0637	0646	0734	M1	
	26	0326	0333	0343	M2	
	26	2028	2032	2049	M5	
	27	1927	1930	1937	M1	
	28	1234	1240	1302	M2.1	
	29	1255	1258	1309	M2.0	
	30	1101	1130	1146	M2.0	
	30	2018	2026	2040	M2.2	
MAY	1	1553	1601	1612	M1.1	
	1	1619	1632	1639	M4.0	
	1	1910	1916	1943	X3.0	
	1	2055	2108	2134	M2.8	
	3	1305	1320	1350	M2.1	
	3	1747	1757	1808	M1.1	
	7	1315	1320	1331	M4.6	
	8	0054	0058	0104	M2.4	
	8	1124	1129	1135	M1.1	
	8	1339	1344	1352	M1.1	
	8	1934	1938	1945	M2.0	
	9	0709	0714	0729	M7.2	
	9	2013	2056	2104	M3.8	
	10	1128	1133	1137	M1.2	
	11	0408	0415	0428	M1.2	
	11	2340	2344	2348	M3.3	
	14	1254	1258	1316	M2.0	
	14	1913	1925	1955	M1.0	
	15	2016	2047	2108	M2.0	
	16	2204	2233	2241	M2.1	
	17	0730	0737	0756	M2.6	
	17	1009	1017	1028	M1.1	
	18	0102	0114	0132	M3.0	
	20	1339	1425	1608	M1.1	
	21	2051	2107	2144	X1.4	

Table 5-11 Summary of Solar X-Ray/Proton Events (MAR-APR-MAY-JUN 1980)
(Reference 22)

MONTH	DAY	GMT			X-RAY CLASS	PCA?
		START	MAX.	END		
MAY	22	2054	2102	2140	M2.1	
	23	2142	2147	2152	M1.1	
	25	0187	0134	0156	M1.9	
	27	2128	0010	0098	M1.0	
	28	0211	0217	0231	M2.2	
	28	1653	1721	1739	M3.6	
	28	1943	1952	1957	X1.1	
	28	2156	2207	2222	M2.8	
	28	2335	2344	0010	M6.9	
	29	0506	0518	0535	M1.8	
JUN	1	1921	1939	2001	M2.7	
	2	0715	0736	0800	M2.6	
	2	0900	0923	0930	M1.0	
	2	2103	2143	2205	M2.1	
	3	0113	0124	0129	M1.0	
	3	0739	0809	0821	M2.1	
	3	1137	1144	1149	M1.1	
	3	1157	1209	1219	M3.7	
	3	2125	2134	2211	M7.2	
	4	0654	0655	0705	M6.7	
	4	0751	0847	0932	M4.0	
	4	2255	2301	2309	X2.2	
	5	0021	0036	0046	M1.3	
	5	1134	1139	1144	M1.1	
	6	2128	2133	2137	M1.4	
	7	0115	0119	0125	M2.5	
	7	0309	0314	0320	M7.3	
	7	1241	1251	1308	M1.6	
	8	1025	1038	1117	M4.4	
	8	1651	1702	1728	M1.7	
	19	1830	1841	1849	M1.2	
	19	1854	1858	1904	M1.1	
	19	1948	2010	2029	M2.3	
	21	0040	0059	0117	M2.7	

MONTH	DAY	GMT			X-RAY CLASS	PCA?
		START	MAX.	END		
JUN	21	0117	0120	0146	X2.6	
	22	1306	1324	1345	M1.9	
	22	1857	1910	1923	M1.3	
	23	0211	0218	0234	M2.1	
	23	0355	0400	0405	M2.1	
	23	1237	1245	1257	M1.0	
	23	2308	2312	2323	M2.2	
	23	2332	2341	0003	M4.6	
	24	1519	1524	1540	M1.1	
	24	1955	2003	2019	M1.0	
	25	1547	1554	1607	M4.8	
	27	0110	0115	0124	M1.0	
	27	1611	1618	1634	M6.7	
	28	0242	0253	0304	M1.0	
	28	0319	0330	0348	M1.4	
	28	0744	0751	0757	M1.3	
	28	1105	1112	1122	M1.3	
	29	0233	0237	0245	M3.6	
	29	1038	1043	1108	M4.2	
	29	1800	1805	1813	M1.0	
	29	1821	1826	1840	M4.2	

Table 5-11 (Continued)

Diurnal amplitude variations of Omega signals were observed at Ascension Island and Blumenau, Brazil. Observations over periods of one day (April 1980) and eight days (16–23 April, 16–23 May 1980) were performed separately. Data obtained during the eight-day observations were averaged to provide single 24-hour plots of signal amplitude for each frequency and station observed. Standard deviations were calculated and plotted along with mean values for the cases that were averaged. Figure 5-2 illustrates an example of the diurnal amplitude-variation plots. The totality of available plots is contained in Reference 22.

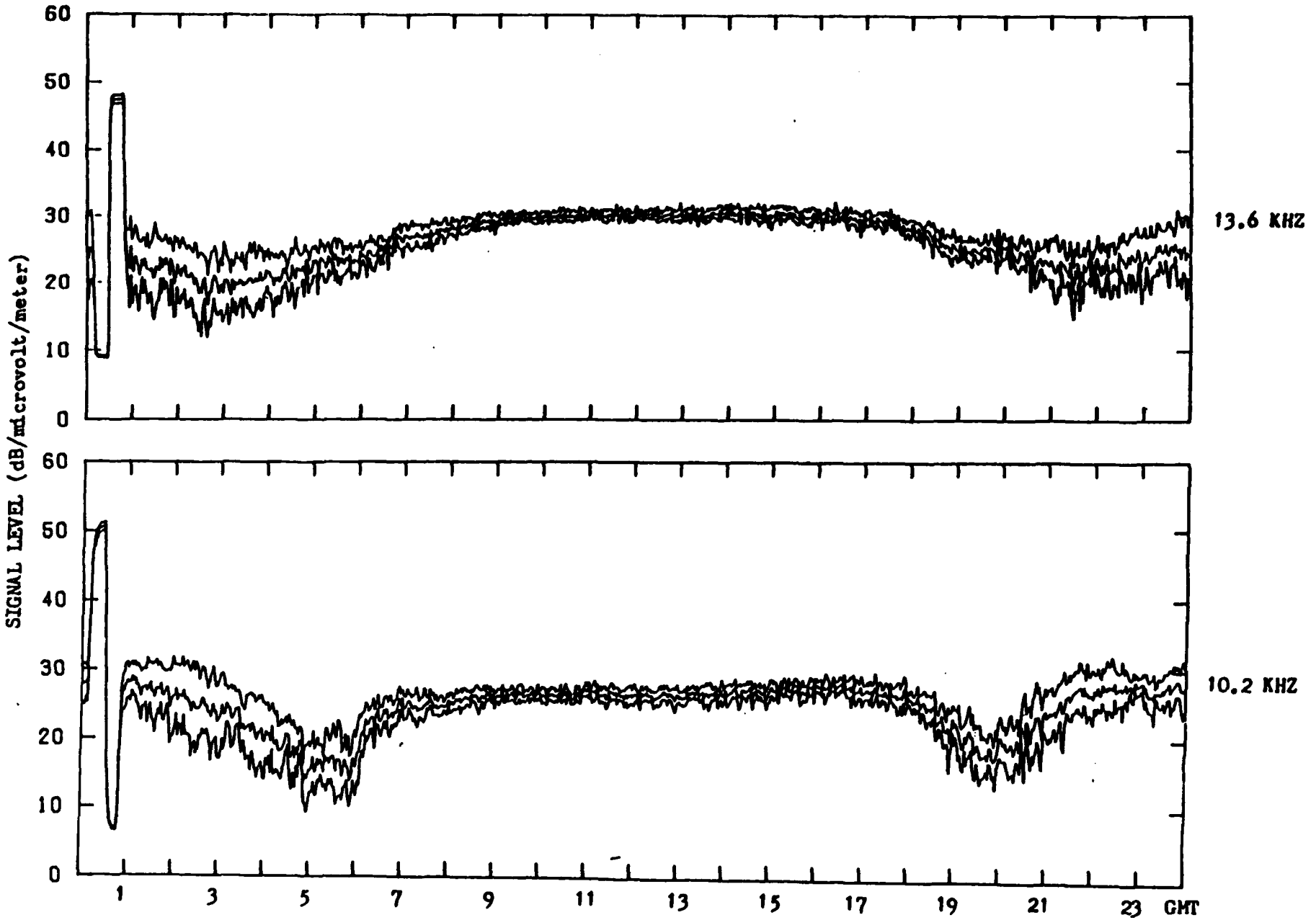

Figure 5-2 Average and Standard Deviation of Observed Signal Level OMEGA Norway at Ascension Island: 16-23 May 1980 (137-144) (Reference 22)

VI. CLASSIFICATION AND SYNTHESIS OF DATA

6.1 ANALYSIS CATEGORIES

The following aspects of Omega performance in the South Atlantic are addressed in this validation study:

(1) Signal Coverage at 10.2 kHz at 0600 and 1800 GMT for February, May, August and November.

(2) Signal Coverage at 13.6 kHz at 0600 and 1800 GMT for February, May, August and November.

(3) Geometric Dilution of Precision (GDOP).

(4) Diurnal Error in LOPs at 10.2 kHz for February, May, August and November.

(5) Diurnal Error in LOPs at 13.6 kHz for February, May, August and November.

(6) LOP Error Statistics at 10.2 kHz at 0600 and 1800 GMT for February, May, August and November.

(7) LOP Error Statistics at 13.6 kHz at 0600 and 1800 GMT for February, May, August and November.

(8) Fix Error Statistics at 10.2 kHz at 0600 and 1800 GMT for February, May, August and November.

(9) Fix Error Statistics at 13.6 kHz at 0600 and 1800 GMT for February, May, August and November.

Each analysis is independent of the others, and requires its own data base. The GDOP analysis requires no data other than Omega transmitter locations. All other analyses are based on actual measurements of Omega signals.

Except for the GDOP case, all these analyses are statistical in nature, and the validity of the results for each analysis is strongly dependent on the size and breadth of the data base used for the analysis, as well as the quality of any measurements that contribute to the data base. In addition, the efficacy of the entire validation process is fundamentally dependent on the quality and reliability of the underlying measurement data. Accordingly,

the analysis of Omega performance categories as described above has been based almost entirely on Masterfile and IOS data, which are the only sources of data representing both high quality and statistical significance.

Sections 6.2 through 6.6 describe each of the analysis categories (a)-(i), the information that is needed for the analysis, and the data that are available and are used to support the analysis.

6.2 SIGNAL COVERAGE AT 10.2 KHZ AND 13.6 KHZ

The analysis of signal coverage at 10.2 kHz involves a comparison of predicted coverage and observed coverage, and a modification of coverage predictions to conform to observations. The two sets of information required for this analysis are (a) predictions of Omega signal coverage in the South Atlantic, and (b) measurements of SNR in the South Atlantic over as wide a range of spatial and temporal conditions as possible.

Omega signal coverage predictions for 10.2 kHz have been calculated by The Analytical Sciences Corporation under a separate contract [18]. The predictions are available in the form of contours on Mercator-projection maps. Predictions are provided for the times 0600 GMT and 1800 GMT and for the months of February, May, August and November. At each GMT/month combination, predictions have been provided that describe the usability of signals from each of the Omega stations A - G, where G is assumed to be in Australia. The usability of Omega signals is defined according to two criteria. Criteria I requires that signal-to-noise ratio SNR be no less than - 20dB in a 100-Hz bandwidth and that modal-interference-induced phase deviation be less than 20 centicycles. Criterion II differs from Criterion I in requiring that SNR be no less than - 30 dB. Symbolically, we have

Criterion I: $SNR \geq -20dB$, $\Delta\phi < 20$ cec.
Criterion II: $SNR \geq -30dB$, $\Delta\phi < 20$ cec.

Contours of SNR = 20 dB, SNR = -30 dB and $\Delta\phi$ = 20 cec are presented on large-scale maps in Reference 4, where each map illustrates the entire globe between latitudes 80^{o} N and 60^{o} S. In the present study, the region of

interest is much smaller, and in order to perform a direct comparison between the theoretical predictions of Reference 18 and the measurement data obtained in this study, it is appropriate to employ smaller-scale representations of the predictions.

Appendix F presents enlarged reproductions of each of the 64 prediction maps (8 transmitters, 4 months, 2 GMTs) from Reference 18 for the South Atlantic region. Except for the enlargement, Appendix F represents no change from the original predictions. However, Appendix F offers a convenient means for comparing the original predictions of Reference 18 with the modified predictons derived from this study.

The data base that is used for validation of Omega signal coverage 10.2 kHz is derived from measurements at ONSOD receiving stations, and integrated Omega-satellite (IOS) measurements aboard maritime vessels. These data are in sufficient abundance to provide a degree of statistical validity. The data also represent reasonable diversity, both reasonably and spatially. The data are in the form of signals measured by Magnavox 1104 and 1105 receivers. The signal readings may be interpreted in terms of the SNR available in a 100-Hz bandwidth by means of a calibration algorithm supplied by Magnavox to ONSOD. SNR data available from ONSOD monitors are described in Section 4.2.2 and SNR data available from IOS measurements are described in Section 4.5.

The data base to be used for validation of Omega signal coverage at 13.6 kHz is derived from the same souce as is the data base for 10.2 kHz. In most cases measurements at both 10.2 kHz and 13.6 kHz are performed simultaneously by the same receiver, both at ONSOD receiving stations and aboard IOS-equipped vessels. Predictions of Omega signal coverage are not presently available at 13.6 kHz, thus no verification of 13.6 kHz predicitions can be performed as a part of this analysis.

6.3 GEOMETRIC DILUTION OF PRECISION

GDOP is calculated entirely on the basis of a location for a hypothetical receiver and the known locations of the Omega transmitter. Locations of Omega transmitters are given in Table 2-1.

6.4 VERIFICATION OF PROPAGATION PREDICTION CORRECTIONS

The efficacy of ONSOD-supplied PPCs can be studied through analysis of diurnal phase difference error (LOP error) obtained from fixed monitor sites. Signal phases are measured hourly at each fixed monitor site. PPCs are applied to the measured phases and corrected LOPs are calculated. These corrected LOPs are compared with ideal LOPs based on monitor location, and the difference is expressed as phase difference error or LOP error. The LOP error provides information about errors in the PPCs used in the calculation.

LOP error data have been obtained from each fixed monitor site at 10.2 kHz and 13.6 kHz for the months of February, May, August and November. Data for an entire month are averaged at each hour in the Masterfile data base. In this study, 24-hour plots are prepared from these data, and presented for Analysis of PPCs. The available data base is described in Table 4-3.

6.5 LOP ERRORS AT 10.2 KHZ AND 13.6 KHZ

LOP errors are determined from Masterfile data obtained at ONSOD fixed monitors, and from LOP error data obtained from IOS receivers aboard maritime vessels. The Masterfile data are described in Table 4-3. It can be seen that the Masterfile data provides, for each LOP error calculation, a sample containing as many as 50 data points.

The availability of LOP error data from IOS receivers is summarized in Table 4-10. The IOS measurements provide, at any one location, a much smaller sample size than is available from Masterfile. On the other hand, the IOS measurements provide spatial diversity to the data base that is not sufficiently available from the ONSOD sites.

There is no significant difference in the sizes of data bases for 10.2 kHz and 13.6 kHz from either Masterfile or IOS sources.

6.6 FIX ERRORS AT 10.2 KHZ AND 13.6 KHZ

Position-fix errors are determined for ONSOD monitor sites from the Masterfile data base, and for oceanic areas from the IOS data base. The fix error calculations from Masterfile data are based on samples averaged over one month of measurements. The fix error calculations from IOS data are based on a sample size that is typically much xmaller. The data base obtained from Masterfile for fix-error calculations is summarized in Table 4-3, where one weighted fix error calculation is available for each site, frequency, month and GMT represented in the Table 4-3. The data base obtained from IOS for fix-error calculations is simply the total number of Omega fixes available in the data widow discussed in Section 4.5.

VII. ANALYSIS AND INTERPRETATION OF DATA

7.1 GENERAL APPROACH

The data base available for the evaluation of Omega performance in the South Atlantic region is described in Sections IV and V. These data were subjected to critical examination and analysis. Data from each source were evaluated separately and then collated with data from other sources to ensure that all possible factors of importance were examined. Two questions were constantly considered during the evaluation process. These questions were:

(1) Does Omega currently provide a reasonable sea and air navigation service in the South Atlantic?

(2) Did any significant negative factor or wide deviation from expected performance appear in the data?

Subsequent sub-sections examine and analyze data received from each source.

The utility of Omega is fundamentally limited by the availability of Omega signals, and the first major analysis is a comparison of predicted and measured availability of Omega signals throughtout the south Atlantic. Section 7.2 presents the results of analysis of measurement data of SNR observed from various platforms and Section 7.3 used the measurement data to obtain modified predictions of Omega signal coverage.

7.2 OBSERVED OMEGA COVERAGE AT 10.2 KHZ

Global coverage of Omega signals 10.2 kHz has been determined theoretically by The Analytical Sciences Corporation (TASC) [18]. The theory and methodology of that study are described thoroughly in Reference 18 and will only be summarized here.

It has been pointed out in Section 3.1 that the threshold for usable Omega signals is either -20 dB or -30 dB SNR depending on which of two criteria is used. Contours for each Omega station corresponding to these two thresholds have been published by TASC in the form of regional and global maps with the contours overlaid. Published contours are available only for two

times (0600 and 1800 GMT) and four months (February, May August and November). No allowance is made in the published contours for long-term variations such as might be associated with the solar cycle. The contours are secondary results of the TASC analysis in that the fundamental variation of SNR is calculated along a series of radials projecting outward from each Omega station.

The contour plots available from TASC are large scale and global in their presentation. In order to focus attention on the South Atlantic, it has been necessary to redraw the contours to a much smaller scale. Appendix F presents redrawn versions of the original 64 contour plots available from TASC. Subsequent comparisons of signal coverage predictions aand observations will use the contours presented in Appendix F.

Sections IV and V have described the measurement data useful for signal analysis of the South Atlantic. The measurement data used for statistical evaluation of SNR in the South Atlantic are fixed-monitor data described in Section 4.2.2, and Tables 4-4, 4-5, and 4-6; and Integrated Omega-satellite data described in Section 4.5 and Table 4-9.

The fixed-monitor data are straightforward in that the data can be associated with a stationary platform and were available at precisely 0600 GMT and 1800 GMT. The IOS data, on the other hand, were obtained aboard moving platforms at random times. The grouping of IOS data in windows has been described in Section 4.5. The grouping technique permits the estimation of an inferred measurement at 0600 GMT or 1800 GMT based on actual measurements at other times.

The spatial correlation to be expected among SNR measurements in the South Atlantic is likely to be fairly high over distance of several hundreds of miles, especially in oceanic areas. Furthermore, the spatial resolution intrinsic to the theoretical signal-coverage predictions is not great since the theoretical calculations were performed along radials from each transmitter that are displaced 15 degrees azimuth intervals. Accordingly, it seems quite reasonable to limit the spatial detail of the SNR data analysis. The approach followed here has been to divide the South Atlantic region onto a grid of rectangular spaces defined by latitude boundaries at 10^{o} intervals and longitude boundaries at 10^{o} intervals. The South Atlantic region of

20^{o} N to 60^{o} S and 70^{o} W to 20^{o} E is then divided into 72 rectangular areas. Within each given area, all available fixed-monitor SNR data for a given circumstance (transmitter, month, GMT) can be statistically combined to yield a single mean and a single standard deviation. Within each area, all available IOS SNR data for a given circumstance (transmitter, month, GMT) can be statistically combined to yield a single mean and a single standard deviation.

The results of all SNR data were plotted on maps that conformed to the maps presented in Appendix F, except that theoretical contours of SNR were replaced with a matrix grid defining the spatial detail of the results. These results were presented to ONSOD for review.

As a result of ONSOD's review and suggestions, the following specific changes were made in the analyzed data:

(1) All data from the ONSOD sote at Rio de Janiero were deleted.

(2) All data indicating SNR $\leq$ -30dB were deleted.

(3) All data within a region where modal interference in predicted to exceed 20 cec were deleted.

(4) The following data associated with the Norway (A) transmitter were deleted:

a. May, 0600 GMT, in the area bounded by 10° S to 20° S and 30° W to 40° W

b. May, 0600 GMT, in the area bounded by 10° S to 20° S and 0° to 10° W

c. May, 1800 GMT, in the area bounded by 20° S to 30° S and 40° W to 50° W

d. November, 1800 GMT, in the area bounded by 20° S to 30° S and 40° W to 50° W.

Appendix G presents the remaining data in the form of means and standard deviations. Appendix G contains 64 maps on which are presented all the analyzed measurement data that are to be compared with theoretical predictions. Each map in Appendix G corresponds to a map of theoretical contours in Appendix F, to the same scale. A comparison of any corresponding maps enables one to make a judgment about the extent, if any, to which a theoretical contour should be modified.

7.3 MODIFIED SIGNAL COVERAGE PREDICTIONS FOR 10.2 KHZ

The theoretical contours of SNR presented in Appendix F and based on the predictions of Reference 18 were modified in accordance with the measurement results obtained in this study and presented in Appendix G. The following rules were followed in modifying the contours:

(1) Smooth curves were employed where ever possible.

(2) Modified contours were defined only in regions where modal interference was predicted to be less than 20 cec.

(3) Modified contours were required to be consistent with measurement data.

(4) Contours were modified only to the extent necessary to accommodate measurement data. Original conours, or segments of original contours were retained wherever possible.

(5) The measurement data in Appendix G demonstrates the well-known tendency of radio noise in the Omega band to be higher over land masses than over oceanic areas. This tendency has been assumed to hold even where no supporting data exist, thus modified SNR contours were drawn to be approximately parallel to coastal outlines in the South Atlantic region.

Appendix H presents modified signal coverage predictions for the South Atlantic region. The predictions are in the same form as the theoretical predictions presented in Appendix F; that is, 64 maps depicting cases for 8 transmitters, 4 months and two GMTs. The maps in Appendix H thus provide a simple and straightforward prediction of Omega availability in the South Atlantic region.

7.4 OBSERVED OMEGA COVERAGE AT 13.6 KHZ

Measurement data on SNR have been obtained at 13.6 kHz as well as at 10.2 kHz. Although signal coverage predictions are not available at 13.6 kHz, nevertheless, it is instructive to examine SNR data at 13.6 kHz and to compare results at 13.6 with results at 10.2 kHz.

Measurement data availability is described in Sectons IV and V for both frequencies. The arguments given earlier to justify a 10^{o} X 10^{o} grid for quantizing data apply here as well. Accordingly, we can plot 13.6 kHz SNR

results in the same manner as was used at 10.2 kHz. Appendix M presents plots of 13.6 kHz SNR statistics obtained from measurement at fixed monitor sites and aboard IOS vessels. Appendix M applies to the same circumstances and is in the same format as Appendix G except that Appendix M contains no prediction contours for modal interference.

A comparison of the 10.2 kHz results shown in Appendix G and the 13.6 kHz results shown in Appendix M indicates a fairly good agreement in both the availability of signals and the SNR of signals at 10.2 kHz and 13.6 kHz. Although signal coverage predictions at 13.6 kHz have not been performed to date, when such predictions become available, the statistical results presented in Appendix M can be used to validate such predictions and to lead to modified coverage diagrams, just as in the case of 10.2 kHz.

7.5 CALCULATION OF GDOP

Geometrical Dilution of Precision (GDOP) is a useful predictor of fix accuracy. GDOP relates achievable fix accuracy for a particular circumstance to the accuracy that would be achievable for an ideal geometry. GDOP is based entirely on relative locations of Omega transmitters and a hypothetical receiver and is independent of phase measurement data.

A knowledge of predicted GDOP, as a function of receiver position, can be very useful to a navigator who is capable of measuring only LOPs, as it provides some guidance as to the best choice of LOPs to use to obtain a position fix.

GDOP is calculated according to a standard algorithm given in Appendix E. GDOP can be calculated for any receiver location and for any pair of LOPs, thus the possible number of GDOP calculations for the South Atlantic region could become prohibitively large unless some effort is made to limit the number of cases.

GDOP calculations are performed in the South Atlantic region according to the following criteria:

(1) GDOP clculations are performed at the center of each 10^{o}x10^{o} grid block defined in Section 3.3, thus 72 hypothetical receive locations are considered.

(2) GDOP calculations are performed for all possible pairs of LOPs, representing all transmitters. No effort is made to limit calculations based on SNR predictions or measurement data.

(3) For any three transmitters, three pairs of LOPs are possible, leading to three GDOP values. For this situation, all three GDOP values are calculated, but only the best (smallest) GDOP is retained for presentation.

(4) Using four transmitters, three pairs of LOPs are possible, leading to three GDOP values. For this situation, all three GDOP values are calculated, but only the best (smallest) GDOP is retained for presentation.

(5) GDOP values greater than 2 are rejected.

Appendix E presents the results of this GDOP analysis. Each grid block is associated with one set of calculations and the GDOP values are considered to be representative of the region represented by the grid block. Appendix E thus presents to a navigator anywhere in the South Atlantic region, achievable GDOP for any possible set of three or more transmitters, unless GDOP >2.

It should be emphasized that there is no direct relationship between the GDOP of a pair of LOPs and the accessability or accuracy of signals from the transmitters involved. The GDOP information presented in Appendix E thus may indicate, in some cases, that certain combinations of transmitters are preferable even though some of the transmitters may not provide accessable signal or the signals may contain large phase errors. GDOP should thus never be considered in isolation from other factors in assessing the efficacy of Omega for any situation.

7.6 DIURNAL VARIATIONS IN LOP ERROR AT 10.2 KHZ and 13.6 KHZ

Appendix I and Appendix N present diurnal plots of phase-difference errors at 10.2kHz and 13.6 kHz, respectively, measured at ONSOD fixed sites and recorded in Masterfile. The plots represent monthly averages of unflagged data and contain no information on day-to-day variations in error values.

It was pointed out in Section 3.6 that phase-difference errors or LOP errors as they are also called, may be equated directly to errors in LOP-PPCs where a LOP-PPC is defined as composite propagation corrections applied to a phase difference measurement to yield a corrected LOP. It was pointed out

that the observed errors in LOP-PPCs provide valuable information regarding the accuracy of propagation corrections that are applied to Omega signals.

The observed LOP errors are associated with the propagation corrections that have actually been applied to signals recorded at the ONSOD monitor sites. It is not known, of couse, what correction algorithms may be in use in various commercial Omega receivers, thus no conclusions can be drawn about the efficacy of such algorithms that may exist other than the ONSOD algorithm. Nevertheless, it is possible, using the LOP errors presented in Appendix I and Appendix N, to estimate the propagation corrections that should have been applied to signals observed at ONSOD sites under the circumstances represented. Such a study is beyond the scope of this report.

The plots in Appendix I and Appendix N provide information from fixed sites at Belem, Buenos Aires, Golfo Nuevo, Monrovia, Natal and Recife, and propagation paths from transmitters at Norway (A) Liberia (B), Hawaii (C), North Dakota (D), La Reunion (E), Argentina (F) and Japan (H), although not every possible combination of transmitters and receivers is represented. In the cases of the monitor at Monrovia receiving signals from Transmitter B, and the monitor at Golfo Nuevo receiving signals from Transmitter F, the proximity of transmitter and receiver means that propagation errors are negligible, hence LOP errors may be interpreted entirely in terms of propagation errors on the other path of the LOP. In these special cases, LOP-PPC errors may be interpreted directly as single-path propagation-correction errors.

In a number of cases, LOP error data are available for the same month during different years. No attempt has been made to combine data from more than one year into a single diurnal plot. Comparing diurnal behavior of LOP errors that represent different years can provide valuable insight into the relationship between propagation errors and solar cycle. At present, this relationship is poorly known, as it is virtually impossible to predict theoretically, an empirical relationships can only be deduced from comparisons of observations made during different parts of the solar cycle.

7.7 LOP ERRORS AT 10.2 KHZ AND 13.6 KHZ

Appendix J and Appendix O present maps of LOP error statistics for 10.2 kHz and 13.6 kHz, respectively, arranged by LOP, month and GMT. The statistics are based on measurements from ONSOD fixed monitor sites and from IOS-equipped vessels.

Results are quantized in 10^0 latitude x 10^0 longitude grid blocks. Within each grid block, LOP errors obtained from fixed monitors are described by a mean value and a standard deviation, and LOP errors obtained from IOS measurements are described by a mean value and a standard deviation.

Each page describes one LOP for one month (February, May, August or November) and one GMT (0600 or 1800). No attempt is made to distinguish between calendar years. Fixed monitor data correspond to specific months and specific times. However, it was pointed out in Section 4.5 that, in order to retain a reasonable sample size in the IOS data base, it has been necessary to establish finite time windows of 4 hours centered on the labeled times of 0600 GMT and 1800 GMT, and date windows of 3 months centered on the labeled months of February, May, August and November. The data windows thus include all 12 months and 8 hours of each day. This scheme accepts some smearing of results over times and over seasons in return for obtaining a meaningful sample size for each case.

7.8 FIX ERRORS AT 10.2 KHZ AND 13.6 KHZ

Fix errors are calculated by comparing an Omega fix with a reference position. In the case of IOS fixes, the reference position of the platform is the position determined from a satellite fix.

Fix errors can be expressed either in vector notation (magnitude and direction) or in terms of orthogonal components. In this study, by convention, all fix errors are expressed in terms of northern and eastern components having dimensions of nautical miles (NM).

The data base for analysis of fix errors is taken both from measurements at ONSOD monitors and from IOS measurements. Each measurement in the data base represents a potential fix derived from phase measurements obtained from

three or more stations. Since any combination of 3 stations yields a potential fix, it follows that several Omega fixes may be associated with a single set of phase measurements. In a situation where more than one Omega fix, at either 10.2 KHz or 13.6 kHz, is available for a particular Omega measurement, the procedure followed in this study is to discard all fixes but the "best" fix, where the best fix is defined as that fix having the smallest error magnitude. Omega fixes are calculated separately at 10.2 kHz and 13.6 kHz, thus for any Omega measurement, a best fix at 10.2 kHz and a best fix at 13.6 kHz are obtained. At each of the frequencies 10.2 kHz and 13.6 kHz, a best fix yields a fix error; this fix error is considered to be the smallest fix error achievable under the circumstances, and is entered into the fix error data base.

Fix errors are calculated, for 10.2 kHz and for 13.6 kHz, at 0600 GMT and at 1800 GMT, and for the months of February, May, August and November. ONSOD monitor data are averaged over one full month of available measurements at exactly 0600 and 1800 GMT. IOS data are used that fall within time windows of 4 hours centered on the times 0600 GMT, and that fall within 3 month windows centered on the validation months of February, May, August* and November. These rather wide windows of data accessability cause some diurnal and seasonal smearing of results, but result in much larger statistical samples than would otherwise be possible. Appendix K presents fix error results obtained at 10.2 kHz and Appendix P presents fix error results obtained at 13.6 kHz.

7.9 SIGNAL AMPLITUDES ALONG TRANSMITTER RADIALS AT 10.2 KHZ AND 13.6 KHZ

7.9.1 General

Section V summarizes the experiments performed by NOSC and the data obtained from the NOSC experiment. References 21 and 22 are the sources for this information.

---

*No IOS data are available for August.

One of the experiments performed by NOSC was a series of aircraft flights along approximate radials for several transmitters. During each flight, signal amplitudes were monitored from several transmitters, as indicated in Table 5-7.

Since the solar illumination condition along the propagation path between transmitter and (airborne) receiver was approximately constant during each flight, then, to a first approximation, each expanded measurement along a radial provided a "snapshot" of signal amplitude variation along the radial at an assumed instant of time.

Omega navigation is based on the assumption that a received signal can be associated with a single, dominant propagation mode. In fact, Omega signal propagation resembles propagation along a waveguide, where a primary mode and one or more higher-order modes are launched by the transmitter into the waveguide set up by the earth and the lower boundary of the ionosphere. Higher-order modes are influenced by geophysical conditions, the discussion of which is beyond the scope of this report. However, it is generally accepted that higher-order modes attenuate with increasing distance from the transmitter more rapidly than does the primary mode.

The presence of higher-order modes gives rise to both amplitude and phase fluctuations of the Omega signal with distance along a radial. Phase fluctuations are a direct cause of navigational errors for Omega. Amplitude fluctuations, while not affecting accuracy directly, indicate the presence of higher-order modes and modal interference.

The direct measurement of phase fluctuations along a radial requires a precise continuous reference position along the radial, such as TACAN or precision tracking radar. In the absence of precise positional information for the aircraft, modal interference must be inferred from measurements of signal amplitude fluctuations along the radial.

Analysis of NOSC airborne amplitude measurements is based on results presented in References 21 and 22. Since the conclusions being sought are transmitter specific, it is convenient to arrange the measurements according to Omega transmitters rather than by flight.

7.9.2 Results Obtained For Norway

Figure 7-1 illustrates radials for Omega Norway in the South Atlantic, along with flight tracks for the various NOSC flights receiving Norway signals during the Omega experiments. It can be seen that each flight can be associated with one or more specific radials from Norway.

Figure 7-2 presents an overlay of theoretical 10.2 kHz signal amplitude profiles for Norway along selected radials, and measured 10.2 kHz signal strength profiles for Norway obtained during Flights 1B, 2, and 3. It is important to note that the theoretical profiles are referenced to a 1-KW transmitter (and probably to a zero-dB transmitter antenna as well), and that the measured data result from a 10-KW transmitter, a real transmitter antenna and a real receiver antenna. Because of these uncertain differences between theoretical and measured signals, no attempt is made here to draw conclusions from absolute differences in signal amplitudes, but the comparison will be limited to profile shapes. Figures 7-3 and 7-4 present corresponding comparisons at 10.2 kHz involving Flight 8 and Flight 10.

Figures 7-1 through 7-4 are duplications of Figures L-1 through L-4 (Appendix L) and are presented here to provide an example of the approach that is used to analyze the NOSC airborne test data. Appendix L presents the available results for all OMEGA transmitters at 10.2 kHz and Appendix Q presents analogous results at 13.6 kHz.

Measurement results at 10.2 kHz from Flights 1B, 2, and 3 compare only moderately well with theoretical results along radials A6 and A7. The measured results suggest modal interference along radials A6 and A7 at ranges between 6 and 10 megameters to a somewhat greater extent than was predicted. Flight 8, along radials A3 and A4 at ranges between 9 and 11 megameters agreed well with predictions in its indication of strong modal interference. Flight 10, along radial A3 at ranges between 8.5 and 10 megameters, produced results that are noisy and difficult to interpret, thus no comparison can be made with predictions. Similar results obtained at 13.6 kHz except that the results from Flight 10 suggest modal interference in agreement with predictions.

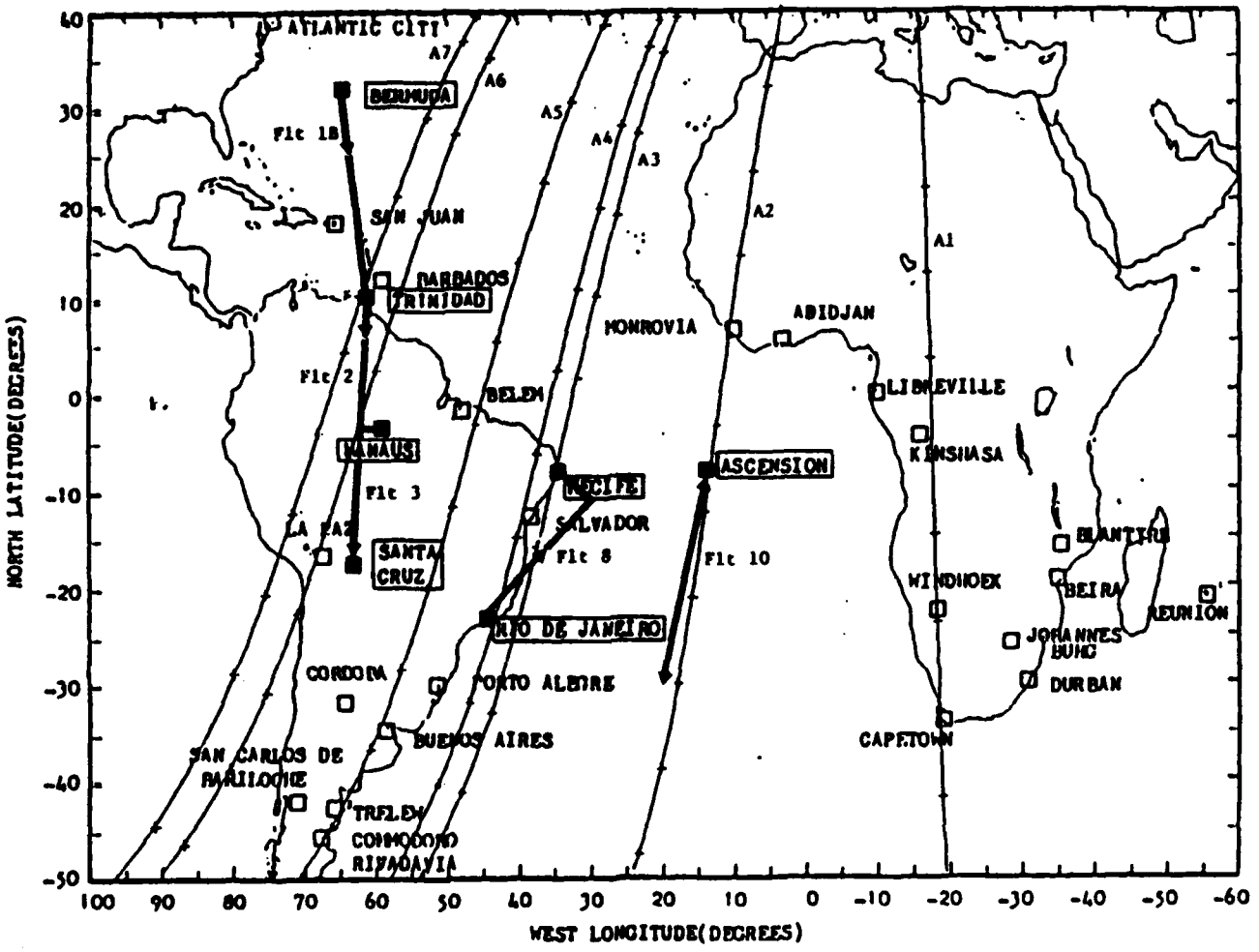

Figure 7-1. Azimuths for predicted radials from Omega Norway and ground tracks for NOSC test flights.

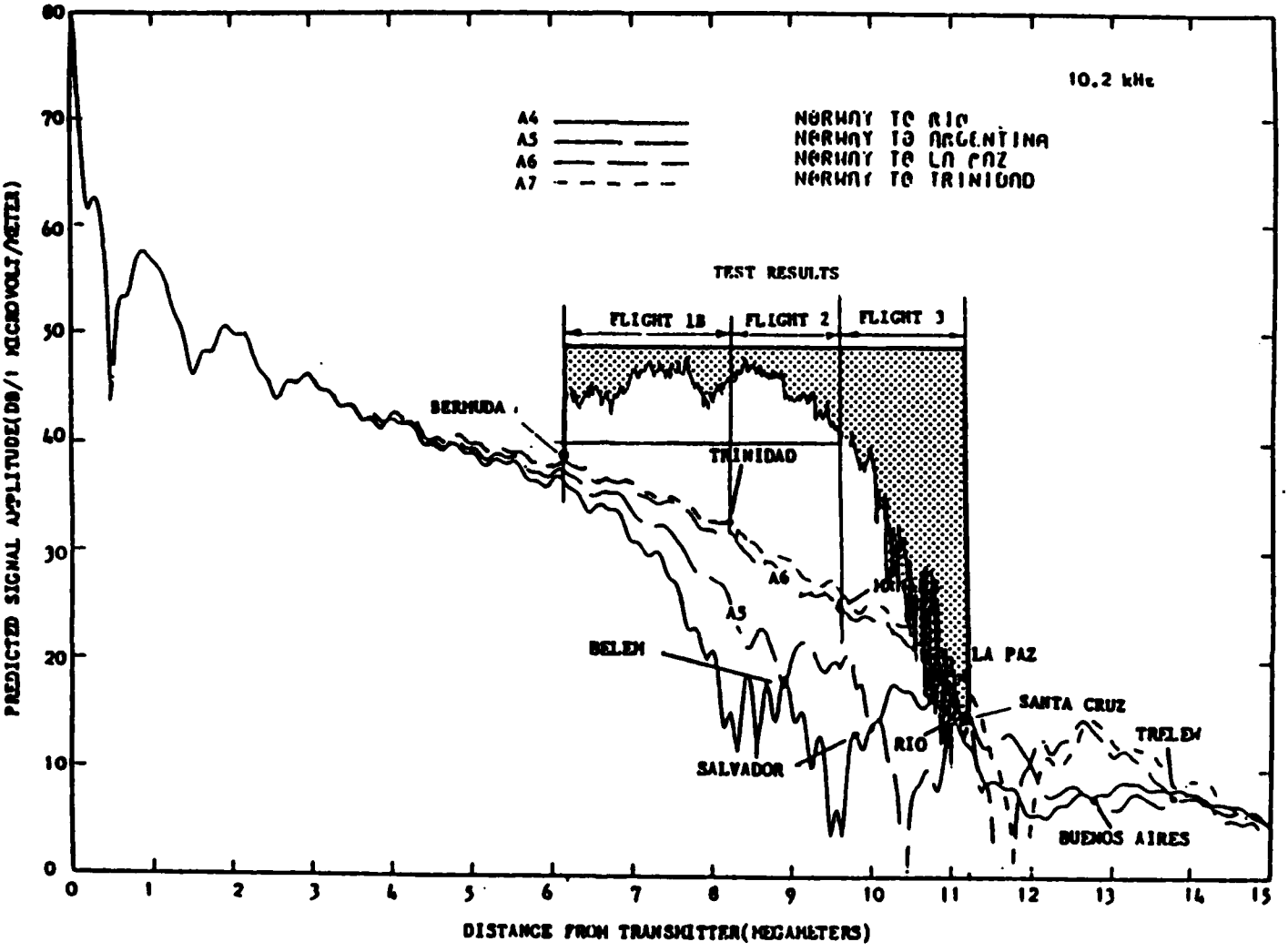

Figure 7-2. Predicted nighttime signal amplitudes at 10.2 kHz as functions of distance from an assumed 1-KW transmitter at Norway along selected radials, and observed signal amplitudes as functions of distance from Norway during Flights 1B, 2 and 3 (References 21 and 22).

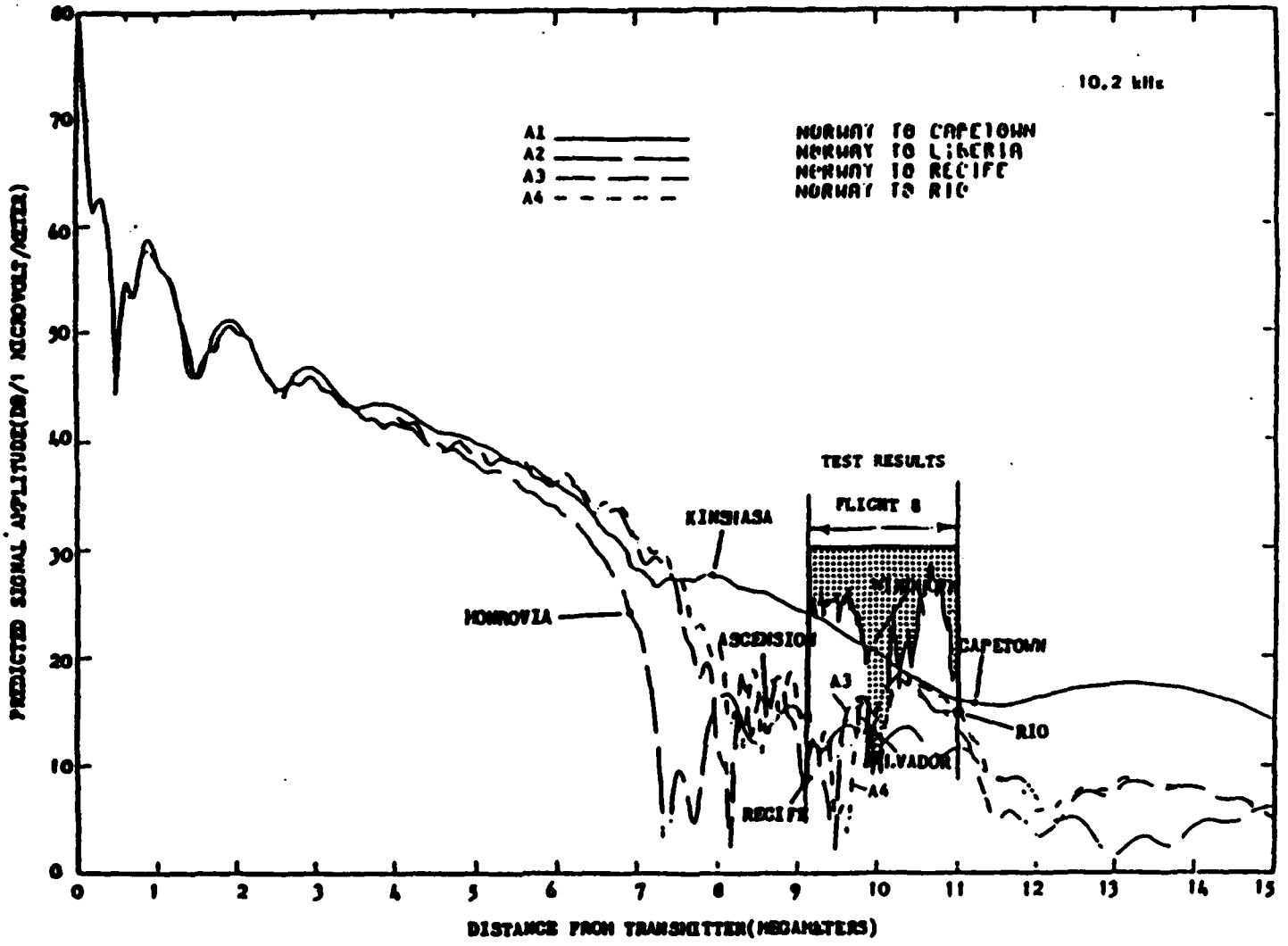

Figure 7-3. Predicted nighttime signal amplitudes at 10.2 kHz as functions of distance from an assumed 1-KW transmitter at Norway along selected radials, and observed signal amplitudes as functions of distance from Norway during Flight 8 (References 21 and 22).

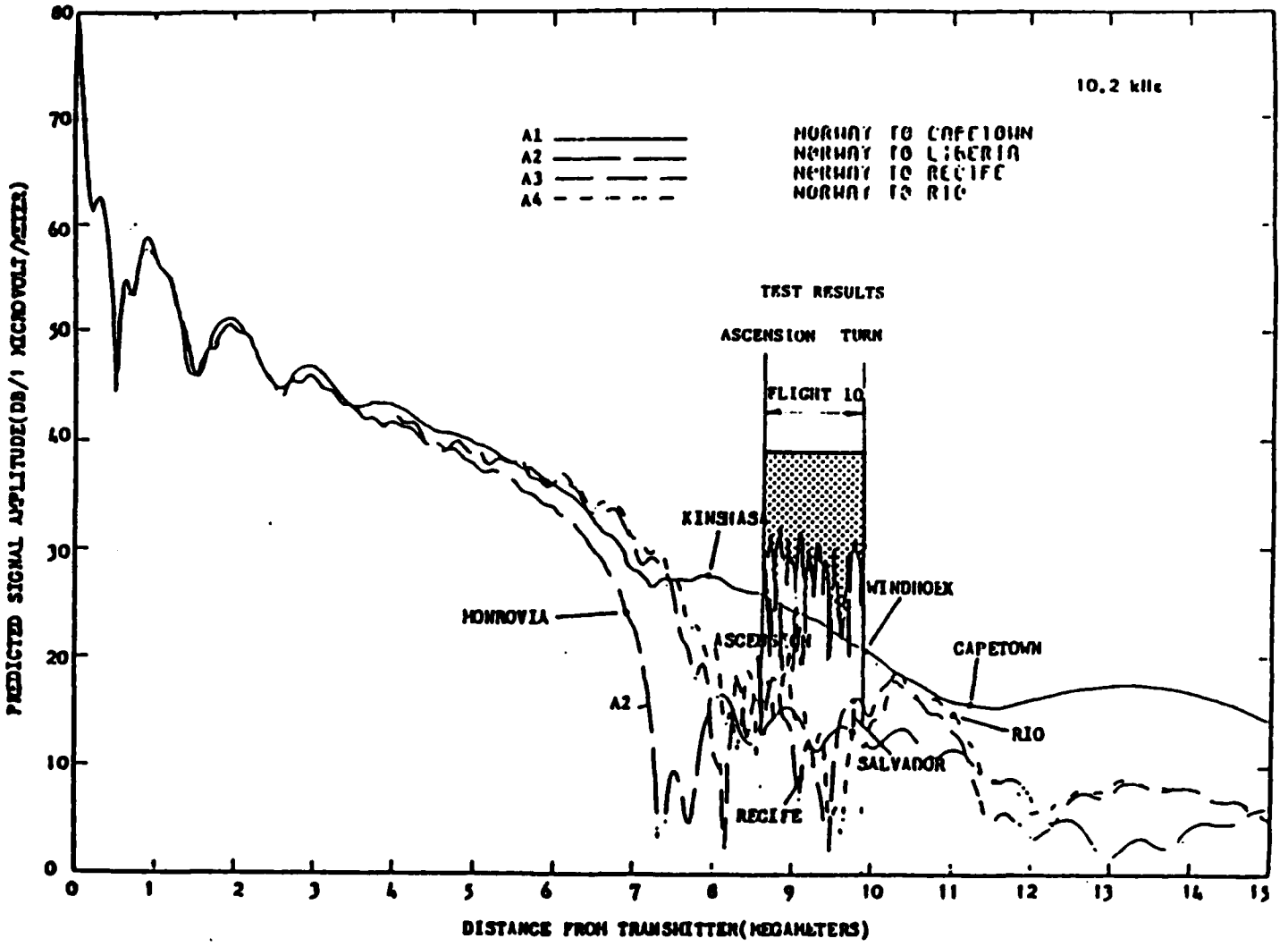

Figure 7-4. Predicted nighttime signal amplitudes at 10.2 kHz as functions of distance from an assumed 1-KW transmitter at Norway along selected radials, and observed signal amplitudes as functions of distance from Norway during Flight 10 (References 21 and 22).

7.9.3 Results Obtained For Liberia

Figures L-5 through L-7 present results obtained for Liberia at 10.2 kHz, and Figures Q-5 through Q-8 present analogous results at 13.6 kHz. At 10.2 kHz, Flight 8, at 2.5 to 5 megameters range along radials B3 and B4, and Flight 10, at 1.5 to 3 megameters range along radial B1, produced measured indications of significant amplitude fluctuations, consistent with predictions of strong modal interference. At 13.6 kHz, Flight 6, at 5 to 8 megameters range along radial B12, produced a weak indication of modal interference, while Flight 8, at 2.5 to 5 megameters range along radials B3 and B4, and Flight 10, at 1.5 to 3 megameters along radial B1, indicated strong modal interference.

7.9.4 Results Obtained For La Reunion

Figures L-8 through L-11 present results obtained for La Reunion at 10.2 kHz, and Figures Q-9 through Q-12 present analogous results at 13.6 kHz. At 10.2 kHz, Flight 7, at 8.5 to 10 megameters range along radials E3 and E4, Flight 9, at 7.5 to 9.5 megameters range along radials E5 and E6, and Flight 11, at 7.5 to 9.5 megameters range along radials E5 and E6, produced measured indications of slight amplitude fluctuations, consistent with predictions of slight modal interference. At 13.6 kHz, Flight 7 and Flight 9 produced uncertain signal fluctuation results, while Flight 11, at 7.5 to 9.5 megameters range along radials E-5 and E-6 produced an inconclusive indication of amplitude fluctuations and modal interference.

7.9.5 Results Obtained For Argentina

Figures L-12 through L-14 present results obtained for Argentina at 10.2 kHz, and Figures Q-13 through Q-15 present analogous results at 13.6 kHz. It can be seen in Figures L-12 and Q-13 that Flights 1B, 2, 3, 4 and 5 were equivalent to a single flight along radial F1 over the range 0 to 8.5 megameters from the transmitter and thus may be treated as a single flight for present purposes. Flights 6 and 8, similarly, may be treated as a single flight along radial F4 over the range 0 to 5 megameters from the transmitter.

At 10.2 kHz, Flights 1-5 indicate strong signal-amplitude fluctuations in the range of 0 to 1 megameter and moderate amplitude fluctuations at ranges greater than 1 megameter along radial F1, consistent with predictions. Flights 6 and 8, taken together, indicate significant signal-amplitude fluctuations at all observed ranges, consistent with predictions.

At 13.6 kHz, Flights 1-5 produced indications of moderate signal-amplitude fluctuations from 0 to about 4 megameters range, in remarkable agreement with predictions. Flight 6 produced indications of very pronounced signal-amplitude fluctuations over the Flight 6 range of 0 to 3 megameters. The Flight 6 results were also in very good agreement with predictions.

VIII. NAVIGATION REQUIREMENTS

As in any objective evaluation of navigation system performance, there is a need first to define and document the requirements. SCT has grappled with this problem on several occasions over the last few years [23, 24]. The difficult part of the problem is translating general requirements, usually based on safety and efficiency, as stated in national and international policy guidelines, into quantified performance parameters against which the navigation system's capability can be measured. The problem appears straightforward intuitively but presents a challenge analytically. Approaches range from a simple estimate of cross-track error and error rate to application of the Reich Model as applied to air navigation requirements [25].

The worldwide air navigation requirements of the International civil Aviation Organization (ICAO) member states, which pertain to requirements specified within member states and for aircraft flying into these states, are specified in five ICAO air navigation regional plan publications [26]. International standards and recommended practices are specified in Annex 10 Aeronautical Telecommunications [27]. More recently, at the 9th Air Navigation Conference of ICAO, the Minimum Navigation Performance Specifications (MNPS) was adopted for consideration on a worldwide basis [28]. This specification is intended to ensure safe separation of aircraft and at the same time enable operators to achieve maximum economic benefit from improvement in accuracy of navigation demonstrated in recent years.

The MNPS has not been implemented in the South Atlantic region, but is presently being used for planning purposes. The MNPS specifies that the standard deviation of lateral track errors shall be less than 6.3 nm. Equivalently, an aircraft must stay within 12.6 nm of track for about 95 of the time. Also, the proportion of the total flight time spent by aircraft 30 nm or more off the cleared track shall be less than 5.3×10^{-4} (one hour in about 200 flight hours), and the proportion of the total flight time spent by aircraft between 50 and 70 nm off the cleared track shall be less than 13×10^{-5} (one hour in about 8,000 flight hours). Furthermore, such navigation performance capability shall be verified by the state of registry (Notice to

Airmen, November 3, 1977). Implementation of these standards generally can be achieved by using Omega or Omega/VLF combinations as an update to previously approved navigation systems, e.g. INS.

Civil air navigation requirements are more complete than most other requirements in the sense that they consider interaction with other flight systems and they are generally specified based on an overall performance measure such as safety, minimum distance, economic considerations, and traffic flow/airspace planning considerations. Less work has been done toward defining the marine requirements which are usually assumed to be less stringent.

No specific international requirements (government regulations)exist for marine navigation. A fundamental requirement based on the Safety of Life at Sea (SOLAS) convention specified basic onboard equipment [29]. The primary objective for marine aids to navigation is similar to the air navigation requirements, mainly to support safe and economic movement of vessels from point of departure to point of arrival. Adequate position-fixing capability is required which is not limited by geographic location or the environment (wind, sea state, visibility). Specific needs of marine navigation have been promulated in he National Plan for Navigation as illustrated in Table 8-1 for high seas [30].

In July 1980, DOD and DOT jointly issued the Federal Radionavigation Plan [31], which establishes, for planning purposes, aviation and marine navigation requirements for both military and civilian users. Tables 8-2 and 8-3 present requirements for civil aviation and civil marine users, respectively, as published in the Federal Radionavigation Plan.

Several sources for the derivation of marine navigation requirements apply to both domestic and foreign users. Capt. A.E. Fiore, USMS, of the National Maritime Research Center presented a paper entitled, "Navigation Requirements of the Maritime Community," at the National Radio Navigation Symposium in November 1973. The history, status, and projections summarized in the paper provide perthaps the best documented basis for maritime navigation requirements available to date. An additional source is the "Ships Routing and Traffic Separation Schemes" published in 1971 by the International Maritime Consultative Organization (IMCO). This document provides

Table 8-1

Marine Navigation Requirements

HIGH SEAS				
ENVIRONMENT	GENERAL REQUIREMENTS	AVAILABILITY	COVERAGE	ACCURACY
• POSITION FIXING BY VISUAL REFERENCE TO LAND OR OTHER FIXED OR FLOATING AIDS IS NOT PRACTICAL	• POSITION FIXES REQUIRED TO EFFICIENTLY DIRECT A COURSE TOWARD DESIRED DESTINATION • OCEANIC AND SURVEY ENDEAVORS REQUIRE POSITION FIXING RELATIVE TO A GEODESY • MUST BE ADEQUATE TO AVOID CHARTED OBSTRUCTIONS INCLUDING REEFS, REMOTE ISLANDS AND COASTS WHERE OTHER NAVAIDS DO NOT EXIST	• CONTINUOUS SYSTEM DESIRABLE • UPPER LIMIT OF 2 HOURS	• GENERALLY WORLDWIDE • U.S. COMMERCIAL MARITIME INTERESTS 90% SATISFIED BY COMPLETE COVERAGE OF NORTH ATLANTIC AND NORTH PACIFIC	• 4 NMI 95% OF THE TIME • FUTURE GOAL OF 2 NMI 95% OF THE TIME BY YEAR 2000

Table 8-2

Controlled Airspace Aviation Navigation Accuracy to Meet Projected Future Requirements

Phase	Sub-Phase		Altitude (Flight Level)	Traffic Density	Route Width (NM)	Accuracy (meters) 2 drms
EnRoute/ Terminal	Oceanic		FL 275 to 400	Normal	less than 60	better than 12.6nm
	Domestic		FL 180 to 600	Normal	8	1000
				High	8	1000
			500 ft to FL 180	Normal	8	1000
	Terminal		500 ft to FL 180	High	4	500
	Remote		500 ft to FL 600	Normal	8 to 20	1000 to 4000
	Helicopter Operations		500 ft to 5000 ft	Low (Off-Shore)	8	1000
			500 ft to 3000 ft	High (Land)	4	500
Approach and Landing	Non-Precision		250 to 3000 ft. above surface	Normal	1 to 2	100
	Precision	Cat I	100 to 3000 ft. above surface	Normal	± 9.1 meters[1]	± 3 meters[2]
					at 100 ft. above Surface	
		Cat II	50 to 3000 ft. above surface	Normal	± 4.6 meters	± 1.4 meters
					at 50 ft. above Surface	
		Cat III	0 to 3000 ft. above surface	Normal	± 4.1 meters	± 0.5 meters
					at Surface	

(1) This column is the 2 sigma lateral accuracy in meters
(2) This column is the 2 sigma vertical accuracy in meters

Table 8-3

Current Maritime User Requirements/Benefits for Purposes of System Planning and Development - Ocean Phase

Requirements	Measures of Minimum Performance Criteria to Meet Requirements									
	Accuracy (2 drms)			Coverage	Availability	Reliability	Fix Rate	Fix Dimension	Capacity	Ambiguity
	Predictable	Repeatable	Relative							
Safety of Navigation – All Craft	2-4NM(3.7-7.4km) Minimum 1-2NM(1.8-3.7km) DESIRABLE	–	–	Worldwide	95% full cap. 99% Fix at least every 12 hours	(2)	15 Mins. or Less Desired; 2 hrs Maximum	Two	Unlimited	Resolvable with 99% Confidence

Benefits	Measures of Minimum Performance Criteria to Achieve Benefits									
Large Ships Maximum Efficiency	0.1-0.25NM (185-460M) (1)	–	–	Worldwide, except Polar Regions	99%	(2)	5 min.	Two	Unlimited	Resolvable with 99% Confidence
Hydrography Science, Resource Exploitation	0.1-0.25NM (185-460M)	Maximum Possible	–	Worldwide	95%	(2)	1 min.	Two	Unlimited	Resolvable with 99% Confidence
Search Operations	0.25NM (460M.)	0.25NM	185 M.	National Maritime SAR Region (NPAC, NWLAN)	99%	(2)	1 min.	Two	Unlimited	Resolvable with 99% Confidence

(1) Requirement subject to confirmation by additional study
(2) Dependent upon mission time

safety-related guidelines. IMCO, supported by the Radio Technical Commisiion for Marine Services (RTCM), is in the process of updating the definition of international marine navigation requirements. A "Preliminary Draft Accuracy Requirements for Navigation" report presents an updated accuracy requirements table for further consideration by the IMCO subcommittee and working group.

The ICAO, IMCO, and NATO documents cited above generally treat navigation accuracy, coverage, and to some extent reliability, as they pertain to the regulation of safety. Navigation requirements derived from these "regulatory" sources are not complete; they must be augmented by more "operational" type considerations, such as ease of utilization, security, and cost. The best sources for such operational considerations are the user groups themselves; however, collecting such information is an arduous, resource-consuming process.

There are two fundamental difficulties in attempting to describe navigation requirements generally. First, the description, if it is to be non-trivial, must address a potentially enormous set of dimensions, including user groups, locations, missions and navigation parameters. Secondly, in many cases quantifiable requirements for navigation parameters have not been established and the best that one can do is to perform a cost-benefit study relating the value of some navigation parameter, such as accuracy, both to the cost of achieving that value of accuracy and to the economic benefit of achieving that value of accuracy.

A very important study on this subject is presently being performed by SCT under contract to the Department of Transportation [32]. The study is entitled, "Economics Requirements Analysis of Civil Navigation Alternatives" (DOT-RC-92008). To provide an indication of the magnitude of this work and its applicability to deriving navigation requirements, particularly for foreign and marine users, several of the more relevant aspects of the study are outlined below.

The DOT study is an extension of an ongoing SCT study for the FAA entitled, "Economic Requirements Analysis for Civil Air Navigation Alternatives." While the FAA study focused only on the U.S.-registered aircraft, the DOT effort explicitly addresses airborne, marine, and land navigation users, both U.S. and foreign-owned (constrained to those which will

be affected directly by U.S. navigation policy decisions, i.e. those which operate in the U.S. or its territories).

The objectives of the DOT effort are described by the following excerpts from the DOT Statement of Work:

"The objective of this effort is to expand the existing FAA navigation model (developed under Contract DOT-FA75WA-3662, Task 9) which addresses air navigation systems, into a multimodal model which will allow an analysis of the economics for both any mode individually and all modes in combination. It will thus provide a tool to assist in making management decisions regarding the mix of future civil navigation systems.

This effort shall be limited to major systems suitable for civil navigation. It will include major military systems having potential civil applications and military use of civil and military systems to the extent that such systems allow the military to navigate in conconance with civil users.... The study shall include systems (both singly and in combination) such as Transit, VOR/DME, Loran-C, Omega and GPS, ..."

The overall approach, utilized in both the FAA and DOT studies, commences with the following activities (also taken from the Statement of Work):

(1) Identifying present and potential navigation user groups.

(2) Developing, or obtaining where available, baseline population estimates for the identified user groups and categorizing each group by elements such as type of vehicle, prime use to which the vehicle is put, and sophistication of navigation equipment.

(3) Developing, or obtaining where available, populations projections for each category and each group identified.

(4) Identifying user needs and system performance requirements for viable alternatives to meeting those needs for the various users."

In summary, it is known that the process of requirements identification, particularly in the marine areas, is a time consuming and costly activity. Furthermore, reasonable levels of subjectivity are required, and the credibility of the results invariably increases with the contractor's experience as well as level of effort. Therefore, it is expected that the DOT study being performed by SCT will permit the incorporation of user requirement information not otherwise obtainable into the Omega validation activity on a

global basis. While the DOT study does not explicitly address users who never operate in the U.S., the scope of users which are being considered is sufficiently broad as to provide valuable and necessary insight regarding the identification of requirements for the purely foreign users.

IX. CONCLUSIONS AND RECOMMENDATIONS

9.1 OVERVIEW

The conclusions to be drawn from any study should include the following elements:

(1) answers to questions explicitly or implicitly posed at the beginning of the study;

(2) a description of significant results that were not expected and were not the basis of inquiry at the beginning of the study

(3) comments on the parameters of the study itself, as opposed to the results obtained; typical parameters might include methodology of the study, data breadth and quality, etc.

In drawing conclusions from this study, not only should one address the above elements, but one must also make a decision, or series of decisions about tradeoffs between generality and specificity of the conclusions. These tradeoffs are properly determined according to the audience one is attempting to reach.

It was stated in Section II that the purpose of the validation effort is to determine the efficacy of Omega as a navigational aid in the South Atlantic Region. In this study, it is assumed that the two most important criteria determining this efficacy are signal coverage and available accuracy. Other possible criteria, such as reliability, power consumption, and user cost, have not been addressed in this study.

Even after limiting the study criteria to coverage and accuracy, a broad spectrum of users must be considered in terms of conclusions to be drawn. For example, the meaning of available accuracy is not immediately apparent, nor is its applicability, inasmuch as the accuracy of Omega navigation depends not only on geophysical variables but on the sophistication of both the user's receiver and the propagation-prediction corrections (PPCs) that are available to the user. A user can provide its own PPCs if it has the motivation and resources to do so, or it can use PPCs that are provided by ONSOD.

Available accuracy is, of course, strongly dependent on the sophistication of a user's receiver. In this study, available accuracy has been characterized according to two levels of receiver sophistication. Specifically, accuracy assessments have been performed for (a) a hypothetical receiver providing single-frequency LOP's and (b) a hypothetical automatic receiver that makes optimal use, in a least squares sense, of all available Omega signals. It is doubtful that even a sophisticated Omega receiver can interpret, in real time, the effects of transient propagation phenomena such as SIDs and PCAs. These phenomena are not predictable, are unavoidable, and cause significant degradation in navigation performance of a users receiver. In this study, attainable accuracy assumes that SIDs and PCAs are absent; that is, accuracy estimates are based on data from which all known SIDs and PCAs have been removed.

Appendix J provides specific conclusions on available accuracy of interest to a user employing a single-frequency LOP receiver at 10.2 kHz. Appendix O provides comparable information at 13.6 kHz. Apppendixes K and P provide specific conclusions on available accuracy of interest to a user employing a sophisticated receiver such as a Magnavox 1104 or 1105. The conclusions presented in Appendixes J, K, O and P are strictly limited by available data and do not extrapolate to unmeasured conditions. Similarly, the rest of the data-based Appendixes G through P present specific conclusions that can be of direct interest to users.

Having argued that Appendixes G through O are themselves conclusions, it is nevertheless appropriate to attempt to summarize those results and to generalize, where possible, about the efficacy of Omega over the entire South Atlantic Region.

9.2 OMEGA SIGNAL COVERAGE

Omega signal coverage at 10.2 kHz in the South Atlantic is presented in Appendix H. The results of this study indicate that Omega signal coverage in the South Atlantic is somewhat better than had been predicted by the TASC study. The results are conservative in the sense that the eventual presence

of a transmitter in Australia can only improve coverage, although the TASC predictions indicate that expected coverage from Station G should be quite poor in the South Atlantic.

There is no comprehensive prediction of Omega signal coverage at 13.6 kHz in the South Atlantic. A comparison of measured results at 13.6 kHz (Appendix M) with measured results at 10.2 kHz (Appendix G) suggests that, broadly speaking, signal coverage at 13.6 kHz is comparable to signal coverage at 10.2 kHz, although large variations exist in particular cases.

Measurement results are quite sparse in the southern part of the South Atlantic, except near the coasts of Africa and South America, and the quality of predictions is lower in those areas without confirming measurements.

The modified predictions resulting from this study suggest that Omega signal coverage, in terms of adequate SNR and freedom from excessive modal interference, should be reasonably good during most times and seasons in the entire South Atlantic from at least three of the Omega stations B, C, D and E.

9.3 OMEGA LOP ERRORS

LOP errors have been considered in two way in this study. First, LOP mean errors obtained at ONSOD monitor sites have been determined on a diurnal basis for specific years and for the possible months of February, May, August and November. The results have been presented in Appendix I for 10.2 kHz and in Appendix N for 13.6 kHz. No further analysis of the results in Appendixes I and N have been performed, as any further analysis would be beyond the scope of this study. However, the results as presented provide potentially valuable input to any study designed to improve the PPC model presently used by ONSOD.

The second consideration of LOP errors has been a statistical analysis of LOP errors at 0600 GMT and 1800 GMT for the months of February, May, August and November. This analysis has used data from IOS vessels, and has averaged measurements over more than one year. Appendix J presents LOP error statistics at 10.2 kHz, and Appendix O presents LOP error statistics at 13.6 kHz.

---

*No August data were available.

Apparent accuracies of LOP measurements in the South Atlantic are moderately good. Within the circumstances actually measured, median LOP errors are typically about 15 cecs, and 90 of the observed mean errors are less than 25 cecs.

The results shown in Appendixes J and O suggest that fix accuracies better than ±2 NM are regularly achievable in the South Atlantic. A caveat to this conclusion is that little or no data are available for the southern part of the region where theoretical predictions of SNR indicate poorer signal quality than in the northern part of the region where most of the data were taken.

9.4 OMEGA FIX ERRORS

Fix errors have been estimated both from ONSOD monitor data and from the IOS data. The IOS data file supplied by ONSOD provides, at each location and at each of the frequencies 10.2 kHz and 13.6 kHz, fix errors for a number of Omega fixes, where the various fixes are obtained using various combinations of available LOPs. Out of each set of fixes obtained at one location using one frequency, one "best" fix is obtained, in the sense of having the smallest total error. Fix errors associated with the best fix characterize the Omega fix accuracy that is attainable under the circumstances for the IOS operation. The ONSOD monitor data obtained from Masterfile is treated in the same way in that various combinations of two LOPs are processed to yield a single fix; then the "best" fix is selected based on the smallest mean error, as described in Section 3.5.

Attainable fix accuracies, described in terms of northern and eastern components, are estimated by averaging individual results. Appendix K presents attainable fix accuracies for 10.2 kHz and Appendix P presents attainable fix accuracies for 13.6 kHz.

As in all other data analyses, conclusions for situations where no data exist must be drawn cautiously. Nevertheless, the results presented in Appendix K and Appendix P indicate that attainable Omega accuracy in the South Atlantic is characterized by a median error of about ± 1 NM and that 90% of all fixes should have errors less than ± 2 NM. Accuracies in the southern

part of the South Atlantic may be somewhat worse than these estimates because of the predicted diminishment of signal quality in the southern part of the region.

9.5 MODAL INTERFERENCE

Modal interference, caused by the presence of higher-order propagation modes, gives rise both to amplitude fluctuations and to phase fluctuations as functions of range along a propagation path. Amplitude fluctuations indicate the presence of modal interference, but do not have an easily calculated quantitative relationship with phase fluctuations. It is thus beyond the scope of this study to interpret observed signal-amplitude fluctuations in terms of phase fluctuations. In particular, no attempt is made here to validate the predicted contours of $\Delta\phi$ = 20 cec which have been provided by TASC and illustrated in Appendix F. The conclusions to be drawn from the results discussed in Section 7.9 will be limited to comments on the extent of agreement between observed and predicted signal-amplitude fluctuations for particular cases.

The results obtained from Norway show substantial, although not complete, agreement between observed and predicted signal amplitude effects due to modal interference. If anything, the observed effects indicate slightly more severe modal interference at 10.2 kHz than has been predicted in the South Atlantic, and also indicate comparable modal interference at 10.2 kHz and 13.6 kHz.

The results obtained from Liberia confirm the predictions of strong modal interference effects, at least along radials to the southwest of Liberia. Observed and predicted effects were consistent in all cases, at both 10.2 kHz and 13.6 kHz.

The results obtained from La Reunion confirm the predictions of moderate to weak modal interference effects in the South Atlantic. Observed and predicted effects were consistent in all cases, at both 10.2 kHz and 13.6 kHz.

The results obtained from Argentina suggest that, while modal interference is present out to ranges of 5.7 megameters, the severity of the modal interference may be less than predicted at 10.2 kHz. At 13.6 kHz, on

the other hand, modal interference may be somewhat more severe than predicted out to ranges exceeding 8 megameters.

9.6 RECOMMENDATIONS

The most serious limitation on the results of this study has been the lack of measurement data over large sections of the South Atlantic Region. This limitation was recognized early in the study. In order to provide for an augmentation of the results should additional data become available at a later time, the analysis results have been quantized into small geographical areas, and presented in this form in the various appendixes. The results have thus been preserved at a fairly detailed level for ease of augmentaiton.

It is recommended that some effort be made to collect more IOS data in geographical areas of the South Atlantic that are presently under-represented. Additional data should include measurements of Station G, in Australia, so that benefits of the Australia signal can be evaluated, especially in the southern part of the South Atlantic Region.

REFERENCES

1. Karkalik, F.G., Sage, G.F., Vincent, W.R., "Western Pacific Omega Validation," Report No. ONSOD 01-78, Volume I and Volume II, April 1978, prepared by Systems Control, Inc. (Vt) for Omega Navigation System Operations Detail.

2. Karkalik, F.G., "Omega Validation Over the Western Pacific Area," presented at the International Omega Association Third Annual Meeting, London, England, September 1978.

3. Kugel, C.P., Rider, K.B. and Bickel, J.E., "Western Pacific Omega Validation Test Plan," prepared by NOSC, for USCG, 1 July 1977.

4. Kugel, C.P., Ferguson, J.A., Bradford, W.R., and Bickel, J.E., "Western Pacific Omega Validation," Preliminary Report, NOSC, TN-340, December 22, 1977.

5. Campbell, L.W., Servaes, T.M. and Grassler, E.R., "North Atlantic Omega Navigation System Validation," Analytical Systems Engineering Corp., ONSOD Report No. CG-ONSOD-01-80, July, 1980.

6. Levine, P.H. and Woods, R.E., "North Pacific Omega Navigation System Validation," Megatek Corporation, December 1981.

7. Nolan, T.P. and Herbert, N.F., "Omega Navigation System Status and Future Plans," May 1976.

8. Scull, D.D. and Kasper, Jr., J.F., "Omega Operational Development Status," presented at First Annual Meeting of the Internatinal Omega Association, Washington, D.C., July 1976.

9. Morris, Peter B. and Cha, Milton Y., "Omega Propagation Corrections: Background and Computational Algorithm," ONSOD-01-74, DOT, U.S. Coast Guard, Omega Navigation System Operations Detail, Washington, D.C., December 1974.

10. Tolstoy, A.I., "New Coefficients for the Swanson PPC Model as Utilized by Omega at 10.2 KHz," Omega Navigation System Operations Detail, October, 1976.

11. Morris, P. and Swanson, E.R., "New Coefficients for th Swanson Propagation Correction Model" presented at the 5th Annual Meeting of the International Omega Association, Bergen, Norway, August, 1980.

12. Fugaro, A.F., "U.S. Coast Guard Radio Navigation Plans and Policies," presented at the First Annual Meeting of the International Omega Association, Washington, D.C., July 1976.

13. "Department of Transportation; National Plan for Navigation: Annex," Department of Transportation, Washington, D.C., July 1974.

14. "Omega Newsletter," Volume 1, No. 2, Summer 1978, U.S. Department of Transportation, U.S. Coast Guard ONSOD.

15. Swanson, E.R. and Dick, M.L., "Propagational Assessment of VLF Navigation Signals in North America and the North Atlantic," FA74WAI-425-2, NELC, San Diego, California, February 1975.

16. "Investigation Into the Propagation of Omega Very Low Frequency Signals and Techniques for Improvement of Navigation Accuracy Including Differential and Composite Omega," Final Report, NASA CR-132276, Research Triangle Institute, Research Triangle Park, North Carolina, February 1973.

17. Swanson, E.R., "VLF Navigation Monitor: Purpose and Function," FA74WAI-425-4, NELC, San Diego, California, May 1975.

18. Gupta, R.R., Donnelly, S.F., Creamer, P.M. and Sayer, S., "Omega Signal Coverage Prediction Diagrams for 10.2 kHz," The Analytical Sciences Corporation, October, 1980.

19. "Solar-Geophysical Data, Part I (Prompt Reports)," U.S. Department of Commerce, Boulder, Colorado.

20. "Solar-Geophysical Data, Part III (Comprehensive Reports)," U.S. Department of Commerce, Boulder, Colorado.

21. Kugel, C.P., Ferguson, J.A. Bradford, W.R. and Bickel, J.E., "South Atlantic Omega Validation Test Plan," NOSC Working Paper prepared for USCG/ONSOD, 1 April 1980.

22. Kugel, C.P. Ferguson, J.A., and Bickel, J.E., "South Atlantic Omega Validation," Naval Ocean Systems Center, September, 1981.

23. Tyler, J.S. and Stepner, D.E., "Oceanic ATC Surveillance Systems STudy," Report No. FAA-RD-73-8, February 1973, prepared by Systems Control, Inc., for Department of Transportation, Federal Aviation Administration.

24. Karkalik, F.G. and McConkey, E.D., "Loran-C, Omega, and Differential Omega Applied to the Civil Air Navigation Requirement of CONUS, Alaska, and Offshore," Vols. I, II, and III, Systems Control, Inc., April 1978, FAA-RD-78-30.

25. Reich, P.G., "Analysis of Long-Range Air Traffic Systems: Separation Standards - Parts I, II, III," Journal of the Institute of Navigation, Vol. 19, No. 1, January 1966; No 2, April 1966; No. 3, July 1966.

26. ICAO Regional Plan Publications.

27. "Annex 10 to the Convention of International Civil Aviation," Vol. II, July 1972.

28. ICAO Annex 2, (MNPS).

29. International Convention for the Safety of Life at Sea, 1974 Message from the President of the United States Transmitting the International Convention for the Safety of Life at Sea, 1974, London, Nov. 1, 1974, U.S. Government Printing Office, 57-1180, 1976.

30. "National Plan for Navigation," U.S. Department of Transportation, November 1977.

31. Federal Radionavigation Plan, published by Department of Defense and Department of Transportation, July 1980.

32. "Economic Analysis of Civil Navigation Alternatives Marine and Air User Benefits," Systems Control Technology, Inc., March 1982 (Draft).

APPENDIX A

SIGNAL-TO-NOISE (SNR) CONVERSION FOR MAGNAVOX RECEIVERS

APPENDIX A

SIGNAL-TO-NOISE (SNR) CONVERSION FOR MAGNAVOX RECEIVERS

dB	Reading	dB	Reading
-40.0	0.01	-9.3	0.28
-36.0	0.02	-8.9	0.29
-30.0	0.03	-8.0	0.30
-28.3	0.04	-8.3	0.31
-26.5	0.05	-8.6	0.32
-24.5	0.06	-7.7	0.33
-22.3	0.07	-7.4	0.34
-20.0	0.08	-7.1	0.35
-19.3	0.09	-6.8	0.36
-18.5	0.10	-6.5	0.37
-18.0	0.11	-6.2	0.38
-17.4	0.12	-5.9	0.39
-16.9	0.13	-5.6	0.40
-16.3	0.14	-5.4	0.41
-15.7	0.15	-5.2	0.42
-15.2	0.16	-5.0	0.43
-14.6	0.17	-4.9	0.44
-14.1	0.18	-4.7	0.45
-13.5	0.19	-4.5	0.46
-13.0	0.20	-4.3	0.47
-12.5	0.21	-4.2	0.48
-12.1	0.22	-4.0	0.49
-11.6	0.23	-3.8	0.50
-11.2	0.24	-3.6	0.51
-10.7	0.25	-3.4	0.52
-10.2	0.26	-3.2	0.53
-9.8	0.27		

APPENDIX A (CONTINUED)

SIGNAL-TO-NOISE (SNR) CONVERSION FOR MAGNAVOX RECEIVERS (CONTINUED)

dB	Reading
-3.0	0.54
-2.8	0.55
-2.6	0.56
-2.4	0.57
-2.2	0.58
-2.0	0.59
-1.6	0.60
-1.5	0.01
-1.2	0.62
- .9	0.63
- .6	0.64
- .3	0.65
.0	0.66
.3	0.67
.6	0.65
.9	0.69
1.2	0.70
1.4	0.71
1.6	0.72
1.7	0.73
1.9	0.74
2.1	0.75
2.3	0.76
2.5	0.77
2.6	0.78
2.8	0.79
3.2	0.80
3.7	0.81
4.4	0.62
5.0	0.83
5.4	0.84
5.9	0.85
7.5	0.86
8.3	0.87
9.0	0.88
9.3	0.89
9.6	0.90
10.0	0.91
11.5	0.92
12.5	0.93
13.8	0.94
15.7	0.95
17.5	0.96
20.0	0.97
30.0	0.98
40.0	0.99
45.0	1.00

APPENDIX B

OMEGA PERFORMANCE SUMMARIES DECEMBER 1977 THROUGH JULY 1978

OMEGA PERFORMANCE SUMMARY

No. 4 31 March 1978

	Since 3/22/78	Total since 12/77
Total flight reports received:	49	250
Unuseable (incomplete) reports:	0	6 (02%)
Both systems operated normally in all respects:	42 (86%)	172 (70%)
One system operated normally in all respects:	4 (08%)	55 (23%)
Malfunction/s reported on part of both systems:	0	7 (03%)
Malfunctions reported on part of one system:	1 (02%)	14 (06%)
One system reported inoperative:	1 (02%)	10 (04%)
Lane slip/s reported on part of both systems:	2 (04%)	16 (07%)
Lane slip/s reported on part of one system:	3 (06%)	31 (13%)

P.R.J. Reynolds
Mgr., Nav. Services

PILOT COMMENTS

1. N892PA GUM/HNL: #2 Omega inop.

2. N404PA Eagle Is./Pt. Menier: Both ONSs ind. on track both dopplers; Ind. on track between Oyster and Klamm Goose Radar showed us 12 n.m. Left of track - after LAR performed ONSs showed us 12 n.m. Left of track.

   Reviewer's Comment: Both ONSs were reported righton over head Eagle Island. It appears that both slipped a lane simultaneously between Ireland and Labrador. Both were right on overhead Pt. Menier subsequent to the reported LAR.

3. N453PA, Eagle Island/Goose Bay: Due to difference in wind and Mag. Heading Omegas diverged a nd it was difficult to resolve ambiguity - LAR was performed on both sets but drifted apart within one hour.

   Reviewer's Comment: The inbound gateway positions show the #2 system to have a radial error of 16.0 n.m./063.2° and the #1 system 5.1/054°. The #2 system appears to have had the problem but it's possible that #1 might have had one also prior to the LAR.

4. N884PA, TYO/GUM: We were not on radial and Omega showed 5 RT - Operation perfect !!

5. N401PA, Skipness/Waco(Que.) 1650Z AMTK display 109° should be 305° - all other functions OK - reads AMTK correctly when queried (flight planning mode?) incorrectly otherwise - waypoints check OK - position OK - offset OK - wind & GS incorrect compared with #2.

   Reviewer's Comment: Apparent enroute malfunction of #1 system - position accuracy was not disturbed but apparent glitch in guidance computation.

6. N455PA, DKR/JFK: ONS #2: deselected Liberia - ONS #1: No deselection.

   Reviewer's Comment: Night-time Liberia procedure was applied,#1 was unaffected.

7. N402PA, DKR/JFK: Station #2 deselected from #2 ONS before takeoff. Approx :45 after T/O△ Position = 4 miles. Station #2 deselected from #1 ONS. Within 10 minutes positions were within 0.5 miles.

8. N402PA, JFK/ROB: Station #2 deselected from #2 ONS on ground. #1 & #2 ONSs were very close together for about 3.5hrs., then gradually separated by 4 miles. Station #2 deselected from #1 ONS @ 0400Z. #1 ONS immediately came within one mile of #2 ONS, and remained there for the remainder of the flight.

   Reviewer's Comment: In both 7 & 8 above the use of Liberia (at night) disturbed the position of the #1 system and the disturbance disappeared when Liberia was deselected.

9. N455PA, DKR/JFK: Deselected Liberia station on #2 Omega. #1 performed normally with Liberia still selected. #1 went in DR for approx. 5 mins. It was receiving no stations - then resumed normal operation.

10. 0715Z #2 mag. track wrong. #1 reads 352° - #2 reads 166° - distance OK, everything else OK - no other indication.

OMEGA PERFORMANCE SUMMARY

No. 9 19 May 1978

	Since 5/10	Since 12/77
Total flight reports received through 18 May:	119	752
Unuseable (incomplete) reports:	3 (02%)	13 (02%)
Flights on which both systems operated normally:	103 (89%)	566 (77%)
Flights on which one system operated normally:	6 (05%)	109 (15%)
Flights reporting malfunctions of both systems:	0	8 (01%)
Flights reporting malfunctions of one system:	6 (05%)	14 (02%)
Flights reporting one system inoperative at departure:	1 (01%)	19 (03%)
Flights reporting apparent lane slip - both systems:	6 (05%)	28 (04%)
Flights reporting apparent lane slip - one system:	5 (04%)	72 (10%)
Flights reporting enroute system failure:	1 (01%)	2 (since 3/20/78)

P.R.J.Reynolds
Mgr., Navigation Services.

PILOT COMMENTS

1. N402PA, San Juan - Asuncion, 5/6/78: Position good over Manaus but the longitude fell out by Asuncion. Sunrise took place in between. After ASU could not get a good LAR due to poor signal strength and geometry.

   Comment: On arrival Buenos Aires the #1 Omega radial position error was 260°/8.3 n.m. The #2 system was reported "out" at that point.

2. N402PA, Asuncion - Margarita, 5/7/78: 0610 GMT - #2 display (CDU) went blank with CDU red light on. Display came back on (red light on, flashing AMB and position in error over 30 n.m.) Then display went blank and repeated this condition several times within a 5 min. period. During time display was on, checked the status code. Left and right both displayed 0. Display (off) again and when it came back on tried Lane Amb. (Status 4 Left reading 1.7, right reading 0) Display again went blank. Turned set off for 10 mins. & back on. Updated to #1. Final readout at JFK as shown. (This referred to the #1 system - 1.6N & 0.2E at JFK) 1318Z - approx 35 nm from JFK #2 ONS red light on; CDU blank - turned pwr. OFF.

3. N409PA, Dakar - JFK, 5/7/78: #2 XTK 5.2 at N1931.0 W2311.0 (#1 1.9 XTK). Attempted LAR on #2 - went to 2 checked station signal and #1 + #4 showing 0. Reselected 1 + 4. Attempted another LAR - normal - both ONS showing same positions.

   Comment: There would have appear to have been an automatic deselection of stations 1 and 4, Norway and N. Dakota. This is not supposed to happen.

4. N410PA, Nantucket - Dakar; 5/4/78: No pilot comments. Apparent dual lane slip if it is assumed aircraft actually overheaded navaid. Radial errors at DKR were 326°/7.7 n.m. and 328°/7.8 n.m. No mention of whether "deselect Liberia" procedure was used.

5. Port of Spain - Brasilia, 5/8/78: At gate in Miami both Omegas slipped lanes and had to be updated twice - airborne both Omegas slipped lanes and were updated over Bimini - enroute Bimini - Grand Turk both Omegas slipped lanes again - update over Grand Turk (NDB) held good for duration of flight (to Rio de Janeiro). GMT/DMY was correct - Positions and waypoints checked good - a real puzzler. Note: Liberia was deselected between Bimini and Grand Turk.

6. N415PA, Nantucket-Dinard, 5/2/78: 0818Z,45N 30W, #1 Omega read over 8 miles difference from #2 in longitude. Updated to #2 position . LAR used & OK.

7. N425PA, Dakar-Nantucket, 5/09/78: Radar vectors (around inbound gateway) but Omega was right on at CODDS. #1 SYN & DR lights on steady due no reception of any stations at 0430Z and again at 0458Z. Again at 0555Z to 0601Z. #1 red light (CDU) inop. during Test.

   Comment: Position accuracy was not degraded by the several short-term desyncs. This familiar fault has been corrected in the revised software now being installed.

8. N455PA, Nantucket to Dakar, 4/21/78: At 0350 #2 sta. (Liberia) removed from #1 ONS. At 0400 LAR performed on #1, after LAR both sets showed 1.5 posn. error but 10 miles discrepancy remained between sets.

   Comment: Radial position errors on ramp at Dakar were 331°/7.1 n.m. and 172°/2.9 n.m. Apparent enroute lane slip on #1 system. Pilot appears unaware that the estimated position error output is an in-lane (only) and not out-of-lane estimate.

9. N492PA, Belfast-St. Anthony, 4/30/78: Both of the Omegas were very close for the entire flight to about 150 miles east of AY (St. Anthony) and then lane slips started - we were navigating on AY VOR. We also got some lane slips on the ground at GXH, updated over Lichfield NDB and ONS worked satisfactorily for the crossing. Over AY we updated both ONS and they still split. We then LARd both ONS and they came together. Both ONS were receiving 5 or 6 stations. No visible reason for the lane slips over AY.

   Comment: Could have been related to PCA following the major solar flare of 4/28/78 although this hypothesis doesn't jibe too well with the successful LARing after AY. The split following the update is not unusual, occasionally the position will settle into the wrong lane before it has time to stabilize.

10. N880PA, Timehri-Brasilia, 5/09/78: 0300Z, #2 Omega does not accept Long. (W8016.9) it jumps to W8026.6. 0050Z DR/SYN/AM lights out. Reinserted, #2 Omega, Lat/long in position. Long. jumps to W8026.9. 0103Z Liberia deselected - position still in error (Long. 80-26.6) 0315Z Attempt LAR #2 0135Z - unable. 0140Z updated to #1- operation OK remainder of flight.

    Comment: Appears to have been a temporary malfunction of the #2 CDU or program/

11. N882PA, Miami-Panama, 5/11/78: Enroute system malfunction - #2 system. Throughout flight #2 ONS would receive only 2-3 stations. 2- 4 & 7 while #1 received 1-4-6-7 & 8. #2 system in DR from 2200Z to 2300Z.

    Comment: The #2 radial position error at Panama was 157°/7.8 n.m., an apparent slip of one lane - cause appeared to be degraded receiver sensitivity.

12. N885PA, Sable Island-Dinard, 5/07/78: Eight mile along-track error - corrected by LAR.

13. N885PA, Cognac-Hyannis, 5/13/78: During first 1/2 of trip Omegas were drifting apart quite a bit - up to 8 n.m. We updated over CMF, LMG &CGC. Liberia was de-selected (even though daytime) in both units. They still were drifting around. LAR #2 = OK, LAR #1 went to 3, then 2, then LAR OK. Performed LAR once more on #2 = OK. Tried 3 LARs on #1 - last one OK. Last 1/2 of flight Omegas operated OK. During first half of flight the wind was way off, e.g. #1 345°/78 kts., #2 372°/34 kts. - #2 was most accurate.

    Comment: The early problem sounds like a signal and/or geometry problem in the early portion of the flight but no signal information was given - Both Omega systems were right on over Hyannis VOR.

14. N887PA, Hickam-Guam, 5/09/78: Numerous lane slips both systems at blox & during taxi at HIK/HNL.

    Comments: No position information whatever was logged. Lane slip on the ground can happen almost anywhere due high local radio noise levels but particularly at Honolulu due to the Hawaii station being subject to near-field constraint.

15. N887PA, Guam-Japan, 5/12/78: #2 ONS lane slip in climb - systems checked at 34 DME from Guam & OK. At BULBS (100 n.m. out) #2 had 8 n.m. error. Updated against #1 ONS and GUM VORTAC - LAR not tried. No position accuracy information recorded on arrival Japan.

16. N897PA, Nantucket-Lisbon, 5/01/78: Deselected Sta. 2 per NOTAM. #1 lane slip between CODDS and PIKE - corrected with LAR. #2 lane slip between Flores and 20W - corrected with LAR.

- o -

1	4/15	2		
2	16			
3	17	1		
4	18			
5	19			
6	20			
7	21	1	1	
8	22			
9	23	1		
10	24	2		
11	25			
12	26			
13	27	1		
14	28			Major Solar Flare
15	29			
16	4/30	2	1	
17	5/1	3	1	
18	2		1	
19	3	3	1	
20	4	5	2	
21	5	12		
22	6	10		
23	7	9	3	
24	8	9		
25	9	9	1	Solar Flare
26	10	6		
27	11	6		
28	12	7		
29	13	1		
30	14	8		
31	5/15	4		

OMEGA PERFORMANCE SUMMARY

No. 13 3 July 1978

	Since 6/17	Since 12/77
Total flight reports received through 27 June:	169	1227
Unuseable (incomplete) reports:	4 (02%)	25 (02%)
Flights upon which both systems operated normally:	157 (95%)	991 (82%)
Flights upon which one system operated normally:	2 (01%)	128 (11%)
Flights reporting malfunctions of both systems:	0	9 (01%)
Flights reporting malfunctions of one system:	3 (02%)	25 (02%)
Flights reporting one system inoperative at departure:	0	20 (02%)
Flights reporting apparent lane-slip - both systems:	3 (02%)	36 (03%)
Flights reporting apparent lane-slip - one system:	2 (01%)	84 (07%)
Flights reporting enroute system failure:(since 3/20/78):	1 (01%)	3 (.25%)

P.R.J.Reynolds
Mgr., Navigation Services

Geographical Distribution of Reporting Flights:

	Flights	Lane Slips
North Atlantic MNPS Area:	123	2
U.S. - Brazil/Argentina:	14	2
U.S./Caribbean - Spain:	10	0
U.S. - West Africa:	8	3
Japan - Guam:	4	0
U.S. - Hawaii:	3	0
Guam - Hawaii:	3	0
Japan - Hawaii:	2	2
Brazil - South Africa:	1	0

Lane Slip Summary:

1. N415PA, Gander-Shannon, 6/7/78: Approx. 30W 0740Z Both systems AMB lights illum. continuously (flashing and steady). Checked station reception.#1 sys. rec. 3, 4, 6 & 7. #2 sys. rec. 2, 6 & 7. LARs unsuccessful - D.R. lgiht occasionally illum. - position on both machines obviously in error. Call Code 0 status reads 1 temporarily, then 0. During LAR attempt status code 2 appears.

   Reviewer's Comment: This flight was reprted to have suffered signal starvation on both systems for most of the flight, e.g. Norway was not received by either system. Shannon ATC radar reported the flight 40 n.m. south of track at 15W. This error appears to have been incurred at about 30W where the #2 system, in use as the steering reference, crossed the Argentina-Trinidad bseline extension while receiveing only Liberia (2), Argentina (6) and Trinidad (7). The #1 Omega system had a radial position error of 087°/7.7 n.m. over the Shannon VOR, the #2 system at this point had a radial error of 015°/44.6 n.m. Both Omega systems ground checked O.K. at London and functioned normally on the return flight to New York.

2. N425PA, Dakar-Nantucket, May 25, 1978: This flight, overhead the Nantucket VOR, reported radial position errors of 218°/6.7 n.m. and 238°/10.5 n.m. Pilots comments were as follows: 0628.5Z - Norway deselected #2 (solar advisory). Liberia deselected on both. Lane slip showed up on #2 12 n.m. offsets - 10 mi. difference dist. to go - LAR not accepted by #2 - AMB on both sets at 0655Z. Position error estimate est. #1 = 5.6 and #2 = 7.4. 0710Z #ONS reinserted sta. 1 & 2. 0716Z LAR #1 4.0-1.7 (?).

   Reviewer's Comment: The problem withthe #2 system appears to have been induced by the precautionary deselection of Norway on the basis of a solar advisory. Both systems appeared to have suffered signal starvation at about 0700Z.

3. N886PA, Zandery-Belo Horizonte, 6/8/78: No pilot comments. The radial position errors over the Belo Horizonte VOR 308°/13.3 n.m. and 306°/14.5 n.m. The close similarity of these errors suggest that the aircraft may have been vectored around, rather than over, the navaid. On the other hand, the time was early morning and it could have been a dual cycle-slippage, possibly.

Lane Slip Summary (cont.)

4. N884PA, Tateyama- Honolulu Terminal, 6/15/78: The radial position errors upon arriving at the gate at Honolulu were 278°/17.8 n.m. and 270°/13.9° n.m. but these may very well have occurred during the landing or taxiing phases (with Hawaii subject to near-field constraint). The pilot reported a 10 n.m. latitude error enroute which was corrected by updating position.

5. N453PA, Glasgow-Goose Bay, 6/15/78: The pilot reported: #1 &#2 were very close until approaching YYR (Goose Bay) - Momentary DR then SYS lite on #2. #2 apparently apparently slipped - could not LAR with Norway out (solar advisory). Updated to #1.

   Reviewer's Comment: This appears to have been a transitory malfunction which resulted in a longitude slip of 1° 32', latitude was not affected. The circumstances suggest a power interruption involving the radio (#2) buss.

6. N882PA, JFK-Robertsfield, 6/23/78: The Omega positions were normally accurate upon arriving at Roberts but the pilot reported a single enroute lane slip which was corrected by updating. One suspects that this involved the #1 system which, procedurally, would be using Liberia unless and until a position error was noted.

Pilot Comments (other than lane slip):

N408PA, Springdale-Shannon, 6/20/78: Both Omegas were totally unreliable for first forty minutes of flight (out of Detroit). AMB lites on steady - couldn't LAR. Updated (position) over Stirling VOR, Beauce VOR and Houlton, then they were OK rest of flight. (Suspect poor signal geometry west of Toronto).

Reviewer's Comment: Typical Omega behaviour in crossing western portion of "Winnipeg Hole" without VLF backup mode. Is now in the process of correction through installation of modified programs containing VLF capability.

N433PA, Gander-Shannon, 6/18/78: #2 AMB light on for entire flight.

Reviewer's Comment: It has to be manually extinguished - it won't go out by itself.

N433PA, Shannon-Gander, 6/26/78: No. 2 intermittent flash of digits across readout with no meaning and if flash occurs during inserting attempt, it cancels out attempt to insert.

Reviewer's comment: A too familiar pecadillo of the Omega program now being replaced. The meaningless data is ordinarily GMT/Date which is briefly displayed at twenty-second intervals. This fault has been corrected in the new program.

N492PA, Waco-Glasgow, 6/23/78: Both systems in SYN on ground DTW (Detroit) Five min. delay for takeoff. Probable cause - lack of stations.

Reviewer's Comment: Correct - Winnipeg Hole effect.

N793PA, Cork-Sable Island, 6/13/78: Note: Updated Omega at Sable - used Ramp #2 position at BOS (Boston) for last pos. which is N12-23 W71-01. Readout #1 = 42-21.9 71-01.8. #2 = 42-22.0 71-01.7.

Pilot Comments (cont.)

N883PA, Dakar-Hyannis, 6/18/78: At 60W both Omegas indicated on track. 150 n.m. beyond 60W they inidcated 11L - waypoints checked OK and doppler course OK. Up to 60W Doppler and Omega had been within limits at all times carrying 1.0E deviation after original update (of dopplers). After flying a/c to 00 XTK dopplers were: #1 = 19R and #2 = 22R.

Reviewer's Comment: Possible compass malfunction. Both Omegas were very accurate overhead the Hyannis VOR.

N887PA, Hawaii-Travis AFB, 6/16/78: "AMB" annunciator lite was illuminated on both sets for 80% of ground operation at Honolulu.

Reviewer's Comment: Not unusual. Probable causes were high local radio noise level and, perhaps more importantly, Hawaii was automatically deselected because of near-field effect. Enroute operation appears to have been normal.

N893PA, 6/21/78, Belo Horizonte-Barbadoes; Longitude of 2 Omegas 9 n.m. apart at 1000Z. No malfunction codes - no AMB lts. - Liberia deselected from #2.

Reviewer's Comment: Good example of modal interference in Liberia signal - it might as well have been deselected from #1 also.

- o -

APPENDIX C

OMEGA LOGS FOR PANAMERICAN FLIGHT NO., 541, APRIL 5-6, 1978
NEW YORK TO SAN JOSE, GUATAMALA TO NEW YORK

O[illegible] [illegible] OF O[illegible] SIGNAL STRENGTHS (CMA 7[illegible]0) ◯

OBSERVER ________

D[illegible] [illegible] [illegible] NO. 541/25 ROUTE OF FLIGHT [illegible]

[illegible]	1-4[illegible]			16[illegible]			1833			1915			1450			2[illegible]		
[illegible] Position ①																		
[illegible] Position ②	40 [illegible] / 73 - 46.2			40 - [illegible] / 23 - 4[illegible]			38 - 14.2 / 77 - 45.9			32 - 48.7 / 81 - 28.6			28 - 35.8 / 83 - 34.6			24 - 02.5 / 86 - 48.1		
[illegible] Position	[illegible] / [illegible] 2.2			40 [illegible] / 73 [illegible]			38 - 15.1 / 77 - 46.1			32 - 46.9 / 81 - 30.0			28 - 26.1 / 83 - [illegible]			24 - 01.0 / 86 - 48.2		
				END [illegible]														
[illegible] (1)	3	19	0	46	21	52 ③	26	19	32	11	15	8 ⑰	18	4	㉔	4	6	㉗
[illegible] (2)	[illegible]	61	28	75	71	76 ①	60	75	72	30	64	32 ⑧	12	26	⑥	7	0	⑤
[illegible] (4)	34	21	19	84	70	82 [illegible]	86	85	87	85	91	81 ㉚	91	91	㉜	89	93	㉙
[illegible] Da[illegible] (1[illegible])	97	96	95	97	96	96 ㉟	98	95	98	97	97	96 ㊸	96	97	[illegible]	97	97	㉗
[illegible] (2)	0	0	10	7	0	43 [illegible]	29	35	31	22	43	45 0	2	41	②	34	45	⑪
[illegible] (2)	1	67	32	61	34	68 ㊹	36	74	62	86	82	72 ㊵	37	65	56	34	63	62
[illegible]	1	52	2	31	0	8 ㊺	21	42	40	24	35	35 57	0	9	[illegible]	57	75	48
[illegible] (2[illegible])	0	14	7	0	10	12 100	5	6	5	14	5	0	5	17	17	30	92	98
[illegible]	[illegible]	[illegible]	[illegible]	52	[illegible]	[illegible]	57	2.??	1.92	757	0.37	1.92	164	0.72	1.17	1.66 / 50	0.72	1.52

SN[illegible] [illegible]

[illegible] 10 - 0 24

③ = VLF

4332	074.1	9074	220.5
4495	184.2	6457	322.0
3886	212.0	4443	64.5
1465	240.7	1591	222.?
8705	[illegible]	2903	222.5
4183	163.0	1070	027.2
7236	124.6	9218	22?.?
6731	132.0	0	[illegible]

OBSERVER [redacted]

DATE 05-06 Apr FLT. NO. 511/512 ROUTE OF FLIGHT New York – San Juan – New York

NYC – SJU SJU – NYC

GMT	2116	0032	1415	1503	1540	1800
Omega Position (1)			← F+H + VLF →			
Omega Position (2)	18-23.5 88-08.8	19-51.1N 85-52.2W	10-[illegible] 84-12.4	10-25.9 85-19.1	13-13.5 88-34.7	17-19.3 90-12.4
INS Position	18-24.4 88-06.2	11-16.6 85-53.1	09-57.8 85-[illegible]	10-25.5 85-18.6	13-13.0 88-34.5	17-18.2 90-11.5

Frequency																		
Norway (1)	9	5	(20)	61	75	70	49	84	69 (31)	26	61	(30)	21	64	(34)	7	11	0
Liberia (2)	13	26	(6)	23	49	11	81	62	16 (3)	48	78	(4)	22	93	(6)	2	64	41
Hawaii (4)	89	93	(4)	88	92	89	91	94	92 (46)	93	95	(40)	73	97	(47)	90	94	96
N. Dakota (10)	97	97	(32)	93	96	92	96	97	97 (37)	96	96	(38)	48	82	(34)	99	98	99
Reunion (22)	35	55	(1)	27	51	19	69	85	77 (31)	78	87	(47)	62	89	(35)	29	67	59
Argentina (42)	60	80	(49)	20	58	24	90	93	85 (50)	84	93	(35)	70	87	(51)	70	94	83
[illegible] (100)	63	2	(41)	53	58	79	85	91	79 (53)	84	70	(56)	09	84	(55)	30	77	63
Japan (209)	41	29	(98)	36	55	48	73	84	77 (70)	85	28	(101)	49	0	(100)	49	72	70
[illegible]	254	0.72	1.56	252	[illegible]	1.44	357	0.67	[illegible]	766	[illegible]	[illegible]	766	[illegible]	[illegible]	257	0.45	1.31
[illegible]							5017	[illegible]	[illegible]	9394	[illegible]							
[illegible]	DF +						4448	[illegible]	[illegible]	6897	[illegible]							
[illegible]	1 3 4 6 +						4176	288.5	[illegible]	4677	[illegible]							
[illegible]							2251	345.1	[illegible]	2122	026.0							
[illegible]		(1) = VLF					+8472	109.5	[illegible]	3966	[illegible]							
[illegible]							3476	166.6	[illegible]	1667	020.6							
[illegible]							7529	[illegible]	[illegible]	7446	[illegible]							
[illegible]							7414	[illegible]	[illegible]	0	226.3							
[illegible]							[illegible]	[illegible]	[illegible]	[illegible]	[illegible]							

OBSERVATIONS OF OMEGA SIGNAL STRENGTHS (CNA 7-0) (3) OBSERVER R. [illegible]

DATE 06 Apr 78 FLT. NO. 542 ROUTE OF FLIGHT San Juan – Guantanamo – New York

GMT	0611/12			2010			9045			1119		
Omega Position (1)										[illegible]		
Omega Position (2)	25-22.2 86-17.7			31-40.3 82-02.6			35-37.0 49-15.6			38-56.2 75-23.9		
INS Position	25+21.5 85+17.2			31+40.8 82-02.5			35-36.3 79+10.4			38-56.5 75-22.1		
Frequency	10.2	13.6	11.3	10.2	13.6	11.3	10.2	13.6	11.3	10.2	13.6	11.3
Norway (1)	0	15	31	5	14	15	35	24	(6)	49	54	68
Liberia (2)	28	65	57	4	42	22	17	4	(2)	7	12	15
Hawaii (4)	91	92	72	72	21	94	35	82	(40)	92	87	91
N. Dakota (10)	97	17	96	96	18	96	75	92	(28)	97	97	97
Reunion (20)	39	57	64	9	30	32	0	14	(47)	5	0	7
Argentina (40)	54	71	74	34	31	31	47	52	(39)	44	64	55
Trinidad (100)	65	54	22	17	29	19	51	46	(12)	27	31	42
Japan (200)	22	33	[illegible]	0	12	8	8	0	100	4	10	1
[illegible]	737	5.67	[illegible]	21	[illegible]	[illegible]	160 17	653	5.13	55	[illegible]	57

OFF VLF

FLT. NO. 541/05 CONSOLIDATED INS/OMEGA DATA FROM JFK-IAD

DATE Apr. 05 78 (1) TO GUA

GMT		Latitude	Longitude	DA	GS	DIS	XTK	W/V	ETA	STATIONS
16[illegible]	INS	40-12.[illegible]	74-[illegible]							
[illegible]	Omega 1									
[illegible]	Omega 2	[illegible]	74-29.7							ABCDFH
[illegible]	Actual	40-12.1	74-29.7			/	/			0.74/1.47
1700	INS	3[illegible]-[illegible]	76-[illegible].2							
[illegible]	Omega #1									
[illegible]	Omega #2	3[illegible]-24.4	76-[illegible].6							[illegible] DFH
VOR	Doppler	3[illegible]-24.7	76-58.7			/	/			0.72/1.43
17[illegible]	INS	[illegible]	77-[illegible]							
[illegible]	Omega #1									
	Omega #2	3[illegible]-56.4	77-[illegible].2							
	Actual	38-56.1	77-27.8			/	/			
1721	INS	38-56.4	77-26.1							
[illegible]	Omega #1	[illegible]-56.6	77-27.0							
[illegible]	Omega #2	[illegible]-56.6	77-24.6							
[illegible]	Actual	38-56.7	77-27.4			/	/			
1805	INS	38 56.[illegible]	77 26.4							
Blcx	Omega #1									
	Omega #2	3[illegible] 57.1	77 26.0							
	Doppler	38-56.7	77 27.4			/	/			
1812	INS	3[illegible] 56.[illegible]	77 [illegible].6							
[illegible]	Omega #1									
30	Omega #2	[illegible] 56.7	77 26.0							
	Doppler	56.1	27.5			/	/			
1[illegible]	INS	37-31.4	77-49.4	6L	440	256	4.26	—	1905.7	
[illegible]	Omega #1									
[illegible]	Omega #2	3[illegible]-31.0	77 48.6	6L	438	256	4.56	—	1906.0	ABCDF
VOR	Doppler	3[illegible]-3[illegible]	77-49.7	[illegible]		/	/			0.70/1.42
1[illegible]	INS	3[illegible]-[illegible]	78-4[illegible]	7L	436	1[illegible]	[illegible]	—	1904.9	
[illegible]	Omega #1									
[illegible]	Omega #2	3[illegible]-[illegible]	78-48.3	8L	466	154	[illegible]	—	1903.4	[illegible]
VOR	Actual	3[illegible]-[illegible]	78-43.0	8L	437	/	/			[illegible]/1.40
1905	INS	3[illegible]-50.1	81-[illegible].4	3L	474	196	0.56	—	19[illegible]	
[illegible]	Omega #1									
VOR	Omega #2	3[illegible]-51.4	81-22.5	5L	[illegible]	197	0.18	—	[illegible]	[illegible]
	Actual	3[illegible]-51.4	81-22.2	5L	[illegible]	/	/			[illegible]
	INS									
	Omega #2									

FLT. NO. 541/05 CONSOLIDATED INS/OMEGA DATA FROM New York

DATE Apr [illegible] 1978 (9) TO [illegible]

GMT		Latitude	Longitude	DA	GS	DIS	XTK	W/V	ETA	STATIONS
1933	INS	30-30.[illegible]	82-32.8	2L	456	50	0.2L	—	1941.0	
Taylor	Omega 1									
VOR.	Omega 2	30-31.8	82-[illegible].1	5L	456	51	1.2L	—	1941.1	ABCDFH
	ACTUAL Doppler	[illegible]	82-33.2	4L	458	/	/			0.70/1.41
1940	INS	29-35.5	83-03.0	3L	469	25	0.5R	—	1949.9	
	Omega #1									
City	Omega #2	29-36.2	83-00.5	5L	466	26	1.0L	—	[illegible]	ABCDFH
VOR	ACTUAL Doppler	29-35.4	83-02.9	5L	470	/	/			0.68/1.42
2015	INS	2[illegible]	87-16.6	4L	454	25[illegible]	0.5L	—	2025.9	
	Omega #1									
	Omega #2	22-28.1	87-16.5	7L	459	259	0.0	—	[illegible]	DF+1234
	Doppler			7L	457	/	/			0.75/1.45
2126	INS	17-30.5	88-17.6	2L	431	74	0.1L	—	2138.8	
Belize	Omega #1	17-31.7	88 16.6							
VOR	Omega #2	17-29.8	88-17.5	4L	426	74	0.3L	—	2138.6	DF+1346
	ACTUAL Doppler	17-2[illegible]	88-18.1	4L	446	/	/			1.02/1.79
2153	INS	14-59.8	90-25.2							
[illegible]	Omega #1									
NDB	Omega #2	15-00.0	90-24.7							DF+1346
	ACTUAL	15-00.5	90-25.[illegible]			/	/			0.78/1.58
2202	INS	14-32.8	90-30.5							
TD	Omega #1									
01	Omega #2	14-33.6	90-30.8							
	ACTUAL	14-34.5	90-31.8			/	/			
2202	INS	14 33.5	90 30.6							
G 6	Omega #1	14 35.4	90 30.5							
	Omega #2	14-33.5	90 31.2							
	ACTUAL	14 35.2	90 31.7			/	/			
[illegible]	INS	[illegible]	90-31.9							
[illegible]	Omega #1									
01	Omega #2	1[illegible]	90-32.4							
	ACTUAL	14-34.2	90-31.9			/	/			
19[illegible]	INS	1[illegible] 10.1	84-07.5	2L	484	50	[illegible]	—	2019.7	
[illegible]	Omega #1									
[illegible]	Omega #2	1[illegible]	84-[illegible]	2L	50[illegible]	[illegible]	[illegible]	—	[illegible]	ABCDFH
	Doppler	1[illegible]	[illegible]			/	/			[illegible]
	INS									
	Omega #2									

FLT. NO. FIT 541 — CONSOLIDATED INS/OMEGA DATA (B) — FROM New York

DATE 05 Apr. 78 — TO San José

GMT		Latitude	Longitude	DA	GS	DIS	XTK	W/V	ETA	STATIONS
0041	INS	10-02.8	84-52.6							
Near	Omega 1	10-								
VOR	Omega 2	09-59.7	84-50.5							
	Actual Doppler	10-03.0	84-51.0							
0156	INS	9 59.5	84 12.[illegible]							
TZ	Omega #1									
R06	Omega #2	09 [illegible]	84 0[illegible]							
	Doppler	9 [illegible]3	84-12.9							
6/[illegible]	INS	10 [illegible]	[illegible]-11.4							
	Omega #1									
	Omega #2	9-59.8	[illegible]4-12.1							
	Doppler	9-59.8	84-12.1							
6/1340	INS									
init	Omega #1		FLT	542	/06	April				
	Omega #2		San José		—	New York				
	Doppler									
1450	INS	09-[illegible]	84-1[illegible].5							
End	Omega #1	10-00.2	84-1[illegible].5							
06	Omega #2	09-59.[illegible]	84-1[illegible]							
	Actual Doppler	09-59.1	84-12.1							
1459	INS	10-01.9	84-54.8	1L	422	62	1.96	—	1509.9	
Chances	Omega #1									
VOR	Omega #2	10-03.3	84-54.8	0	441	61	0.1R	—	1509.5	F+H+1345
	Doppler	10-03.0	[illegible]-51.0	3L	429					0.40/1.41
1530	INS	12-46.6	87-56.0	2R	432	84	0.51	—	1545.1	
	Omega #1									
	Omega #2	12-44.1	87-56.5	0	430	[illegible]	2.46	—	1545.1	F+H+1[illegible]
	Doppler			1[illegible]	427					
1544	INS	[illegible]-40.1	89-0[illegible]	0	450	[illegible]	0.5[illegible]	—	[illegible]	
No pay	Omega #1									
	Omega #2	13-40.9	89-07.9	2L	4[illegible]	[illegible]	2.2L	—	1612	F+H+13456
VOR-	Actual	[illegible]-41.5	89-0[illegible]	1L	448					
1600	INS	14-2[illegible]	90-0[illegible]							
[illegible]	Omega #1									
01	Omega #2	1[illegible]	1[illegible]-31.2							
	[illegible]	35.5	8							
[illegible]	INS	14 [illegible]	[illegible] 31.9							
[illegible]	Omega #1	[illegible] 35 [illegible]	[illegible] 31.4							
	[illegible]	[illegible]	[illegible]							

[illegible] 35 [illegible] 30.7

FLT. NO. 542/66 CONSOLIDATED INS/OMEGA DATA (4) FROM Guatemala

DATE 1 Apr TO New York

GMT		Latitude	Longitude	DA	GS	DIS	XTK	W/V	ETA	STATIONS
[illegible]/17[illegible]	INS	14-3[illegible].0	90-31.9							
END	Omega 1									
Rwy	Omega 2	14-34.4	90-30.9							
01	ACTUAL Doppler	14-34.2	90-31.9							
1740	INS	14-58.3	90-29.9	2R	408					
Rabinal	Omega #1									
NDB	Omega #2	14-5[illegible]	90-30.1	1L	410					ABCDFH
	Doppler	15-00.5	90-28.2							0.65/1.31
1815	INS	1[illegible]-11.[illegible]	8[illegible]-42.1	[illegible]	447	88	1.1R	—	18[illegible]	
	Omega #1									
	Omega #2	1[illegible]-13.[illegible]	8[illegible]-42.1	4R	457	88	1.[illegible]	—	1829	ABCDFH
	Doppler			6R	457					0.65/1.31
1830	INS	20-56.1	89-3[illegible].7	11R	461	130	0.1L	—	1849.6	
Merida	Omega #1	20-[illegible]	89 38.6							ABCDFGH
VOR	Omega #2	20-56.1	89-38.7	8R	4[illegible]	130	0.4L	—	1849.7	ABCDFH
	ACTUAL Doppler	20-56.4	89-34.9	10R	472					0.65/1.31
1953	INS	24-37.1	83-02.7	8R	450	44	0.2R	—	2000.4	
Cross	Omega #1	24 36.[illegible]	83 0[illegible]							
City	Omega #2	24-36.9	83-02.4	5R	456	44	0.9R	—	2000.4	ABCDFH
VOR	ACTUAL Doppler	24-35.9	83-02.9	8R	462					0.69/1.46
[illegible]	INS	[illegible]	[illegible]							
Taylor	Omega #1	[illegible]	[illegible]1.9							
VOR	Omega #2	30-31.7	82-37.4							
	ACTUAL Doppler	[illegible]	[illegible]							
2037	INS	33-52.6	81-02.0	7R	4[illegible]	40[illegible]	0.[illegible]	—	21[illegible]	
	Omega #1									
VOR	Omega #2	[illegible]-52.7	[illegible]1-05.9	4R	49[illegible]	40[illegible]	[illegible]	—	[illegible]	ACDF
	Doppler	[illegible]	[illegible]	4R	[illegible]					0.79/1.52
[illegible]	INS	[illegible]	7[illegible]-2[illegible]	6R	49[illegible]	195	4.7[illegible]	—	21[illegible]	
	Omega #1									
	Omega #2	3[illegible]-03.6	7[illegible]-2[illegible]	4R	492	197	4.7R	—	[illegible]	A[illegible]DF
	Doppler			5R	500					[illegible]4/1.50
2149	INS	40 39.9	73-45.1							
13	Omega #1									
L	Omega #2	40 39.9	73 47.6							
	ACTUAL Doppler	40-3[illegible]	73-47.0							
21[illegible]	INS	40 [illegible]	73-[illegible]							
	Omega #1	40 38.0	73 46.2							
	[illegible]	40 3[illegible]	[illegible]							

[illegible] 40-3[illegible] 73-47.2

APPENDIX D

WINDOWS OF IOS DATA AVAILABILITY

APPENDIX D

WINDOWS OF IOS DATA AVAILABILITY BY TRANSMITTER, MONTH, AND GMT

NORWAY (A)

MONTH	GMT	D/N	GMT	D/N
January	0400-0800	N	1600-2000	N
February	0400-0626	N	1600-2000	N
March	0400-0435	N	1739-2000	N
April	0435-0800	D	1600-1739	D
May	0400-0800	D	1600-2000	D
June	0400-0800	D	1600-2000	D
July	0400-0800	D	1600-2000	D
August	0400-0800	D	1600-1827	D
September	0543-0800	D	1600-1632	D
October	0400-0543	N	1632-2000	N
November	0400-0800	N	1600-2000	N
December	0400-0800	N	1600-2000	N

LIBERIA (B)

MONTH	GMT	D/N	GMT	D/N
January	0400-0653	N	1600-1833	D
February	0400-0647	N	1600-1839	D
March	0400-0641	N	1600-1844	D
April	0400-0636	N	1600-1844	D
May	0400-0633	N	1600-1849	D
June	0400-0633	N	1600-1852	D
July	0400-0632	N	1600-1851	D
August	0400-0634	N	1600-1846	D
September	0400-0639	N	1600-1841	D
October	0400-0644	N	1600-1836	D
November	0400-0649	N	1600-1833	D
December	0400-0652	N	1600-1832	D

APPENDIX D
(CONTINUED)

WINDOWS OF IOS DATA AVAILABILITY
BY TRANSMITTER, MONTH, AND GMT

HAWAII (C)

MONTH	GMT	D/N	GMT	D/N
January	0402-0800	N	1707-2000	D
February	0419-0800	N	1700-2000	D
March	0436-0800	N	1644-2000	D
April	0454-0800	N	1626-2000	D
May	0506-0800	N	1609-2000	D
June	0510-0800	N	1557-2000	D
July	0508-0800	N	1603-2000	D
August	0500-0800	N	1619-2000	D
September	0444-0800	N	1638-2000	D
October	0426-0800	N	1655-2000	D
November	0408-0800	N	1707-2000	D
December	0356-0800	N	1710-2000	D

NORTH DAKOTA (D)

MONTH	GMT	D/N	GMT	D/N
January	0400-0800	N	1600-2000	D
February	0400-0800	N	1600-2000	D
March	0400-0800	N	1600-2000	D
April	0400-0800	N	1600-2000	D
May	0400-0800	N	1600-2000	D
June	0400-0800	N	1600-2000	D
July	0400-0800	N	1600-2000	D
August	0400-0800	N	1600-2000	D
September	0400-0800	N	1600-2000	D
October	0400-0800	N	1600-2000	D
November	0400-0800	N	1600-2000	D
December	0400-0800	N	1600-2000	D

APPENDIX D
(CONTINUED)

WINDOWS OF IOS DATA AVAILABILITY BY TRANSMITTER, MONTH, AND GMT

LA REUNION (E)

MONTH	GMT	D/N	GMT	D/N
January	0400-0800	D	1600-2000	N
February	0400-0800	D	1600-2000	N
March	0400-0800	D	1600-2000	N
April	0400-0800	D	1600-2000	N
May	0400-0800	D	1600-2000	N
June	0400-0800	D	1600-2000	N
July	0400-0800	D	1600-2000	N
August	0400-0800	D	1600-2000	N
September	0400-0800	D	1600-2000	N
October	0400-0800	D	1600-2000	N
November	0400-0800	D	1600-2000	N
December	0400-0800	D	1600-2000	N

GOLFO NEUVO (F)

MONTH	GMT	D/N	GMT	D/N
January	0400-0800	N	1600-2000	D
February	0400-0800	N	1600-2000	D
March	0400-0800	N	1600-2000	D
April	0400-0800	N	1600-2000	D
May	0400-0800	N	1600-2000	D
June	0400-0800	N	1600-2000	D
July	0400-0800	N	1600-2000	D
August	0400-0800	N	1600-2000	D
September	0400-0800	N	1600-2000	D
October	0400-0800	N	1600-2000	D
November	0400-0800	N	1600-2000	D
December	0400-0800	N	1600-2000	D

APPENDIX D
(CONTINUED)

WINDOWS OF IOS DATA AVAILABILITY
BY TRANSMITTER, MONTH, AND GMT

JAPAN (H)

MONTH	GMT	D/N	GMT	D/N
January	0400-0800	D	1600-2000	N
February	0400-0800	D	1600-2000	N
March	0400-0800	D	1600-2000	N
April	0400-0800	D	1600-2000	N
May	0400-0800	D	1600-2000	N
June	0400-0800	D	1600-2000	N
July	0400-0800	D	1600-2000	N
August	0400-0800	D	1600-2000	N
September	0400-0800	D	1600-2000	N
October	0400-0800	D	1600-2000	N
November	0400-0800	D	1600-2000	N
December	0400-0800	D	1600-2000	N

APPENDIX E

GDOP VALUES IN SOUTH ATLANTIC REGION

APPENDIX E

GDOP VALUES IN SOUTH ATLANTIC REGION

GDOP is calculated at the center of all 10^{0}x10^{0} grids in the South Atlantic between 20^{0}N and 60^{0} S Latitude and 70^{0} W and 20^{0} E Longitude, according to the algorithm included herein.

```
      SUBROUTINE GDOPC
        COMMON / CONSTS / CONS, RNTDG, DGTRN, PI, TWOPI, CONS02, CONS36,
        1        PI02
        COMMON / GDOP   / CTHETA, GDOP, THETA(2,8), ALOPBR(6)
        COMMON / PROCES / II, JJ
        COMMON / TABLE6 / TRANS(2,6), BLAT(6), BLON(6), ALOPBP(6), FLG(24,6)
C
C         COMPUTE LANE WIDTH
C
      AB = ABS(THETA(1,II) - THETA(2,II))
      ABBAR=ABS(180-AB)
      BW=AMIN1(AB,ABBAR)
      ALW=1./SIN(BW/2)
      BAB = ABS(THETA(1,JJ) - THETA(2,JJ))
      BABBAR=ABS(180-BAB)
      BBW=AMIN1(BAB,BABBAR)
      BLW=1./SIN(BBW/2)
      W12=AMIN1(ALW,BLW)
      W34=AMAX1(ALW,BLW)
C
C         IF THERE ARE ONLY THREE STATIONS,SKIP NEXT EQUATION
C
      DO 90 I = 1, 2
        N = I
        DO 90 K = 1, 2
          IF (TRANS(I,II) .EQ. TRANS(K,JJ)) GO TO 9000
   90   CONTINUE
C
C         THE GDOP EQUATION FOR 4 STATIONS FIRST COMPUTE CROSSING ANGLE
C
      C1 = ABS(ALOPBR(II) - ALOPBR(JJ))
      C2 = ABS(PI - C1)
      CTHETA=AMIN1(C1,C2)
      GDOP=W12*SQRT(1+(W34/W12)**2)/(SQRT(2.)*SIN(CTHETA))
      RETURN
C
C         THIS IS THE THREE STATION GDOP THE CROSSING ANGLE IS A SUBROUT
C
 9000 BRCOM = THETA(N,II)
      CALL CROSS3(BRCOM)
      RADICL=SQRT(1+(W34/W12)**2+(W34/W12)*COS(CTHETA))
      GDOP=RADICL*W12/(SIN(CTHETA)*SQRT(2.))
      RETURN
      END
```

```
      SUBROUTINE CROSS3(BRCOM)
      COMMON / CONSTS / CONS, RNTD0, DGTRN, PI, TWOPI, CONS02, CONS36,
     1       PID2
      COMMON / GDOP   / CTHETA, GDOP, THETA(2,8), ALOPBR(6)
      COMMON / PROCES / II, JJ
      DIMENSION ALOP(6),CALOP(3)
      I = II
      J = JJ
      DO 6 K=1,6
    6 ALOP(K)=ALOPBR(K)
      NFLAG=0
      CALOP(1)=ALOP(I)+PI
      CALOP(2)=ALOP(J)+PI
      CALOP(3)=BRCOM+PI
   50 DO 2 K=1,3
    2    IF (CALOP(K)  GT  TWOPI) CALOP(K) = CALOP(K) - TWOPI
      IF((ALOP(I) LT BRCOM) AND (BRCOM LT ALOP(J))
     1      AND (CALOP(1) LT CALOP(3)) AND (CALOP(3) LT CALOP(2)))
     2     GO TO 40
      IF ((ALOP(J) LT BRCOM) AND (BRCOM LT ALOP(I))
     1      AND (CALOP(2) LT CALOP(3)) AND (CALOP(3) LT CALOP(1)))
     2     GO TO 40
      IF ((ALOP(I) LT CALOP(3)) AND (CALOP(3) LT ALOP(J))
     1      AND (CALOP(1) LT BRCOM) AND (BRCOM LT CALOP(2)))
     2     GO TO 40
      IF((ALOP(J) LT CALOP(3)) AND (CALOP(3) LT ALOP(I))
     1      AND (CALOP(2) LT BRCOM) AND (BRCOM LT CALOP(1)))
     2     GO TO 40
      IF (NFLAG NE.0) GO TO 30
C
C          CHECK THESE CASES AGAIN WITH A 90 DEGREE ROTATION
C
      NFLAG=1
      ALOP(I)=ALOP(I)+ PID2
      ALOP(J)=ALOP(J)+ PID2
      DO 3 K=1,3
    3 CALOP(K)=CALOP(K)+ PID2
      IF (ALOP(I)  GT  TWOPI) ALOP(I) = ALOP(I) - TWOPI
      IF (ALOP(J)  GT  TWOPI) ALOP(J) = ALOP(J) - TWOPI
      GO TO 50
   40 CTHETA=AMIN1(ABS(ALOP(I)-CALOP(2)),ABS(ALOP(J)-CALOP(1)))
      RETURN
   30 CTHETA=AMIN1(ABS(ALOP(I)-ALOP(J)),ABS(CALOP(1)-CALOP(2)))
      RETURN
        END
```

LAT=15°N LONG=65°W

LOP PAIRS	CROSSING ANGLE	GDOP
AB-AC	80.88	1.67
AB-AG	65.13	1.73
AC-AE	87.06	1.48
AC-AF	55.59	1.66
AD-AF	72.58	1.78
AE-AG	58.95	1.69
BC-BF	55.59	1.71
BD-BF	72.58	1.45
BD-BG	50.98	1.64
BF-BH	82.29	1.40
BG-BH	60.69	1.50
CE-CG	58.95	1.87
CF-CH	82.29	1.86
DE-DG	58.95	1.54
EF-EH	82.29	1.48
EG-EH	60.69	1.48
AE-BC	52.74	1.64
AF-BC	89.92	1.02
AG-BC	68.32	1.09
AF-BD	73.09	1.12
AG-BD	85.31	1.07
AF-CE	83.90	1.02
AG-CE	74.50	1.05
AG-CF	68.15	1.20
AF-DE	66.91	1.13
AG-DE	88.50	1.04
AG-DF	51.16	1.32
BF-CE	61.78	1.42
BG-CE	40.18	1.63
BG-CF	77.53	1.19
BF-DE	78.77	1.30
BG-DE	57.17	1.29
BG-DF	85.48	1.08
BH-DG	55.43	1.53
BH-EF	76.10	1.50
BH-EG	54.50	1.47
CH-DE	77.36	1.79
CH-DF	65.29	1.91
CG-EF	65.46	1.89
DG-EF	48.47	1.98

LAT=5°N LONG=65°W

LOP PAIRS	CROSSING ANGLE	GDOP
AB-AC	77.16	1.81
AB-AG	65.05	1.84
AC-AE	89.90	1.42
AC-AF	55.66	1.66
AD-AF	75.13	1.89
AE-AG	52.32	1.78
BC-BF	55.66	1.65
BD-BF	75.13	1.40
BD-BG	57.25	1.53
BF-BH	80.92	1.39
BG-BH	63.04	1.48
CE-CG	52.32	1.93
CF-CH	80.92	1.95
DE-DG	52.32	1.63
EF-EH	80.92	1.55
EG-EH	63.04	1.47
AE-BC	58.70	1.46
AF-BC	86.86	1.02
AG-BC	68.98	1.09
AF-BD	73.68	1.15
AG-BD	88.44	1.10
AF-CE	80.41	1.02
AG-CE	81.71	1.01
AG-CF	63.84	1.24
AF-DE	60.94	1.19
AG-DE	78.82	1.05
AG-DF	44.38	1.46
BF-CE	68.39	1.29
BG-CE	50.52	1.36
BG-CF	84.96	1.16
BF-DE	87.86	1.22
BG-DE	69.98	1.15
BG-DF	75.58	1.10
BH-DF	41.38	1.75
BH-DG	59.26	1.43
BH-EF	68.19	1.66
BH-EG	50.31	1.65
CH-DE	84.10	1.83
CG-EF	72.02	1.79
DG-EF	52.56	1.90

LAT=5°S LONG=65°W

LOP PAIRS	CROSSING ANGLE	GDOP
AB-AC	73.87	1.99
AB-AG	66.13	1.96
AC-AE	87.45	1.40
AC-AF	55.43	1.67
AD-AF	76.76	1.97
AE-AG	47.46	1.88
BC-BF	55.43	1.61
BC-BG	39.99	1.93
BD-BF	76.76	1.38
BD-BG	61.32	1.80
BF-BH	78.61	1.38
BG-BH	63.18	1.48
DE-DG	47.46	1.72
EF-EH	78.61	1.63
EG-EH	63.18	1.91
AE-BC	64.69	1.38
AF-BC	83.28	1.04
AG-BC	67.85	1.10
AE-BD	43.36	1.92
AF-BD	75.39	1.18
AG-BD	89.18	1.14
AF-CE	78.05	1.83
AG-CE	86.52	1.00
AG-CF	61.45	1.27
AF-DE	56.71	1.24
AG-DE	72.15	1.08
AG-DF	40.12	1.97
AH-DG	87.87	1.99
BF-CE	74.10	1.30
BG-CE	58.66	1.23
BG-CF	89.31	1.16
BF-DE	84.57	1.19
BG-DE	79.99	1.09
BG-DF	67.98	1.14
BH-DF	48.84	1.88
BH-DG	64.28	1.38
BH-EF	59.94	1.87
BH-EG	44.51	1.89
CH-DE	89.31	1.99
CG-EF	77.11	1.77
DG-EF	55.78	1.88

LAT=15°S LONG=65°W

LOP PAIRS	CROSSING ANGLE	GDOP
AC-AE	85.02	1.39
AC-AF	54.88	1.67
AE-AG	43.95	1.98
AE-AH	75.54	1.97
AF-AH	74.33	1.86
BC-BE	85.02	1.94
BC-BF	54.88	1.59
BC-BG	41.07	1.91
BD-BF	77.78	1.39
BD-BG	63.96	1.49
BF-BH	74.33	1.39
BG-BH	60.52	1.51
DE-DG	43.95	1.82
EF-EH	74.33	1.74
EG-EH	60.52	1.60
AE-BC	70.47	1.28
AF-BC	79.40	1.06
AG-BC	65.59	1.13
AE-BD	47.58	1.81
AF-BD	77.71	1.22
AG-BD	88.48	1.18
AF-CE	76.81	1.04
AG-CE	89.37	1.00
AG-CF	60.49	1.28
AH-CG	72.80	1.97
AF-DE	53.92	1.28
AG-DE	67.73	1.11
AG-DF	37.60	1.66
AH-DF	81.88	1.72
AH-DG	84.31	1.74
BF-CE	78.67	1.15
BG-CE	64.86	1.15
BG-CF	85.01	1.16
BH-CG	48.29	1.88
BF-DE	78.44	1.17
BG-DE	87.75	1.07
BG-DF	62.12	1.19
BH-DF	57.36	1.37
BH-DG	71.18	1.26
CG-EF	81.17	1.79
DG-EF	58.28	1.90

LAT=25°S LONG=65°W

LOP PAIRS	CROSSING ANGLE	GDOP
AC-AE	82.78	1.39
AC-AF	54.01	1.67
AE-AH	86.04	1.53
AF-AH	65.19	1.66
AG-AH	52.46	1.96
BC-BE	82.78	1.74
BC-BF	54.01	1.59
BC-BG	41.28	1.90
BD-BF	78.32	1.40
BD-BG	65.59	1.51
BE-BH	86.04	1.78
BF-BH	65.19	1.44
BG-BH	52.46	1.62
DE-DG	41.50	1.90
EF-EH	65.19	1.94
EG-EH	52.46	1.83
AE-BC	79.95	1.24
AF-BC	75.29	1.08
AG-BC	62.56	1.17
AE-BD	51.64	1.78
AF-BD	80.41	1.25
AG-BD	86.86	1.23
AF-CE	76.73	1.04
AG-CE	89.46	1.00
AG-CF	60.70	1.29
AH-CF	66.84	1.60
AH-CG	79.57	1.62
AF-DE	52.42	1.30
AG-DE	65.16	1.13
AH-DE	62.39	1.57
AG-DF	36.39	1.70
AH-DF	88.85	1.38
AH-DG	76.12	1.46
BF-CE	81.99	1.12
BG-CE	69.26	1.11
BG-CF	81.97	1.17
BH-CF	45.57	1.69
BH-CG	58.30	1.60
BF-DE	73.70	1.17
BG-DE	86.43	1.06
BH-DE	41.11	1.69
BG-DF	57.66	1.24
BH-DF	69.88	1.17
BH-DG	82.61	1.15
CG-EF	84.49	1.83
DG-EF	60.19	1.92

LAT=35°S LONG=65°W

LOP PAIRS	CROSSING ANGLE	GDOP
AC-AE	80.71	1.38
AC-AF	52.66	1.68
AG-AF	78.32	1.97
AE-AH	73.69	1.48
AF-AH	45.63	1.88
BC-BE	80.71	1.64
BC-BF	52.66	1.61
BC-BG	40.77	1.98
BD-BE	73.62	1.91
BD-BF	78.32	1.43
BD-BG	66.44	1.53
BE-BH	73.69	1.70
BF-BH	45.63	1.79
CD-CE	73.62	1.98
CD-CF	78.32	1.98
DE-DG	39.94	1.98
DF-DH	73.69	1.66
AE-BC	81.16	1.22
AF-BC	70.78	1.11
AG-BC	38.90	1.21
AE-BD	55.50	1.70
AF-BD	83.55	1.28
AG-BD	84.56	1.27
AH-BD	50.81	1.74
AH-BE	55.56	1.94
AF-CE	78.00	1.04
AG-CE	89.88	1.04
AH-CE	56.37	1.33
AG-CF	61.82	1.29
AH-CF	84.43	1.23
AH-CG	83.69	1.38
AF-DE	52.34	1.31
AG-DE	64.22	1.13
AH-DE	82.03	1.13
AG-DF	36.16	1.71
AH-DF	69.91	1.18
AH-DG	58.03	1.38
BF-CE	83.88	1.10
BG-CE	71.99	1.09
BH-CE	38.24	1.68
BG-CF	79.95	1.10
BH-CF	66.30	1.26
BH-CG	78.10	1.34
BF-DE	70.46	1.17
BG-DE	82.15	1.06
BH-DE	63.70	1.16
BG-DF	54.49	1.28
BH-DF	88.04	1.03
BH-DG	76.16	1.10
CG-EF	87.40	1.08
DG-EF	61.74	1.92

LAT=45°S LONG=65°W.

LOP PAIRS	CROSSING ANGLE	GDOP
AC-AE	78 82	1 38
AE-AH	52 91	1 69
BC-BE	78 82	1 38
BC-BG	39 65	1 96
BD-BE	74 21	1 86
BD-BG	66 61	1 56
BD-BH	52 88	1 84
BF-BG	75 80	1 67
BF-BH	62 06	1 89
CD-CE	74 21	1 88
CE-CF	65 02	1 68
CF-CG	75 80	1 78
DE-DG	39 18	1 98
DF-DH	52 91	1 64
EF-EG	75 80	1 49
EF-EH	62 06	1 48
AE-BC	86 23	1 22
AG-BC	54 59	1 28
AH-BC	40 85	1 61
AE-BD	59 27	1 67
AG-BD	81 55	1 31
AH-BD	67 82	1 41
AG-BF	89 26	1 53
AH-BF	77 00	1 97
AG-CE	88 11	1 01
AH-CE	74 37	1 06
AH-CG	66 45	1 44
AG-DE	64 93	1 13
AH-DE	78 66	1 08
AH-DG	39 48	1 66
AG-EF	55 74	1 27
AH-EF	69 48	1 13
BG-CE	73 17	1 08
BH-CE	59 43	1 17
BH-CG	81 39	1 33
BG-DE	79 87	1 06
BH-DE	86 40	1 02
BH-DG	54 42	1 29
BG-EF	70 68	1 14
BH-EF	84 42	1 06
BH-FG	45 24	1 43
CF-DE	88 01	1 41
CH-EG	87 44	1 97
DH-EF	43 73	1 71
DH-EG	60 47	1 64
EH-FG	78 76	1 17

LAT=55°S LONG=65°W

LOP PAIRS	CROSSING ANGLE	GDOP
AC-AE	77 12	1 40
AD-AE	74 69	1 96
AD-AG	66 14	1 94
BC-BE	77 12	1 36
BD-BE	74 69	1 83
BD-BG	66 14	1 58
BD-BH	62 34	1 84
BF-BG	77 39	1 77
BF-BH	73 99	1 81
CD-CE	74 69	1 81
CE-CF	63 44	1 63
CF-CG	77 39	1 73
CF-CH	73 99	1 87
DE-DG	39 17	1 99
DE-DH	62 97	1 86
EF-EG	77 39	1 47
EF-EH	73 99	1 48
AE-BC	88 37	1 24
AG-BC	49 40	1 37
AH-BC	45 60	1 44
AE-BD	63 23	1 60
AG-BD	77 60	1 34
AH-BD	73 80	1 37
AG-BF	88 84	1 64
AH-BF	85 04	1 68
AG-CE	84 32	1 82
AH-CE	80 52	1 83
AH-CG	60 31	1 38
AG-DE	67 48	1 10
AH-DE	71 28	1 88
AH-DG	32 11	1 97
AG-EF	56 24	1 28
AH-EF	60 04	1 22
AH-EG	42 98	1 96
BG-CE	72 87	1 88
BH-CE	69 07	1 10
BH-CG	71 76	1 43
BG-DE	78 94	1 86
BH-DE	82 74	1 84
BH-DG	43 57	1 34
BG-EF	67 69	1 17
BH-EF	71 49	1 13
BH-FG	32 32	1 91
CF-DE	88 37	1 33
CH-EG	80 92	1 71
DH-EG	70 89	1 46
EH-FG	67 24	1 37

LAT=15°N LONG=55°W

LOP PAIRS	CROSSING ANGLE	GDOP
AB-AC	81 17	1 36
AB-AG	59 16	1 32
AC-AE	84 28	1 [illegible]
AC-AF	58 44	1 [illegible]
AD-AE	73 22	1 [illegible]
AD-AF	65 72	1 [illegible]
AE-AG	54 84	1 [illegible]
BC-BF	58 44	1 [illegible]
BD-BF	65 72	1 [illegible]
BD-BG	58 73	1 [illegible]
BF-BH	83 23	1 [illegible]
BG-BH	79 28	1 [illegible]
CE-CG	54 84	1 [illegible]
CF-CH	83 23	1 [illegible]
DF-DF	41 84	1 [illegible]
DE-DG	54 84	1 [illegible]
EF-EH	83 23	1 [illegible]
EG-EH	79 28	1 [illegible]
AE-BC	64 97	1 [illegible]
AF-BC	88 97	1 [illegible]
AG-BC	75 99	1 [illegible]
AF-BD	77 97	1 [illegible]
AG-BD	85 85	1 [illegible]
AF-CF	85 91	1 [illegible]
AG-CE	81 10	1 [illegible]
AG-CF	57 84	1 [illegible]
AF-DE	72 84	1 [illegible]
AG-DE	85 84	1 [illegible]
AG-EF	44 78	1 [illegible]
BF-CE	57 77	1 [illegible]
BG-CE	44 79	1 [illegible]
BG-CF	85 85	1 [illegible]
BF-DE	79 83	1 [illegible]
BG-DE	57 85	1 [illegible]
BG-EF	81 85	1 [illegible]
BH-DG	41 64	1 [illegible]
BH-EF	78 12	1 [illegible]
BH-EG	65 14	1 [illegible]
CH-DE	68 76	1 [illegible]
CH-EF	79 17	1 [illegible]
CH-EG	57 19	1 [illegible]
CG-EF	73 36	1 [illegible]
DG-EF	68 24	1 [illegible]

LAT=5°N LONG=55°W

LOP PAIRS	CROSSING ANGLE	GDOP
AB-AC	76.68	1.81
AB-AG	60.62	1.91
AC-AE	88.87	1.44
AC-AF	51.42	1.79
AD-AE	72.77	2.00
AD-AF	67.52	1.89
AE-AG	48.42	1.90
BC-BF	51.42	1.69
BC-BG	42.70	1.88
BD-BF	67.52	1.43
BD-BG	58.01	1.51
BF-BH	82.18	1.39
BG-BH	73.46	1.42
CE-CG	48.42	1.93
CF-CH	82.18	1.72
CG-CH	73.46	1.93
DE-DF	39.71	1.96
DE-DG	40.42	1.71
EF-EH	82.18	1.44
EG-EH	73.46	1.40
AE-BC	57.07	1.49
AF-BC	83.22	1.02
AG-BC	74.51	1.05
AE-BD	40.96	1.99
AF-BD	80.67	1.09
AG-BD	89.38	1.08
AF-CE	84.58	1.01
AG-CE	86.70	1.00
AG-CF	53.59	1.43
AF-DE	68.48	1.10
AG-DE	77.19	1.05
AG-DF	37.48	1.71
BF-CE	63.61	1.28
BG-CE	54.89	1.32
BG-CF	85.39	1.22
BF-DE	79.72	1.18
BG-DE	71.00	1.16
BG-DF	69.29	1.19
BH-DG	45.96	1.79
BH-EF	69.98	1.58
BH-EG	61.27	1.56
CH-DE	74.22	1.63
CH-DF	66.07	1.73
CH-DG	57.36	1.91
CG-EF	80.16	1.54
DG-FF	64.05	1.54

LAT=5°S LONG=55°W

LOP PAIRS	CROSSING ANGLE	GDOP
AC-AE	[illegible].37	1.41
AC-AF	49.46	1.[illegible]
AD-AF	[illegible].14	1.[illegible]
AE-AG	44.63	2.[illegible]
BC-BF	49.46	1.69
BC-BG	43.93	1.[illegible]
BD-BF	[illegible] 14	1.[illegible]
BD-BG	62.62	1.47
BF-BH	[illegible] 37	1.[illegible]
BG-BH	74.[illegible]	1.[illegible]
CE-CH	60.92	1.[illegible]
CF-CH	[illegible] 37	1.7[illegible]
CG-CH	74.[illegible]	1.[illegible]
DE-DF	39 11	1.[illegible]
DE-DG	44.63	1.[illegible]
EF-EH	[illegible].37	1 46
EG-EH	74.[illegible]	1.42
AE-BC	64 30	1.37
AF-BC	76.59	1.[illegible]
AG-BC	71.07	1.[illegible]
AE-BD	45.62	1.04
AF-BD	[illegible].73	1.13
AG-BD	[illegible] 75	1.12
AF-CE	[illegible].68	1.01
AG-CE	[illegible].80	1.[illegible]
AG-CF	51 09	1 [illegible]
AF-DE	65.99	1.12
AG-DE	71 52	1.[illegible]
AG-DF	32 41	1.94
BF-CE	68 19	1.10
BG-CE	62.67	1 19
BG-CF	78.22	1 28
BF-DE	86.87	1.12
BG-DE	81 35	1 10
BG-DF	59.54	1.27
BH-DF	45.61	1.[illegible]
BH-DG	51 13	1 70
BH-EF	61 64	1 78
BH-EG	56.12	1 76
CH-DE	79 20	1.59
CH-DF	61 69	1.79
CH-DG	56 17	1 91
CG-EF	85.91	1.[illegible]
DG-EF	67 23	1 49

LAT=15°S LONG=55°W

LOP PAIRS	CROSSING ANGLE	GDOP
AC-AE	86.07	1.[illegible]
AC-AF	46 43	1.9[illegible]
AC-AG	44 [illegible]	2.[illegible]
BC-BE	86 07	1.[illegible]
BC-BF	46 43	1 76
BC-BG	44 [illegible]	1 [illegible]
BD-BF	67 43	1 [illegible]
BD-BG	65 [illegible]	1 [illegible]
BF-BH	76 94	1 [illegible]
BG-BH	74.33	1.[illegible]
CE-CH	63 42	1.[illegible]
CF-CH	76 94	1.[illegible]
CG-CH	74 33	1 [illegible]
DE-DF	39 64	1 96
DE-DG	42 [illegible]	1 [illegible]
EF-EH	76 94	1 67
EG-EH	74.33	1 [illegible]
AE-BC	71 [illegible]	1.[illegible]
AF-BC	69 15	1 11
AG-BC	66.74	1 13
AE-BD	[illegible] 21	1 76
AF-BD	[illegible]	1 [illegible]
AG-BD	87 74	1 [illegible]
AF-CE	86 92	1 [illegible]
AG-CE	[illegible] 93	1 [illegible]
AG-CF	49 30	1 [illegible]
AF-DE	65 [illegible]	1 13
AG-DE	67 93	1.[illegible]
AG-EF	44 64	1.07
BF-CE	70 76	1 12
BG-CE	68 36	1 13
BG-CF	72 02	1 31
BF-DE	[illegible] 24	1 [illegible]
BG-DE	59 36	1 07
BG-DF	51 01	1 40
BH-DF	54 45	1.67
BH-DG	56 86	1 63
BH-EF	52 62	1 [illegible]
CH-DE	84 42	1 [illegible]
CH-DF	58 94	1 92
CH-DG	53 93	1.[illegible]
CG-EF	[illegible] 40	1 94
DG-EF	70 52	1 44

LAT=25°S LONG=55°W

LOP PAIRS	CROSSING ANGLE	GDOP
AC-AE	83.63	1.39
AC-AG	43.28	1.99
BC-BE	83.63	1.70
BC-BF	41.29	1.90
BC-BG	43.28	1.83
BD-BE	73.19	1.98
BD-BF	64.47	1.53
BD-BG	66.45	1.50
BF-BH	68.37	1.54
BG-BH	70.36	1.51
CE-CH	69.29	1.95
DE-DF	42.34	1.87
DE-DG	40.35	1.94
EF-EH	68.37	1.51
EG-EH	70.36	1.52
AE-BC	77.61	1.26
AF-BC	60.05	1.20
AG-BC	62.04	1.18
AE-BD	54.44	1.71
AF-BD	83.22	1.24
AG-BD	85.21	1.24
AF-CE	88.84	1.00
AG-CE	89.18	1.00
AG-CF	46.84	1.76
AF-DE	67.99	1.10
AG-DE	66.00	1.12
AG-EF	49.53	1.66
BF-CE	70.08	1.10
BG-CE	72.07	1.09
BG-CF	65.59	1.44
BF-DE	86.75	1.05
BG-DE	84.76	1.06
BG-DF	42.42	1.61
BH-DF	67.22	1.45
BH-DG	65.23	1.47
BG-FH	38.51	1.72
CH-DE	87.54	1.72
CG-EF	81.65	1.49
DG-EF	75.18	1.35

LAT=35°S LONG=55°W

LOP PAIRS	CROSSING ANGLE	GDOP
AC-AE	81 30	1 39
AE-AF	51 42	1 79
AF-AH	73 29	1 41
BC-BE	81 30	1 61
BC-BG	41 91	1 88
BD-BE	73 47	1 90
BD-BF	55 11	1 76
BD-BG	67 14	1 94
BE-BH	73 29	1 68
CD-CE	73 47	1 98
DE-DF	51 42	1 44
DE-DG	39 39	1 97
DE-DH	73 29	1 64
AE-BC	83 48	1 24
AF-BC	45 10	1 48
AG-BC	57 13	1 25
AE-BD	58 24	1 69
AF-BD	70 33	1 37
AG-BD	82 36	1 29
AH-BD	48 47	1 88
AH-BE	58 07	1 84
AF-CE	77 19	1 04
AG-CE	89 22	1 01
AH-CE	55 32	1 32
AH-CF	73 25	1 71
AH-CG	85 28	1 34
AF-DE	77 58	1 08
AG-DE	65 55	1 12
AH-DE	80 56	1 12
AH-DF	48 02	1 60
AH-DG	60 05	1 30
AG-EF	59 34	1 34
BF-CE	61 97	1 14
BG-CE	74 00	1 08
BH-CE	40 10	1 59
BG-CF	54 58	1 97
BH-CF	88 47	1 60
BH-CG	79 49	1 31
BF-DE	87 20	1 03
BG-DE	80 77	1 06
BH-DE	45 33	1 14
BH-DF	63 24	1 27
BH-DG	75 27	1 10
BG-EF	44 12	1 68
CG-EF	69 27	1 49
DG-EF	85 50	1 19

LAT=45°S LONG=55°W

LOP PAIRS	CROSSING ANGLE	GDOP
AC-AE	79 12	1 39
AD-AG	67 18	1 96
AD-AH	65 88	1 99
AE-AF	81 26	1 39
AF-AG	42 18	1 98
BC-BE	79 12	1 36
BC-BG	40 83	1 95
BD-BE	73 74	1 86
BD-BG	67 18	1 97
BD-BH	65 80	1 89
BE-BF	81 26	1 38
BF-BG	42 18	1 88
BF-BH	40 80	1 87
CD-CE	73 74	1 87
DE-DF	81 26	1 99
DE-DG	39 08	1 99
DE-DH	40 46	1 94
AE-BC	88 94	1 28
AG-BC	51 98	1 38
AH-BC	50 60	1 38
AE-BD	61 79	1 60
AG-BD	79 13	1 36
AH-BD	77 79	1 38
AF-BE	69 31	1 60
AG-BF	54 12	1 38
AH-BF	52 74	1 38
AF-CE	44 11	1 60
AG-CE	86 29	1 01
AH-CE	84 91	1 01
AH-CG	36 01	1 88
AH-DE	71 26	1 88
AG-DF	66 37	1 11
AH-DE	67 94	1 10
AG-EF	88 43	1 01
AH-EF	87 09	1 01
AH-EG	44 88	1 88
AH-FG	53 87	1 37
BF-CE	32 17	2 00
BG-CE	74 34	1 07
BH-CE	72 96	1 07
BH-CG	67 95	1 43
BF-DE	59 31	1 28
BG-DE	78 51	1 06
BH-DE	79 09	1 06
BH-DG	40 81	1 62
BG-EF	76 48	1 06
BH-EF	75 11	1 06
BH-FG	65 81	1 41
CH-EG	80 49	1 62
DG-EF	64 08	1 17
DH-EF	65 46	1 16
DH-EG	72 36	1 43
EH-FG	79 88	1 34

LAT=55°S LONG=55°W

LOP PAIRS	CROSSING ANGLE	GDOP
AC-AE	77.15	1.41
AC-AH	41.03	1.96
AD-AE	74.03	1.93
AD-AG	66.58	1.86
AD-AH	69.85	1.81
AE-AF	75.72	1.84
AF-AG	64.89	1.83
AF-AH	68.16	1.77
BC-BE	77.15	1.55
BC-BH	41.03	1.91
BD-BE	74.03	1.85
BD-BG	66.58	1.60
BD-BH	69.85	1.56
BE-BF	75.72	1.79
BF-BG	64.89	1.59
BF-BH	68.16	1.55
CD-CE	74.03	1.79
CE-CF	75.72	1.85
DE-DG	39.39	1.98
EF-EG	64.89	1.61
EF-EH	68.16	1.63
AE-BC	85.79	1.27
AG-BC	46.41	1.44
AH-BC	49.68	1.38
AE-BD	65.39	1.68
AG-BD	75.22	1.39
AH-BD	78.49	1.37
AF-BE	84.36	1.83
AG-BF	73.54	1.36
AH-BF	76.80	1.35
AG-CE	81.95	1.03
AH-CE	85.22	1.02
AH-CG	55.40	1.65
AG-DE	69.24	1.09
AH-DE	65.97	1.12
AG-EF	70.92	1.08
AH-EF	67.66	1.11
AH-EG	47.45	1.80
BG-CE	73.30	1.08
BH-CE	76.57	1.07
BH-CG	64.04	1.53
BG-DE	77.88	1.06
BH-DE	74.61	1.09
BH-DG	35.23	1.86
BG-EF	79.57	1.05
BH-EF	76.30	1.07
BH-EG	36.91	1.80
CF-DE	75.46	1.77
CH-EG	73.88	1.61
DG-EF	41.07	1.62
DH-EF	37.81	1.71
DH-EG	77.30	1.38
EH-FG	72.45	1.50

LAT=15°N LONG=45°W

LOP PAIRS	CROSSING ANGLE	GDOP
AB-AC	81.65	1.60
AB-AD	71.92	1.94
AB-AG	50.37	1.98
AC-AE	85.39	1.51
AC-AF	50.29	1.87
AC-AG	47.98	1.98
AD-AE	75.66	1.82
AD-AF	60.02	1.89
AD-AG	57.71	1.98
AE-AG	46.64	1.98
BC-BF	50.29	1.77
BC-BG	47.98	1.80
BD-BF	60.02	1.88
BD-BG	57.71	1.87
BF-BH	84.59	1.39
BG-BH	82.28	1.39
CE-CF	44.32	1.93
CE-CG	46.64	1.80
CF-CH	84.59	1.60
CG-CH	82.28	1.64
DE-DF	44.32	1.82
DE-DG	46.64	1.77
DF-DH	84.59	1.93
DG-DH	82.28	1.96
EF-EH	84.59	1.40
EG-EH	82.28	1.39
AE-BC	46.19	1.78
AF-BC	89.48	1.01
AG-BC	87.17	1.01
AF-BD	80.79	1.04
AG-BD	83.10	1.03
AG-BF	36.88	1.97
AF-CE	86.78	1.00
AG-CE	89.09	1.00
AG-CF	44.77	1.65
AF-DE	77.05	1.04
AG-DE	79.36	1.03
AG-DF	35.04	1.88
AG-EF	40.62	1.90
BF-CE	54.02	1.47
BG-CE	51.71	1.48
BG-CF	83.96	1.31
BF-DE	63.76	1.34
BG-DE	61.45	1.34
BG-DF	74.23	1.28
BH-EF	80.85	1.41
BH-EG	78.54	1.40
CG-DE	36.90	2.00
CH-DE	60.82	1.66
CH-DF	74.85	1.55
CH-DG	72.54	1.58
CG-EF	83.08	1.40
DG-EF	73.34	1.37

LAT=5°N LONG=45°W

LOP PAIRS	CROSSING ANGLE	GDOP
AB-AC	75.74	1.88
AB-AF	36.37	1.95
AC-AE	87.88	1.44
AC-AF	47.89	1.94
AC-AG	49.29	1.85
AD-AE	74.69	1.91
AD-AF	61.04	1.88
AD-AG	62.45	1.94
BC-BF	47.89	1.74
BC-BG	49.29	1.71
BD-BF	61.04	1.48
BD-BG	62.45	1.47
BF-BH	84.13	1.44
BG-BH	85.54	1.44
CE-CF	44.26	1.97
CE-CH	91.61	2.00
CF-CH	84.13	1.88
CG-CH	85.54	1.88
DE-DF	44.26	1.88
DE-DG	42.86	1.88
EF-EH	84.13	1.40
EG-EH	85.54	1.41
AE-BC	58.21	1.91
AF-BC	80.52	1.03
AG-BC	81.93	1.03
AE-BD	42.05	1.91
AF-BD	86.32	1.07
AG-BD	84.91	1.07
AG-BF	34.09	1.97
AF-CE	87.37	1.00
AG-CE	85.96	1.00
AG-CF	41.69	1.78
AF-DE	74.21	1.04
AG-DE	72.80	1.07
AG-EF	46.16	1.71
BF-CE	59.99	1.28
BG-CE	61.40	1.27
BG-CF	74.33	1.34
BF-DE	73.15	1.17
BG-DE	74.56	1.18
BG-DF	61.17	1.38
BH-EF	72.02	1.88
BH-EG	73.43	1.95
CH-DE	64.76	1.89
CH-DF	70.97	1.33
CH-DG	72.38	1.31
CG-EF	89.26	1.38
DG-EF	76.10	1.33

LAT=5°S LONG=45°W

LOP PAIRS	CROSSING ANGLE	GDOP
AC-AE	89.59	1.41
AC-AG	48.99	1.87
AD-AE	74.10	1.98
AD-AG	65.31	1.96
AE-AF	45.13	1.98
BC-BF	44.45	1.80
BC-BG	48.99	1.69
BD-BF	60.77	1.49
BD-BG	65.31	1.44
BF-BH	83.49	1.61
BG-BH	88.03	1.59
CE-CH	51.38	1.92
CF-CH	83.49	1.56
CG-CH	88.03	1.48
DE-DF	45.13	1.79
DE-DG	40.59	1.93
EF-EH	83.49	1.39
EG-EH	88.03	1.43
AE-BC	64.38	1.37
AF-BC	70.48	1.09
AG-BC	75.02	1.07
AE-BD	48.07	1.77
AF-BD	86.80	1.12
AG-BD	88.66	1.12
AF-CE	89.64	1.00
AG-CE	85.09	1.00
AG-CF	39.96	1.92
AF-DE	73.32	1.06
AG-DE	68.78	1.10
AG-EF	50.45	1.59
BF-CE	64.33	1.17
BG-CE	68.88	1.15
BG-CF	65.99	1.42
BF-DE	80.65	1.09
BG-DE	85.19	1.10
BG-DF	49.67	1.51
BH-EF	63.61	1.88
BH-EG	68.15	1.87
CH-DE	67.69	1.45
CH-DF	67.17	1.50
CH-DG	71.72	1.44
CG-EF	85.04	1.37
DG-EF	78.64	1.29

LAT=15°S LONG=45°W

LOP PAIRS	CROSSING ANGLE	GDOP
AC-AE	86.94	1.40
AC-AG	47.71	1.87
AD-AG	67.04	1.98
AE-AF	47.41	1.88
BC-BE	86.94	1.80
BC-BF	39.53	1.97
BC-BG	47.71	1.71
BD-BF	58.86	1.88
BD-BG	67.04	1.46
BF-BH	82.82	1.97
BG-BH	89.00	1.94
CE-CH	49.77	1.87
CF-CH	82.82	1.57
CG-CH	89.00	1.41
DE-DF	47.41	1.74
DE-DG	39.23	1.98
DF-DH	82.82	1.99
DG-DH	89.00	1.91
EF-EH	82.82	1.39
EG-EH	89.00	1.46
AE-BC	72.79	1.30
AF-BC	59.80	1.21
AG-BC	67.98	1.13
AE-BD	53.45	1.70
AF-BD	79.13	1.21
AG-BD	87.31	1.19
AF-CE	86.00	1.00
AG-CE	85.82	1.00
AF-DE	74.66	1.06
AG-DE	66.48	1.12
AG-EF	54.65	1.46
BF-CE	65.73	1.12
BG-CE	73.91	1.09
BG-CF	58.68	1.59
BF-DE	85.07	1.08
BG-DE	86.75	1.07
BG-DF	39.34	1.79
CH-DE	69.10	1.36
CH-DF	63.48	1.48
CH-DG	71.66	1.38
CG-EF	78.76	1.38
DG-EF	81.90	1.24

LAT=25°S LONG=45°W

LOP PAIRS	CROSSING ANGLE	GDOP
AC-AE	84.25	1.39
AC-AG	49.72	1.89
AD-AG	67.99	1.97
AE-AF	52.18	1.74
BC-BE	84.25	1.49
BC-BG	49.72	1.52
BD-BE	73.48	1.82
BD-BF	54.33	1.78
BD-BG	67.99	1.51
CE-CH	49.93	1.83
CF-CH	83.87	1.44
CG-CH	88.44	1.38
DE-DF	52.18	1.68
DF-DH	83.87	1.72
DG-DH	88.44	1.48
EF-EH	83.87	1.48
EG-EH	88.44	1.50
AE-BC	80.14	1.57
AF-BC	47.48	1.63
AG-BC	61.33	1.80
AE-BD	57.87	1.45
AF-BD	69.94	1.37
AG-BD	83.60	1.57
AF-CE	78.50	1.88
AG-CE	87.84	1.01
AF-DE	79.23	1.80
AG-DE	69.57	1.13
AG-EF	60.09	1.38
BF-CE	62.87	1.13
BG-CE	76.98	1.07
BG-CF	51.27	1.96
BF-DE	88.16	1.83
BG-DE	81.19	1.07
BG-EF	64.48	1.47
CH-DE	64.20	1.57
CH-DF	61.62	1.48
CH-DG	75.28	1.32
CG-EF	70.97	1.41
DG-EF	67.14	1.18

LAT=35°S LONG=45°W

LOP PAIRS	CROSSING ANGLE	GDOP
AC-AE	81.60	1.39
AC-AG	43.24	1.94
AC-AH	88.60	1.51
AD-AG	68.30	1.94
AE-AF	61.92	1.55
AF-AH	71.72	1.59
BC-BE	81.60	1.55
BC-BG	43.24	1.84
BC-BH	88.60	1.91
BD-BE	73.34	1.88
BD-BG	68.30	1.56
BE-BF	61.92	1.80
CD-CE	73.34	1.99
CG-CH	48.16	1.92
DE-DF	61.92	1.56
DF-DH	71.72	1.44
DG-DH	48.16	1.70
AE-BC	86.54	1.26
AG-BC	55.10	1.29
AH-BC	76.74	1.48
AE-BD	61.48	1.69
AF-BD	56.60	1.60
AG-BD	80.16	1.34
AF-BE	50.06	1.92
AG-BF	35.42	1.73
AH-BF	83.58	1.41
AH-BG	60.02	1.63
AF-CE	65.46	1.13
AG-CE	89.02	1.01
AF-DE	89.48	1.05
AG-DE	65.92	1.12
AG-EF	69.34	1.14
AH-EF	62.50	1.63
AH-EG	86.06	1.66
BF-CE	53.59	1.25
BG-CE	77.16	1.06
BF-DE	78.65	1.05
BG-DE	77.78	1.07
BG-EF	57.48	1.30
BH-EF	74.36	1.98
CH-DE	34.86	1.79
CG-DF	48.62	1.92
CH-DF	83.22	1.24
CH-DG	73.22	1.09
CG-EF	58.04	1.54
DG-EF	83.10	1.11
DH-EF	34.94	1.96
DH-EG	58.50	1.63

LAT=45°S LONG=45°W

LOP PAIRS	CROSSING ANGLE	GDOP
AC-AE	79.11	1.40
AC-AH	57.18	1.84
AD-AE	73.29	1.98
AD-AG	68.03	1.88
AD-AH	84.78	1.69
AE-AF	79.28	1.40
AF-AG	40.60	2.00
AF-AH	57.35	1.84
BC-BE	79.11	1.83
BC-BG	40.43	1.94
BC-BH	57.18	1.83
BD-BE	73.29	1.87
BD-BG	68.03	1.60
BD-BH	84.78	1.47
BE-BF	79.28	1.83
BF-BG	40.60	1.93
BF-BH	57.35	1.83
CD-CE	73.29	1.86
CD-CH	84.78	1.78
DE-DF	79.28	1.80
AE-BC	87.79	1.88
AG-BC	49.12	1.40
AH-BC	65.86	1.20
AE-BD	64.61	1.70
AG-BD	76.72	1.40
AH-BD	86.54	1.40
AF-BE	70.60	1.57
AG-BF	49.28	1.39
AH-BF	66.03	1.20
AF-CE	44.25	1.60
AG-CE	84.85	1.02
AH-CE	78.40	1.08
AF-CH	66.19	1.31
AF-DE	71.85	1.18
AG-DE	67.55	1.11
AH-DE	50.80	1.38
AG-EF	89.02	1.02
AH-EF	78.23	1.08
AH-EG	61.16	1.56
BF-CE	35.57	1.83
BG-CE	76.17	1.06
BH-CE	87.08	1.11
BF-CH	57.50	1.36
BH-CG	48.41	1.84
BF-DE	63.17	1.20
BG-DE	76.23	1.07
BH-DE	59.48	1.30
BG-EF	76.34	1.06
BH-EF	86.92	1.11
BH-EG	52.48	1.77
BH-FG	48.24	1.84
CH-DF	84.95	1.76
CH-DG	44.34	1.62
CH-EG	62.37	1.99
DG-EF	64.11	1.19
DH-EF	49.37	1.33
DH-EG	89.97	1.24

LAT=55°S LONG=45°W

LOP PAIRS	CROSSING ANGLE	GDOP
AC-AE	76.93	1.44
AC-AH	48.62	1.78
AD-AE	73.38	1.82
AD-AG	67.17	1.88
AD-AH	78.32	1.64
AE-AF	83.20	1.86
AF-AG	57.35	1.78
AF-AH	68.90	1.88
BC-BE	76.93	1.82
BC-BH	48.62	1.87
BD-BE	73.38	1.87
BD-BG	67.17	1.63
BD-BH	78.32	1.81
BE-BF	83.20	1.82
BF-BG	57.36	1.46
BF-BH	68.90	1.44
CD-CE	73.38	1.77
CD-CH	78.32	1.82
BE-BG	39.45	1.97
EF-EG	57.36	1.78
EF-EH	68.90	1.98
AE-BC	82.63	1.84
AG-BC	43.17	1.84
AH-BC	54.32	1.28
AE-BD	67.48	1.71
AG-BD	72.87	1.44
AH-BD	84.01	1.48
AF-BE	88.89	1.88
AG-BF	63.06	1.38
AH-BF	74.19	1.88
AG-CE	79.69	1.84
AH-CE	89.16	1.84
AH-CG	69.71	1.81
AF-DE	82.04	1.49
AG-DE	78.61	1.89
AH-DE	59.47	1.88
AG-EF	80.44	1.88
AH-EF	69.29	1.11
AH-EG	93.36	1.67
BG-CE	73.99	1.87
BH-CE	86.14	1.87
BH-CG	55.41	1.79
BF-DE	46.34	1.89
BG-DE	76.31	1.87
BH-DE	65.16	1.18
BG-EF	84.13	1.88
BH-EF	74.99	1.89
BH-EG	47.44	1.84
BH-FG	38.93	1.87
CH-DG	40.84	1.84
CH-EG	63.78	1.88
DG-EF	69.27	1.38
DH-EF	38.13	1.44
DH-EG	84.32	1.82
EH-FG	72.06	1.88

LAT=15°N LONG=35°W

LOP PAIRS	CROSSING ANGLE	GDOP
AB-AC	82.85	1.58
AB-AD	76.15	1.81
AB-AF	48.40	1.91
AC-AE	84.28	1.54
AC-AG	58.95	1.72
AD-AE	77.59	1.78
AD-AG	65.65	1.78
AE-AF	46.97	1.93
BC-BF	48.75	1.81
BC-BG	58.95	1.75
BD-BF	55.44	1.64
BD-BG	65.65	1.62
BF-BH	86.12	1.40
BG-BH	83.68	1.56
CE-CF	46.97	1.86
CF-CH	86.12	1.53
CG-CH	83.68	1.47
DE-DF	46.97	1.78
DF-DH	86.12	1.66
DG-DH	83.68	1.64
EF-EH	86.12	1.39
EG-EH	83.68	1.58
AE-BC	40.68	1.88
AF-BC	87.65	1.01
AG-BC	77.44	1.03
AF-BD	80.95	1.03
AG-BD	70.74	1.08
AG-BF	53.82	1.47
AF-CE	86.22	1.01
AG-CE	76.01	1.04
AF-DE	79.52	1.03
AG-DE	69.31	1.09
AG-EF	55.25	1.46
BF-CE	50.18	1.54
BG-CE	60.39	1.55
BG-CF	72.64	1.55
BF-DE	56.88	1.42
BG-DE	67.08	1.47
BG-DF	65.95	1.57
BH-EF	84.68	1.39
BH-EG	85.11	1.55
CF-DE	40.27	1.84
CH-DE	53.61	1.70
CH-DF	79.42	1.47
CH-DG	89.63	1.40
CG-EF	85.51	1.28
DG-EF	87.79	1.24

LAT=5°N LONG=35°W

LOP PAIRS	CROSSING ANGLE	GDOP
AB-AC	74.18	1.86
AB-AF	60.44	1.88
AC-AE	86.68	1.49
AC-AG	87.37	1.73
AD-AE	76.26	1.86
AD-AG	67.79	1.88
AE-AF	47.91	1.87
BC-BF	48.40	1.79
BC-BG	57.37	1.60
BD-BF	55.82	1.58
BD-BG	67.79	1.48
BF-BH	86.29	1.38
BG-BH	81.74	1.67
CE-CF	47.91	1.89
CF-CH	86.29	1.49
CG-CH	81.74	1.43
DE-DF	47.91	1.78
DF-DH	86.29	1.66
DG-DH	81.74	1.68
EF-EH	86.29	1.40
EG-EH	81.74	1.63
AE-BC	53.10	1.93
AF-BC	78.99	1.84
AG-BC	89.04	1.88
AE-BD	42.68	1.86
AF-BD	89.41	1.84
AG-BD	78.62	1.89
AG-BF	45.55	1.98
AF-CE	88.48	1.88
AG-CE	76.91	1.83
AE-CH	86.36	1.46
AF-DE	78.06	1.84
AG-DE	66.09	1.12
AG-EF	58.09	1.40
BF-CE	57.94	1.87
BG-CE	69.90	1.86
BG-CF	62.18	1.98
BF-DE	68.36	1.17
BG-DE	80.32	1.81
BG-DF	91.76	1.62
BH-EF	73.76	1.67
BH-EG	89.73	1.77
CH-DE	56.22	1.97
CH-DF	75.87	1.42
CH-DG	87.84	1.32
CG-EF	81.35	1.28
DG-EF	88.23	1.22

LAT=9°S LONG=35°W

LOP PAIRS	CROSSING ANGLE	GDOP
AC-AE	89.38	1.88
AC-AG	84.99	1.88
AD-AE	75.28	1.88
AD-AG	65.11	1.88
AE-AF	45.84	1.88
BC-BE	85.38	1.88
BC-BF	48.81	1.88
BC-BG	54.99	1.88
BD-BF	54.93	1.88
BD-BG	65.11	1.88
CE-CF	45.84	1.88
CF-CH	86.74	1.88
CG-CH	79.68	1.88
DE-DF	45.84	1.88
DF-DH	86.74	1.88
DG-DH	79.68	1.88
EF-EH	86.74	1.88
EG-EH	79.68	1.88
AE-BC	48.58	1.88
AF-BC	64.64	1.88
AG-BC	78.82	1.88
AE-BD	91.39	1.88
AF-BD	78.77	1.88
AG-BD	67.68	1.88
AG-BF	38.81	1.88
AF-CE	87.38	1.88
AG-CE	78.44	1.88
AE-CH	86.19	1.88
AF-DE	78.49	1.88
AG-DE	64.31	1.88
AG-EF	60.78	1.88
BF-CE	63.98	1.88
BG-CE	77.73	1.88
BG-CF	68.43	1.88
BF-DE	77.48	1.88
BG-DE	88.14	1.88
BG-DF	38.38	1.88
CH-DE	87.84	1.88
CH-DF	78.42	1.88
CH-DG	84.80	1.88
CG-EF	76.47	1.88
DG-EF	89.41	1.88

LAT=15°S LONG=35°W

LOP PAIRS	CROSSING ANGLE	GDOP
AC-AE	87.74	1.40
AC-AG	51.96	1.76
AD-AE	74.38	1.98
AD-AG	69.84	1.89
AE-AF	53.15	1.72
BC-BE	87.74	1.64
BC-BG	51.96	1.62
BD-BE	74.38	1.92
BD-BF	52.47	1.77
BD-BG	69.84	1.47
CF-CH	88.09	1.54
CG-CH	74.53	1.39
DE-DF	53.15	1.64
DF-DH	88.09	1.52
DG-DH	74.53	1.57
EF-EH	88.09	1.45
EG-EH	74.53	1.83
AE-BC	75.78	1.30
AF-BC	51.06	1.38
AG-BC	68.44	1.15
AE-BD	57.90	1.66
AF-BD	68.95	1.33
AG-BD	86.32	1.24
AG-BF	33.86	1.81
AF-CE	81.05	1.02
AG-CE	81.57	1.02
AF-DE	81.07	1.04
AG-DE	63.69	1.14
AG-EF	63.84	1.27
BF-CE	64.57	1.11
BG-CE	81.05	1.06
BF-DE	82.45	1.03
BG-DF	80.17	1.08
BG-EF	47.36	1.60
CH-DE	56.64	1.37
CH-DF	70.21	1.33
CH-DG	87.58	1.16
CG-EF	70.36	1.34
DG-EF	88.24	1.16

LAT=25°S LONG=35°W

LOP PAIRS	CROSSING ANGLE	GDOP
AC-AE	84.65	1.39
AC-AG	48.42	1.80
AD-AE	73.69	2.00
AD-AG	70.08	1.89
AE-AF	58.56	1.61
BC-BE	84.65	1.53
BC-BG	48.42	1.70
BD-BE	73.69	1.87
BD-BG	70.08	1.54
BE-BF	58.56	1.86
CF-CH	87.71	1.80
CG-CH	65.38	1.47
DE-DF	58.56	1.58
DF-DH	87.71	1.40
DG-DH	65.38	1.52
EF-EH	87.71	1.69
AE-BC	83.92	1.28
AF-BC	37.52	1.79
AG-BC	59.84	1.25
AE-BD	62.27	1.68
AF-BD	59.18	1.55
AG-BD	81.50	1.34
AF-BE	47.14	1.98
AG-BF	33.75	1.81
AF-CE	71.91	1.07
AG-CE	85.76	1.01
AF-DE	86.43	1.04
AG-DE	64.10	1.14
AG-EF	68.15	1.18
BF-CE	60.49	1.15
BG-CE	82.82	1.04
BF-DE	82.15	1.03
BG-DE	75.52	1.09
BG-EF	56.72	1.34
CH-DE	50.81	1.38
CG-DF	43.98	1.94
CH-DF	70.64	1.30
CH-DG	87.04	1.08
CG-EF	62.33	1.42
DG-EF	83.99	1.13

LAT=35°S LONG=35°W

LOP PAIRS	CROSSING ANGLE	GDOP
AC-AE	81.58	1.40
AC-AG	44.56	1.87
AC-AH	88.30	1.84
AD-AE	73.14	1.99
AD-AG	69.85	1.87
AE-AF	67.16	1.49
AF-AH	77.29	1.97
BC-BE	81.58	1.49
BC-BG	44.56	1.81
BC-BH	88.30	1.78
BD-BE	73.14	1.88
BD-BG	69.85	1.60
BE-BF	67.16	1.63
BF-BH	77.29	1.85
CD-CE	73.14	1.98
CG-CH	47.14	1.93
DE-DF	67.16	1.57
DF-DH	77.29	1.47
DG-DH	47.14	1.73
AE-BC	89.42	1.29
AG-BC	52.40	1.36
AH-BC	80.46	1.51
AE-BD	65.30	1.72
AF-BD	47.54	1.92
AG-BD	77.69	1.42
AF-BE	59.32	1.63
AG-BF	37.99	1.66
AH-BF	85.13	1.45
AH-BG	54.98	1.77
AF-CE	59.04	1.22
AG-CE	89.19	1.01
AF-DE	84.33	1.07
AG-DE	65.52	1.13
AG-EF	74.78	1.09
AH-EF	58.08	1.73
AH-EG	88.23	1.71
BF-CE	51.20	1.31
BG-CE	81.35	1.04
BF-DE	76.49	1.07
BG-DE	73.36	1.09
BG-EF	66.94	1.16
BH-EF	65.92	1.92
BH-EG	83.93	1.98
CH-DE	35.41	1.77
CG-DF	55.43	1.82
CH-DF	77.42	1.35
CH-DG	72.43	1.08
CG-EF	51.43	1.62
DG-EF	76.71	1.10
DH-EG	59.72	1.64

AD-A181 508 SOUTH ATLANTIC OMEGA VALIDATION VOLUME 1 SUMMARY ANALYSIS APPENDICES A-E(U) SYSTEMS CONTROL TECHNOLOGY INC PALO ALTO CA T M WATT ET AL. JAN 83 3/3

UNCLASSIFIED DTCG23-81-C-40023 F/G 17/7.3 NL

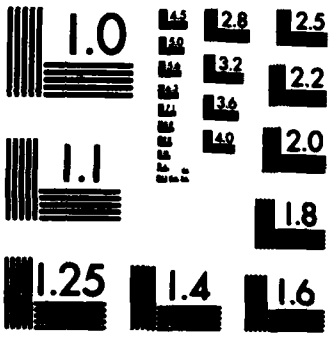

LAT=45°S LONG=35°W

LOP PAIRS	CROSSING ANGLE	GDOP
AC-AE	78.74	1.42
AC-AG	40.65	1.97
AC-AH	68.54	1.42
AD-AE	72.77	1.97
AD-AG	69.14	1.82
AD-AH	82.97	1.73
AE-AF	79.54	1.42
AF-AG	41.44	1.93
AF-AH	69.33	1.41
BC-BE	78.74	1.49
BC-BG	40.65	1.94
BC-BH	68.54	1.44
BD-BE	72.77	1.89
BD-BG	69.14	1.65
BD-BH	82.97	1.62
BE-BF	79.54	1.48
BF-BG	41.44	1.91
BF-BH	69.33	1.44
CD-CE	72.77	1.82
CD-CH	82.97	1.72
DE-DF	79.54	1.78
DF-DH	69.33	1.91
AE-BC	83.80	1.31
AG-BC	45.71	1.49
AH-BC	73.60	1.24
AE-BD	67.71	1.74
AG-BD	74.19	1.48
AH-BD	77.92	1.55
AF-BE	74.48	1.48
AG-BF	46.50	1.48
AH-BF	74.39	1.24
AF-CE	42.05	1.65
AG-CE	83.50	1.02
AH-CE	68.61	1.23
AF-DE	70.54	1.19
AG-DE	68.01	1.11
AH-DE	40.12	1.79
AG-EF	84.29	1.02
AH-EF	67.82	1.23
AH-EG	70.74	1.53
BF-CE	37.00	1.78
BG-CE	78.44	1.05
BH-CE	73.67	1.24
BF-DE	65.49	1.19
BG-DE	73.07	1.09
BH-DE	45.18	1.70
BG-EF	79.24	1.04
BH-EF	72.88	1.25
BH-EG	65.68	1.63
CG-DF	69.93	1.99
CH-DF	82.18	1.72
CH-DG	56.38	1.29
CH-EG	50.85	1.77
DG-EF	65.79	1.14
DH-EF	37.90	1.65
DH-EG	79.34	1.37

LAT=55°S LONG=35°W

LOP PAIRS	CROSSING ANGLE	GDOP
AC-AE	76.39	1.46
AC-AH	54.85	1.56
AD-AE	72.66	1.92
AD-AG	67.89	1.75
AD-AH	85.80	1.58
AE-AF	86.86	1.49
AF-AG	53.69	1.70
AF-AH	71.60	1.43
BC-BE	76.39	1.51
BC-BH	54.85	1.57
BD-BE	72.66	1.90
BD-BG	67.89	1.67
BD-BH	85.80	1.51
BE-BF	86.86	1.51
BF-BG	53.69	1.67
BF-BH	71.60	1.41
CD-CE	72.66	1.73
CD-CH	85.80	1.66
DE-DG	39.45	1.97
EF-EG	53.69	1.84
AE-BC	78.97	1.36
AG-BC	39.52	1.66
AH-BC	57.43	1.32
AE-BD	70.08	1.75
AG-BD	70.47	1.52
AH-BD	88.38	1.47
AF-BE	89.44	1.51
AG-BF	56.27	1.42
AH-BF	74.18	1.28
AG-CE	77.33	1.05
AH-CE	84.76	1.09
AF-DE	54.59	1.50
AG-DE	71.73	1.09
AH-DE	53.82	1.35
AG-EF	85.93	1.01
AH-EF	68.02	1.15
AH-EG	58.30	1.61
BG-CE	74.75	1.06
BH-CE	87.34	1.10
BH-CG	47.89	1.93
BF-DE	52.01	1.51
BG-DE	74.31	1.08
BH-DE	56.40	1.33
BG-EF	88.51	1.01
BH-EF	70.60	1.15
BH-EG	55.71	1.67
CH-DG	48.86	1.53
CH-EG	58.48	1.65
DG-EF	53.65	1.29
DH-EF	35.74	1.72
DH-EG	89.43	1.32

LAT=15°N LONG=25°W

LOP PAIRS	CROSSING ANGLE	GDOP
AB-AC	86.54	1.56
AB-AD	82.87	1.69
AB-AF	45.19	1.88
AC-AE	82.85	1.62
AC-AG	71.00	1.62
AD-AE	79.19	1.76
AD-AG	74.66	1.69
AE-AF	48.88	1.81
BC-BF	48.27	1.88
BD-BF	91.93	1.77
BF-BH	87.60	1.40
CE-CF	48.88	1.81
CF-CH	87.60	1.48
CG-CH	69.67	1.54
DE-DF	48.88	1.76
DF-DH	87.60	1.39
DG-DH	69.67	1.42
EF-EH	87.60	1.41
AF-BC	80.26	1.02
AG-BC	57.52	1.21
AF-BD	76.60	1.04
AG-BD	53.86	1.27
AG-BF	74.21	1.29
AF-CE	83.94	1.01
AG-CE	61.21	1.17
AF-DE	80.28	1.03
AG-DE	57.55	1.22
AG-EF	70.52	1.27
BF-CE	44.58	1.75
BH-CE	43.02	1.76
BF-DE	48.24	1.65
BH-DE	39.35	1.90
BH-EF	88.71	1.35
CF-DE	45.22	1.68
CH-DE	47.18	1.81
CH-DF	83.94	1.44
CH-DG	73.33	1.39
CG-EF	74.42	1.25
DG-EF	78.08	1.22

LAT=5°N LONG=25°W

LOP PAIRS	CROSSING ANGLE	GDOP
AB-AC	71.33	1.95
AB-AF	64.45	1.75
AC-AE	85.20	1.54
AC-AG	66.25	1.64
AD-AE	77.57	1.85
AD-AG	73.88	1.77
AE-AF	50.57	1.76
BC-BF	44.22	1.81
BC-BG	66.25	1.53
BD-BF	51.85	1.62
BD-BG	73.88	1.45
BF-BH	88.23	1.74
CE-CF	50.57	1.83
CF-CH	88.23	1.45
CG-CH	69.74	1.47
DE-DF	50.57	1.71
DF-DH	88.23	1.50
DG-DH	69.74	1.60
EF-EH	88.23	1.42
AE-BC	50.98	1.56
AF-BC	78.45	1.06
AG-BC	79.53	1.06
AE-BD	43.35	1.80
AF-BD	86.08	1.07
AG-BD	71.90	1.13
AG-BF	56.25	1.29
AF-CE	87.67	1.01
AG-CE	65.65	1.11
AF-DE	80.04	1.03
AG-DE	58.02	1.21
AG-EF	70.13	1.24
BF-CE	58.10	1.25
BG-CE	80.13	1.28
BG-CF	49.30	1.92
BF-DE	65.73	1.17
BG-DE	87.76	1.27
BH-EF	74.35	1.86
CF-DE	42.94	1.83
CH-DE	48.82	1.66
CH-DF	80.60	1.38
CH-DG	77.37	1.29
CG-EF	72.77	1.25
DG-EF	80.40	1.19

LAT=5°S LONG=25°W

LOP PAIRS	CROSSING ANGLE	GDOP
AC-AE	88.06	1.46
AC-AG	61.60	1.65
AD-AE	76.15	1.92
AD-AG	73.51	1.82
AE-AF	53.24	1.69
BC-BE	88.06	1.68
BC-BG	61.60	1.47
BD-BE	76.15	1.89
BD-BF	50.61	1.78
BD-BG	73.51	1.41
CE-CF	53.24	1.88
CF-CH	89.28	1.46
CG-CH	67.82	1.43
DE-DF	53.24	1.66
DF-DH	89.28	1.46
DG-DH	67.82	1.58
EF-EH	89.28	1.46
AE-BC	69.48	1.35
AF-BC	57.28	1.30
AG-BC	80.18	1.11
AE-BD	57.57	1.61
AF-BD	69.19	1.29
AG-BD	87.90	1.21
AG-BF	41.49	1.53
AF-CE	86.50	1.01
AG-CE	70.60	1.07
AF-DE	81.59	1.04
AG-DE	58.69	1.20
AG-EF	70.70	1.21
BF-CE	67.91	1.08
BG-CE	89.19	1.08
BF-DE	79.82	1.04
BG-DE	77.27	1.12
BG-EF	52.12	1.53
CH-DE	49.39	1.54
CH-DF	77.37	1.33
CH-DG	79.73	1.19
CG-EF	69.04	1.28
DG-EF	80.95	1.16

LAT=15°S LONG=25°W

LOP PAIRS	CROSSING ANGLE	GDOP
AC-AE	88.57	1.41
AC-AG	56.56	1.67
AD-AE	74.87	1.96
AD-AG	73.12	1.84
AE-AF	57.15	1.62
BC-BE	88.57	1.47
BC-BG	56.56	1.56
BD-BE	74.87	1.81
BD-BG	73.12	1.53
BE-BF	57.15	1.83
CF-CH	88.80	1.59
CG-CH	63.64	1.49
DE-DF	57.15	1.61
DF-DH	88.80	1.41
DG-DH	63.64	1.96
EF-EH	88.80	1.40
AE-BC	81.23	1.31
AF-BC	41.62	1.70
AG-BC	66.77	1.23
AE-BD	64.67	1.66
AF-BD	58.18	1.60
AG-BD	83.33	1.36
AF-BE	46.94	1.90
AG-BF	35.35	1.75
AF-CE	78.36	1.04
AG-CE	76.49	1.04
AF-DE	85.07	1.04
AG-DE	59.93	1.19
AG-EF	72.09	1.16
BF-CE	68.16	1.08
BG-CE	86.69	1.04
BF-DE	84.72	1.02
BG-DE	70.13	1.12
BG-EF	61.89	1.28
CH-DE	48.21	1.47
CG-DF	41.71	1.92
CH-DF	74.64	1.30
CH-DG	80.22	1.12
CG-EF	63.42	1.34
DG-EF	79.98	1.14

LAT=25°S LONG=25°W

LOP PAIRS	CROSSING ANGLE	GDOP
AC-AE	84.84	1.39
AC-AG	51.12	1.72
AD-AE	73.74	1.99
AD-AG	72.55	1.84
AE-AF	62.70	1.54
AF-AH	85.23	1.99
BC-BE	84.84	1.44
BC-BG	51.12	1.67
BD-BE	73.74	1.87
BD-BG	72.55	1.63
BE-BF	62.70	1.64
CG-CH	56.24	1.59
DE-DF	62.70	1.57
DF-DH	85.23	1.40
DG-DH	56.24	1.59
AE-BC	89.38	1.31
AG-BC	56.90	1.34
AE-BD	67.96	1.73
AF-BD	49.34	1.94
AG-BD	78.32	1.49
AF-BE	56.92	1.59
AG-BF	34.77	1.79
AH-BF	88.99	1.95
AF-CE	67.73	1.11
AG-CE	83.28	1.02
AF-DE	89.15	1.09
AG-DE	61.86	1.17
AG-EF	74.58	1.11
BF-CE	61.95	1.15
BG-CE	89.06	1.02
BF-DE	83.37	1.04
BG-DE	67.64	1.13
BG-EF	68.80	1.16
CH-DE	43.95	1.51
CG-DF	50.41	1.78
CH-DF	73.35	1.32
CH-DG	77.67	1.07
CG-EF	55.85	1.46
DG-EF	77.28	1.11

LAT=35°S LONG=25°W

LOP PAIRS	CROSSING ANGLE	GDOP
AC-AE	81.13	1.40
AC-AG	45.59	1.82
AC-AH	89.52	1.52
AD-AE	72.78	1.99
AD-AG	71.67	1.82
AE-AF	70.39	1.47
AF-AH	79.74	1.55
BC-BE	81.13	1.43
BC-BG	45.59	1.80
BC-BH	89.52	1.60
BD-BE	72.78	1.92
BD-BG	71.67	1.70
BE-BF	70.39	1.51
BF-BH	79.74	1.64
CD-CE	72.78	1.94
CG-CH	44.90	1.99
DE-DF	70.39	1.59
DF-DH	79.74	1.50
DG-DH	44.90	1.79
AE-BC	84.19	1.33
AG-BC	48.64	1.47
AH-BC	86.46	1.51
AE-BD	69.72	1.79
AG-BD	74.73	1.57
AF-BE	67.33	1.44
AG-BF	37.90	1.70
AH-BF	82.80	1.47
AH-BG	47.96	1.95
AF-CE	54.49	1.30
AG-CE	89.34	1.01
AF-DE	80.58	1.09
AG-DE	64.57	1.14
AG-EF	78.60	1.06
AH-EF	56.50	1.75
AH-EG	88.65	1.75
BF-CE	51.43	1.33
BG-CE	86.28	1.02
BF-DE	77.52	1.09
BG-DE	67.63	1.12
BG-EF	75.54	1.08
BH-EF	59.56	1.80
BH-EG	85.59	1.83
CH-DE	35.45	1.77
CG-DF	60.93	1.76
CH-DF	74.17	1.43
CH-DG	70.99	1.09
CG-EF	46.28	1.72
DG-EF	72.37	1.11
DH-EG	62.32	1.64

LAT=45°S LONG=25°W

LOP PAIRS	CROSSING ANGLE	GDOP
AC-AE	77.89	1.44
AC-AG	40.41	1.96
AC-AH	72.69	1.42
AD-AE	72.10	1.97
AD-AG	70.42	1.77
AD-AH	77.30	1.82
AE-AF	80.36	1.43
AF-AG	42.88	1.89
AF-AH	75.15	1.41
BC-BE	77.89	1.45
BC-BG	40.41	1.96
BC-BH	72.69	1.43
BD-BE	72.10	1.95
BD-BG	70.42	1.73
BD-BH	77.30	1.80
BE-BF	80.36	1.44
BF-BG	42.88	1.88
BF-BH	75.15	1.41
CD-CE	72.10	1.77
CD-CH	77.30	1.71
DE-DF	80.36	1.78
DF-DH	75.15	1.84
AE-BC	78.96	1.36
AG-BC	41.48	1.63
AH-BC	73.75	1.31
AE-BD	71.03	1.82
AG-BD	71.49	1.61
AH-BD	76.23	1.71
AF-BE	79.29	1.40
AG-BF	43.94	1.58
AH-BF	76.22	1.31
AF-CE	38.97	1.75
AG-CE	81.84	1.03
AH-CE	65.88	1.33
AF-DE	68.98	1.19
AG-DE	68.15	1.12
AG-EF	84.31	1.02
AH-EF	63.41	1.35
AH-EG	73.71	1.58
BF-CE	37.90	1.78
BG-CE	80.78	1.04
BH-CE	66.95	1.33
BF-DE	67.91	1.20
BG-DE	69.21	1.11
BG-EF	83.24	1.03
BH-EF	64.48	1.35
BH-EG	72.64	1.60
CG-DF	72.89	1.97
CH-DF	74.83	1.76
CH-DG	62.29	1.19
CH-EG	45.61	1.93
DG-EF	65.03	1.15
DH-EF	32.75	1.88
DH-EG	75.62	1.41

LAT=55°S LONG=25°W

LOP PAIRS	CROSSING ANGLE	GDOP
AC-AE	75.47	1.50
AC-AH	58.59	1.82
AD-AE	71.82	1.94
AD-AG	68.69	1.71
AD-AH	88.69	1.86
AE-AF	88.40	1.47
AF-AG	52.10	1.70
AF-AH	74.72	1.39
BC-BE	75.47	1.49
BC-BH	58.59	1.52
BD-BE	71.82	1.95
BD-BG	68.69	1.73
BD-BH	88.69	1.58
BE-BF	88.40	1.47
BF-BG	52.10	1.70
BF-BH	74.72	1.39
CD-CE	71.82	1.68
CD-CH	88.69	1.56
DE-DG	39.49	1.97
EF-EG	52.10	1.89
AE-BC	74.77	1.43
AG-BC	35.28	1.84
AH-BC	57.90	1.37
AE-BD	72.51	1.82
AG-BD	67.99	1.62
AH-BD	89.39	1.57
AF-BE	87.71	1.45
AG-BF	51.41	1.51
AH-BF	74.03	1.32
AG-CE	74.58	1.07
AH-CE	82.80	1.14
AF-DE	55.19	1.45
AG-DE	72.71	1.09
AH-DE	50.09	1.48
AG-EF	89.29	1.01
AH-EF	66.67	1.21
AH-EG	61.22	1.60
BG-CE	75.27	1.06
BH-CE	82.11	1.13
BF-DE	55.88	1.44
BG-DE	72.01	1.09
BH-DE	49.39	1.49
BG-EF	88.60	1.01
BH-EF	65.98	1.21
BH-EG	61.92	1.59
CH-DG	55.33	1.37
CH-EG	52.85	1.74
CH-FG	38.75	1.95
DG-EF	56.08	1.29
DH-EF	33.46	1.81
DH-EG	85.56	1.32

LAT=15°N LONG=15°W

LOP PAIRS	CROSSING ANGLE	GDOP
AB-AC	80.32	1.69
AB-AD	80.63	1.70
AC-AE	80.93	1.77
AC-AG	82.06	1.68
AD-AE	80.61	1.79
AD-AG	82.38	1.69
AE-AF	49.98	1.73
BC-BH	39.82	2.00
BF-BH	88.90	1.60
CE-CF	49.98	1.76
CF-CH	88.90	1.48
CG-CH	58.12	1.72
DE-DF	49.98	1.76
DF-DH	88.90	1.46
DG-DH	58.12	1.73
EF-EH	88.90	1.42
FG-FH	58.12	1.93
AD-BC	69.65	1.72
AF-BC	60.94	1.16
AF-BD	60.63	1.17
AG-BF	77.05	1.60
AF-CE	79.69	1.03
AG-CE	46.72	1.44
AF-DE	79.38	1.03
AG-DE	46.40	1.44
AG-EF	84.19	1.20
BH-CE	58.57	1.27
BH-CG	41.56	1.64
BH-DE	58.25	1.28
BH-DG	41.25	1.65
BH-EF	72.34	1.29
BH-FG	89.35	1.54
CF-DE	49.64	1.55
CH-DE	41.43	1.99
CH-DF	88.59	1.44
CH-DG	58.44	1.54
CG-EF	66.09	1.28
DG-EF	66.41	1.27
EH-FG	71.90	1.77

LAT=5°N LONG=15°W

LOP PAIRS	CROSSING ANGLE	GDOP
AB-AF	72.51	1.75
AC-AE	83.16	1.66
AC-AG	75.23	1.65
AD-AE	78.72	1.87
AD-AG	79.68	1.77
AE-AF	52.24	1.68
BC-BF	44.60	1.80
BC-BG	75.23	1.45
BD-BF	49.04	1.70
BD-BG	79.68	1.43
CE-CF	52.24	1.77
CF-CH	89.78	1.42
CG-CH	59.58	1.60
DE-DF	52.24	1.70
DF-DH	89.78	1.43
DG-DH	59.58	1.67
EF-EH	89.78	1.44
FG-FH	59.58	1.98
AE-BC	52.73	1.82
AF-BC	75.03	1.11
AG-BC	74.34	1.13
AE-BD	48.29	1.65
AF-BD	79.47	1.12
AG-BD	69.89	1.19
AG-BF	61.07	1.20
AF-CE	84.70	1.02
AG-CE	54.06	1.27
AF-DE	80.25	1.04
AG-DE	49.42	1.36
AG-EF	81.34	1.18
BF-CE	64.87	1.14
BG-CE	84.49	1.28
BF-DE	69.31	1.11
BG-DE	80.05	1.30
BG-EF	50.91	1.79
CF-DE	47.80	1.67
CH-DE	42.42	1.82
CH-DF	85.34	1.37
CH-DG	64.02	1.37
CG-EF	66.20	1.26
DG-EF	70.64	1.22
EH-FG	68.18	1.94

LAT=5°S LONG=15°W

LOP PAIRS	CROSSING ANGLE	GDOP
AC-AE	86.27	1.53
AC-AG	68.60	1.61
AD-AE	76.91	1.94
AD-AG	77.96	1.81
AE-AF	55.46	1.62
BC-BE	86.27	1.49
BC-BG	68.60	1.52
BD-BE	76.91	1.80
BD-BG	77.96	1.63
BE-BF	55.46	1.69
CE-CF	55.46	1.83
CF-CH	88.98	1.45
CG-CH	58.65	1.53
DE-DF	55.46	1.65
DF-DH	88.98	1.41
DG-DH	58.65	1.64
EF-EH	88.98	1.55
AE-BC	81.41	1.43
AF-BC	43.13	1.89
AG-BC	73.46	1.35
AE-BD	72.05	1.70
AF-BD	52.49	1.91
AG-BD	82.82	1.53
AF-BE	50.60	1.61
AG-BF	35.20	1.78
AF-CE	87.82	1.02
AG-CE	61.84	1.16
AF-DE	82.82	1.04
AG-DE	52.48	1.30
AG-EF	79.89	1.15
BF-CE	82.96	1.02
BG-CE	66.71	1.13
BF-DE	87.68	1.02
BG-DE	57.35	1.24
BG-EF	75.03	1.18
CF-DE	46.10	1.88
CH-DE	42.88	1.69
CG-DF	39.69	1.91
CH-DF	81.66	1.32
CH-DG	68.01	1.24
CG-EF	63.39	1.28
DG-EF	72.75	1.18

LAT=15°S LONG=15°W

LOP PAIRS	CROSSING ANGLE	GDOP
AC-AE	89.60	1.42
AC-AG	61.36	1.61
AD-AE	75.18	1.98
AD-AG	76.58	1.83
AE-AF	59.81	1.56
BC-BE	89.60	1.42
BC-BG	61.36	1.60
BD-BE	75.18	1.96
BD-BG	76.58	1.81
BE-BF	59.81	1.56
CF-CH	87.16	1.45
CG-CH	55.59	1.58
DE-DF	59.81	1.60
DF-DH	87.16	1.40
DG-DH	55.59	1.64
EF-EH	87.16	1.76
AE-BC	90.00	1.41
AG-BC	61.75	1.64
AE-BD	74.79	1.86
AG-BD	76.97	1.73
AF-BE	59.42	1.41
AG-BF	31.95	1.96
AF-CE	77.65	1.05
AG-CE	70.79	1.08
AF-DE	87.13	1.04
AG-DE	55.57	1.28
AE-DH	54.68	1.48
AG-EF	79.42	1.11
BF-CE	77.26	1.08
BG-CE	71.18	1.07
BF-DE	87.52	1.04
BG-DE	55.96	1.28
BG-EF	79.03	1.12
CH-DE	42.56	1.60
CG-DF	46.78	1.76
CH-DF	77.63	1.31
CH-DG	70.81	1.14
CG-EF	58.04	1.38
DG-EF	73.26	1.14

LAT=25°S LONG=15°W

LOP PAIRS	CROSSING ANGLE	GDOP
AC-AE	84.76	1.39
AC-AG	53.54	1.66
AC-AH	76.23	1.98
AD-AG	75.21	1.82
AE-AF	65.48	1.58
AF-AH	84.50	1.79
BC-BE	84.76	1.39
BC-BG	53.54	1.68
BC-BH	76.23	1.93
BD-BG	75.21	1.88
BE-BF	65.48	1.47
BF-BH	84.50	1.73
CG-CH	50.23	1.70
DE-DF	65.48	1.57
DF-DH	84.50	1.42
DG-DH	50.23	1.69
AE-BC	83.43	1.38
AG-BC	52.21	1.51
AH-BC	77.56	1.88
AE-BD	74.90	1.93
AG-BD	73.88	1.81
AF-BE	64.81	1.34
AG-BF	32.93	1.94
AH-BF	83.17	1.77
AF-CE	64.93	1.15
AG-CE	80.81	1.03
AF-DE	86.60	1.04
AG-DE	59.13	1.21
AG-EF	79.92	1.08
BF-CE	66.26	1.14
BG-CE	79.48	1.03
BF-DE	87.93	1.04
BG-DE	57.81	1.22
BG-EF	81.24	1.07
CH-DE	40.69	1.89
CG-DF	55.94	1.48
CH-DF	73.83	1.26
CH-DG	71.91	1.09
CG-EF	50.50	1.82
DG-EF	72.17	1.12
DH-EG	84.20	1.98

LAT=35°S LONG=15°W

LOP PAIRS	CROSSING ANGLE	GDOP
AC-AE	80.04	1.41
AC-AG	45.89	1.80
AC-AH	88.48	1.51
AD-AG	73.67	1.78
AE-AF	72.69	1.46
AF-AH	81.14	1.54
BC-BE	80.04	1.40
BC-BG	45.89	1.82
BC-BH	88.48	1.47
BD-BG	73.67	1.89
BE-BF	72.69	1.43
BF-BH	81.14	1.49
CD-CE	72.18	1.86
DE-DF	72.69	1.60
DF-DH	81.14	1.53
DG-DH	42.59	1.86
AE-BC	77.69	1.38
AG-BC	43.54	1.64
AH-BC	86.13	1.52
AE-BD	74.52	1.95
AG-BD	71.33	1.82
AF-BE	75.04	1.31
AG-BF	36.20	1.83
AH-BF	78.79	1.51
AF-CE	50.37	1.38
AG-CE	88.91	1.02
AH-CE	48.49	1.92
AF-DE	78.16	1.10
AG-DE	63.30	1.16
AG-EF	81.57	1.09
AH-EF	55.84	1.75
AH-EG	85.62	1.78
BF-CE	52.72	1.35
BG-CE	88.74	1.02
BH-CE	46.15	1.91
BF-DE	80.50	1.11
BG-DE	60.95	1.18
BG-EF	83.92	1.04
BH-EF	53.49	1.73
BH-EG	87.97	1.72
CH-DE	36.23	1.74
CG-DF	66.33	1.72
CH-DF	71.08	1.50
CH-DG	70.38	1.08
CG-EF	41.49	1.86
DG-EF	69.28	1.12
DH-EG	65.23	1.64

LAT=45°S LONG=15°W

LOP PAIRS	CROSSING ANGLE	GDOP
AC-AE	76.36	1.47
AC-AG	39.35	1.99
AC-AH	73.08	1.48
AD-AE	71.18	1.99
AD-AG	71.82	1.73
AD-AH	74.45	1.89
AE-AF	81.46	1.44
AF-AG	44.45	1.83
AF-AH	78.18	1.42
BC-BE	76.36	1.43
BC-BH	73.08	1.42
BD-BG	71.82	1.86
BD-BH	74.45	1.97
BE-BF	81.46	1.41
BF-BG	44.45	1.86
BF-BH	78.18	1.39
CD-CE	71.18	1.69
CD-CG	71.82	1.93
CD-CH	74.45	1.66
DE-DF	81.46	1.78
DF-DH	78.18	1.81
AE-BC	73.17	1.43
AG-BC	36.17	1.86
AH-BC	69.90	1.40
AE-BD	74.36	1.94
AG-BD	68.63	1.80
AH-BD	77.64	1.87
AF-BE	84.64	1.33
AG-BE	40.19	1.96
AG-BF	41.26	1.71
AH-BF	75.00	1.39
AF-CE	34.94	1.93
AG-CE	79.39	1.05
AH-CE	66.88	1.37
AF-DE	67.41	1.21
AG-DE	68.14	1.12
AG-EF	84.49	1.02
AH-EF	61.78	1.42
AH-EG	73.77	1.63
BF-CE	38.13	1.82
BG-CE	82.87	1.03
BH-CE	63.69	1.36
BF-DE	70.59	1.21
BG-DE	64.96	1.14
BG-EF	87.67	1.01
BH-EF	58.60	1.42
BH-EG	76.95	1.57
CG-DF	76.92	1.95
CH-DF	69.35	1.82
CH-DG	66.20	1.15
CH-FG	38.83	2.00
DG-EF	64.38	1.14
DH-EG	78.09	1.43

LAT=55°S LONG=15°W

LOP PAIRS	CROSSING ANGLE	GDOP
AC-AE	74.08	1.55
AC-AH	59.89	1.83
AD-AE	70.78	1.98
AD-AG	69.52	1.67
AD-AH	84.96	1.60
AE-AF	88.71	1.49
AF-AG	51.59	1.68
AF-AH	77.11	1.38
BC-BE	74.08	1.47
BC-BH	59.89	1.50
BD-BG	69.52	1.81
BD-BH	84.96	1.70
BE-BF	88.71	1.45
BF-BG	51.59	1.73
BF-BH	77.11	1.39
CD-CE	70.78	1.62
CD-CH	84.96	1.51
DE-DG	39.70	1.96
EF-EG	51.59	1.90
AE-BC	70.01	1.91
AH-BC	55.83	1.48
AE-BD	74.85	1.91
AG-BD	65.45	1.75
AH-BD	89.03	1.48
AF-BE	84.64	1.41
AG-BE	43.77	1.88
AG-BF	47.52	1.63
AH-BF	73.04	1.38
AF-CD	51.23	1.95
AG-CE	71.13	1.89
AH-CE	83.35	1.18
AF-DE	54.69	1.45
AG-DE	73.72	1.89
AH-DE	48.20	1.98
AG-EF	88.34	1.81
AH-EF	66.13	1.86
AH-EG	62.28	1.62
BG-CE	75.20	1.66
BH-CE	79.28	1.15
BF-DE	58.76	1.42
BG-DE	69.65	1.11
BH-DE	44.13	1.64
BG-EF	87.59	1.01
BH-EF	62.04	1.86
BH-EG	66.39	1.53
CH-DG	60.67	1.38
CH-EG	48.55	1.84
CH-FG	42.74	1.79
DG-EF	57.63	1.82
DH-EF	32.11	1.89
DH-EG	83.70	1.32

LAT=15°N LONG=5°W

LOP PAIRS	CROSSING ANGLE	GDOP
AB-AE	46.75	1.78
AC-AG	88.24	1.98
AD-AE	82.01	1.87
AD-AG	88.11	1.77
AE-AF	50.20	1.69
AF-AG	40.32	1.94
BC-BE	78.36	1.39
BC-BG	88.24	1.47
BD-BE	82.01	1.39
BD-BG	88.11	1.50
BD-BH	42.21	2.00
CE-CF	50.20	1.73
CF-CH	89.99	1.48
CG-CH	49.68	1.99
DE-DF	50.20	1.77
DF-DH	89.99	1.42
DG-DH	49.68	1.90
EF-EH	89.99	1.44
FG-FH	49.68	1.94
AD-BC	74.23	1.87
AF-BE	51.93	1.55
AG-BE	87.76	1.25
AF-CE	73.19	1.08
AG-CE	32.87	1.96
AF-DE	76.83	1.05
AG-DE	36.52	1.78
AG-EF	84.31	1.21
BG-CE	45.01	1.95
BH-CE	85.32	1.01
BG-CF	84.80	1.49
BH-CF	35.12	2.00
BH-CG	75.44	1.03
BH-DE	88.96	1.01
BG-DF	88.44	1.52
BH-DF	38.76	1.90
BH-DG	79.08	1.02
BH-EF	43.24	1.70
BH-FG	53.12	1.63
CF-DE	53.84	1.43
CG-DF	36.67	1.99
CH-DF	86.35	1.49
CH-DG	46.03	1.86
CG-EF	61.32	1.32
DG-EF	57.67	1.37
EH-FG	80.12	1.58

LAT=5°N LONG=5°W

LOP PAIRS	CROSSING ANGLE	GDOP
AB-AE	83.66	1.41
AB-AG	68.12	1.51
AC-AE	80.19	1.92
AC-AG	84.26	1.81
AD-AE	79.82	1.94
AD-AG	84.43	1.83
AE-AF	52.90	1.64
BF-BH	89.03	1.61
BG-BH	51.68	1.63
CE-CF	52.90	1.72
CF-CH	89.03	1.41
CG-CH	51.68	1.80
DE-DF	52.90	1.71
DF-DH	89.03	1.41
DG-DH	51.68	1.80
EF-EH	89.03	1.50
FG-FH	51.68	1.96
AF-BE	84.72	1.03
AG-BE	57.93	1.22
AF-CE	79.13	1.08
AG-CE	41.78	1.56
AF-DE	78.74	1.08
AG-DE	41.41	1.98
AG-EF	88.69	1.16
BH-CE	92.28	1.37
BG-CF	53.50	1.83
BH-CF	74.82	1.31
BH-CG	67.82	1.17
BH-DE	92.65	1.37
BG-DF	53.87	1.82
BH-DF	74.46	1.31
BH-DG	68.19	1.16
BG-EF	46.31	1.62
CF-DE	52.53	1.82
CG-DF	37.72	1.96
CH-DF	89.40	1.40
CH-DG	52.04	1.87
CG-EF	62.46	1.88
DG-EF	62.82	1.88
EH-FG	78.43	1.73

LAT=5°S LONG=5°W

LOP PAIRS	CROSSING ANGLE	GDOP
AC-AE	83.44	1.67
AC-AG	74.23	1.66
AD-AE	77.58	1.99
AD-AG	82.10	1.88
AE-AF	54.61	1.58
BE-BF	54.61	1.56
BF-BH	87.82	1.46
BG-BH	51.53	1.98
CE-CF	54.61	1.76
CF-CH	87.82	1.45
CG-CH	51.53	1.68
DE-DF	54.61	1.68
DF-DH	87.82	1.40
DG-DH	51.53	1.76
EF-EH	87.82	1.68
AF-BE	73.72	1.11
AG-BE	37.43	1.78
AF-CE	88.20	1.03
AG-CE	51.91	1.31
AF-DE	82.34	1.08
AG-DE	46.05	1.44
AG-EF	88.14	1.13
BF-CE	71.10	1.19
BG-CE	34.81	1.76
BH-CF	73.33	1.67
BF-DE	69.23	1.25
BH-DF	79.19	1.55
BH-DG	42.90	1.99
BG-EF	74.75	1.14
CF-DE	50.75	1.70
CH-DE	37.07	1.91
CG-DF	42.15	1.63
CH-DF	86.32	1.33
CH-DG	57.39	1.36
CG-EF	60.27	1.29
DG-EF	66.13	1.31
EH-FG	71.86	1.91

LAT=15°S LONG=5°W

LOP PAIRS	CROSSING ANGLE	GDOP
AC-AE	88.78	1.46
AC-AG	66.50	1.58
AD-AG	79.97	1.85
AE-AF	61.42	1.52
AF-AH	86.25	1.90
BC-BE	88.78	1.70
BC-BG	66.50	1.93
BE-BF	61.42	1.47
BF-BH	86.25	1.50
CE-CF	61.42	1.97
CF-CH	86.25	1.65
CG-CH	49.54	1.67
DE-DF	61.42	1.59
DF-DH	86.25	1.41
DG-DH	49.54	1.75
EF-EH	86.25	1.89
AE-BC	80.00	1.78
AF-BE	72.64	1.16
AG-BE	35.94	1.87
AH-BF	75.03	1.98
AF-CE	78.93	1.05
AG-CE	64.36	1.13
AF-DE	87.59	1.05
AG-DE	50.89	1.34
AG-EF	85.84	1.09
BF-CE	89.85	1.09
BG-CE	53.14	1.25
BF-DE	76.38	1.14
BG-DE	39.67	1.60
BH-DF	71.30	1.68
BG-EF	82.94	1.06
CH-DE	38.30	1.73
CG-DF	50.18	1.68
CH-DF	80.28	1.32
CH-DG	63.02	1.20
CG-EF	54.52	1.37
DG-EF	67.99	1.16

LAT=25°S LONG=5°W

LOP PAIRS	CROSSING ANGLE	GDOP
AC-AE	84.21	1.39
AC-AG	55.26	1.62
AC-AH	78.93	1.83
AD-AG	77.93	1.82
AE-AF	67.41	1.47
AF-AH	84.26	1.69
BC-BE	84.21	1.42
BC-BG	55.26	1.77
BC-BH	78.93	1.68
BE-BF	67.41	1.42
BF-BH	84.26	1.46
CG-CH	45.81	1.81
DE-DF	67.41	1.57
DF-DH	84.26	1.44
DG-DH	45.81	1.80
AE-BC	75.24	1.51
AG-BC	46.29	1.81
AH-BC	92.10	1.81
AF-BE	76.38	1.19
AG-BE	37.92	1.84
AH-BF	75.30	1.74
AF-CE	62.71	1.18
AG-CE	78.84	1.04
AF-DE	85.39	1.07
AG-DE	56.16	1.28
AG-EF	84.36	1.06
BF-CE	71.68	1.16
BG-CE	69.87	1.07
BF-DE	85.64	1.12
BG-DE	47.19	1.40
BH-DF	64.03	1.75
BG-EF	86.67	1.05
BH-EG	79.31	1.89
CH-DE	39.53	1.62
CG-DF	61.13	1.61
CH-DF	73.06	1.39
CH-DG	68.49	1.10
CG-EF	45.76	1.61
DG-EF	68.44	1.13
DH-EG	61.08	1.93

LAT=35°S LONG=5°W

LOP PAIRS	CROSSING ANGLE	GDOP
AC-AE	77.80	1.43
AC-AG	44.76	1.81
AC-AH	85.22	1.88
AD-AG	78.75	1.77
AE-AF	74.57	1.48
AF-AG	41.53	1.91
AF-AH	81.99	1.83
BC-BE	77.80	1.38
BC-BG	44.76	1.89
BC-BH	85.22	1.41
BE-BF	74.57	1.39
BF-BG	41.53	1.97
BF-BH	81.99	1.41
CD-CE	71.21	1.75
CD-CG	78.75	1.86
CD-CH	63.79	1.87
DE-DF	74.57	1.60
DF-DH	81.99	1.84
DG-DH	40.46	1.94
AE-BC	69.88	1.47
AG-BC	36.83	1.93
AH-BC	77.29	1.57
AF-BE	82.50	1.22
AG-BE	40.96	1.79
AH-BF	74.07	1.57
AF-CE	45.53	1.50
AG-CE	87.06	1.03
AH-CE	52.48	1.81
AF-DE	76.52	1.12
AG-DE	61.95	1.18
AG-EF	83.84	1.04
AH-EF	55.71	1.74
AH-EG	82.76	1.81
BE-CD	56.82	1.97
BH-CD	64.24	1.91
BF-CE	53.45	1.40
BG-CE	85.02	1.02
BH-CE	44.56	1.81
BF-DE	84.45	1.15
BG-DE	54.02	1.28
BH-DF	61.01	1.87
BG-EF	88.24	1.02
BH-EF	47.78	1.72
BH-EG	89.31	1.44
CH-DE	38.41	1.66
CG-DF	72.53	1.69
CH-DF	67.02	1.87
CH-DG	71.45	1.07
DG-EF	67.26	1.12
DH-EG	68.33	1.63

LAT=45°S LONG=5°W

LOP PAIRS	CROSSING ANGLE	GDOP
AC-AE	73.83	1.51
AC-AH	70.93	1.49
AD-AG	73.26	1.70
AD-AH	72.78	1.94
AE-AF	82.82	1.46
AF-AG	45.96	1.78
AF-AH	79.93	1.43
BC-BE	73.83	1.42
BC-BH	70.93	1.42
BE-BF	82.82	1.39
BF-BG	45.96	1.86
BF-BH	79.93	1.38
CD-CE	69.88	1.61
CD-CG	73.26	1.87
CD-CH	72.78	1.57
DE-DF	82.82	1.77
DF-DH	79.93	1.80
AE-BC	66.35	1.53
AH-BC	63.45	1.50
AF-BE	89.70	1.29
AG-BE	44.34	1.75
AG-BF	38.49	1.87
AH-BF	72.45	1.47
AG-CE	75.48	1.07
AH-CE	70.56	1.38
AF-DE	65.81	1.23
AG-DE	68.23	1.13
AG-EF	84.48	1.03
AH-EF	61.56	1.46
AH-EG	72.48	1.67
BF-CE	36.99	1.94
BG-CE	82.96	1.03
BH-CE	63.08	1.34
BF-DE	73.29	1.23
BG-DE	60.75	1.19
BG-EF	88.04	1.01
BH-EF	54.08	1.46
BH-EG	79.95	1.53
CH-DE	33.39	1.93
CG-DF	82.25	1.96
CH-DF	63.78	1.91
CH-DG	70.25	1.12
CH-FG	42.96	1.81
DG-EF	64.15	1.14
DH-EG	76.15	1.43

LAT=55°S LONG=5°W

LOP PAIRS	CROSSING ANGLE	GDOP
AC-AE	72.15	1.62
AC-AH	59.12	1.57
AD-AG	70.32	1.64
AD-AH	82.49	1.63
AE-AF	88.17	1.53
AF-AG	51.61	1.67
AF-AH	78.80	1.39
BC-BE	72.15	1.47
BC-BH	59.12	1.51
BD-BG	70.32	1.92
BD-BH	82.49	1.83
BE-BF	88.17	1.45
BF-BG	51.61	1.76
BF-BH	78.80	1.39
CD-CE	69.46	1.56
CD-CH	82.49	1.46
DE-DG	40.22	1.94
EF-EG	51.61	1.88
AE-BC	64.71	1.62
AH-BC	51.68	1.57
AG-BD	62.88	1.92
AH-BD	90.07	1.81
AF-BE	80.72	1.39
AG-BE	47.67	1.74
AG-BF	44.17	1.76
AH-BF	71.36	1.45
AF-CD	54.42	1.77
AG-CE	66.65	1.14
AH-CE	86.16	1.21
AF-DE	53.43	1.44
AG-DE	74.96	1.09
AH-DE	47.77	1.64
AG-EF	86.33	1.02
AH-EF	66.48	1.30
AH-EG	61.91	1.65
BG-CE	74.09	1.07
BH-CE	78.71	1.16
BF-DE	60.87	1.42
BG-DE	67.52	1.12
BH-DE	40.32	1.77
BG-EF	86.23	1.01
BH-EF	59.03	1.30
BH-EG	69.36	1.49
CH-DG	65.59	1.22
CH-EG	44.96	1.94
CH-FG	46.88	1.67
DG-EF	38.93	1.20
DH-EF	31.74	1.91
DH-EG	83.35	1.32

LAT=15°N LONG=5°E

LOP PAIRS	CROSSING ANGLE	GDOP
AB-AE	58.75	1.51
AB-AG	54.60	1.57
AD-AG	87.67	1.97
AE-AF	49.43	1.60
AF-AG	45.29	1.78
BC-BE	75.04	1.41
BC-BG	79.19	1.39
BD-BE	83.53	1.47
BD-BG	87.67	1.46
BG-BH	43.78	1.89
CE-CF	49.43	1.7.
CF-CG	45.29	1.83
CF-CH	89.07	1.50
DE-DF	49.43	1.81
DF-DG	45.29	1.98
DF-DH	89.07	1.41
EF-EH	89.07	1.45
AE-BC	44.01	1.83
AG-BC	39.86	1.96
AF-BE	69.62	1.19
AG-BE	65.10	1.26
AF-CE	64.17	1.17
AF-DE	72.66	1.08
AG-EF	74.41	1.26
BG-CE	42.06	1.69
BH-CE	85.84	1.03
BG-CF	88.50	1.22
BH-CF	44.72	1.59
BH-CG	89.99	1.01
BH-DE	77.36	1.03
BG-DF	83.01	1.31
BH-DF	53.21	1.50
BH-DG	81.50	1.02
CF-DE	57.92	1.32
CH-DF	80.58	1.58
CG-EF	59.68	1.36
DG-EF	51.19	1.50
EH-FG	86.78	1.49

LAT=5°N LONG=5°E

LOP PAIRS	CROSSING ANGLE	GDOP
AB-AE	77.99	1.41
AB-AG	67.76	1.49
AD-AG	88.74	1.96
AE-AF	52.48	1.62
AF-AG	42.25	1.87
BC-BE	75.78	1.89
BC-BG	86.01	1.80
BF-BH	88.10	1.83
BG-BH	45.85	1.76
CE-CF	52.48	1.66
CF-CG	42.25	1.99
CF-CH	88.10	1.43
DE-DF	52.48	1.73
DF-DH	88.10	1.40
DG-DH	45.85	1.96
EF-EH	88.10	1.52
AF-BE	83.43	1.05
AG-BE	54.32	1.29
AF-CE	70.34	1.11
AF-DE	75.59	1.07
AG-DE	33.34	1.90
AG-EF	79.83	1.19
BH-CE	61.84	1.20
BG-CF	68.48	1.27
BH-CF	65.67	1.30
BH-CG	72.08	1.10
BH-DE	56.59	1.26
BG-DF	63.23	1.39
BH-DF	70.92	1.32
BH-DG	66.83	1.14
CF-DE	57.73	1.36
CH-DF	82.85	1.48
CG-EF	61.97	1.29
DG-EF	56.72	1.36
EH-FG	81.67	1.62

LAT=5°S LONG=5°E

LOP PAIRS	CROSSING ANGLE	GDOP
AB-AE	83.64	1.75
AB-AG	80.45	1.72
AC-AG	85.66	1.94
AD-AG	85.83	1.95
AE-AF	56.71	1.55
AF-AG	40.80	1.92
AF-AH	86.99	1.89
BE-BF	56.71	1.76
BF-BH	86.99	1.44
BG-BH	46.19	1.82
CE-CF	56.71	1.66
CF-CH	86.99	1.40
CG-CH	46.19	1.89
DE-DF	56.71	1.66
DF-DH	86.99	1.40
DG-DH	46.19	1.90
EF-EH	86.99	1.66
AF-BE	85.62	1.04
AG-BE	44.82	1.47
AF-CE	80.40	1.06
AG-CE	39.60	1.63
AF-DE	80.24	1.06
AG-DE	39.44	1.64
AG-EF	84.47	1.14
BF-CE	51.50	1.69
BH-CE	35.49	1.96
BG-CF	46.01	1.71
BH-CF	87.80	1.34
BH-CG	51.41	1.45
BF-DE	51.33	1.69
BH-DE	35.66	1.95
BG-DF	46.18	1.70
BH-DF	87.63	1.33
BH-DG	51.57	1.44
BG-EF	55.56	1.34
CF-DE	56.55	1.48
CG-DF	40.97	1.87
CH-DF	87.16	1.38
CH-DG	46.36	1.64
CG-EF	60.78	1.26
DG-EF	60.95	1.26
EH-FG	77.10	1.82

LAT=15°S LONG=5°E

LOP PAIRS	CROSSING ANGLE	GDOP
AC-AE	85.46	1.58
AC-AG	73.02	1.61
AD-AG	83.22	1.91
AE-AF	62.17	1.50
AF-AG	40.66	1.93
AF-AH	85.68	1.75
BE-BF	62.17	1.53
BF-BH	85.68	1.39
BG-BH	45.03	1.98
CE-CF	62.17	1.85
CF-CH	85.68	1.57
CG-CH	45.03	1.79
DE-DF	62.17	1.59
DF-DH	85.68	1.41
DG-DH	45.03	1.88
EF-EH	85.68	1.98
AF-BE	82.44	1.08
AG-BE	41.79	1.88
AF-CE	83.15	1.08
AG-CE	36.19	1.84
AF-DE	86.65	1.06
AG-DE	45.99	1.45
AG-EF	88.56	1.09
BF-CE	76.57	1.24
BG-CE	39.92	1.71
BH-CF	71.28	1.72
BF-DE	66.37	1.23
BH-DF	81.48	1.43
BH-DG	40.82	1.83
BG-EF	68.28	1.15
CF-DE	51.97	1.92
CH-DE	33.71	1.98
CG-DF	50.85	1.65
CH-DF	84.12	1.32
CH-DG	55.22	1.31
CG-EF	53.88	1.38
DG-EF	64.08	1.19

LAT=25°S LONG=5°E

LOP PAIRS	CROSSING ANGLE	GDOP
AC-AE	82.49	1.39
AC-AG	55.41	1.61
AC-AH	82.12	1.72
AD-AG	80.64	1.85
AE-AF	68.78	1.46
AF-AG	41.70	1.89
AF-AH	84.17	1.63
BC-BE	82.49	1.51
BC-BG	55.41	1.91
BC-BH	82.12	1.62
BE-BF	68.78	1.43
BF-BH	84.17	1.39
CD-CE	72.28	2.00
CD-CG	80.64	1.96
CG-CH	42.47	1.93
DE-DF	68.78	1.56
DF-DH	84.17	1.45
DG-DH	42.47	1.92
AE-BC	66.82	1.70
AH-BC	82.20	1.85
AF-BE	84.46	1.12
AG-BE	42.76	1.60
AH-BF	68.49	1.79
AF-CE	59.94	1.22
AG-CE	78.36	1.05
AF-DE	85.17	1.08
AG-DE	53.13	1.31
AG-EF	87.93	1.06
BE-CD	72.12	1.94
BH-CD	87.51	1.93
BF-CE	75.62	1.21
BG-CE	62.68	1.13
BF-DE	79.15	1.21
BG-DE	37.46	1.69
BH-DF	73.80	1.55
BG-EF	76.39	1.07
BH-EG	75.62	1.89
CH-DE	40.61	1.58
CG-DF	66.93	1.54
CH-DF	70.60	1.41
CH-DG	67.70	1.09
CG-EF	40.79	1.75
DG-EF	66.02	1.14
DH-EG	65.25	1.95

LAT=35°S LONG=5°E

LOP PAIRS	CROSSING ANGLE	GDOP
AC-AE	73.21	1.47
AC-AG	40.76	1.93
AC-AH	79.39	1.54
AD-AG	77.85	1.77
AE-AF	76.35	1.45
AF-AG	43.91	1.83
AF-AH	82.53	1.52
BC-BE	73.21	1.39
BC-BH	79.39	1.38
BE-BF	76.35	1.39
BF-BG	43.91	1.96
BF-BH	82.53	1.38
CD-CE	69.70	1.59
CD-CG	77.85	1.72
CD-CH	63.53	1.68
DE-DF	76.35	1.59
DF-DH	82.53	1.55
AE-BC	60.14	1.61
AH-BC	66.31	1.64
AF-BE	89.43	1.18
AG-BE	45.52	1.60
AH-BF	69.45	1.65
AF-CE	38.25	1.76
AG-CE	82.15	1.05
AH-CE	59.23	1.67
AF-DE	75.33	1.14
AG-DE	60.76	1.21
AG-EF	85.30	1.04
AH-EF	56.08	1.72
AH-EG	80.01	1.83
BE-CD	57.97	1.72
BH-CD	64.15	1.67
BF-CE	51.32	1.53
BG-CE	84.77	1.03
BH-CE	46.15	1.67
BF-DE	88.41	1.20
BG-DE	47.68	1.40
BH-DF	67.29	1.71
BG-EF	81.63	1.03
BH-EF	43.01	1.75
BH-EG	86.92	1.63
CH-DE	43.26	1.52
CG-DF	81.00	1.69
CH-DF	60.38	1.68
CH-DG	75.71	1.05
CH-FG	41.76	1.87
DG-EF	66.39	1.12
DH-EG	71.68	1.62

LAT=45°S LONG=5°E

LOP PAIRS	CROSSING ANGLE	GDOP
AC-AE	69.89	1.60
AC-AH	66.33	1.87
AD-AG	74.69	1.69
AD-AH	71.61	1.97
AE-AF	84.57	1.48
AF-AG	47.31	1.74
AF-AH	81.01	1.44
BC-BE	69.90	1.43
BC-BH	66.33	1.44
BE-BF	84.57	1.39
BF-BG	47.31	1.87
BF-BH	81.01	1.39
CD-CE	68.05	1.52
CD-CG	74.69	1.85
CD-CH	71.61	1.48
DE-DF	84.57	1.76
DF-DH	81.01	1.78
AD-BC	53.61	1.96
AE-BC	58.34	1.68
AH-BC	54.78	1.64
AF-BE	83.88	1.27
AG-BE	48.82	1.60
AH-BF	69.45	1.56
AF-CD	46.08	1.86
AG-CE	69.28	1.13
AH-CE	77.02	1.36
AF-DE	64.03	1.28
AG-DE	68.67	1.14
AG-EF	83.95	1.03
AH-EF	62.35	1.47
AH-EG	70.35	1.70
BE-CD	50.05	1.85
BH-CD	46.49	1.91
BG-CE	80.84	1.05
BH-CE	65.46	1.29
BF-DE	75.58	1.27
BG-DE	57.11	1.24
BG-EF	84.49	1.01
BH-EF	50.79	1.48
BH-EG	81.90	1.49
CH-DE	38.49	1.74
CH-DG	75.75	1.10
CH-FG	48.37	1.65
DG-EF	64.64	1.13
DH-EG	78.25	1.42

LAT=55°S LONG=5°E

LOP PAIRS	CROSSING ANGLE	GDOP
AC-AE	69.71	1.72
AC-AH	56.62	1.65
AD-AG	71.03	1.61
AD-AH	80.86	1.65
AE-AF	86.91	1.60
AF-AG	51.88	1.65
AF-AH	80.00	1.40
BC-BE	69.71	1.48
BC-BH	56.62	1.55
BD-BH	80.86	1.98
BE-BF	86.91	1.48
BF-BG	51.88	1.79
BF-BH	80.00	1.41
CD-CE	67.76	1.51
CD-CH	80.86	1.42
CE-CF	86.91	1.96
DE-DG	41.21	1.90
EF-EG	51.88	1.85
AD-BC	53.23	1.80
AE-BC	59.01	1.78
AH-BC	45.91	1.75
AH-BD	88.43	1.96
AF-BE	76.20	1.39
AG-BE	51.92	1.62
AG-BF	41.17	1.91
AH-BF	69.29	1.52
AF-CD	58.81	1.59
AG-CE	60.84	1.21
AH-CE	88.95	1.25
AF-DE	51.48	1.48
AG-DE	76.64	1.09
AH-DE	48.52	1.67
AG-EF	84.22	1.03
AH-EF	67.67	1.32
AH-EG	60.45	1.68
BF-CD	48.10	1.96
BG-CE	71.55	1.09
BH-CE	80.34	1.15
BF-DE	62.19	1.44
BG-DE	65.93	1.14
BH-DE	37.82	1.87
BG-EF	85.08	1.01
BH-EF	56.96	1.32
BH-EG	71.16	1.45
CH-DG	70.64	1.20
CH-FG	51.49	1.58
DG-EF	60.35	1.18
DH-EF	32.24	1.89
DH-EG	84.12	1.30

LAT=15°N LONG=15°E

LOP PAIRS	CROSSING ANGLE	GDOP
AB-AE	61.29	1.50
AB-AG	62.28	1.48
AE-AF	47.53	1.71
AF-AG	48.52	1.69
AF-AH	88.26	1.84
BC-BE	71.17	1.42
BC-BG	70.17	1.43
BD-BE	85.36	1.55
BD-BG	84.37	1.55
BE-BH	40.73	1.95
BG-BH	39.74	1.98
CE-CF	47.53	1.72
CF-CG	48.52	1.70
CF-CH	88.26	1.62
DE-DF	47.53	1.87
DF-DG	48.52	1.84
DF-DH	88.26	1.41
EF-EH	88.26	1.46
AE-BC	56.19	1.48
AG-BC	57.18	1.47
AH-BC	83.08	1.92
AF-BE	79.83	1.13
AG-BE	51.65	1.43
AF-CE	52.63	1.35
AG-CF	43.42	1.63
AH-CF	83.16	1.85
AF-DE	66.82	1.14
AG-EF	65.41	1.36
BE-CF	84.93	1.14
BG-CE	48.54	1.46
BH-CE	88.28	1.04
BG-CF	83.93	1.14
BH-CF	44.20	1.55
BH-CG	87.28	1.04
BG-DE	34.34	1.89
BH-DE	74.08	1.05
BG-DF	81.87	1.27
BH-DF	58.39	1.42
BH-DG	73.09	1.06
CF-DE	61.73	1.22
CH-DF	74.06	1.76
CG-EF	60.31	1.40
DG-EF	46.12	1.66
EH-FG	87.27	1.44

LAT=5°N LONG=15°E

LOP PAIRS	CROSSING ANGLE	GDOP
AB-AE	74.76	1.45
AB-AG	69.55	1.49
AE-AF	50.82	1.64
AF-AG	45.61	1.76
AF-AH	87.33	1.79
BC-BE	69.67	1.63
BC-BG	74.88	1.57
BD-BG	87.77	2.00
BF-BH	87.33	1.92
BG-BH	41.72	1.88
CE-CF	50.82	1.65
CF-CG	45.61	1.79
CF-CH	87.33	1.55
DE-DF	50.82	1.78
DF-DG	45.61	1.94
DF-DH	87.33	1.40
EF-EH	87.33	1.82
AE-BC	67.83	1.57
AG-BC	62.62	1.62
AF-BE	86.68	1.07
AG-BE	47.71	1.43
AF-CE	57.75	1.28
AG-CF	38.68	1.79
AH-CF	80.40	1.82
AF-DE	70.63	1.11
AG-EF	71.65	1.25
BH-CE	72.08	1.12
BG-CF	81.18	1.13
BH-CF	57.10	1.33
BH-CG	77.29	1.08
BH-DE	59.20	1.21
BG-DF	68.29	1.33
BH-DF	69.98	1.31
BH-DG	64.40	1.15
CF-DE	63.70	1.21
CH-DF	74.45	1.48
CG-EF	64.71	1.29
DG-EF	51.83	1.47
EH-FG	87.46	1.95

LAT=5°S LONG=15°E

LOP PAIRS	CROSSING ANGLE	GDOP
AB-AE	88.78	1.55
AB-AG	77.14	1.62
AE-AF	55.64	1.56
AF-AG	44.00	1.81
AF-AH	86.34	1.73
BE-BF	55.64	1.99
BF-BH	86.34	1.55
BG-BH	42.34	1.89
CE-CF	55.64	1.57
CF-CG	44.00	1.88
CF-CH	86.34	1.45
DE-DF	55.64	1.68
DF-DH	86.34	1.40
EF-EH	86.34	1.65
AF-BE	88.51	1.05
AG-BE	44.51	1.47
AF-CE	66.44	1.18
AH-CF	75.55	1.81
AF-DE	76.42	1.09
AG-DE	32.42	1.94
AH-DF	65.56	2.00
AG-EF	77.65	1.17
BH-CE	52.78	1.39
BG-CF	66.07	1.23
BH-CF	71.58	1.25
BH-CG	64.42	1.20
BH-DE	42.79	1.60
BG-DF	56.08	1.48
BH-DF	81.57	1.30
BH-DG	54.43	1.32
BG-EF	44.78	1.59
CF-DE	65.62	1.23
CH-DF	76.36	1.56
CG-EF	66.85	1.21
DG-EF	56.86	1.33
EH-FG	82.02	1.74

LAT=15°S LONG=15°E

LOP PAIRS	CROSSING ANGLE	GDOP
AB-AE	78.43	1.98
AB-AG	83.04	1.85
AE-AF	62.06	1.48
AF-AG	43.52	1.83
AF-AH	85.26	1.66
BE-BF	62.06	1.68
BF-BH	85.26	1.44
BG-BH	41.74	1.96
CE-CF	62.06	1.59
CF-CH	85.26	1.41
DE-DF	62.06	1.59
DF-DH	85.26	1.41
AF-BE	87.65	1.06
AG-BE	44.13	1.49
AF-CE	84.56	1.07
AG-CE	41.04	1.59
AH-CF	62.76	1.99
AF-DE	84.35	1.07
AG-DE	40.82	1.60
AH-DF	62.98	1.99
AG-EF	83.64	1.10
BF-CE	58.97	1.55
BG-CF	46.62	1.74
BH-CF	88.36	1.35
BH-CG	44.83	1.58
BF-DE	58.75	1.56
BG-DF	46.83	1.73
BH-DF	88.57	1.35
BH-DG	45.05	1.58
BG-EF	58.05	1.26
CF-DE	61.84	1.45
CG-DF	43.74	1.82
CH-DF	85.48	1.38
CH-DG	41.96	1.71
CG-EF	61.14	1.22
DG-EF	61.36	1.22

LAT=25°S LONG=15°E

LOP PAIRS	CROSSING ANGLE	GDOP
AC-AE	75.36	1.41
AC-AG	49.61	1.68
AC-AH	89.60	1.57
AD-AG	83.34	1.92
AE-AF	69.85	1.44
AF-AG	44.10	1.81
AF-AH	84.09	1.59
BC-BE	75.36	1.52
BC-BH	89.60	1.46
BE-BF	69.85	1.48
BF-BH	84.09	1.41
CD-CE	70.91	1.66
CD-CG	83.34	1.63
CD-CH	56.67	1.94
DE-DF	69.85	1.84
DF-DH	84.09	1.44
AE-BC	54.70	1.86
AH-BC	68.94	1.89
AF-BE	89.49	1.10
AG-BE	46.41	1.47
AH-BF	63.43	1.88
AF-CE	51.99	1.36
AG-CE	83.91	1.05
AF-DE	85.72	1.09
AG-DE	50.19	1.37
AG-EF	89.43	1.06
BE-CD	71.59	1.57
BH-CD	85.83	1.56
BF-CE	72.65	1.33
BG-CE	63.25	1.14
BF-DE	73.62	1.33
BH-DF	80.31	1.45
BH-DG	36.22	1.92
BG-EF	68.77	1.11
BH-EG	72.87	1.94
CH-DE	47.97	1.39
CG-DF	77.82	1.49
CH-DF	62.19	1.80
CH-DG	73.72	1.08
DG-EF	64.99	1.14
DH-EG	69.10	1.96

LAT=35°S LONG=15°E

LOP PAIRS	CROSSING ANGLE	GDOP
AC-AE	63.78	1.61
AC-AH	68.27	1.65
AD-AG	79.98	1.79
AE-AF	78.37	1.46
AF-AG	45.71	1.77
AF-AH	82.86	1.51
BC-BE	63.79	1.45
BC-BH	68.27	1.42
BE-BF	78.37	1.41
BF-BG	45.71	1.99
BF-BH	82.86	1.40
CD-CE	67.36	1.45
CD-CG	79.98	1.75
CD-CH	62.87	1.50
DE-DF	78.37	1.57
DF-DH	82.86	1.54
AD-BC	66.24	1.91
AE-BC	46.39	1.90
AH-BC	50.88	1.90
AF-BE	84.24	1.17
AG-BE	50.05	1.46
AH-BF	65.47	1.74
AF-CD	41.97	1.85
AG-CE	71.11	1.14
AH-CE	71.75	1.83
AF-DE	74.25	1.15
AG-DE	60.04	1.23
AG-EF	85.69	1.04
AH-EF	57.16	1.69
AH-EG	77.13	1.83
BE-CD	53.80	1.56
BH-CD	58.28	1.52
BF-CE	42.79	1.89
BG-CE	88.50	1.06
BH-CE	54.36	1.46
BF-DE	88.36	1.27
BG-DE	42.65	1.54
BH-DF	72.87	1.61
BG-EF	76.92	1.04
BH-EF	39.77	1.79
BH-EG	85.48	1.59
CH-DE	53.34	1.38
CG-DF	85.44	1.86
CH-DF	48.29	1.97
CH-DG	86.00	1.05
CH-FG	51.73	1.59
DG-EF	66.93	1.11
DH-EG	75.49	1.58

LAT=45°S LONG=15°E

LOP PAIRS	CROSSING ANGLE	GDOP
AC-AE	64.46	1.79
AC-AH	59.25	1.71
AD-AG	76.07	1.68
AE-AF	86.91	1.53
AF-AG	48.40	1.71
AF-AH	81.70	1.45
BC-BE	64.46	1.48
BC-BH	59.25	1.51
BE-BF	86.91	1.40
BF-BG	48.40	1.90
BF-BH	81.70	1.40
CD-CE	69.42	1.46
CD-CH	70.63	1.41
DE-DF	86.91	1.73
DF-DH	81.70	1.76
AD-BC	69.33	1.72
AE-BC	49.25	1.98
AF-BC	37.66	1.86
AH-BC	44.04	1.95
AF-BE	77.88	1.27
AG-BE	53.72	1.48
AH-BF	66.49	1.65
AF-CD	53.72	1.53
AG-CE	60.10	1.24
AH-CE	86.60	1.37
AF-DE	61.82	1.29
AG-DE	69.78	1.14
AG-EF	82.55	1.03
AH-EF	64.15	1.47
AH-EG	67.44	1.72
BE-CD	48.40	1.79
BH-CD	43.19	1.88
BG-CE	79.32	1.09
BH-CE	71.39	1.23
BF-DE	77.03	1.32
BG-DE	94.57	1.29
BH-DF	69.64	1.92
BG-EF	82.24	1.01
BH-EF	48.94	1.49
BH-EG	82.66	1.44
CH-DE	44.91	1.60
CH-DG	83.41	1.11
CH-FG	59.75	1.32
DG-EF	66.17	1.11
DH-EF	32.88	1.90
DH-EG	81.28	1.38

LAT=55°S LONG=15°E

LOP PAIRS	CROSSING ANGLE	GDOP
AC-AE	67.02	1.87
AC-AH	58.78	1.77
AD-AG	71.87	1.59
AD-AH	79.83	1.67
AE-AF	84.93	1.71
AF-AG	58.24	1.64
AF-AH	80.84	1.41
BC-BE	67.02	1.91
BC-BH	58.78	1.69
BE-BF	84.93	1.88
BF-BG	58.24	1.85
BF-BH	80.84	1.48
CD-CE	65.60	1.48
CD-CH	79.83	1.39
CE-CF	84.93	1.72
CF-CH	80.84	1.83
DE-DG	42.84	1.88
EF-EG	58.24	1.81
AD-BC	61.15	1.68
AF-BC	41.82	1.71
AF-BE	71.16	1.48
AG-BE	56.60	1.88
AH-BF	67.08	1.60
AF-CD	64.23	1.43
AG-CE	83.60	1.33
AH-CE	82.30	1.29
AF-DE	48.75	1.84
AG-DE	79.01	1.09
AH-DE	80.41	1.67
AG-EF	81.64	1.84
AH-EF	69.74	1.35
AH-EG	88.02	1.72
BF-CD	50.47	1.86
BG-CE	67.36	1.13
BH-CE	84.03	1.14
BF-DE	62.52	1.48
BG-DE	65.25	1.16
BH-DE	34.64	1.98
BG-EF	84.58	1.91
BH-EF	85.97	1.33
BH-EG	71.79	1.41
CH-DG	79.99	1.19
CH-FG	56.66	1.91
DG-EF	62.17	1.16
DH-EF	33.56	1.83
DH-EG	83.80	1.37

END

7-87

DTIC